

What is the carbon storage potential of scrubland created by rewilding?



Nancy C. Burrell
St Edmund Hall
University of Oxford

A thesis submitted for the degree of
Doctor of Philosophy
MICHAELMAS 2024

Declaration

I declare that this thesis was composed by myself and that the work contained herein is my own except where explicitly stated in the text. The work has not been submitted for any degree or professional qualification except as specified.

Nancy Burrell, MICHAELMAS 2024

Word count: 39,000

Acknowledgements

It has been an extraordinary privilege to have Kathy Willis as lead supervisor on this DPhil. Her boundless energy, positivity and holistic, out-of-the-box, process-led thinking is an inspiration that I will carry with me for the rest of my life. Marc Macias-Fauria introduced me to the extraordinary, thrilling, fast-evolving world of drone technology and machine learning – something that lifted this project, quite literally, into dimensions I could never have imagined. Thank you for persuading me to rise to the challenge! Lizzy Jeffers' probing questions and insightful guidance have pushed my critical thinking and helped me grow as a researcher. Together, as a supervisory team, they have guided and supported me in ways they probably don't even realise. I am deeply thankful for their collective intelligence, kindness and patience.

Several people I hugely admire contributed to the thinking behind this DPhil, especially in the early phases, helping me ground and expand my ideas. Thank you, Mick Crawley, Ted Green and Bill Sutherland for inspiring conversations and providing insights into the worlds of plants, trees, fungi and the dynamic, often unexpected processes of natural disturbance.

Without the indomitable destructive sampling team battling winter weather and heavy Sussex clay to pull up 300 trees, this research project could not have been realised. It was a truly Herculean task. Thank you, Aaron Europa and Stuart White, for your dedication and unflagging good cheer.

To Ewan Marsh and James Burrows, your help in processing thousands of samples with such patience and meticulousness created a really significant dataset. Thank you to Marcus Spiegel and Jeff Kerby for introducing me to the astonishing world of remote sensing.

My friends and family: thank you for holding me to my Pomodoro timer, diving into sampling chaos, and making the past four years inspiring, exciting, and fun. You turned challenges into cherished memories.

Finally, to my parents, Isabella Tree and Charlie Burrell, to whom I dedicate this thesis: you are my steadfast pillars, my greatest inspiration, and the reason I believe in a better future for our planet. Watching you bring a vision to life—restoring the land and championing rewilding—has shaped this project and my sense of purpose. You are the deep, carbon-rich roots of this work, and I dedicate it to you with love and pride.

Funding Acknowledgements

This research was made possible through the generous financial support of Nattergal Ltd and Virgin Media O2.

Publications

The following publications have arisen from this thesis:

Chapter 2:

Burrell, N.C., Jeffers, E.S., Macias-Fauria, M. and Willis, K.J., 2024. The inadequacy of current carbon storage assessment methods for rewilding: A Knepp Estate case study. *Ecological Solutions and Evidence*, 5(1), p.e12301.

Thesis abstract

Climate change represents the most urgent challenge humanity has ever faced, spurring a global race to devise solutions that can prevent irreversible harm to our planet and future generations. Alongside massive and rapid decarbonisation, nature-based solutions are considered to be the most effective way of combating climate change through protection, restoration and sustainable management of natural carbon sinks and reservoirs. Predominant amongst these is reforestation - planting trees to absorb carbon dioxide from the atmosphere. But as governments, NGOs and businesses the world over undertake large-scale tree planting schemes the environmental sector is raising concerns that tree planting does not adequately address the twin crisis of biodiversity loss. Indeed, it may, in some circumstances, actually harm ecosystems and increase carbon emissions. Scientists have, on this account, spelled out the importance of natural regeneration - allowing trees and shrubs to recolonise through natural processes - as a means of establishing tree cover for carbon storage while at the same time helping to restore ecosystems and biodiversity. Rewilding is a particularly effective way of providing conditions for natural regeneration, but its carbon storage potential is poorly understood. There is an assumption that young trees naturally colonising in rewilding projects are adversely affected by the presence of grazing and browsing animals, and smaller woody shrubs characteristic of emergent vegetation are rarely factored into carbon storage calculations. This thesis aims to quantify carbon storage in woody shrubs and emergent trees within a rewilding context and develops a replicable method for calculating above- and below-ground carbon. The goal is to create a landscape-scale method applicable to woody vegetation in temperate rewilding projects, enabling more accurate assessment of its potential as a nature-based climate solution.

Contents

Declaration	2
Publications.....	5
Thesis abstract	6
List of Figures	13
List of Tables.....	18
Chapter 1: Introduction.....	23
1.1 Valuing Natural Capital: A Framework for Sustainable Ecosystem Management .23	
1.2 Plantation Forestry Bias in Nature-based Solutions to Climate Change.....26	
1.3 Natural Regeneration of Trees and Woody Shrubs in the Rewilding Scenario	31
1.4 Assessing the Carbon Storage Potential of Scrubland in the Trophic Rewilding Scenario	36
1.5 The Southern Block of Knepp Wildland as Study Site	41
1.6 Thesis Aims and Research Objectives.....	44
1.7 Reference List	47
Chapter 2: The inadequacy of current carbon storage assessment methods for rewilding: A Knepp Estate case study.	61
2.0 Abstract.....	62
2.1 Introduction.....	63

2.2 Materials & Methods.....	68
2.2.1 Site location.....	68
2.2.2 Stratified sampling.....	69
2.2.3 Data collection and analysis.....	70
2.2.4 i-Tree Eco model	71
2.2.5 Preliminary destructive sampling of the scrubland	71
2.2.6 Statistical analysis.....	73
2.3 Results.....	74
2.3.1 Species composition	74
2.3.2 The relationship between tree height (m) and DBH (cm).....	74
2.3.3 Belowground biomass.....	77
2.4 Discussion	79
2.4.1 Allometric equations used to determine aboveground carbon storage	81
2.4.2 Belowground carbon storage	82
2.5 Conclusion	83
2.5.2 Acknowledgements	84
2.5.3 Peer review	84
2.5.4 Date availability statement	84
2.6 Reference List	85
2.7 Supplementary Materials	90

Chapter 3: Quantifying Carbon Storage in Rewilded Scrubland: Developing Allometric Equations through Destructive Sampling.....	93
3.0 Abstract	94
3.1 Introduction.....	95
3.2 Materials and Methods	99
3.2.1 Site Location and Sample Selection.....	100
3.2.2. Individual Tree /Shrub Selection and Sample Collection Process.....	103
3.2.3 Destructive sampling	105
3.2.4 Field sampling.....	105
3.2.5. Allometric model development and statistical analysis	113
3.3 Results	116
3.3.1 Model outputs	119
3.3.2 Variation in Root:Shoot Ratio in Relation to Browse Line	124
3.3.3 Allometric equations	125
3.4 Discussion	130
3.4.1. Scrub-specific allometric equations and explanation	130
3.4.2. Impact of Browsing on Biomass Allocation	134
3.5 Conclusion	137
3.6 Reference list.....	138
3.7 Supplementary Material	150

Chapter 4: Quantifying Carbon Content in Rewilded Scrublands: Challenging the '50% Rule' through Elemental Analysis.....	168
4.0 Abstract	169
4.1 Introduction.....	170
4.2 Materials and Methods	176
4.2.1 Site location.....	176
4.2.2 Destructive Sampling	177
4.2.3 Elemental Analysis	178
4.3 Results	180
4.3.1. Carbon content of studied taxa.....	180
4.3.2. Carbon Content in Aboveground vs. Belowground Parts by Taxon.....	182
4.3.3. Relationship between tree height and taxon-specific carbon content.....	184
4.3.4 Exposure Impact on Carbon Content	185
4.4 Discussion	188
4.4.1. Factors Contributing to Lower Carbon Content in Scrub Trees	189
4.4.2. Carbon content variation by tree part across taxa	192
4.5 Conclusion	193
4.6 References	194
4.7 Supplementary Materials	204

Chapter 5: Integrating Structure from Motion and 5-Band Imaging to Estimate Above- and Belowground Biomass in a Rewilded Scrubland Ecosystem.....205

5.0 Abstract206

5.1 Introduction207

5.2 Materials and methods.....212

 5.2.1 Study site.....212

 5.2.2 UAV surveys.....213

 5.2.3 Imagery processing.....215

 5.2.4 Canopy features from SfM217

 5.2.5 Taxonomic classification of scrubland taxa from multispectral orthomosaics221

 5.2.6 Estimating carbon and biomass from allometric equations222

5.3 Results224

 5.3.1 Extracting predictor variables from the SfM model224

 5.3.2 Taxonomic classification of scrub from multispectral orthomosaics225

 5.3.3 allometric equations233

 5.3.4 Biomass and carbon estimates233

5.4 Discussion 240

 5.4.1 Generating predictor variables through Structure from Motion (SfM)240

 5.4.2 Multi-spectral imaging to identify scrub taxa243

 5.4.3 Scrub biomass and carbon estimation245

5.5 Conclusion	249
5.6 References	250
5.7 Supplementary materials.....	263
Chapter 6: Conclusion.....	269
6.1 Main Findings	269
6.2 Future directions.....	286
6.3 Concluding Remarks.....	289
6.4 References	290

List of Figures

Figure 1.1: Framework illustrating the flow from natural capital to societal benefits through ecosystem services.

Figure 1.2: A young *Quercus robur* (oak) sapling, commonly known as a "Vera oak," growing within dense scrubland at the Knepp Estate, West Sussex, UK. The surrounding hawthorn (*Crataegus monogyna*) and bramble (*Rubus fruticosus*) protect the sapling from browsing animals (Tree & Burrell, 2019; Vera 200; Hodder et al., 2005).

Figure 1.3: Herbivores impact oak morphology in Crete's wood-pasture landscapes. Image [A] (with the author) shows an oak (*Quercus spp.*) with a dense "pin cushion" form below the ~2 m herbivore browse line, while image [B] depicts a more conventional tree form above it (Rackham, 1998).

Figure 1.4: Two different woodlands found at Knepp Wildland, West Sussex. [A] scrubland generated by 'rewilding'; [B] mixed woodland plantation.

Figure 1.5: Arable reversion to scrubland through natural colonisation in the presence of grazing and browsing large herbivores. A field in the Southern Block of the Knepp Estate, Image A was taken in 2001, Image B was taken in 2023.

Figure 2.1: The Southern Block of the Knepp Estate (50.9817° N, 0.3664° W), showing the 5 landcover classes that were sampled, the green areas denote hedgerows, the black area is the Southern Block boundary. The black dots represent the plots that were sampled.

Figure 2.2: the relationship between the log-transformed height and the long diameter at breast height (dbh) of trees in the study area, stratified by tree height. The grey line represents trees taller than 2.5 m (above the browse line), while the black line represents trees shorter than 2.5 m (below the browse line). Panels [A-F] show trees with different numbers of stems, with panel [A] showing trees with a single stem, and panels [B-F] showing trees with 2, 3, 4, 5, and 6 stems, respectively. The results of the Spearman's rank correlation are displayed as a ρ value with NS denotes a non-significance of the p-value outcome.

Figure 2.3: A comparison between the i-Tree estimates and the actual values of the destructive samples. Panel [A] exhibits the root:shoot ratio of the destructive samples, with $n = 39$. The solid line illustrates the i-Tree Eco predicted root:shoot ratio, which was 0.26, while the dotted line depicts the sample mean root:shoot ratio, which was 1.07. Panel [B] displays a comparison of the total belowground fresh weight (BGB, black bars) to the i-Tree prediction of belowground biomass (BGB, grey bars) for five different species. The number of samples (n) for each species is provided in parentheses: blackthorn (*Prunus spinosa*, $n = 16$), dog rose (*Rosa canina*, $n = 5$), hawthorn (*Crataegus spp.*, $n = 6$), oak (*Quercus spp.*, $n = 11$), and willow (*Salix spp.*, $n = 1$).

Figure 3.1: The Southern Block of the Knepp Estate (50.975781°N, 0.344819°W), showing the three possible sampling site locations (1-3) that were selected based on their heterogeneous land-cover classification. The blue area is the Southern Block boundary.

Figure 3.2: The left panel shows the 3,300 possible individual scrub taxa, including blackthorn (*Prunus spinosa*), dog rose (*Rosa canina*), hawthorn (*Crataegus monogyna*), willow (*Salix spp.*), and oak (*Quercus spp.*). The right panel displays the randomly selected samples to be destructively sampled for each taxon chosen from the initial pool under the specified browsing conditions.

Figure 3.3: Methodology undertaken to sample aboveground biomass and belowground biomass of different scrub species.

Figure 3.4: Destructive sampling process in the field and in the laboratory [A] combination of the mini digger and the compressed air to extract a scrub tree; [B] samples in paper bags in ovens; [C] trench dug 0.5 m deep to extract the root ball of a larger tree.

Figure 3.5: Laboratory measurements and processes of destructively sampled scrub trees [A] processed samples in paper bags ready for oven drying; [B] size categorisation of root classes based on diameter; [C] precision balance scales used to weigh samples, including the excess saw dust created during the processing (displayed here); [D] digital crane scale used to weigh the total weight of the scrub tree.

Figure 3.6: Distribution of tree sizes by refined tree height (cm), the preliminary population of scrub trees (Figure S3.1A) was analysed for summary statistics (min, max and mean values) to determine height classes for the destructive sampling of scrub (displaying in Figure 3.7).

Figure 3.7: Height distribution (density as proportion) of five scrub species sampled for allometric equation development: blackthorn (*Prunus spinosa*), dog rose (*Rosa canina*), hawthorn (*Crataegus monogyna*), oak (*Quercus robur*), and willow (*Salix cinerea*). Density values represent the proportion of individuals within each height class.

Figure 3.8: Relationships between predictor variables (log height, log dbh, and log canopy area) and three biomass components (A) log aboveground biomass, (B) log belowground biomass, and (C) log total biomass across five taxa (blackthorn, dog rose, hawthorn, oak, and willow) and two conditions (exposed in grey and protected in yellow). Symbols represent different taxa: blackthorn (square), dog rose (diamond), hawthorn (triangle), oak (circle), and willow (cross). (D) Box-and-whisker plots of log root:shoot ratio by taxon and condition.

Figure 3.9: root:shoot ratio for various scrub taxa (blackthorn, dog rose, hawthorn, oak, and willow) and their relationship with the browse line (below and above 2.5 meters) and condition (exposed and protected).

Figure 3.10: Predicted versus actual log-transformed biomass components for five taxa (blackthorn, willow, hawthorn, dog rose, and oak), showing aboveground biomass (AGB), belowground biomass (BGB), and total biomass (TB) in panels A–O. Each panel represents a separate model for each biomass component across different taxa, with R^2 values indicating model fit. Points are coloured by taxa: blackthorn (A–C, blue), willow (D–F, green), hawthorn (G–I, pink), dog rose (J–L, orange), and oak (M–O, yellow). Equations used for each model are displayed in table 3.4.

Figure 4.1: Distribution of observed carbon content (%) compared to the 50% assumption value (red dotted line) for five tree taxa: blackthorn (*Prunus spinosa*) n=36, dog rose (*Rosa canina*) n=42, hawthorn (*Crataegus spp.*) n=54, willow (*Salix spp.*) n=39 and oak (*Quercus spp.*) n=30.

Figure 4.2: Variation in carbon content (%) across five different tree taxa: blackthorn (*Prunus spinosa*) n=36, dog rose (*Rosa canina*) n=42, hawthorn (*Crataegus spp.*) n=54, willow (*Salix spp.*) n=39 and oak (*Quercus spp.*) n=30.

Figure 4.3: The carbon content (%) in aboveground (shoot) and belowground (root) parts for five tree taxa: blackthorn (*Prunus spinosa*), dog rose (*Rosa canina*), hawthorn (*Crataegus spp.*), oak (*Quercus spp.*), and willow (*Salix spp.*).

Figure 4.4: The mean carbon content in relation to tree size and taxa. [A]: Mean carbon content by tree size (large: >150 cm, medium <150 cm >50 cm, small: <50 cm). [B]: Mean carbon content by taxon (blackthorn (*Prunus spinosa*), dog rose (*Rosa canina*), hawthorn (*Crataegus spp.*), oak (*Quercus spp.*), willow (*Salix spp.*)) and size categories. Each taxon is further divided into size categories (large, medium, small).

Figure 4.5: Mean carbon content, divided by tree part (shoot or root) of the five taxa (blackthorn (*Prunus spinosa*), dog rose (*Rosa canina*), hawthorn (*Crataegus spp.*), oak (*Quercus spp.*), willow (*Salix spp.*)). Each taxon is further divided into exposure categories: exposed (not found within a bramble patch) and protected (found within a bramble patch).

Figure S4.1: relationship between mean carbon content (%) and mean dry density (g/cm³) for aboveground (shoots) and belowground (roots) biomass. Red circles represent shoot density versus carbon, while orange triangles represent root density versus carbon.

Figure 5.1: Study site 3 (red line) within the Southern Block of Knepp Wildland (50.975781°N, 0.344819°W). Black dots represent the 14 ground control points (GCPs) used for georeferencing.

Figure 5.2: Spatial distribution of vegetation characteristics within the study area. Panel A shows the maximum canopy height (m) derived from SfM data, with taller canopies highlighted in brighter colours. Panel B visualises the spatial arrangement of canopy interactions, categorising areas as "touching bramble" (blue), "outside bramble" (red), and "bramble" (yellow).

Figure 5.3: Confusion matrix illustrating the classification performance of the XGBoost model for six taxa: blackthorn, bramble, dog rose, hawthorn, oak, and willow. The rows represent the predicted taxa, and the columns represent the actual taxa. Diagonal cells indicate correct classifications, while off-diagonal cells represent misclassifications. The colour intensity corresponds to the number of samples, with darker shades (red) indicating higher counts. The heatmap represents the 30% evaluation dataset, separated from the training data using a 70:30 random split to ensure robust model evaluation.

Figure 5.4: Top 20 features ranked by Gain (the relative contribution of the feature to improving the model's accuracy) in the XGBoost model for taxa classification.

Figure 5.5: Spatial distribution of classified taxa across the study area based on XGBoost model predictions. Each polygon represents an individual canopy, color-coded by predicted taxon: blackthorn (green), bramble (yellow), dog rose (red), hawthorn (purple), oak (blue), and willow (orange).

Figure 5.6: Distribution of canopy area and height for destructively sampled scrub and Structure-from-Motion (SfM) models. Panels [A] and [B] show the distribution of canopy area (cm²) for both models, while panels [C] and [D] display the distribution of canopy height (cm) for the same.

Figure 5.7: Total biomass and distribution of aboveground and belowground biomass across five taxa. (a) total aboveground biomass (blue) and belowground biomass (aqua) in kilograms (kg) per taxon, aggregated across 13 hectares. (b) the distribution of individual biomass values (log scale) for aboveground (blue) and belowground (aqua) biomass across taxa. Taxa include blackthorn, dog rose, hawthorn, oak, and willow.

Figure 6.1: Diagrams (A – D) summarising the findings of this thesis. Created in <https://BioRender.com>

List of Tables

Table 2.1: The characteristics of different tree species measured in the southern block, along with their corresponding allometric equations for estimating biomass using i-Tree Eco. The table includes the number of individuals (n) for each species, as well as the average tree height and diameter at breast height (dbh) with their corresponding standard deviations. The final column indicates the closest taxonomic level to associate with an i-Tree equation for estimating biomass. Where no associated equation was found, the field was left blank.

Table S2.1: Landcover classes observed in the Southern Block of the Knepp rewilding project in 2021, illustrating the vegetation cover that has emerged due to the rewilding efforts. Classes chosen for i-Tree sampling are marked with asterisks.

Table S2.2: Destructive samples (n=39) of individual trees and shrubs sourced from the Southern Block of the Knepp rewilding project. Listed samples include their common name, measured aboveground biomass (AGB), and belowground biomass (BGB). i-Tree predictions of BGB are derived from the actual AGB weight, using a factor of 0.26 to represent the anticipated root:shoot ratio.

Table 3.1: Description of different scales, balances, and equipment used in the field and laboratory.

Table 3.2: Number of samples extracted per scrub taxa according to their size class and exposure to browsing. Small <75 cm; medium 75 – 210 cm; large >210 cm.

Table 3.3A: The response variables (aboveground biomass (AGB), belowground biomass (BGB), total biomass and root:shoot ratio) for each taxon (blackthorn, dog rose, hawthorn, oak, sallow) as a function of single predictor variables (height, dbh and canopy area) on the log scale. Estimates, Standard Error (S.E) and p-values recorded.

Table 3.3B: The response variables (aboveground biomass (AGB), belowground biomass (BGB), total biomass and root:shoot ratio) for each taxon (blackthorn, dog rose, hawthorn, oak, sallow) as a function of condition of browsing (exposed or

protected) in relation to single predictor variables (height, dbh and canopy). Interactive term, Standard Error (S.E) and p-values recorded.

Table 3.4 : Summary of linear regression models used to predict biomass components (W) (aboveground biomass (AGB), belowground biomass (BGB), and total biomass (Total)) across five taxa (blackthorn, dog rose, hawthorn, oak, and willow). Each model incorporates predictor variables—height (h), diameter at Breast Height (d), and canopy area (A)—as well as interactions with browsing condition (x_c) where specified. The models include combinations of main effects and interactions, up to a maximum model structure with all possible interaction terms (Equation 1). Model performance is evaluated using the coefficient of determination (R^2), residual sum of squares (RSS), and Akaike Information Criterion (AIC). Taxon specific biomass coefficient values ($\beta_0 - \beta_{15}$) can be found in Table 3.5.

Table 3.5: Coefficient values (β) for models predicting aboveground biomass (AGB), belowground biomass (BGB), and total biomass (Total) for five scrub taxa (blackthorn, dog rose, hawthorn, oak, and willow). Each coefficient (β) corresponds to a predictor or interaction term in the model, where W represents the biomass component, β_0 is the intercept, and β_1 through β_{15} are coefficients for predictor variables and their interactions. Predictor terms include log (height) (tree height), log (dbh) (diameter at breast height), log (canopy area) (canopy area), and the browsing condition factor (conditionprotected), along with their interactions. Coefficients are ordered from the intercept (β_0) to the highest-order interaction term, “conditionprotected:log_height:log_dbh:log_canopy_area” (β_{15}). NA values indicate terms that were not included in the final model for that specific taxon and biomass component. The full table of coefficients with Standard Error (SE), T-Value and P-value can be found in Table S3.2.

Table S3.1: Summary of biomass models for above-ground biomass (AGB), below-ground biomass (BGB), and total biomass across different taxa. Models include combinations of log-transformed height, diameter at breast height (DBH), canopy area, condition, and their interactions. Model fit improves with additional predictors and interactions, indicated by higher R^2 and lower AIC values.

Table S3.2: The table presents the estimated coefficients for the maximum model $\log(\text{biomass}) \sim \text{condition} * \log(\text{height}) * \log(\text{canopy_area}) * \log(\text{dbh})$, fitted separately for each taxon and biomass type (AGB = Above-Ground Biomass, BGB = Below-Ground

Biomass, TB = Total Biomass). Each row shows the taxon, biomass type, coefficient estimate (β), standard error (s.e.), t-value (t), along with the beta identifier (b0 to b15) corresponding to the intercept, main effects, and interaction terms. The intercept is b0, while the highest-order interaction term (b15) captures the combined effect of condition, height, canopy area, and dbh. p-values are excluded from this table as uninformative to these model comparisons. Each of the terms included in the various models (Table 3.4) were significant ($p < 0.05$) (see Tables 3.3a and 3.3b).

Table S3.3: Summary of model results for relationships between ecological variables and response variables across different taxa. The table provides coefficients (Estimate), standard errors (S.E.), t-values, and p-values for predictors such as log-transformed density, canopy area, height, and interactions involving these variables. Significant effects ($p < 0.05$) are highlighted for each taxon and response type.

Table 4.1: Number of representative trees per category used for elemental analysis, including taxa, size and exposure to/protection from herbivory. Each tree is made up of six representative sub-samples – three from aboveground tree parts and three from the roots.

Table S4.1: Linear regression analysis results for the relationships between mean carbon content (%) and mean dry density (g/cm^3) for shoots and roots. The table includes the slope, intercept, R-squared value, p-value, and standard error (s.e.) for each variable pair. Results indicate weak correlations, with no statistically significant relationships at the 0.05 level.

Table 5.1: Description of drone surveys and their photogrammetric models. The February survey included a dual-flight approach with a multispectral survey, capturing both nadir and oblique (20° from nadir) imagery. All other flights followed a standardised mission plan with set waypoints, though launch point variations led to slight differences in altitude and resolution. Automated camera triggering occasionally caused minor inconsistencies in image count. Each survey includes details on camera type, ground resolution, point density, total images, dense point cloud size, and RMS reprojection error.

Table 5.2: Class-wise statistics derived from the confusion matrix for the XGBoost model, showing the performance metrics for each taxon (blackthorn, bramble, dog

rose, hawthorn, oak, and willow). The evaluated metrics: Sensitivity (proportion of correctly identified samples for each taxon), Specificity (proportion of correctly identified non-samples for each taxon), Positive Predictive Value (precision of predictions for each taxon), Negative Predictive Value (proportion of correctly excluded samples), and Balanced Accuracy (the average of Sensitivity and Specificity for each taxon).

Table 5.3: The top 20 features ranked by their importance in the XGBoost model for taxa classification. The month from which the feature was derived, the statistical metric used (including standard deviation, mean, and median), the spectral band number associated with the feature, Gain (the relative contribution of the feature to improving the model's accuracy), Cover (the proportion of samples affected by the feature during tree splits), and Frequency (the number of times the feature was used in splitting data across all decision trees in the model).

Table 5.4: Summary of linear regression models used to predict biomass components (W) (aboveground biomass (AGB) and belowground biomass (BGB)) across five taxa (blackthorn, dog rose, hawthorn, oak, and willow). Each model incorporates predictor variables—height (h) and canopy area (A)—as well as interactions with browsing condition (x_c) where specified. The models include combinations of main effects and interactions, up to a maximum model structure with all possible interaction terms (Equation 1). Model performance is evaluated using the coefficient of determination (R^2), residual sum of squares (RSS), and Akaike Information Criterion (AIC). Taxon specific biomass coefficient values ($\beta_0 - \beta_7$) are displayed, coefficients are ordered from the intercept (β_0) to the highest-order interaction term, “conditionprotected:log_height:log_canopy_area” (β_7). NA values indicate terms that were not included in the final model for that specific taxon and biomass component. The full table of coefficients with Standard Error (SE), T-Value and P-value can be found in Table S5.2.

Table 5.5: Summary of total aboveground biomass (AGB) and belowground biomass (BGB) for each taxon across 13 hectares, along with their corresponding carbon estimates. The table includes total biomass (kg), carbon storage (kg), root-to-shoot ratios, and the minimum, maximum, and mean biomass values per individual (kg). Additionally, the per-hectare biomass and carbon values for both AGB and BGB are presented.

Table S5.1: results of multiple linear regression models fitted to predict above-ground biomass (AGB) and below-ground biomass (BGB) for each taxon. Model performance is evaluated using R^2 , Residual Sum of Squares (RSS), and Akaike Information Criterion (AIC). The tested models include combinations and interactions of predictor variables: log-transformed height, canopy area, and condition. Results are presented unfiltered to display the full range of tested models. P-values are excluded from this table as uninformative to these model comparisons. Each of the terms included in the various models (column 2) was significant ($p < 0.05$).

Table S5.2: linear models predicting aboveground biomass (AGB) and belowground biomass (BGB) for different taxa using the maximal model: Biomass~condition×log(height)×log(canopy area). Each row represents a model term, with corresponding estimates, standard errors and T-values. P-values are excluded from this table as uninformative to these model comparisons. Each of the terms included in the various models (Table 5.4) was significant ($p < 0.05$).

Chapter 1: Introduction

1.1 Valuing Natural Capital: A Framework for Sustainable Ecosystem Management

As we confront the accelerating threats of climate change and biodiversity loss, numerous studies are being undertaken to identify a framework that can be applied to natural landscapes so that their contributions to human well-being, sustainable economic development, and the overall health of the planet can be accurately valued (Arias-Arevalo et al., 2023; IUCN, 2022; Sajeva, 2023; Costanza et al., 1997). The concept of natural capital has become fundamental to a new way of thinking about the world's stock of finite natural resources including geology, soil, air, water, and all living organisms (Costanza et al., 1997; Daily, 1997; Millennium Ecosystem Assessment, 2005; IPCC, 2014; IPBES, 2019). It identifies and quantifies the provision of ecosystem services, the array of benefits derived by humans from natural ecosystems, including provisioning (food, raw materials, fresh water, medicines), cultural and health services, and regulating services (natural functions that help regulate climate, hydrology, air, and pests and disease) (IPBES, 2019). Carbon storage by trees (Zellweger et al., 2022), vegetation and soil is fundamental to climate regulation (Lal et al., 2021). Quantifying carbon storage under different land management regimes provides crucial evidence to support nature-based climate solutions.

In recent years, a growing emphasis has been placed on the 'stacking' of ecosystem services – i.e. packaging different services produced from a given piece of land together, sometimes with a range of different value and payment mechanisms attached to them (Dunklin et al., 2024; GOV.UK, 2023) (Figure 1.1).

(Díaz et al., 2019, Isaac et al., 2018, Costanza et al., 1997, Daily et al., 2000, Millenium Ecosystem Assessment, 2005). Adopting a natural capital framework can contribute to the development of policy and market instruments (e.g. subsidies, tradable permits and payments for ecosystem services) that internalise the value of ecosystem services, ultimately promoting their conservation and sustainable use (Bishop et al., 2010, Barbier, 2011, Johnson et al., 2023) (Figure 1.1). In light of these considerations, it is imperative that research continues to identify, quantify and value ecosystem services within a natural capital perspective, thereby fostering a deeper appreciation of the intrinsic and instrumental value of nature in the pursuit of a more sustainable future.

The importance of ecosystem services is becoming increasingly apparent as habitats and natural landscapes face mounting threats (McLellan et al., 2014, Cardinale et al., 2012, Vitousek et al., 1997, Foley et al., 2005, Johnson et al., 2023, Costanza, 2020, Bateman and Mace, 2020). By focusing research efforts on ecosystem services and framing them through a natural capital lens, a more holistic and integrated understanding of the value of nature can be achieved, enabling more effective decision-making processes and environmental management (Pettorelli et al., 2018, Guerry et al., 2015, Daily et al., 2009, Mandle et al., 2021). This approach facilitates the recognition of trade-offs and synergies between various ecosystem services (Bennett et al., 2009, Feng et al., 2021), while promoting sustainable land use practices and conservation strategies that account for the complex interdependencies within ecosystems (Liu et al., 2007, Mace et al., 2012, Jansen, 2023). By contrast, prioritising one ecosystem service through financial incentives to the exclusion of others can lead to a reduction in ecosystem provision across the board and even to environmental degradation and further carbon and biodiversity loss from the system in the long term (Roe et al., 2021;

Kelly-Quinn, 2020). This is particularly true in the assessment of carbon stocks. Focusing on carbon storage primarily through one single approach such as plantation forestry – i.e. large-scale manual planting of trees - for example, can adversely affect biodiversity, soil, hydrology and other natural processes, which all feed into natural carbon storage long-term (Tudge et al., 2023, Aguirre-Gutierrez et al., 2023). Many scholars have therefore argued that it is important, to maintain a holistic approach to the nature-based climate solution of carbon storage.

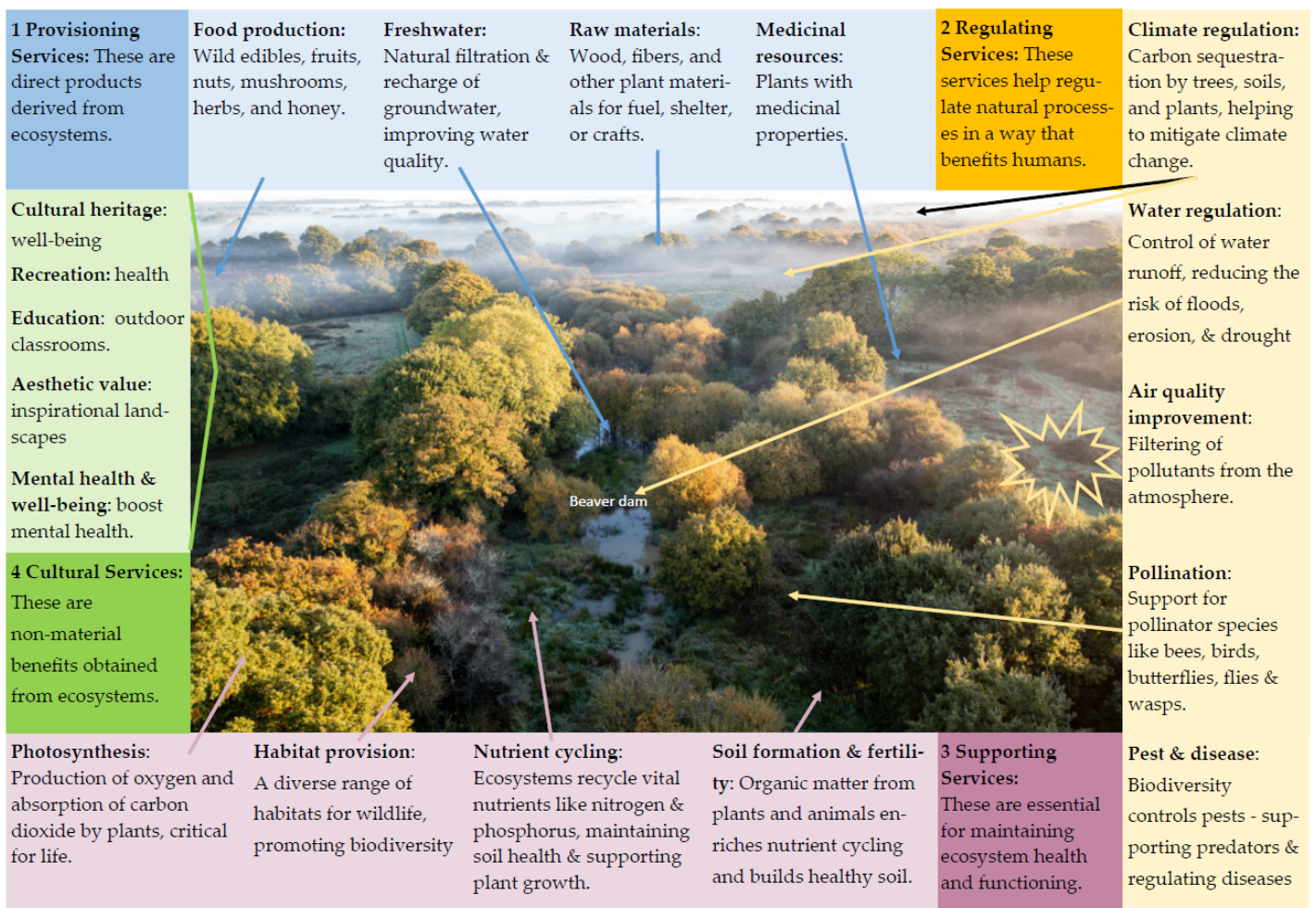


Figure 1.1: Framework illustrating the flow from natural capital to societal benefits through ecosystem services.

1.2 Plantation Forestry Bias in Nature-based Solutions to Climate Change

Modern forestry was established as a scientific discipline in the late 18th century by a coterie of German silviculturists including Johann Heinrich Cotta (1763-1844), founder of the Royal Saxon Academy of Forestry. The plantation model they pioneered focused on establishing areas of trees exclusively for timber production and the development of techniques for artificially propagating and planting saplings close together to grow straight timber (Johan., 2006). This involved fencing livestock out of forestry plantations, and thus negated the need for thorny scrub to act as natural sapling protection. They also established methods to calculate the wood mass of individual trees as well as the yield of entire forested regions, linking growth rates with economic value (Frangsmyr et al., 2023). The influence of plantation forestry on the global mindset has been profound and produced a bias in favour of manual tree planting as the default mechanism for re-establishing trees the world over (Di Sacco et al., 2021; Johnan., 2006). Consequently, the natural processes of tree colonisation and regeneration as happen in the wild or when land is left to its own devices, have largely been forgotten.

In addition to timber production, plantation forests may be established for other objectives, including fuelwood provision, erosion control and flood management (UK Forestry Commission, 2022). In recent decades, however, CO₂ reduction and climate change mitigation have become important drivers (Besar et al. 2020; IPCC, 2013; Zarin et al., 2016). Governments frequently pledge to plant millions of trees in order to harness the inherent capacity of trees to sequester CO₂ through photosynthesis, serving as carbon sinks ((Mada et al., 2022) Luyssaert et al., 2008). National commitments and global campaigns such as the Bonn

Challenge or the Trillion Tree Campaign serve as significant political statements (Cook-Patton et al., 2020, Fleischman et al., 2020, Bastin et al., 2019, Holl and Brancalion, 2020, Reid, 2021, Skidmore, 2019) and plantation forestry has strongly influenced the emerging carbon market (Girardin et al., 2021, Lewis et al., 2019, Ickowitz et al., 2022) (Mada et al., 2022) Luysaert et al., 2008) - a trading system by which companies and individuals can compensate for their greenhouse gas emissions (Forster et al., 2021).

The prominence of plantation forestry in current carbon offsetting efforts can be explained by several factors. Its simplicity enhances comprehension among both the public and policymakers, contributing to its widespread acceptance (Holl and Brancalion, 2020, Fleischman, 2014, Lewis et al., 2019). The tangible 'hands-on' nature of this model serves as a symbol of environmental stewardship, further bolstering its appeal in public relations and policy domains. Its economic feasibility marks it as a cost-effective approach compared to other climate change mitigation strategies, including blue carbon (Johannessen, 2022; Macreadie et al., 2021; Taillardat et al., 2018) and technological innovations such as Direct Air Carbon Capture and Storage (DACCS) (using chemical bonding to remove CO₂ directly from the atmosphere storing it underground or elsewhere) (Fawzy et al., 2020) and others (Williamson et al., 2012; Kantola et al., 2017; Renforth & Henderson, 2017). Plus, the growth and success rates of plantation forestry are relatively easy to predict, unlike natural regeneration (i.e. allowing trees to seed and colonise naturally) which, although beneficial - as I will discuss shortly - is highly uncertain and challenging to control. Factors such as seed dispersal, establishment timing, and survival rates can vary widely when left to natural processes, meaning it is often difficult to predict when or if new trees will successfully colonise an area (Kim et al., 2022; Marchin & Yuan, 2023). By contrast, plantation forestry operates

under controlled conditions, with trees planted, managed and harvested on a predictable schedule, offering clear timelines and returns for carbon sequestration (Busch et al., 2024; Nichol & Abbas, 2021; Guariguata et al., 2019). The ability to forecast these outcomes makes plantations more attractive for grant funding and large-scale carbon offset projects, where reliable results are prioritised (Randle & Jenkins, 2011).

However, manual tree planting, particularly at large-scale, also presents significant disbenefits which are of increasing concern to environmentalists. Plantation forestry can have adverse effects on the natural environment, impacting biodiversity (Veldman et al., 2019, Tölgyesi et al., 2022), and may lead to the release of carbon from other stocks (Helm et al., 2020). Notably, planting non-native species such as Sitka spruce in UK peatlands can result in significant carbon release (Smyth, 2023, Sloan et al., 2018). The drive to plant trees can also result in the establishment of forestry in regions not naturally forested (Tölgyesi et al., 2022).

Manually planting trees is also costly both financially (in terms of labour and propagation) and in carbon expenditure (in terms of intensive, high-energy propagation systems, transport to site, use of on-site herbicides, protective plastic tubing and artificial drainage, etc) – factors rarely incorporated into the carbon storage calculations of a plantation (Pacheco et al., 2024).

In terms of what tree species are planted, forestry plantations tend to be characterised by just a few types of tree, sometimes only one species if they are for commercial timber (Wang et al., 2022) (US EPA (2018), which makes them vulnerable to pests and disease. Since the saplings have been propagated artificially in nurseries, without the support of mycorrhizal associations available in natural systems, the genetic resilience of the trees themselves is low, making them further susceptible to disease and changes in local conditions (Begum et al., 2019; Barto et al., 2011). Being of a single generation or age class, and packed tight together, plantation trees are

also vulnerable to windblow (Forest Research, 2022; MDPI, 2022). All of which undermines the ecological balance and health of these hand-made forests (Dietrich et al., 2021, Alexander, 1999, Alexander, 2012, Rutten et al., 2021).

Significantly, too, plantations tend to produce habitats of low biodiversity (Wang et al., 2022). The practice of manual planting generally involves clearing from site any other vegetation and woody species deemed as competing with the young saplings, including understory shrubs such as hazel (*Corylus avellana*), dogwood (*Cornus sanguinea*), box (*Buxus sempervirens*), spindle (*Euonymus europaeus*), holly (*Ilex aquifolium*), gorse (*Ulex europaeus*), and hawthorn (*Crataegus monogyna*) that would once have formed part of the vegetation structure of ancient woodland and provided cover and nesting habitat for birds and small mammals (Rackham, 1986). The plantation forestry model with trees planted close together produces dark, closed-canopy conditions depriving other flora such as wildflowers and nectar- and berry-producing shrubs such as juniper (*Juniperus communis*), crab apple (*Malus sylvestris*), rowan (*Sorbus aucuparia*), blackthorn (*Prunus spinosa*), wild pear (*Pyrus pyraster*), and dog rose (*Rosa canina*) of the light they require to thrive (Hill et al., 1999; Vera, 2000). In contrast to naturally regenerated or open-structured systems with open-grown, light-demanding trees and woody shrubs, plantations are therefore generally characterised by a lack of understory and ground flora (Kirby et al., 2017; Vera, 2000).

Government and private funding for plantation forests and the vested interests of the forestry industry has meant that natural regeneration, or 'colonisation' as it is also known, is undervalued as an ecosystem service (Di Sacco et al., 2021, Merryweather, 2014). Thanks largely to the plantation forestry bias, a widespread historical and cultural prejudice against understory shrubs and open scrubland itself, now often considered to be useless 'wasteland',

has arisen (Randle & Jenkins, 2011). Consequently, thorny scrub is barely tolerated in the modern landscape, and these species along with the presence of native herbivores, such as deer (*Cervidae spp.*), hares (*Lepus europaeus*), rabbits (*Oryctolagus cuniculus*) and others in the UK, is often considered a hindrance to woodland creation due to their negative impact on vegetation recruitment (Candaele et al., 2023; Gill, 2006, Tanentzap et al., 2023, Tanentzap and Coomes, 2012).

Recently, though, the rewilding of land – the restoration of ecosystems by enabling natural processes to repair degraded landscapes – has gone some way to promoting the value of scrubland by demonstrating its importance as a productive habitat for wildlife (Pringle et al. 2023, Svenning et al., 2024; Svenning, 2020). However, the services provided by scrubland for the natural regeneration of trees remain poorly researched and are still considered antithetical to the prevailing funding models which rely on quantifiable numbers of trees established and predictable outcomes (Mercer & Gregg., 2023; Pettorelli et al. 2018). This oversight is often attributed to the perception that natural colonisation of woody vegetation is less efficient in establishing trees compared to the plantation forestry model (Holl, 2017). However, this view is still waiting to be validated with accurate, field-based data, highlighting a crucial area of knowledge that is currently lacking.

In addition, rewilding has not been seriously considered with regard to carbon sequestration (Schmitz et al., 2023; Mercer & Gregg, 2023; Cerqueira et al., 2015). There are standardised methods to measure and monitor the carbon stock specifically of a forested system but not of a rewilding landscape (Cord et al., 2017, Pettorelli et al., 2018)Burrell et al., 2024). This scarcity of study has led to a degree of scepticism among scientists when evaluating scrubland as an option for carbon sequestration and storage (Arts et al., 2016, Bulkens et al., 2016, Lorimer and

Driessen, 2014, Tanentzap et al., 2023). In this study, I aim to quantify the carbon storage values of woody shrubs and naturally colonising trees in a rewilding scenario, addressing gaps in evidence needed to evaluate rewilding as an approach to ecosystem service provision and nature-based solutions for climate change.

1.3 Natural Regeneration of Trees and Woody Shrubs in the Rewilding Scenario

'Rewilding' – enabling natural processes to repair damaged ecosystems – is a nature restoration strategy now being deployed in many countries across the world (Pettorelli et al., 2018). It has been specifically lauded for its effective delivery of one particular ecosystem service: the creation of habitats for biodiversity (Svenning, 2020, Svenning et al., 2019, Wang et al., 2023).

Allowing vegetation to recover is a key aspect of rewilding. Indeed, until recently, vegetation succession was considered the primary natural process or driving force of nature in temperate regions of the world (Clements, 1916; Tansley, 1940). The large-scale abandonment of land from agricultural production in Europe over recent decades (estimated to be more than 5 million hectares by 2030) (European Parliament, 2020) has shown how readily afforestation can occur, even in remote areas and on marginal land – a process known as 'passive rewilding' (Broughton, 2021; Martín-Forés, 2020).

However, the restoration of natural water systems and, in particular, the reintroduction of large free-roaming herbivores and missing keystone species have become defining characteristics of the rewilding model known as 'trophic rewilding' – a model that focusses

on the restoration and creation of complex and dynamic habitats as opposed to the more static and predictable ecosystem embodied by closed-cover forest (Schmitz et al., 2023; Hall, 2019, Garrido et al., 2021, Pettoirelli et al., 2018, Garrido et al., 2019, Apollonio et al., 2010, van Klink et al., 2020, Schulze, 2018, Ledger et al., 2022). In large rewilding projects in Europe (and even smaller ones, down to 330ha in Kraansvlak, Netherlands) large herbivores such as bison (*Bison bonasus*), water buffalo (*Bubalus bubalis*), horses (*Equus spp.*), red deer (*Cervus elaphus*), pigs (*Sus spp.*), and cattle (*Bos taurus*), introduced into the modern landscape as "ecosystem engineers" have been shown to drive species recovery (Seddon et al., 2014, Naundrup and Svenning, 2015, Ceaușu et al., 2015, Dvorský et al., 2021, Kristensen et al., 2022). This concept is primarily based on the premise that, before the late Quaternary mass extinctions of global megafauna populations (Stuart, 2015), large herbivores were the drivers behind ecosystem function and complexity (Vera, 2000; Levy, 2011; Kurten., 2017; Martin, 2005), and hence species diversity and abundance. The theory contends that their different grazing and browsing preferences create openness and dynamism in a landscape, generating habitat complexity (Bakker et al., 2016, Kristensen et al., 2022) and species diversity. Even in the absence of many of the large herbivores of the past, surviving species and 'proxies' (domesticated descendants or close relatives of the original species) have been shown to have positive effects for ecosystem recovery (Wang et al., 2023, Bakker et al., 2016, Soulé and Noss, 1998, Cromsigt et al., 2018).

The presence of large herbivores on the landscape has been shown to promote a number of important ecosystem processes. For example, large herbivores transfer nutrients across the landscape by eating in one place and dunging, passing urine, and (if legislation allows) eventually dying and decaying in another, affecting the fertility of the soil (Putman et al.,

2011). Their role as vectors of seeds (carried in fur, hooves, and gut) increases the complexity of the flora (both in number of plant species and vegetation structure) and the distribution of plants, thus increasing and sustaining biodiversity (Svenning, 2002, Malhi et al., 2022, Janzen, 1984, Miller and Coe, 1993). Also, their many physical disturbances through wallowing, rootling, rolling, rubbing and trampling, breaking branches and pushing over and de-barking trees, adds further dynamism and complexity to the ecosystem, creating myriad niches and opportunities for other life forms (Dvorský et al., 2021, Hanberry and Faison, 2023, Bakker et al., 2016, Peterken, 1996). Overall, the presence of large herbivores on the landscape has been shown to create a more open, dynamic and complex mosaic of habitats than presented by the kind of static, single age-class forest typified by plantation forestry and even more natural areas of closed canopy woodland where these big disturbers are absent. The number of free-roaming herbivores is key (Tree & Burrell, 2023). Too few, and their repressive effect on vegetation succession begins to fail, allowing woody shrubs and trees to dominate, shading and crowding out the more open, floristically rich areas. Too many, and vegetation complexity and abundance are adversely affected, reducing habitat and sustenance for other species, and resulting in a simplified, open grassland system. In the absence of apex predators as a controlling influence over herbivore population growth, and in more populated areas of Europe where people are unwilling to witness population die-offs through starvation or disease as happens in the wild (Kopnina et al., 2019), human management is needed to control numbers. This has led to some criticism of rewilding as being 'managed wilderness' with 'arbitrary standards for wildness' – i.e., not as wild and process-led as rewilders claim (Von Essen & Allen, 2015; Gammon, 2015).

In addition to positives for biodiversity, trophic rewilding has been shown to contribute to the enhancement of other ecosystem services, too, demonstrating its value as a holistic land management approach that embraces the many aspects of the natural capital perspective. The diverse ecosystems that rewilding generates, exhibit more efficient nutrient cycles and greater primary productivity, thereby supporting services such as nutrient cycling, soil formation, and primary production (Broughton et al., 2021, Ustaoglu and Collier, 2018). Rewilding has also been shown to reduce the risk of flooding (Dutton et al., 2018, Laurel and Wohl, 2019, Shurin et al., 2020, Harvey and Henshaw, Harvey and Henshaw, 2023), improve ecosystem resilience (Malhi et al., 2022, Wang et al., 2023) and increase pollinating insects, dung beetles (Garrido et al., 2019, Brompton, 2018, Andriuzzi and Wall, 2018, Howison et al., 2016) and insect predators which are vital to the agricultural sector. By providing wild spaces for human recreation and enjoyment rewilding can also provide significant benefits to human physical and mental health (VanVolkenburg et al., 2022, Kumar et al., 2023).

Rewilding projects are now also increasingly recognised for their capacity to generate scrubland habitats which can serve as a driver of the natural regeneration of trees in the landscape—another emerging ecosystem service (Watts and Jump, 2022; Tree, 2018). A particular feature of rewilding in temperate zone Europe is the emergence of environments abundant with woody shrubs such as bramble (*Rubus fruticosus*), hawthorn (*Crataegus monogyna*), sallow (*Salix spp.*), dog rose (*Rosa canina*), gorse (*Ulex europaeus*), dogwood (*Cornus spp.*), juniper (*Juniperus spp.*), holly (*Ilex spp.*) and blackthorn (*Prunus spinosa*) - that act as effective nurseries for naturally colonising saplings of trees such as oak (*Quercus spp.*), ash (*Fraxinus spp.*), alder (*Alnus spp.*) (etc) (Vera, 2000) (Figure 1.2).



Figure 1.2: A young *Quercus robur* (oak) sapling, commonly known as a "Vera oak," growing within dense scrubland at the Knepp Estate, West Sussex, UK. The surrounding hawthorn (*Crataegus monogyna*) and bramble (*Rubus fruticosus*) protect the sapling from browsing animals (Tree & Burrell, 2019; Vera 200; Hodder et al., 2005).

Historically, scrubland was highly valued, especially during the medieval period (Rackham, 1986). It was a primary source of essential materials used for food, medicines, tool handles, gunpowder, fuel and livestock fodder (Gerard, 1633; Leonti, 2012). Traditionally, thorny scrub was also particularly valued for its dual role in protecting naturally regenerating tree saplings from herbivory while simultaneously fostering a favourable microclimate for their growth (Standish, 1611; Rotherham, 2013; Stewart et al., 2000) (Figure 1.2). The nursery role of scrubland has been highlighted by several researchers, who emphasise its importance in offering saplings protection from environmental factors such as wind, sun, rain, and frost

(Vera, 2000; Hodder & Bullock, 2009). In addition, it promotes air circulation and moisture retention, contributing to pest and disease prevention in developing saplings (Torroba-Balmori et al., 2015; Dobson & Crawley, 1994). Recent studies also suggest that these nurseries may provide nutrients to growing trees through mycorrhizal associations with other woody species (Schaffer-Morrison & Zak, 2023; Simard, 2021). Additionally, research by Cavers & Cottrell (2014) highlights that genetic diversity within these regenerating environments, supported by scrub habitats, enhances resilience against climate change and disease. Furthermore, natural regeneration does not involve any of the costs associated with propagation and manual planting, it is a comparatively inexpensive way of establishing trees and shrubs, and involves zero expenditure of carbon. All of which makes natural regeneration in both the passive and trophic rewilding scenarios worth considering as an alternative – or, at least, in addition - to the forestry plantation model. Quantifying the carbon storage of natural regeneration within the trophic rewilding scenario, which is the specific aim of this study, will add important further evidence of the value of this alternative to plantation forestry as well as contribute to the total ecosystem services provided by trophic rewilding.

1.4 Assessing the Carbon Storage Potential of Scrubland in the Trophic Rewilding Scenario

Both passive and trophic rewilding are largely overlooked as nature-based solutions for carbon storage and climate change mitigation (Schmitz et al., 2023; Cromsigt et al., 2018). The lack of empirical studies supporting the carbon storage potential of trophic rewilding, in particular, complicates its promotion as a favoured management approach, one that could potentially stack together multiple ecosystem services. including the dual roles of biodiversity enhancement and carbon storage (Lorimer et al., 2015; Svenning et al., 2016).

Carbon storage associated with natural colonisation and rewilding is a complex process (Tree, 2018; Vera, 2000). A significant factor is the influence of large herbivores on the growth and carbon storage of woody plants (Figure 1.3A). For example, Rackham (1998) described a wood-pasture landscape in Crete, where oak trees under 2 metres exhibited a "pin cushion" appearance. However, once they grew above the herbivore browse line (~2 metres), they transitioned into a "conventional" tree form (Figure 1.3B). Similarly, Perkovich and Ward (2021) observed that oak (*Quercus spp.*) adapts to herbivory by reallocating biomass belowground. Additionally, Axe *et al.* (2017) reported increased carbon sequestration in hedgerow species when subjected to moderate hedge-trimming. Tree and scrub species also display a number of other strategies to act as protection against herbivory, such as promoting tannins (Iqbal & Poor, 2024), thorns (Facciolati *et al.*, 2024; Balaji & Jambagi., 2024; Skarpe & Hester, 2008; Hanley *et al.*, 2007), growing scar tissue over stripped bark (Shelp *et al.*, 2021) and deep incisions, and sprouting new growth from broken stems (Kant *et al.*, 2015), may also increase carbon storage levels within the plant (Guo *et al.*, 2023).

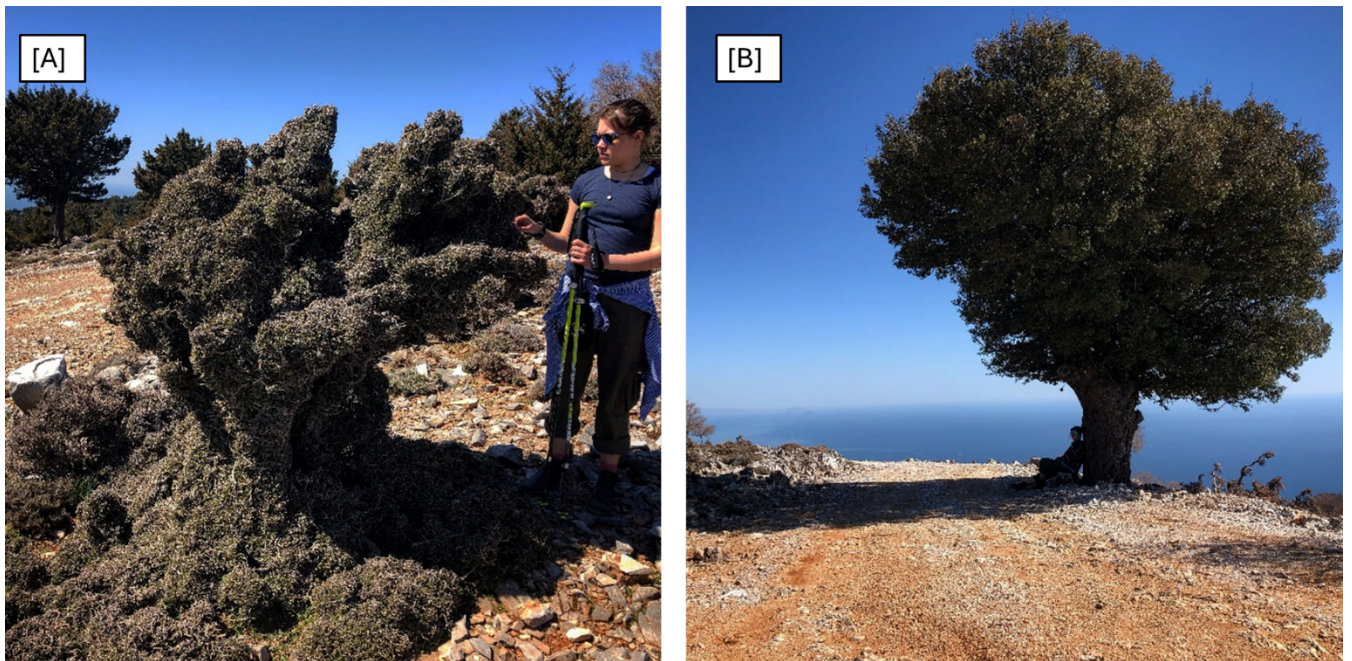


Figure 1.3: Herbivores impact oak morphology in Crete's wood-pasture landscapes. Image [A] (with the author) shows an oak (*Quercus* spp.) with a dense "pin cushion" form below the ~2 m herbivore browse line, while image [B] depicts a more conventional tree form above it (Rackham, 1998).

These findings raise the question of what the carbon content of rewilded ecosystems is, given the diverse plant strategies that occur in response to herbivory and other animal disturbances. For example, do current methodologies, which rely heavily on plantation-based allometry (Conti et al., 2013; Chen et al., 2024) under or overestimate the carbon storage of rewilded landscapes?

Traditional carbon offset models, such as those utilised in standards like the Verified Carbon Standard Association (VERRA) and the Gold Standard Foundation, are commonly used to estimate the amount of carbon storage within a block of trees on a landscape. These methodologies often rely on standardised assumptions about growth rates to calculate carbon sequestration potential. For example, VERRA's methodologies operate on a 5 to 30-year

growth timeline, while the Gold Standard employs a 20 to 100-year growth timeframe, incorporating detailed modelling to account for variability in carbon sequestration (Verra, 2024; Gold Standard, 2023).

Similarly, the Woodland Carbon Code (WCC), a widely adopted standard for measuring carbon offsets in woodlands, particularly in the UK, uses a 5- to 25-year growth model with linear growth assumptions (Woodland Carbon Code, 2019). These frameworks play a vital role in quantifying and verifying carbon credits; however, they differ in their approaches to modelling, timelines, and assumptions, reflecting the diverse ecological and economic contexts in which they are applied.

Importantly, none of these methods (VERRA, Gold or WCC) have been tested to determine whether the slower and more variable growth patterns of trees and scrub species on rewilded landscapes have a significant impact on the amount of carbon stored both above and below-ground. What might be assumed is that a model based on metrics predominantly derived from plantation forests (Figure 1.4B) will fail to account for the structural complexity and unique characteristics of rewilded wood pasture and scrubland landscapes (Figure 1.4A), and potentially underestimate their carbon sequestration potential. Further research is therefore needed to incorporate more nuanced growth rate calculations and consider the possible

implications of the extended maturation periods of rewilded landscapes. This would lead to more accurate carbon offset predictions and highlight the broader benefits of rewilded



Figure 1.4: Two different woodlands found at Knepp Wildland, West Sussex. [A] scrubland generated by 'rewilding'; [B] mixed woodland plantation.

In particular, the unpredictability of scrub regeneration and tree recruitment needs to be taken into consideration, along with the long-term stability of stored carbon (Tanentzap et al., 2023).

Finally, the impact of herbivores on recruitment rates of native trees and shrubs in trophic rewilding is largely unknown and adds another layer of complexity when assessing how this approach compares with plantation forestry as a model for establishing trees for carbon capture (Smit et al., 2015; Tanentzap and Coomes, 2012).

1.5 The Southern Block of Knepp Wildland as Study Site

The Knepp Estate, comprising 3,500 acres of post-agricultural farmland in the Sussex Weald, began rewilding in 2000 (Tree, 2018). Inspired by the work of Dutch ecologist Dr. Frans Vera, it became the first large-scale rewilding project in lowland England. Since its inception, the Knepp Estate has been closely monitored through scientific studies.

The 450-hectare Southern Block of Knepp Estate presents particularly useful context for this study. Beginning in 2001, the fields were withdrawn piecemeal from arable production over a period of five years, allowing thorny scrub to colonise the fields after their last harvest (Figure 1.5). With no thick grass cover such as permanent pasture to hold back natural colonisation, and only rabbits (*Oryctolagus cuniculus*) and roe deer (*Capreolus capreolus*) present as browsers, blackthorn (*Prunus spinosa*), hawthorn (*Crataegus monogyna*), dog rose (*Rosa canina*), bramble (*Rubus fruticosus*), oak (*Quercus robur*), wild service (*Sorbus torminalis*), birch (*Betula pendula*), crab apple (*Malus sylvestris*), and hazel (*Corylus avellana*) germinated profusely in the open stubble of the former arable fields (Tree, 2018). A process of vegetation succession characteristic of passive rewilding was underway. In 2009, further changes were implemented in the Southern Block of Knepp, supported by Higher Level Stewardship funding. This included ringfencing the area and introducing large free-roaming herbivores as part of an experimental approach to European-style trophic rewilding (Tree, 2018).

Before 2009, a period of 4–8 years without significant herbivory (other than rabbits (*Oryctolagus cuniculus*) and roe deer (*Capreolus capreolus*)) allowed the emergent woody shrubs and young saplings in the southern block to properly establish. By the time larger herbivores—deer (fallow *Dama dama* and red *Cervus elaphus*), cattle (longhorn *Bos taurus*),

ponies (Exmoor *Equus ferus caballus*), and pigs (Tamworth *Sus scrofa domestica*)—were introduced, this vegetation was sufficiently mature to employ defensive mechanisms to survive and ‘fight back’ against herbivory.

Already, research at Knepp Wildland has suggested that rewilding can store carbon. A recent Queen Mary University study using drone mounted LiDAR found that rewilding habitats at Knepp probably sequester around 3.3–3.4 tCO₂e/ha/year over in above-ground biomass, a rate comparable to new native woodland creation projects (Knepp Wildland Carbon Project, 2024). Another study measuring carbon in the soils in the Southern Block estimated that 3.3–4.8 tCO₂e/ha/year is sequestered in these soils, with a midpoint estimate of 4.05 tCO₂e/ha/year, also comparable to rates for woodland establishment (Knepp Wildland Carbon Project, 2024). However, these previous data on carbon sequestration in scrub and mixed habitats remain limited, as they are based on estimations without detailed on-the-ground field measurements. Additionally, they lack insights into changes in the root:shoot ratio caused by browsing pressure – an essential factor for accurately estimating below-ground carbon storage.



Figure 1.5: Arable reversion to scrubland through natural colonisation in the presence of grazing and browsing large herbivores. A field in the Southern Block of the Knepp Estate, Image A was taken in 2001, Image B was taken in 2023.

1.6 Thesis Aims and Research Objectives

The aim of this thesis is to investigate the carbon storage potential of scrubland resulting from rewilding, to provide a more comprehensive understanding of the multifaceted benefits that rewilding may provide. I address the central research question – “What is the carbon storage potential of scrubland created by rewilding?” using six interlinked research objectives:

- i. Evaluation of whether the current methodologies for estimating carbon storage in trees are applicable to scrubland species in a rewilding context.
- ii. Determination of the carbon storage potential of scrubland through destructive sampling and the development of above- and below-ground, taxa-specific allometric equations of a 25-year-old rewilded landscape.
- iii. Investigation into the impact of browsing on the carbon storage of scrubland taxa both above- and below-ground and develop a model to describe this impact.
- iv. Quantification of carbon content in above- and below-ground biomass across five target scrub taxa, assessing the 50% carbon-to-dry-weight assumption and examining the influence of herbivory on carbon content.
- v. Evaluation of the potential for remotely sensing carbon storage in scrubland ecosystems by combining UAV RGB imaging with a Structure-from-Motion workflow alongside multispectral imaging.

- vi. Development of a predictive tool to estimate total carbon storage in rewilded scrubland by integrating Structure-from-Motion data, multispectral imaging, scrub-specific carbon content values and taxa-specific above- and below-ground carbon models at a landscape scale.

My thesis describes the outcome of this research and is arranged into five further chapters as follows:

Chapter 2 evaluates the applicability of current allometric-based models for estimating carbon storage potential in scrubland ecosystems. Specifically, I compared the output of the i-Tree Eco model—a tool commonly used for carbon storage estimation—applied to scrub trees at the Knepp Estate, with field data obtained from destructively sampled scrub. The aim was to determine whether the i-Tree Eco model's assumed root:shoot ratio of 0.26 accurately represents belowground biomass in scrubland taxa.

Chapter 3 addresses the knowledge gap identified in Chapter 2 by developing a scrub-taxa-specific allometric model. A total of 270 individual shrub trees, including roots, were destructively sampled across five different scrub taxa. These samples were categorised based on exposure to browsing (exposed or protected) and grouped into three distinct size classes. The chapter also examines the root and shoot responses to aboveground herbivory and the effects of browsing on carbon storage and biomass allocation. Samples within natural thorny protection, out of reach of large herbivores, were compared to freestanding samples exposed to browsing. This comparison served as a proxy for assessing the impact of browsing on carbon storage and biomass allocation in scrub trees.

Chapter 4 details the analysis of a subset of 34 out of the 270 destructively sampled trees, using elemental analysis by dry combustion to compare the carbon percentage across different scrub species and their various tree components. These values were also evaluated against the commonly used assumption that "50% of dry biomass is carbon," originally developed for mature trees, to determine its applicability to scrub species.

Chapter 5 describes the development of a UAV-based remote sensing approach, utilising a Structure-from-Motion workflow to generate a 3D point cloud of the study site, combined with data from a multi-spectral 10-band camera for taxa identification. This method aimed to create an accessible and replicable way to correlate aboveground vegetation characteristics, such as canopy height and canopy area, with actual biomass measurements (from Chapter 3) and carbon content data (from Chapter 4) in taxa-specific scrubland ecosystems.

Chapter 6 concludes my thesis by discussing the implications of my findings and their potential integration into future rewilding and land management schemes. It also addresses the critical knowledge gap by providing quantitative data that can be incorporated into a natural capital framework.

1.7 Reference List

- Aguirre-Gutiérrez, J., Stevens, N. and Berenguer, E., 2023. Valuing the functionality of tropical ecosystems beyond carbon. *Trends in Ecology & Evolution*, 38(12), pp.1109-1111.
- Alexander, K., 1999. Britain's wood pastures. *British Wildlife*.
- Alexander, K.N., 2012. What do saproxylic (wood-decay) beetles really want? Conservation should be based on practical observation rather than unstable theory. In: Rotherham, I.D. (Ed.), *Trees beyond the wood*. Wildtrack Publishing, Sheffield, pp. 33-46.
- Andriuzzi, W.S. and Wall, D.H., 2018. Soil biological responses to, and feedbacks on, trophic rewilding. *Philosophical Transactions of the Royal Society B*, 373(20170448). <https://doi.org/10.1098/rstb.2017.0448>.
- Apollonio, M., Andersen, R. and Putman, R., 2010. *European ungulates and their management in the 21st century*. Cambridge University Press.
- Arias-Arévalo, P., Lazos-Chavero, E., Monroy-Sais, A.S., Nelson, S.H., Pawlowska-Mainville, A., Vatn, A., Cantú-Fernández, M., Murali, R., Muraca, B. and Pascual, U., 2023. The role of power in leveraging the diverse values of nature for transformative change. *Current Opinion in Environmental Sustainability*, 64, p.101352.
- Arts, K., Fischer, A. and Van Der Wal, R., 2016. Boundaries of the wolf and the wild: A conceptual examination of the relationship between rewilding and animal reintroduction. *Restoration Ecology*, 24(1), pp. 27-34. <https://doi.org/10.1111/rec.12356>.
- Assessment, M.E., 2005. *Ecosystems and human well-being: wetlands and water*. World Resources Institute.
- Axe, M.S., Grange, I.D. and Conway, J.S., 2017. Carbon storage in hedge biomass—A case study of actively managed hedges in England. *Agriculture, Ecosystems & Environment*, 250, pp. 81-88. <https://doi.org/10.1016/j.agee.2017.08.018>.
- Bakker, E.S., Gill, J.L., Johnson, C.N., Vera, F.W.M., Sandom, C.J., Asner, G.P. and Svenning, J.-C., 2016. Combining paleo-data and modern exclosure experiments to assess the impact of megafauna extinctions on woody vegetation. *Proceedings of the National Academy of Sciences*, 113(4), pp. 847-855. <https://doi.org/10.1073/pnas.1502545112>.
- Balaji, B.N. and Jambagi, S.R., 2024. Structural Defences in Plants against Herbivores-A Review. *Indian Journal of Entomology*, pp.1-9.
- Barbier, E.B., 2011. Pricing nature. *Annual Review of Resource Economics*, 3, pp. 337-353. <https://doi.org/10.1146/annurev-resource-083110-115954>.
- Barto, E.K., Hilker, M., Müller, F., Mohny, B.K., Weidenhamer, J.D. and Rillig, M.C., 2011. The fungal fast lane: common mycorrhizal networks extend bioactive zones of

- allelochemicals in soils. *PLoS One*, 6(11), e27195.
<https://doi.org/10.1371/journal.pone.0027195>.
- Bastin, J.-F., Finegold, Y., Garcia, C., Mollicone, D., Rezende, M., Routh, D., Zohner, C.M. and Crowther, T.W., 2019. The global tree restoration potential. *Science*, 365(6448), pp. 76-79.
<https://doi.org/10.1126/science.aax0848>.
- Bateman, I.J. and Mace, G.M., 2020. The natural capital framework for sustainably efficient and equitable decision making. *Nature Sustainability*, 3, pp. 776-783.
<https://doi.org/10.1038/s41893-020-0537-2>.
- Begum, N., Qin, C., Ahanger, M.A., Raza, S., Khan, M.I., Ashraf, M., Ahmed, N. and Zhang, L., 2019. Role of arbuscular mycorrhizal fungi in plant growth regulation: implications in abiotic stress tolerance. *Frontiers in Plant Science*, 10, p. 1068.
<https://doi.org/10.3389/fpls.2019.01068>.
- Bennett, E.M., Peterson, G.D. and Gordon, L.J., 2009. Understanding relationships among multiple ecosystem services. *Environmental Letters*, 12(12), pp. 1394-1404.
<https://doi.org/10.1029/2009GL038161>.
- Besar, N.A., Suardi, H., Phua, M.H., James, D., Mokhtar, M.B. and Ahmed, M.F., 2020. Carbon stock and sequestration potential of an agroforestry system in Sabah, Malaysia. *Forests*, 11(2), p. 210. <https://doi.org/10.3390/f11020210>.
- Bishop, J., Brink, P.T., Gundimeda, H., Kumar, P., Nesshöver, C., Schröter-Schlaack, C., Simmons, B., Sukhdev, P. and Wittmer, H., 2010. The economics of ecosystems and biodiversity: mainstreaming the economics of nature: a synthesis of the approach, conclusions and recommendations of TEEB.
- Brompton, S., 2018. Does rewilding benefit dung beetle biodiversity? University of Bristol.
- Broughton, R.K., Bullock, J.M., George, C., Hill, R.A., Hinsley, S.A., Maziarz, M., Melin, M., Mountford, J.O., Sparks, T.H. and Pywell, R.F., 2021. Long-term woodland restoration on lowland farmland through passive rewilding. *PLoS One*, 16(5), e0252466.
<https://doi.org/10.1371/journal.pone.0252466>.
- Bulkens, M., Muzaini, H. and Minca, C., 2016. Dutch new nature: (re) landscaping the Millingerwaard. *Journal of Environmental Planning and Management*, 59(5), pp. 808-825.
<https://doi.org/10.1080/09640568.2015.1035771>.
- Burrell, N.C., Jeffers, E.S., Macias-Fauria, M. and Willis, K.J., 2024. The inadequacy of current carbon storage assessment methods for rewilding: A Knepp Estate case study. *Ecological Solutions and Evidence*, 5(1), p. e12301. <https://doi.org/10.1002/2688-8319.12301>.
- Busch, J., Bukoski, J.J., Cook-Patton, S.C., Griscom, B., Kaczan, D., Potts, M.D., Yi, Y. and Vincent, J.R., 2024. Cost-effectiveness of natural forest regeneration and plantations for climate mitigation. *Nature Climate Change*, pp.1-7.
- Candaele, R., Ligot, G., Licoppe, A., Lievens, J., Fichet, V., Jonard, M., André, F. and Lejeune, P., 2023. Interspecific Growth Reductions Caused by Wild Ungulates on Tree Seedlings and Their Implications for Temperate Quercus-Fagus Forests. *Forests*, 14(7), p.1330.

- Cardinale, B.J., Duffy, J.E., Gonzalez, A., Hooper, D.U., Perrings, C., Venail, P., Narwani, A., Mace, G.M., Tilman, D. and Wardle, D.A., 2012. Biodiversity loss and its impact on humanity. *Nature*, 486(7401), pp. 59-67. <https://doi.org/10.1038/nature11148>.
- Cavers, S. and Cottrell, J.E., 2015. The basis of resilience in forest tree species and its use in adaptive forest management in Britain. *Forestry: An International Journal of Forest Research*, 88(1), pp.13-26.
- Ceașu, S., Hofmann, M., Navarro, L.M., Carver, S., Verburg, P.H. and Pereira, H.M., 2015. Mapping opportunities and challenges for rewilding in Europe. *Conservation Biology*, 29, pp.1017-1027.
- Cerqueira, Y., Navarro, L.M., Maes, J., Marta-Pedroso, C., Pradinho Honrado, J. and Pereira, H.M., 2015. Ecosystem services: the opportunities of rewilding in Europe. *Rewilding European Landscapes*, pp.47-64.
- Chen, J., Fang, X., Wu, A., Xiang, W., Lei, P. and Ouyang, S., 2024. Allometric equations for estimating biomass of natural shrubs and young trees of subtropical forests. *New Forests*, 55(1), pp.15-46.
- Clements, F.E., 1916. *Plant succession: an analysis of the development of vegetation* (No. 242). Carnegie institution of Washington.
- Conti, G., Enrico, L., Casanoves, F. and Díaz, S., 2013. Shrub biomass estimation in the semiarid Chaco forest: a contribution to the quantification of an underrated carbon stock. *Annals of Forest Science*, 70, pp.515-524.
- Cook-Patton, S.C., Leavitt, S.M., Gibbs, D., Harris, N.L., Lister, K., Anderson-Teixeira, K.J., Briggs, R.D., Chazdon, R.L., Crowther, T.W. and Ellis, P.W., 2020. Mapping carbon accumulation potential from global natural forest regrowth. *Nature*, 585, pp.545-550.
- Cord, A.F., Brauman, K.A., Chaplin-Kramer, R., Huth, A., Ziv, G. and Seppelt, R., 2017. Priorities to advance monitoring of ecosystem services using earth observation. *Trends in Ecology & Evolution*, 32, pp.416-428.
- Costanza, R., 2020. Valuing natural capital and ecosystem services toward the goals of efficiency, fairness, and sustainability. *Ecosystem Services*, 43, p.101096.
- Costanza, R., D'Arge, R., De Groot, R., Farber, S., Grasso, M., Hannon, B., Limburg, K., Naeem, S., O'Neill, R.V. and Paruelo, J., 1997. The value of the world's ecosystem services and natural capital. *Nature*, 387, pp.253-260.
- Cromsigt, J.P., Te Beest, M., Kerley, G.I., Landman, M., Le Roux, E. and Smith, F.A., 2018. Trophic rewilding as a climate change mitigation strategy? *Philosophical Transactions of the Royal Society B: Biological Sciences*, 373, p.20170440.
- Daily, G.C., Polasky, S., Goldstein, J., Kareiva, P.M., Mooney, H.A., Pejchar, L., Ricketts, T.H., Salzman, J. and Shallenberger, R.J., 2009. Ecosystem services in decision making: time to deliver. *Frontiers in Ecology and the Environment*, 7, pp.21-28.
- Daily, G.C., Söderqvist, T., Aniyar, S., Arrow, K., Dasgupta, P., Ehrlich, P.R., Folke, C., Jansson, A., Jansson, B.O. and Kautsky, N., 2000. The value of nature and the nature of value. *Science*, 289, pp.395-396.

- Di Sacco, A., Hardwick, K.A., Blakesley, D., Brancalion, P.H., Breman, E., Cecilio Rebola, L., Chomba, S., Dixon, K., Elliott, S., Ruyonga, G. and Shaw, K., 2021. Ten golden rules for reforestation to optimize carbon sequestration, biodiversity recovery and livelihood benefits. *Global Change Biology*, 27(7), pp.1328-1348.
- Díaz, S., Settele, J., Brondízio, E.S., Ngo, H.T., Agard, J., Arneth, A., Balvanera, P., Brauman, K.A., Butchart, S.H. and Chan, K.M., 2019. Pervasive human-driven decline of life on Earth points to the need for transformative change. *Science*, 366, p.eaax3100.
- Dietrich, P., Cesarz, S., Liu, T., Roscher, C. and Eisenhauer, N., 2021. Effects of plant species diversity on nematode community composition and diversity in a long-term biodiversity experiment. *Oecologia*, 197, pp.297-311.
- Dobson, A. and Crawley, M., 1994. Pathogens and the structure of plant communities. *Trends in ecology & evolution*, 9(10), pp.393-398.
- Domke, G., Oswald, S., Walters, B., Morin, R. and Estes, J., 2020. Tree planting has the potential to increase carbon sequestration capacity of forests in the United States. *Proceedings of the National Academy of Sciences*, 117.
- Dunklin, P., Parry, J. and Gegg, T., 2024. Should nature restoration projects be able to stack multiple revenue streams from ecosystem services? Full impact accounting as a clear way forward. *Nature-Based Solutions*, p.100141.
- Dutton, C.L., Subalusky, A.L., Anisfeld, S.C., Njoroge, L., Rosi, E.J. and Post, D.M., 2018. The influence of a semi-arid sub-catchment on suspended sediments in the Mara River, Kenya. *PLoS One*, 13, p.e0192828.
- Dvorský, M., Mudrák, O., Doležal, J. and Jirků, M., 2021. Rewilding with large herbivores helped increase plant species richness in dry grasslands.
- European Parliament, 2020. *The challenge of land abandonment after 2020 and options for mitigation measures*. [online] Available at: [https://www.europarl.europa.eu/RegData/etudes/STUD/2020/652238/IPOL_STU\(2020\)652238_EN.pdf](https://www.europarl.europa.eu/RegData/etudes/STUD/2020/652238/IPOL_STU(2020)652238_EN.pdf) [Accessed 18 Nov. 2024].
- Facciolati, V., Zarek, M., Blonska, E., Lasota, J., Orman, O. and Ciach, M., 2024. To be browsed or not to be browsed: differences in nutritional characteristics of blackthorn *Prunus spinosa* subject to the long-term pressure of herbivores. *bioRxiv*, pp.2024-04.
- Fawzy, S., Osman, A.I., Doran, J. and Rooney, D.W., 2020. Strategies for mitigation of climate change: a review. *Environmental Chemistry Letters*, 18, pp.2069-2094.
- Feng, Z., Jin, X., Chen, T. and Wu, J., 2021. Understanding trade-offs and synergies of ecosystem services to support the decision-making in the Beijing–Tianjin–Hebei region. *Land Use Policy*, 106, p.105446.
- Fleischman, F., Basant, S., Chhatre, A., Coleman, E.A., Fischer, H.W., Gupta, D., Güneralp, B., Kashwan, P., Khatri, D. and Muscarella, R., 2020. Pitfalls of tree planting show why we need people-centered natural climate solutions. *BioScience*, 70, pp.947-950.
- Fleischman, F.D., 2014. Why do foresters plant trees? Testing theories of bureaucratic decision-making in Central India. *World Development*, 62, pp.62-74.

Foley, J.A., DeFries, R., Asner, G.P., Barford, C., Bonan, G., Carpenter, S.R., Chapin, F.S., Coe, M.T., Daily, G.C. and Gibbs, H.K., 2005. Global consequences of land use. *Science*, 309, pp.570-574.

Forest Research, 2022. Tree stability and wind risk to forests. Available at: <https://www.forestresearch.gov.uk/> (Accessed: 24 September 2024).

Forster, E.J., Healey, J.R., Dymond, C. and Styles, D., 2021. Commercial afforestation can deliver effective climate change mitigation under multiple decarbonisation pathways. *Nature Communications*, 12, p.3831.

Frangmyr, T., Heilbron, J.L. and Rider, R.E. eds., 2023. *The quantifying spirit in the eighteenth century*. Univ of California Press.

Gammon, A.R., 2018. The many meanings of rewilding: An introduction and the case for a broad conceptualisation. *Environmental Values*, 27(4), pp.331-350.

Garrido, P., Edenius, L., Mikusiński, G., Skarin, A., Jansson, A. and Thulin, C.-G., 2021. Experimental rewilding may restore abandoned wood-pastures if policy allows. *Ambio*, 50, pp.101-112.

Garrido, P., Mårell, A., Öckinger, E., Skarin, A., Jansson, A. and Thulin, C.-G., 2019. Experimental rewilding enhances grassland functional composition and pollinator habitat use. *Journal of Applied Ecology*, 56, pp.946-955.

Gerard, J., 2015. *The herbal or general history of plants: the complete 1633 edition as revised and enlarged by Thomas Johnson*. Courier Dover Publications.

Gill, R., 2006. Influence of large herbivores on tree recruitment and forest dynamics. *Forest Ecology and Management*, 234, pp.143-153.

Girardin, C.A., Jenkins, S., Seddon, N., Allen, M., Lewis, S.L., Wheeler, C.E., Griscom, B.W. and Malhi, Y., 2021. Nature-based solutions can help cool the planet—if we act now. *Nature*, 593, pp.191-194.

Gold Standard, 2023. Agroforestry and reforestation with the Gold Standard - Decision Analysis of a voluntary carbon offset label. Available at: <https://link.springer.com/article/10.1007/s11027-020-09935-x> (Accessed: 24 September 2024).

GOV.UK, 2023. *Combining environmental payments, biodiversity net gain (BNG) and nutrient mitigation*. [online] Available at: <https://www.gov.uk/guidance/combining-environmental-payments-biodiversity-net-gain-bng-and-nutrient-mitigation> [Accessed 14 October 2024].

Guariguata, M.R., Chazdon, R.L., Brancalion, P.H.S. and David, L., 2019. Forests: When natural regeneration is unrealistic. *Nature*, 570, p.164.

Guerry, A.D., Polasky, S., Lubchenco, J., Chaplin-Kramer, R., Daily, G.C., Griffin, R., Ruckelshaus, M., Bateman, I.J., Duraiappah, A. and Elmqvist, T., 2015. Natural capital and ecosystem services informing decisions: From promise to practice. *Proceedings of the National Academy of Sciences*, 112, pp.7348-7355.

Guo, Z., Gong, J., Luo, S., Zuo, Y. and Shen, Y., 2023. Role of gamma-aminobutyric acid in plant defense response. *Metabolites*, 13(6), p.741.

- Hall, C.M., 2019. Tourism and rewilding: an introduction–definition, issues and review. *Journal of Ecotourism*, 18, pp.1-18.
- Hanberry, B.B. and Faison, E.K., 2023. Re-framing deer herbivory as a natural disturbance regime with ecological and socioeconomic outcomes in the eastern United States. *Science of the Total Environment*, 868, p.161669.
- Hanley, M.E., Lamont, B.B., Fairbanks, M.M. and Rafferty, C.M., 2007. Plant structural traits and their role in anti-herbivore defence. *Perspectives in Plant Ecology, Evolution and Systematics*, 8(4), pp.157-178.
- Harvey, G.L. and Henshaw, A.J., 2023. Rewilding and the water cycle. *WIREs Water*, 10, e1686.
- Helm, D., Austen, M., Bateman, I.J., Collins, C., Leinster, P., Mayer, C. and Willis, K., 2020. Natural Capital Committee end of term report.
- Hill, M.O., Mountford, J.O., Roy, D.B. and Bunce, R.G.H., 1999. *Ellenberg's indicator values for British plants. ECOFACT Volume 2 Technical Annex* (Vol. 2). Institute of Terrestrial Ecology.
- Hodder, K.H. and Bullock, J.M., 2009. Really Wild? Naturalistic grazing in modern landscapes. *British Wildlife*, 20(5), pp.37-43.
- Holl, K.D. and Brancalion, P.H., 2020. Tree planting is not a simple solution. *Science*, 368, pp.580-581.
- Holl, K.D., 2017. Restoring tropical forests from the bottom up. *Science*, 355, pp.455-456.
- Howison, R.A., Berg, M.P., Smit, C., Van Dijk, K. and Olff, H., 2016. The importance of coprophagous macrodetritivores for the maintenance of vegetation heterogeneity in an African savannah. *Ecosystems*, 19, pp.674-684.
- Ickowitz, A., McMullin, S., Rosenstock, T., Dawson, I., Rowland, D., Powell, B., Mausch, K., Djoudi, H., Sunderland, T., Nurhasan, M., Nowak, A., Gitz, V., Meybeck, A., Jamnadass, R., Guariguata, M.R., Termote, C. and Nasi, R., 2022. Transforming food systems with trees and forests. *The Lancet Planetary Health*, 6, e632-e639.
- IPBES, 2019. Global assessment report on biodiversity and ecosystem services. Available at: <https://ipbes.net/global-assessment> (Accessed: 24 September 2024).
- IPCC, 2013. Climate Change 2013: The Physical Science Basis. Contribution of Working Group I to the Fifth Assessment Report of the Intergovernmental Panel on Climate Change. Cambridge: Cambridge University Press. Available at: <https://www.ipcc.ch/report/ar5/wg1/> (Accessed: 24 September 2024).
- IPCC, 2014. Climate Change 2014: Synthesis Report. Contribution of Working Groups I, II and III to the Fifth Assessment Report of the Intergovernmental Panel on Climate Change. Geneva: IPCC. Available at: <https://www.ipcc.ch/report/ar5/syr/> (Accessed: 24 September 2024).
- Iqbal, N. and Poór, P., 2024. Plant Protection by Tannins Depends on Defence-Related Phytohormones. *Journal of Plant Growth Regulation*, pp.1-18.

Isaac, N.J., Brotherton, P.N., Bullock, J.M., Gregory, R.D., Boehning-Gaese, K., Connor, B., Crick, H.Q., Freckleton, R.P., Gill, J.A. and Hails, R.S., 2018. Defining and delivering resilient ecological networks: Nature conservation in England. *Journal of Applied Ecology*, 55, pp.2537-2543.

IUCN, 2022. Nature-based Solutions in the Global Biodiversity Framework. Available at: <https://www.iucn.org/> (Accessed: 24 September 2024).

Jansen, R., 2023. Today's public costs - tomorrow's private costs? Master's thesis. Leuphana Universität Lüneburg. Available at: <https://pubdata.leuphana.de/handle/20.500.14123/931> [Accessed 24 September 2024].

Janzen, D.H., 1984. Dispersal of small seeds by big herbivores: foliage is the fruit. *American Naturalist*, 123, pp.338-353.

Johann, E., 2006. Historical development of nature-based forestry in Central Europe. *Nature-based forestry in Central Europe. Alternatives to industrial forestry and strict preservation*, pp.1-18.

Johannessen, S.C., 2022. How can blue carbon burial in seagrass meadows increase long-term, net sequestration of carbon? A critical review. *Environmental Research Letters*, 17(9), p.093004.

Johnson, J.A., Baldos, U.L., Corong, E., Hertel, T., Polasky, S., Cervigni, R., Roxburgh, T., Ruta, G., Salemi, C. and Thakrar, S., 2023. Investing in nature can improve equity and economic returns. *Proceedings of the National Academy of Sciences*, 120, p.e2220401120.

Kant, M.R., Jonckheere, W., Knecht, B., Lemos, F., Liu, J., Schimmel, B.C.J., Villarroel, C.A., Ataide, L.M.S., Dermauw, W., Glas, J.J. and Egas, M., 2015. Mechanisms and ecological consequences of plant defence induction and suppression in herbivore communities. *Annals of botany*, 115(7), pp.1015-1051.

Kantola, I.B., Masters, M.D., Beerling, D.J., Long, S.P. and DeLucia, E.H., 2017. Potential of global croplands and bioenergy crops for climate change mitigation through deployment for enhanced weathering. *Biology letters*, 13(4), p.20160714.

Kelly-Quinn, M., Christie, M., Bodoque, J.M. and Schoenrock, K., 2020. Ecosystem services approach and natures contributions to people (NCP) help achieve SDG6. In *Clean Water and Sanitation* (pp. 1-13). Cham: Springer International Publishing.

Kim, M., Lee, S., Lee, S., Yi, K., Kim, H.S., Chung, S., Chung, J., Kim, H.S. and Yoon, T.K., 2022. Seed dispersal models for natural regeneration: A review and prospects. *Forests*, 13(5), p.659.

Kirby, K.J., Goldberg, E.A. and Orchard, N., 2017. Long-term changes in the flora of oak forests and of oak: spruce mixtures following removal of conifers. *Forestry: An International Journal of Forest Research*, 90(1), pp.136-147.

Knepp Wildland Carbon Project (2024) *Knepp Wildland Carbon Project Report*. Queen Mary University of London. Available at: <https://knepp.co.uk/rewilding/ecosystem-services/carbon-sequestration/> (Accessed: 18 November 2024).

Kopnina, H., Leadbeater, S. and Cryer, P., 2019. The golden rules of rewilding: Examining the case of Oostvaardersplassen. *Ecology*, 40(6), pp.1-16.

- Kristensen, J.A., Svenning, J.-C., Georgiou, K. and Malhi, Y., 2022. Can large herbivores enhance ecosystem carbon persistence? *Trends in Ecology & Evolution*, 37, pp.117-128.
- Kumar, P., Thonning, J., Santosh, A. and Barnes, N., 2023. Rewilding Medical Education. *BJPsych Open*, 9, p.S28.
- Kurten, B., 2017. *Pleistocene mammals of Europe*. Routledge.
- Lal, R., Monger, C., Nave, L. and Smith, P., 2021. The role of soil in regulation of climate. *Philosophical Transactions of the Royal Society B*, 376(1834), p.20210084.
- Lamy, T., Liss, K.N., Gonzalez, A. and Bennett, E.M., 2016. Landscape structure affects the provision of multiple ecosystem services. *Environmental Research Letters*, 11(12), p.124017.
- Laurel, D. and Wohl, E., 2019. The persistence of beaver-induced geomorphic heterogeneity and organic carbon stock in river corridors. *Geomorphology*, 44, pp.342-353.
- Lawton, J., 2011. Making space for nature. *Envtl. L. Rev.*, 13, p.1.
- Ledger, S.E., Rutherford, C.A., Benham, C., Burfield, I.J., Deinet, S., Eaton, M., Freeman, R., Gray, C., Herrando, S. and Puleston, H., 2022. Wildlife Comeback in Europe: Opportunities and challenges for species recovery. *Rewilding Europe Report*.
- Leonti, M., 2012. The co-evolutionary perspective of the food-medicine continuum and wild gathered and cultivated vegetables. *Genetic Resources and Crop Evolution*, 59(7), pp.1295-1302.
- Levy, S., 2011. *Once and Future Giants: What Ice Age Extinctions Tell Us about the Fate of Earth's Largest Animals*. Oxford University Press.
- Lewis, S.L., Wheeler, C.E., Mitchard, E.T. and Koch, A., 2019. Restoring natural forests is the best way to remove atmospheric carbon. *Nature*, 568, pp.25-28.
- Liu, J., Dietz, T., Carpenter, S.R., Alberti, M., Folke, C., Moran, E., Pell, A.N., Deadman, P., Kratz, T. and Lubchenco, J., 2007. Complexity of coupled human and natural systems. *Science*, 317, pp.1513-1516.
- Lorimer, J. and Driessen, C., 2014. Wild experiments at the Oostvaardersplassen: rethinking environmentalism in the Anthropocene. *Transactions of the Institute of British Geographers*, 39, pp.169-181.
- Luyssaert, S., Schulze, E.D., Börner, A., Knohl, A., Hessenmöller, D., Law, B.E., Ciais, P. and Grace, J., 2008. Old-growth forests as global carbon sinks. *Nature*, 455(7210), pp.213-215.
- Mace, G.M., Norris, K. and Fitter, A.H., 2012. Biodiversity and ecosystem services: a multilayered relationship. *Trends in Ecology & Evolution*, 27, pp.19-26.
- Macreadie, P.I., Costa, M.D., Atwood, T.B., Friess, D.A., Kelleway, J.J., Kennedy, H., Lovelock, C.E., Serrano, O. and Duarte, C.M., 2021. Blue carbon as a natural climate solution. *Nature Reviews Earth & Environment*, 2(12), pp.826-839.
- Mada, G., Anjulo, A. and Gelaw, A., 2022. Estimation of biomass and carbon sequestration capacity of the Surra mountain plantation forest in Gamo Highlands, Southern Ethiopia. *Ecology and Evolution*, 11, p.e399.

- Malhi, Y., Lander, T., Le Roux, E., Stevens, N., Macias-Fauria, M., Wedding, L., Girardin, C., Kristensen, J.Å., Sandom, C.J. and Evans, T.D., 2022. The role of large wild animals in climate change mitigation and adaptation. *Current Biology*, 32, pp.R181-R196.
- Mandle, L., Shields-Estrada, A., Chaplin-Kramer, R., Mitchell, M.G.E., Bremer, L.L., Gourevitch, J.D., Hawthorne, P., Johnson, J.A., Robinson, B.E., Smith, J.R., Sonter, L.J., Verutes, G.M., Vogl, A.L., Daily, G.C. and Ricketts, T.H., 2021. Increasing decision relevance of ecosystem service science. *Nature Sustainability*, 4, pp.161-169.
- Marchin, R.M. and Yuan, Z., 2023. Natural tree seedling establishment and forest regeneration under climate change. *Frontiers in Forests and Global Change*, 6, p.1256577.
- Martin, P.S., 2005. *Twilight of the mammoths: Ice Age extinctions and the rewilding of America* (Vol. 8). Univ of California Press.
- Martín-Forés, I., Magro, S., Bravo-Oviedo, A., Alfaro-Sánchez, R., Espelta, J.M., Frei, T., Valdés-Correcher, E., Rodríguez Fernández-Blanco, C., Winkel, G., Gerzabek, G. and González-Martínez, S.C., 2020. Spontaneous forest regrowth in South-West Europe: Consequences for nature's contributions to people. *People and Nature*, 2(4), pp.980-994.
- McLellan, R., Iyengar, L., Jeffries, B. and Oerlemans, N., 2014. *Living planet report 2014: species and spaces, people and places*. WWF International.
- MDPI, 2022. Assessment of Effective Wind Loads on Individual Plantation-Grown Forest Trees. Available at: MDPI (Accessed: 24 September 2024).
- Mercer, L. and Gregg, R., 2023. Exploring the carbon sequestration potential of rewilding in the UK: Policy and data needs to support net zero.
- Merryweather, J., 2014. *Gorse: Woodland in Waiting. Nature in Focus*.
- Millennium Ecosystem Assessment, 2005. *Ecosystems and human well-being: synthesis*. Washington, DC: Island Press. Available at: <https://www.millenniumassessment.org/en/Synthesis.html> (Accessed: 24 September 2024).
- Miller, M.F. and Coe, M., 1993. Is It Advantageous for Acacia Seeds to Be Eaten by Ungulates? *Oikos*, 66, pp.364-368.
- Naundrup, P.J. and Svenning, J.-C., 2015. A geographic assessment of the global scope for rewilding with wild-living horses (*Equus ferus*). *PLoS One*, 10, p.e0132359.
- Nichol, J.E. and Abbas, S., 2021. Evaluating plantation forest vs. Natural forest regeneration for biodiversity enhancement in Hong Kong. *Forests*, 12(5), p.593.
- Nogués-Bravo, D., Simberloff, D., Rahbek, C. and Sanders, N.J., 2016. Rewilding is the new Pandora's box in conservation. *Current Biology*, 26, pp.R87-R91.
- Pacheco, P., Beatty, C. and Patel, J., 2024. An economic view on the costs and benefits of forest restoration. *Restoring Forests and Trees for Sustainable Development: Policies, Practices, Impacts, and Ways Forward*, p.238.

- Perkovich, C. and Ward, D., 2021. Aboveground herbivory causes belowground changes in twelve oak *Quercus* species: a phylogenetic analysis of root biomass and non-structural carbohydrate storage. *Oikos*, 130, pp.1797-1812.
- Peterken, G.F., 1996. *Natural woodland: ecology and conservation in northern temperate regions*. Cambridge: Cambridge University Press.
- Pettorelli, N., Barlow, J., Stephens, P.A., Durant, S.M., Connor, B., Schulte to Bühne, H., Sandom, C.J., Wentworth, J. and Du Toit, J.T., 2018. Making rewilding fit for policy. *Journal of Applied Ecology*, 55, pp.1114-1125.
- Pringle, R.M., Abraham, J.O., Anderson, T.M., Coverdale, T.C., Davies, A.B., Dutton, C.L., Gaylard, A., Goheen, J.R., Holdo, R.M., Hutchinson, M.C. and Kimuyu, D.M., 2023. Impacts of large herbivores on terrestrial ecosystems. *Current Biology*, 33(11), pp.R584-R610.
- Putman, R., Apollonio, M. and Andersen, R. eds., 2011. *Ungulate management in Europe: problems and practices*. Cambridge University Press.
- Rackham, O., 1986. *The history of the countryside: the full fascinating story of Britain's landscape*. London: J.M. Dent & Sons Ltd.
- Rackham, O., 1998. Savanna in Europe. *Studies in European Savannas*, pp.1-24.
- Rana, P. and Varshney, L.R., 2023. Exploring limits to tree planting as a natural climate solution. *Journal of Cleaner Production*, 384, p.135566.
- Randle, T. and Jenkins, T., 2011. The construction of lookup tables for estimating changes in carbon stocks in forestry projects. A background document for users of the Forestry Commissions' Woodland Carbon Code. *Forestry Commission*.
- Reid, C.E.A., 2021. State of the UK's Woods and Trees. In: *Woodland Trust, Inquiry into the Adaptation of Agriculture and Forestry to Climate Change - the EU Policy Response*. House of Lords European Union Committee.
- Renforth, P. and Henderson, G., 2017. Assessing ocean alkalinity for carbon sequestration. *Reviews of Geophysics*, 55(3), pp.636-674.
- Roe, S., Streck, C., Beach, R., Busch, J., Chapman, M., Daioglou, V., Deppermann, A., Doelman, J., Emmet-Booth, J., Engelmann, J. and Fricko, O., 2021. Land-based measures to mitigate climate change: Potential and feasibility by country. *Global Change Biology*, 27(23), pp.6025-6058.
- Rotherham, I.D., 2013. *Trees, forested landscapes and grazing animals*. Earthscan from Routledge.
- Rutten, G., Hönig, L., Schwaß, R., Braun, U., Saadani, M., Schuldt, A., Michalski, S.G. and Bruelheide, H., 2021. More diverse tree communities promote foliar fungal pathogen diversity, but decrease infestation rates per tree species, in a subtropical biodiversity experiment. *Journal of Ecology*, 109, pp.2068-2080.
- Sajeva, G., 2023. Assessing the values of nature to promote a sustainable future. *Ecosystem Services*.

- Sandom, C.J., Middleton, O., Lundgren, E., Rowan, J., Schowanek, S.D., Svenning, J.C. and Faurby, S., 2020. Trophic rewilding presents regionally specific opportunities for mitigating climate change. *Philosophical Transactions of the Royal Society B*, 375(1794), p.20190125.
- Schaffer-Morrison, S.A. and Zak, D.R., 2023. Mycorrhizal fungal and tree root functional traits: Strategies for integration and future directions. *Ecosphere*, 14(2), p.e4437.
- Schmitz, O.J., Sylvén, M., Atwood, T.B., Bakker, E.S., Berzaghi, F., Brodie, J.F., Cromsigt, J.P., Davies, A.B., Leroux, S.J., Schepers, F.J. and Smith, F.A., 2023. Trophic rewilding can expand natural climate solutions. *Nature Climate Change*, 13(4), pp.324-333.
- Schulze, E.D., 2018. Effects of forest management on biodiversity in temperate deciduous forests: An overview based on Central European beech forests. *Forest Ecology and Management*, 43, pp.213-226.
- Seddon, P.J., Griffiths, C.J., Soorae, P.S. and Armstrong, D.P., 2014. Reversing defaunation: restoring species in a changing world. *Science*, 345, pp.406-412.
- Shelp, B.J., Aghdam, M.S. and Flaherty, E.J., 2021. γ -Aminobutyrate (GABA) regulated plant defense: Mechanisms and opportunities. *Plants*, 10(9), p.1939.
- Shurin, J.B., Aranguren-Riaño, N., Duque Negro, D., Echeverri Lopez, D., Jones, N.T., Laverde-R, O., Neu, A. and Pedroza Ramos, A., 2020. Ecosystem effects of the world's largest invasive animal. *Ecology*, 101, p.e03005.
- Simard, S., 2021. *Finding the mother tree: Uncovering the wisdom and intelligence of the forest*. Penguin UK.
- Skarpe, C. and Hester, A.J., 2008. Plant traits, browsing and gazing herbivores, and vegetation dynamics. *Ecological Studies*, 195, p.217.
- Skidmore, C., 2019. UK Becomes First Major Economy to Pass Net Zero Emissions Law. *UK Government News*.
- Sloan, T., Payne, R.J., Bain, C., Chapman, S., Cowie, N., Gilbert, P., Lindsay, R., Mauquoy, D., Newton, A. and Andersen, R., 2018. Peatland afforestation in the UK and consequences for carbon storage. *Global Change Biology*, 24, pp.479-490.
- Smit, C., Ruifrok, J.L., van Klink, R. and Olf, H., 2015. Rewilding with large herbivores: The importance of grazing refuges for sapling establishment and wood-pasture formation. *Biological Conservation*, 182, pp.134-142.
- Smyth, M.-A., 2023. Plantation forestry: Carbon and climate impacts. *Land Use Policy*, 130, p.106677.
- Soulé, M. and Noss, R.J., 1998. Rewilding and biodiversity: complementary goals for continental conservation. *Wild Earth*, 8, pp.18-28.
- Standish, A. (1611) *The Commons Complaint*. London: William Stansby
- Stewart, K.M., Fulbright, T.E. and Drawe, D.L., 2000. White-tailed deer use of clearings relative to forage availability. *Journal of Wildlife Management*, 64(3), pp.733-741.

- Stuart, A.J., 2015. Late Quaternary megafaunal extinctions on the continents: a short review. *Geological Journal*, 50, pp.338-363.
- Svenning, J.-C., 2002. A review of natural vegetation openness in north-western Europe. *Biological Conservation*, 104, pp.133-148.
- Svenning, J.-C., 2020. Rewilding should be central to global restoration efforts. *One Earth*, 3, pp.657-660.
- Svenning, J.C., Buitenwerf, R. and Le Roux, E., 2024. Trophic rewilding as a restoration approach under emerging novel biosphere conditions. *Current Biology*, 34(9), pp.R435-R451.
- Svenning, J.-C., Munk, M. and Schweiger, A., 2019. Trophic rewilding: ecological restoration of top-down trophic interactions to promote self-regulating biodiverse ecosystems. In: *Rewilding*, pp.73-98.
- Svenning, J.C., Pedersen, P.B., Donlan, C.J., Ejrnæs, R., Faurby, S., Galetti, M., Hansen, D.M., Sandel, B., Sandom, C.J., Terborgh, J.W. and Vera, F.W., 2016. Science for a wilder Anthropocene: Synthesis and future directions for trophic rewilding research. *Proceedings of the National Academy of Sciences*, 113(4), pp.898-906.
- Taillardat, P., Friess, D.A. and Lupascu, M., 2018. Mangrove blue carbon strategies for climate change mitigation are most effective at the national scale. *Biology letters*, 14(10), p.20180251.
- Tanentzap, A.J. and Coomes, D.A., 2012. Carbon storage in terrestrial ecosystems: do browsing and grazing herbivores matter? *Biological Reviews*, 87, pp.72-94.
- Tanentzap, A.J., Daykin, G., Fennell, T., Hearne, E., Wilkinson, M., Carey, P.D., Woodcock, B.A. and Heard, M.S., 2023. Trade-offs between passive and trophic rewilding for biodiversity and ecosystem functioning. *Biological Conservation*, 281, p.110005.
- Tansley, A.G., 1940. The British Islands and Their Vegetation. *The Geographical Journal*, 95(1), p.57.
- Tölgyesi, C., Buisson, E., Helm, A., Temperton, V.M. and Török, P., 2022. Urgent need for updating the slogan of global climate actions from “tree planting” to “restore native vegetation”. *Restoration Ecology*, 30, p.e13594.
- Torroba-Balmori, P., Zaldívar, P., Alday, J.G., Fernández-Santos, B. and Martínez-Ruiz, C., 2015. Recovering *Quercus* species on reclaimed coal wastes using native shrubs as restoration nurse plants. *Ecological engineering*, 77, pp.146-153.
- Tree, I. & Burrell, C. (2023) *The Book of Wilding*. Bloomsbury.
- Tree, I., 2018. *Wilding: The return of nature to a British farm*. Pan Macmillan.
- Tudge, S.J., Harris, Z.M., Murphy, R.J., Purvis, A. and De Palma, A., 2023. Global trends in biodiversity with tree plantation age. *Global Ecology and Conservation*, 48, p.e02751.
- UK Forestry Commission, n.d. **First-ever UK Woodland Natural Flood Management Guide Published**. [online] Available at: <https://www.gov.uk/government/news/first-ever-uk-woodland-natural-flood-management-guide-published> [Accessed 6 Dec. 2024].

- US Environmental Protection Agency, 2018. Mixed-species versus monocultures in plantation forestry. Available at: [US EPA HERO Database](#) (Accessed: 24 September 2024).
- Ustaoglu, E. and Collier, M.J., 2018. Farmland abandonment in Europe: An overview of drivers, consequences, and assessment of the sustainability implications. *Environmental Reviews*, 26, pp.396-416.
- Van Klink, R., Van Laar-Wiersma, J., Vorst, O. and Smit, C., 2020. Rewilding with large herbivores: Positive direct and delayed effects of carrion on plant and arthropod communities. *PLoS One*, 15, p.e0226946.
- Vanvolkenburg, H., Beyers, R., Nelson, C., Vasseur, L., Andrade, A., Convery, I. and Carver, S., 2022. Rewilding and human health. In: *Routledge Handbook of Rewilding*. Routledge.
- Veldman, J.W., Aleman, J.C., Alvarado, S.T., Anderson, T.M., Archibald, S., Bond, W.J., Boutton, T.W., Buchmann, N., Buisson, E. and Canadell, J.G., 2019. Comment on "The global tree restoration potential". *Science*, 366, p.eaay7976.
- Vera, F.W.M., 2000. *Grazing ecology and forest history*. Wallingford: CABI.
- Verra, 2024. Verified Carbon Standard: Verified Carbon Units (VCUs). Available at: [Verra](#) (Accessed: 24 September 2024).
- Vitousek, P.M., Mooney, H.A., Lubchenco, J. and Melillo, J.M., 1997. Human domination of Earth's ecosystems. *Science*, 277, pp.494-499.
- Von Essen, E. and Allen, M.P., 2015. Wild-but-not-too-wild animals: Challenging goldilocks standards in rewilding. *Between the Species*, 19(1), p.4.
- Wang, C., Zhang, W., Li, X. and Wu, J., 2022. A global meta-analysis of the impacts of tree plantations on biodiversity. *Global Ecology and Biogeography*, 31(3), pp.576-587.
- Wang, L., Pedersen, P.B.M. and Svenning, J.-C., 2023. Rewilding abandoned farmland has greater sustainability benefits than afforestation. *Nature-Based Solutions*, 2, p.5.
- Watts, S.H. and Jump, A.S., 2022. The benefits of mountain woodland restoration. *Restoration Ecology*, 30, p.e13701.
- Williamson, P., Wallace, D.W., Law, C.S., Boyd, P.W., Collos, Y., Croot, P., Denman, K., Riebesell, U., Takeda, S. and Vivian, C., 2012. Ocean fertilization for geoengineering: a review of effectiveness, environmental impacts and emerging governance. *Process Safety and Environmental Protection*, 90(6), pp.475-488.
- Woodland Carbon Code (WCC): Forestry Commission, 2019. Learn about the Woodland Carbon Code. Available at: <https://forestrycommission.blog.gov.uk/2019/08/01/learn-about-the-woodland-carbon-code/> (Accessed: 24 September 2024).
- Zarin, D.J., Harris, N.L., Baccini, A., Aksenov, D., Hansen, M.C., Azevedo-Ramos, C., Azevedo, T., Margono, B.A., Alencar, A.C., Gabris, C. and Allegretti, A., 2016. Can carbon emissions from tropical deforestation drop by 50% in 5 years?. *Global Change Biology*, 22(4), pp.1336-1347.

Zellweger, F., Flack-Prain, S., Footring, J., Wilebore, B. and Willis, K.J., 2022. Carbon storage and sequestration rates of trees inside and outside forests in Great Britain. *Environmental Research Letters*, 17(7), p.074004.

Chapter 2: The inadequacy of current carbon storage assessment methods for rewilding: A Knepp Estate case study.

Nancy C. Burrell¹, Marc Macias-Fauria², Elizabeth Jeffers¹, Katherine J. Willis¹

¹Department of Biology, University of Oxford, Oxford, UK

²School of Geography and the Environment, University of Oxford, Oxford, UK

Author contributions: Nancy C. Burrell led the conceptualisation, methodology development, formal analysis, investigation and data curation of the study. She was responsible for creating the original draft, revising it, visualising data and acted as the project lead. Kathy J. Willis supervised the project, assisted in designing the methodology, and revised and edited the manuscript. Elizabeth S. Jeffers also had a supervisory role, participated in designing the methodology, and edited the original draft. Marc Macias-Fauria's contributed in validating the study's findings, provided additional supervision and reviewed and edited the final draft.

Published in **Ecological Solutions & Evidence** in January 2024

As a clarifying point, pedunculate oaks (*Quercus spp.*) do not naturally have thorns but have been observed to develop thorn-like structures under browsing pressure. This characteristic is discussed further within this chapter.

2.0 Abstract

In the context of global climate change mitigation, carbon storage in woody vegetation plays a crucial role. Recognising the value of the i-Tree Eco model for carbon storage in urban and forestry settings, this study aimed to explore its applicability to rewilded landscapes. Using direct measurements from destructively sampled scrub from the Knepp Estate, our goal was to determine the model's suitability to this landscape. Our findings reveal that these methods are not appropriate for multi-stemmed trees below browsing height, as we observed no significant relationship between stem basal diameter and height. The i-Tree tool's assumption of belowground biomass being 26% of aboveground biomass may not be applicable to herbivore-influenced landscapes. Additionally, we found that, on average, scrub at Knepp had more biomass below the ground than above, with a root:shoot ratio of 1.07, which is more than four times the amount predicted by current models using the 0.26 estimate ratio. This study underscores the need for novel allometric approaches that consider species-specific biomass and the impact of external factors, such as herbivory, on carbon storage. Accurate carbon accounting in future rewilding projects is essential for their contribution to both biodiversity enhancement and climate change mitigation. While the i-Tree Eco model provides valuable insights for many ecosystems, our findings suggest that its applicability may be limited in scrubland ecosystems, especially in rewilded landscapes where natural processes create semi-stable scrub and open wood pastures. Nonetheless, with suitable adjustments or when complemented with other methods, the i-Tree Eco model could be a valuable tool for specific scrub or rewilding scenarios.

Key words: Allometry, carbon sequestration, climate change mitigation, rewilding, scrubland, carbon stocks.

2.1 Introduction

Targeted forestation will be necessary to mitigate greenhouse gas (GHG) emissions in order to limit global warming to 1.5°C above preindustrial levels (Bonan, 2008). Young, growing woodland can rapidly sequester carbon dioxide (CO₂) and may simultaneously provide other ecosystem services such as flood hazard mitigation (Bernhardt et al, 2005; Stutter et al, 2012) and improved air quality (Bytnerowicz et al, 2007). The default approach in the UK to increasing tree cover is via plantations, with mechanical or hand-planting of tree saplings (Department for Environment, 2021). The establishment of plantations has been widely acknowledged for its significant contribution towards meeting the ever-increasing demand for timber and other forest products. Nevertheless, the practice has been accompanied by several drawbacks, including the considerable carbon cost associated with artificial propagation, transport and planting. In addition, the monoculture nature of plantations, dominated by a single or a few species, has been reported to lead to the development of closed-canopy systems that are notably inadequate for biodiversity conservation. These findings have been previously reported by Pereira & Navarro (2012) and have been a subject of growing concern in the field of forestry and ecology.

An alternative approach to tree planting for carbon offsets therefore rising in popularity amongst land managers is natural colonisation, particularly associated with the process of rewilding (Mikołajczak et al, 2022; Sandom et al, 2019). Natural colonisation, where trees take

over naturally from existing seed sources, is considered to be a low cost, low carbon and low disease-risk alternative to the artificial system of planting (Di Sacco et al, 2021; Garrido et al, 2021; Keesstra et al, 2018), with evidence of biodiversity benefits (Biermann & Anderson, 2017; Corlett, 2016; Fernández et al, 2017; Jepson, 2016; Keesstra et al, 2018; Rewilding-Britain, 2020).

The Knepp Estate, situated in southern England, has undergone rewilding efforts since 2001, spanning a considerable area of 1,400 ha. This project serves as an exemplary demonstration of the capacity of trees to establish rapidly and densely on former arable land, especially in the presence of low densities of herbivores such as roe deer (*Capreolus capreolus*) and rabbits (*Oryctolagus cuniculus*). After establishment, woody plants continue to naturally regenerate even when exposed to a much larger population of herbivores, once the thorny scrub is established, which serves as a structural defence against browsing (Broughton et al, 2021; Navarro & Pereira, 2015). Notably, free-roaming herbivores were introduced to the Knepp Estate in 2009 (Tree, 2018), making it one of several rewilding projects in Europe that have positively impacted wood-pasture succession, ecosystem function and complexity, leading to woodland recovery and enhanced biodiversity (Ceaşu et al, 2015; Naundrup & Svenning, 2015; Seddon et al, 2014; Vera et al, 2000).

The benefits of rewilding for biodiversity have been demonstrated in several studies (Cerqueira et al, 2015; Hodder et al, 2014; Keesstra et al, 2018; Tree, 2017). However, the potential benefits of rewilding for carbon sequestration in scrubland are still unclear. It has been argued that planting trees is more efficient at establishing a greater volume of trees than natural colonisation (Meli et al, 2017). Additionally, the presence of some herbivores, both domestic and wild, has been suggested to hinder vegetation recruitment and prevent the creation of woodland (Gill & Fuller, 2007). Nevertheless, ecological research into natural

regeneration and rewilding challenges this notion (Tree 2018, Vera 2000). The carbon storage potential of scrubland created by rewilding could be significant.

Given the existing knowledge gaps, the investigation of carbon storage potential in scrubland species is of great significance and requires immediate attention. In this context, while traditional methods for evaluating carbon storage in various woody species have been effective, their applicability to scrubland species remains uncertain. For instance, UK-based research, such as work by the Forestry Commission (Matthews & Mackie, 2006) has provided valuable insight into best practices in British forestry with detailed methodologies for timber measurement. However, further exploration in this specific field is essential to understand the full potential of rewilding, as elaborated in the following paragraph.

The i-Tree Eco model, widely recognised for its value in urban and forestry applications, emerges as a potential tool to bridge this gap. Its utility in estimating carbon storage has been demonstrated in diverse settings, yet its efficacy for rewilded scrubland remains an open question. Our study, therefore, aims to assess the potential use of i-Tree Eco in this context, comparing the predicted biomass of five scrub species to their actual measurements.

The most common approach to estimate carbon storage of different tree species is to use allometric equations that predict C content by incorporating variables such as height (h), diameter at breast height (dbh), and canopy area of the species (Ngomanda et al, 2014). These forest mensuration methods are based on the relationship between biomass of tree components and easily measurable independent variables (Brown, 1997; Chave et al, 2005; Pati et al, 2022; Vorster et al, 2020). Lookup tables are used to estimate carbon storage of different species within a given landscape from these variables. However, these tables focus mainly on commonly cultivated forest trees of a specific size, representing only a select

number of species. These species then act as surrogates for those not covered, inherently limiting the tables' applicability (Randle & Jenkins, 2011). The Woodland Carbon Code (WCC) is a UK-based voluntary standard for woodland creation projects, aiming to certify the amount of carbon captured and stored in afforestation and reforestation activities. For instance, the WCC defines trees as having a dbh > 7 cm, and anything below this size is regarded as "unmeasurable" (Randle and Jenkins, 2011). The exclusion of smaller trees from these estimates is mainly because they are assumed to have no timber volume and, hence, negligible carbon storage potential in a landscape (Matthews, 2017). This size limitation has led to rewilded scrubland being disregarded when measuring carbon storage of woodlands using the WCC. This leaves a significant knowledge gap in the potential contribution of these scrubland species to carbon sequestration.

Unlike the WCC, the i-Tree Eco model can be used to estimate carbon storage for smaller diameter woody species. i-Tree Eco was developed by the United States Department of Agriculture Forest Service to analyse forest structure and composition to generate estimates of selected ecosystem services, including carbon sequestration (Nowak, 2019). Although developed in the US, the model is applicable on a global scale and incorporates data sets from around the world including the UK (i-Tree Eco Manual, 2020). As a result, i-Tree Eco has been applied in 130 countries (Nowak et al, 2018). In the UK, there have been more than 20 i-Tree Eco projects since 2011 (Raum et al, 2019). In this tool, the gross amount of carbon sequestered and stored in a tree, both above- and below-ground, is calculated using allometry-derived data from the i-Tree database (Nowak et al, 2008). Compared to other models, i-Tree defines a tree as any woody plant with a diameter at breast height (dbh - 1.37 m) greater than or equal to 2.54 cm, making it suitable for estimating carbon storage in smaller woody species (i-Tree

manual, 2020). i-Tree has been used in many studies to assess the ecosystem services provided by trees, including their carbon storage capacity, in a variety of settings, such as urban areas, private lands and forests (Dale, 2013; Ma et al, 2021; Morani et al, 2014; Qian et al, 2019). The lower size threshold of i-Tree makes it applicable to a significant proportion of the scrub found at Knepp, which is why we chose to use this method in our study.

The i-Tree Eco requires input data on tree height and dbh and uses whole-tree carbon estimates from the GlobAllomeTree (2017) database as well as other biomass equations extracted from scientific literature (Nowak & Crane, 2002; Nowak, 1994) to predict carbon sequestration. The i-Tree Eco model then estimates an annual carbon sequestration value by associating size and species of tree with age and specific annual growth. The i-Tree Eco model has been used to assess the carbon storage potential of woody biomass throughout the UK (Hutchings et al, 2012; Monteiro et al, 2019), including by the Forestry Commission (Doick et al, 2017; Raum et al, 2019). Its adaptability and economic conversion have bolstered its reputation as a valuable tool for carbon sequestration estimation, particularly in urban settings.

However, as with the WCC, i-Tree Eco does not consider the role of browsing animals and their effect on woody plant strategy in terms of structural differences and biomass reallocation. Trees have been known to adopt a thorny strategy (Bannister & Watt, 1995; Churski et al, 2022) to defend against browsing and to reallocate a larger proportion of biomass belowground (Perkovich & Ward, 2021). It is typically assumed, in many models, including the i-Tree model, that belowground root biomass is 26% of the amount of aboveground stem biomass (Cairns et al., 1997). This estimation is based on height and dbh.

Therefore, the standard model of C allocation in trees could significantly underestimate the belowground carbon storage potential of rewilded landscapes.

In this study, we sought to evaluate the suitability of the i-Tree methodology, which has been primarily developed based on data from closed-canopy systems, in estimating carbon storage in scrubland species where herbivore interactions may play a crucial role. To this end, we employed the rewilded Knepp Estate as a model system to investigate the efficacy of this standardised approach in capturing the carbon sequestered by scrubland trees. Additionally, we performed a preliminary destructive sampling study to test the accuracy of the 0.26 predictive estimate of below-ground biomass (BGB) in predicting scrub root biomass. By shedding light on this crucial aspect of carbon storage, our research emphasises the need for a more comprehensive understanding of the intricate relationships between biotic and abiotic factors in ecosystem functioning.

2.2 Materials & Methods

2.2.1 Site location

Our study was conducted in the 'Southern Block' of Knepp Estate (50.975781N, 0.344819W), West Sussex, UK, covering 445 ha and comprising 59 former arable fields (Figure 2.1). The Estate is located in an area where soils are poorly drained and predominantly heavy clay (Type 18 SoilScapes – British Geological Survey, n.d.). Since World War II, the Knepp Estate operated a mixed farming system, with intensive arable and dairy enterprises (Tree, 2018). However, in 2001, farming operations ceased across the estate, and a rewilding project modelled on Oostvaardersplassen in the Netherlands was initiated (Vera, 2000). As part of

this project, Knepp Estate was divided into three blocks: Northern, Middle and Southern. The Southern Block was left fallow between 2001-2006 to allow for natural regeneration, and herbivores were introduced in 2009, including old English longhorn cattle (*Bos primigenius taurus*), Exmoor ponies (*E. ferus caballus*) and fallow deer (*Dama dama*), as well as Tamworth pigs (*Sus scrofa domesticus*). Red deer (*Cervus elaphus*) were introduced in 2013.

2.2.2 Stratified sampling

The Southern Block has been separated into 12 different landcover types based on the vegetation that dominated that area (Table S2.1). Permission was granted for fieldwork by the Knepp Castle Estate. We divided the landscape into strata polygons (one stratum per landcover class) and randomly selected five polygons for sampling of the scrubland vegetation. Within these five landcover classes we randomly designated 18 plots of 0.1 ha for data collection (Figure 2.1). Sampling locations within each polygon were randomly generated using ArcGIS v 10.6.1 and the "Create Random Points" tool. Areas of scrubland were defined as having a predominance of shrubs characterised as woody plants not exceeding 5 meters in height if having a single stem, or 8 meters if multi-stemmed, with many shrubs being thorny and browsed by animals (Harden, 1990).



Figure 2.1: The Southern Block of the Knepp Estate (50.9817° N, 0.3664° W), showing the 5 landcover classes that were sampled, the green areas denote hedgerows, the black area is the Southern Block boundary. The black dots represent the plots that were sampled.

2.2.3 Data collection and analysis

The study was conducted from June to July 2021 to measure scrub trees in a specific area using a standardised sampling protocol. For each plot selected, tree species were identified using PlantATT (2004) and the Collins Tree Guide (2004). All woody vegetation taller than 40 cm was measured and recorded within circular sampling plots of 0.1 ha, and only individuals that grew entirely within the plot, including the full extent of branches, were included.

According to the i-Tree Eco manual (2020) trees with multiple stems branching above the ground were treated as the same tree. In these cases, the dbh of up to six stems were to be measured separately. When a tree has more than six stems with a dbh ≥ 1 inch, the measurement height is lowered to 1 ft above the ground, and up to six of the largest stems are

to be recorded, disregarding the others. If the pith union is below ground, each stem is regarded as an individual tree. For multi-stemmed trees the combined dbh was calculated using the following equation:

$$\sqrt{(dbh1^2 + dbh2^2 + dbh3^2 + \dots)}$$

The characteristics of each individual, including the number of stems, stem circumference (measured in cm) and total height (measured in meters), were recorded. For trees taller than 3 meters, tree height was measured using a clinometer or a similar instrument, following the protocol recommended by i-Tree Eco's field manual (2020) to measure the angle between the observer and the top of the tree.

2.2.4. i-Tree Eco model

To estimate the potential carbon storage of the Southern Block, we utilised the i-Tree Forecast Eco v6.0.22. Consistent with the guidelines outlined in the i-Tree Eco manual, we measured the diameter at ground level for trees whose diameter we were unable to measure at breast height (1.37 m). i-Tree Eco accommodates this adjustment, permitting the measurement to be taken at the base when standard dbh cannot be taken. There is no minimum tree height for i-Tree; instead, the focus is on dbh. This approach ensures that smaller trees will not be excluded.

2.2.5. Preliminary destructive sampling of the scrubland

The validation of i-Tree allometry for scrubland species involved destructive sampling of individuals, which encompassed the complete recovery of above- and belowground plant

material. This study was carried out over a period of two months, from February to March 2022. A total of 39 individual trees and/or shrubs were collected from a study site that was randomly chosen from four potential sites based on their heterogeneous land cover. Permissions limited our access to certain areas, leading to an uneven sample size across different species. The sample consisted of 11 oak (*Quercus robur*), 16 blackthorn (*Prunus spinosa*), 5 dog rose (*Rosa canina*), 6 hawthorn (*Crataegus spp.*) and 1 willow (*Salix spp.*) The study site was selected based on its heterogeneity to ensure that the samples collected were representative of the range of scrubland species found within the area.

The entire plant was removed and separated into crown, stem and root ball. For clarity, the stem and crown were differentiated at the live crown base – the point on the main stem where the lowest live branch with foliage begins. In the context of the root ball, any section below the top 1 cm above the soil was classified as such.

To standardise the measurement of belowground biomass, an area with a diameter equivalent to three times the canopy width down to a depth of 1 meter was dug, following the approach used by Picard et al. (2012) and Snowdon et al. (2000). All roots were carefully washed using a pressure hose to remove soil, ensuring that the bark remained intact during the process. Roots were then categorised based on their diameter: small roots (<2 mm), medium roots (2 mm < diameter < 10 mm) and large roots (>10 mm). Branches were categorised into small (<4 cm), medium (4 cm < diameter < 7 cm) and large (>7 cm).

Following the excavation and preparation, each component – crown, stem and roots - was weighed on a digital weighing scale. Their respective lengths (cm) and diameters (cm) were measured. The samples were subdivided and dried at 100°C until their weight remained constant, which was achieved in all cases after 72 hours. Both aboveground biomass (AGB)

and belowground biomass (BGB) weights of these samples were recorded. I-Tree Eco uses a root:shoot ratio of 0.26 (Nowak, 2019) to predict belowground biomass. Our objective was to evaluate the accuracy of this estimate by directly comparing the measured and estimated root:shoot ratios. The measured AGB weight from our samples was used to determine this ratio, which was then compared to the actual BGB weights to assess the reliability of the 0.26 ratio prediction.

2.2.6 Statistical analysis

The statistical analysis and graph creation were performed in R Studio version 2022.7.2.576 (RStudio Team, 2022), with the graphs created using the ggplot2 package (Wickham, 2016) in R Studio. The relationship between tree height (m) and diameter at breast height (dbh) (cm) was estimated for each species based on the number of stems, after which trees were divided into two height categories: those > 2.5 m and <2.5 m; that is, above and below the browse line, respectively. This browse line height has been widely accepted by researchers (e.g. Van Uytvanck et al. 2010). A Shapiro-Wilk Normality test (Crawley, 2012) was conducted to assess normality of the data. Due to non-normality in the data, a Spearman's Rank Correlation was used to measure the linear association between the continuous variables. Since preliminary results revealed a skewed variation in tree height, we used a Siegel nonparametric linear regression analysis with the relationship evaluated on a log-transformed height and a log-transformed dbh. In view of the considerable sample size for the destructively sampled trees, a one-sample t-test was employed to evaluate the root:shoot ratio of the preliminary findings against the anticipated value of 0.26 derived from i-Tree, notwithstanding its non-normal distribution (Crawley, 2012).

2.3 Results

2.3.1 Species composition

In our study, we identified a total of 1580 woody plants, comprising 15 species from 14 different genera. The most prevalent species in the sample population were *Salix spp.* (60.0%), *Prunus spinosa* (11.9%), *Crataegus spp.* (10.1%), followed by *Quercus robur* (8.3%), *Prunus avium* (2.7%), *Fraxinus excelsior* (2.2%), *Acer campestre* (1.5%) and *Rosa canina* (1.1%) (Table 2.1). Of the 15 species measured, 8 (16.90% of the total trees) had a genus-related allometric equation from the i-Tree database, while only 1 of the 15 species measured (0.13% of total sample population) had a species-specific allometric equation (Table 2.1). The i-Tree database applied the 'next relevant taxonomic group' coefficient to individual tree species within the remaining sample population, which included six different species and accounted for 83.10% of the total trees measured. According to the i-Tree Eco manual, when a particular tree species does not have a species-level or genus-level equation available, i-Tree Eco selects the next most relevant taxonomic group to apply equations to that particular species of tree.

2.3.2 The relationship between tree height (m) and DBH (cm)

We found that the diameter at breast height (dbh) and height (h) of single stem trees above the browse line had a moderate positive correlation ($n = 415$, $\rho = 0.53$, $p < 0.0001$), while single stem trees below the browse line had only a weak positive correlation between these two variables ($n = 558$, $\rho = 0.35$, $p < 0.0001$). All trees above the browse line (>2.5 m) with 1 ($n = 415$, $\rho = 0.53$, $p < 0.0001$), 2 ($n = 83$, $\rho = 0.53$, $p < 0.0001$), 3 ($n = 82$, $\rho = 0.57$, $p < 0.0001$), 4 ($n =$

= 58, $\rho = 0.57$, $p < 0.0001$) or 5 ($n = 48$, $\rho = 0.4$, $p < 0.005$) stems showed a significant moderate positive correlation between dbh and h (Figure 2.2). But with six stems, no significant correlation between dbh and h ($n = 88$, $\rho = 0.028$, $p\text{-value} > 0.05$) was present. The correlation strength comparatively changed with all species of tree below the browse line (<2.5 m) with 1 ($n = 558$, $\rho = 0.35$, $p < 0.0001$), 2 ($n = 88$, $\rho = 0.35$, $p < 0.001$), 3 ($n = 88$, $\rho = 0.33$, $p < 0.01$) or 4 ($n = 61$, $\rho = 0.33$, $p < 0.01$) stems exhibited a weak positive correlation between h and dbh (Figure 2.2), while trees below the browse line with 5 ($n = 29$, $\rho = 0.27$, $p > 0.1$) or 6 ($n = 46$, $\rho = 0.24$, $p > 0.1$) stems had no significant relationship between h and dbh.

Table 2.1: The characteristics of different tree species measured in the southern block, along with their corresponding allometric equations for estimating biomass using i-Tree Eco. The table includes the number of individuals (n) for each species, as well as the average tree height and diameter at breast height (dbh) with their corresponding standard deviations. The final column indicates the closest taxonomic level to associate with an i-Tree equation for estimating biomass. Where no associated equation was found, the field was left blank.

Species	total	Avg. Height (m)	± SD	Avg. dbh (cm)	± SD	closest taxa level	i-Tree equations
<i>Acer campestre</i>	23	10.92	15.9	17.59	7.3	genus	$Y=eA + B * \ln(x) + (C / 2)$; $Y=A+Bx+Cx^2+Dx^3+Ex^4+Fx^5+Gx^6$; $Y=AxB$; $Y=A+Bx+Cx^2+Dx^3+Ex^4+Fx^5+Gx^6$
<i>Alnus spp.</i>	1	10.03	N/A	17.5	N/A	genus	$Y=Ax^2$
<i>Betula pendula</i>	4	9.65	19.1	22.15	7.43	genus	$Y=A+Bx+Cx^2+Dx^3+Ex^4+Fx^5$; $Y=eA + B * \ln(x) + (C / 2)$
<i>Corylus avellana</i>	27	7.49	4.04	12.36	8.69	nothing	
<i>Crataegus spp.</i>	128	2.68	15.3	5.16	6.67	nothing	
<i>Fagus spp.</i>	3	15.72	4.2	22.67	6.59	genus	$Y=A+Bx+Cx^2+Dx^3+Ex^4+Fx^5+Gx^6$
<i>Fraxinus excelsior</i>	24	10.98	15.8	11.11	7.32	genus	$Y=eA + B * \ln(x) + (C / 2)$
<i>Malus sylvestris</i>	3	5.23	3.49	5.61	7.52	unknown	
<i>Pinus sylvestris</i>	2	13.43	16.1	30.2	6.99	species	$Y=A+Bx+Cx^2+Dx^3+Ex^4+Fx^5$
<i>Prunus avium</i>	31	12.01	15.8	19.64	7.33	genus	$Y=eA + B * \ln(x) + (C / 2)$
<i>Prunus spinosa</i>	90	1.63	15.1	2.65	7.09	genus	$Y=eA + B * \ln(x) + (C / 2)$
<i>Quercus spp.</i>	89	10.37	15	13.66	7.1	genus	$Y=(Ax^2)+B$
<i>Rosa canina</i>	2	3.37	18.3	1.65	6.09	nothing	
<i>Salix spp.</i>	1151	6.61	15.2	10.49	6.86	family	
<i>Sorbus terminalis</i>	2	8.46	16.4	15.4	6.53	family	
Total	1580	8.57	4.06	13.86	8.09		

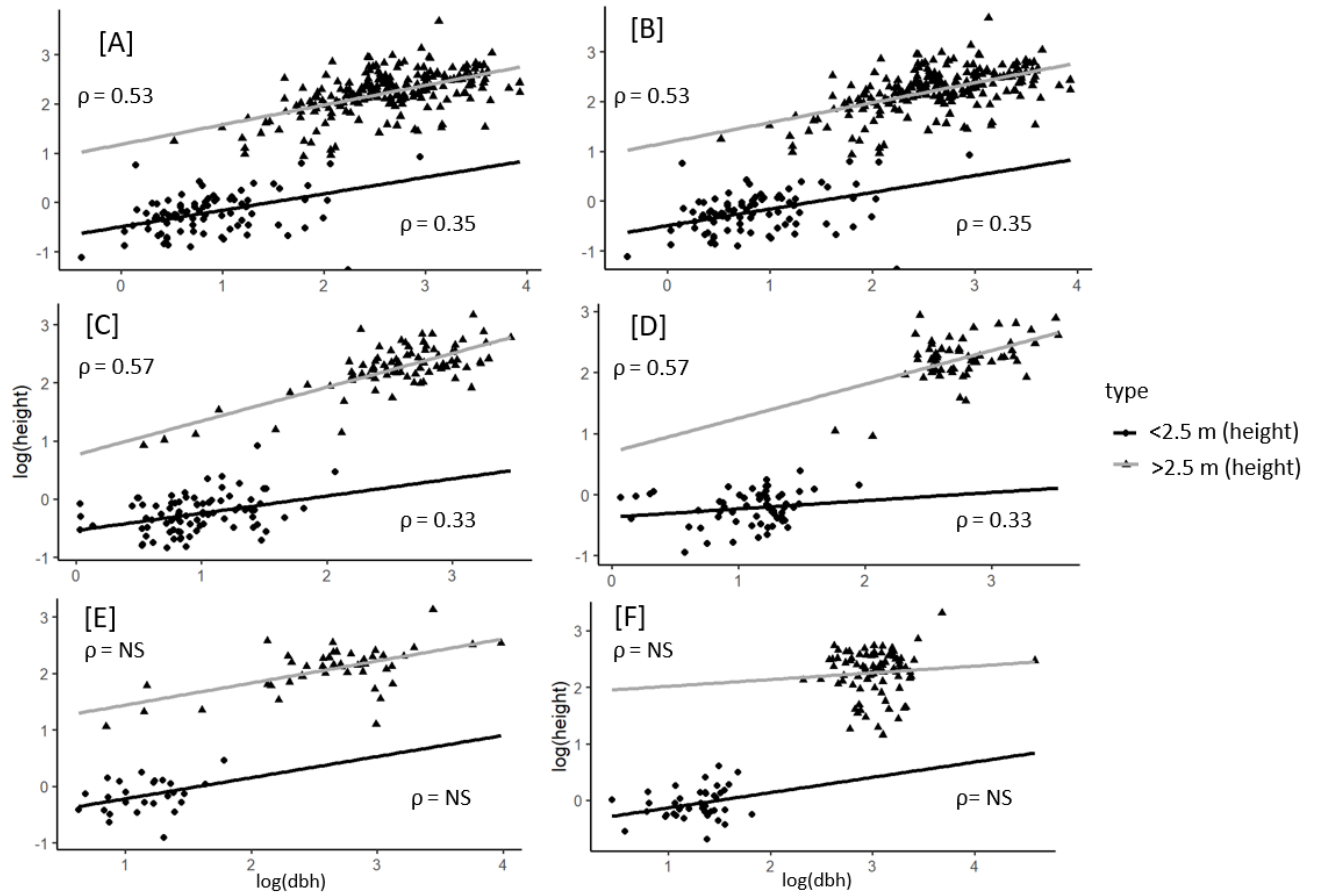


Figure 2.2: the relationship between the log-transformed height and the long diameter at breast height (dbh) of trees in the study area, stratified by tree height. The grey line represents trees taller than 2.5 m (above the browse line), while the black line represents trees shorter than 2.5 m (below the browse line). Panels [A-F] show trees with different numbers of stems, with panel [A] showing trees with a single stem, and panels [B-F] showing trees with 2, 3, 4, 5, and 6 stems, respectively. The results of the Spearman's rank correlation are displayed as a ρ value with NS denotes a non-significance of the p-value outcome.

2.3.3 Belowground biomass

The destructively sampled tree results revealed a skewed variation in tree height (min 23.10 cm, median 59.50 cm, mean 72.70 cm, max 155.50 cm). A Siegel nonparametric linear regression analysis showed that tree height was significantly correlated with both aboveground biomass (AGB; v value = 496, $p < 0.0001$) and belowground biomass (BGB; min

10.57 g, median 79.24 g, mean 194.67 g, max 903.83 g; v value = 494, $p < 0.0001$). However, due to the species-specific nature of carbon storage and the lack of species-specific data available in i-Tree, we focused our analysis on biomass rather than carbon stock. The significant variation in tree species and height, along with a small sample size for each species (oak = 11, sallow = 1, hawthorn = 6, dog rose = 5, blackthorn = 16), made it difficult to compare the i-Tree predicted carbon stock between species and size. Therefore, instead of comparing carbon stock, we focused on comparing the total scrub aboveground biomass (AGB) to the total belowground biomass (BGB) and the predicted belowground biomass from i-Tree, which was based on the assumed root:shoot ratio of 0.26 (see Table S2.2).

The i-Tree prediction of BGB ranged from min = 1.59 g to max = 853.57 g, with a median of 22.77 g and a mean of 89.25 g. These results from the destructive sampling showed that the mean root:shoot ratio from 39 trees was 1.07 - significantly greater than the predicted root:shoot ratio of 0.26 ($t(38) = 5.51$, $p = 0.0000027$, $d = 0.871$), as determined by a one-sample t-test (Figure 2.3A). Destructive sampling of 39 trees yielded higher estimates of BGB than the i-Tree predictions, with an average 7% larger proportion of BGB to AGB. All samples had a greater belowground biomass than the i-Tree prediction, with individual blackthorn, dog rose and hawthorn trees having a greater proportion of belowground biomass to aboveground biomass (10%, 35%, and 5%, respectively), while oak and sallow trees had a greater proportion of total biomass above the ground (4% and 41%, respectively) (Figure 2.3B).

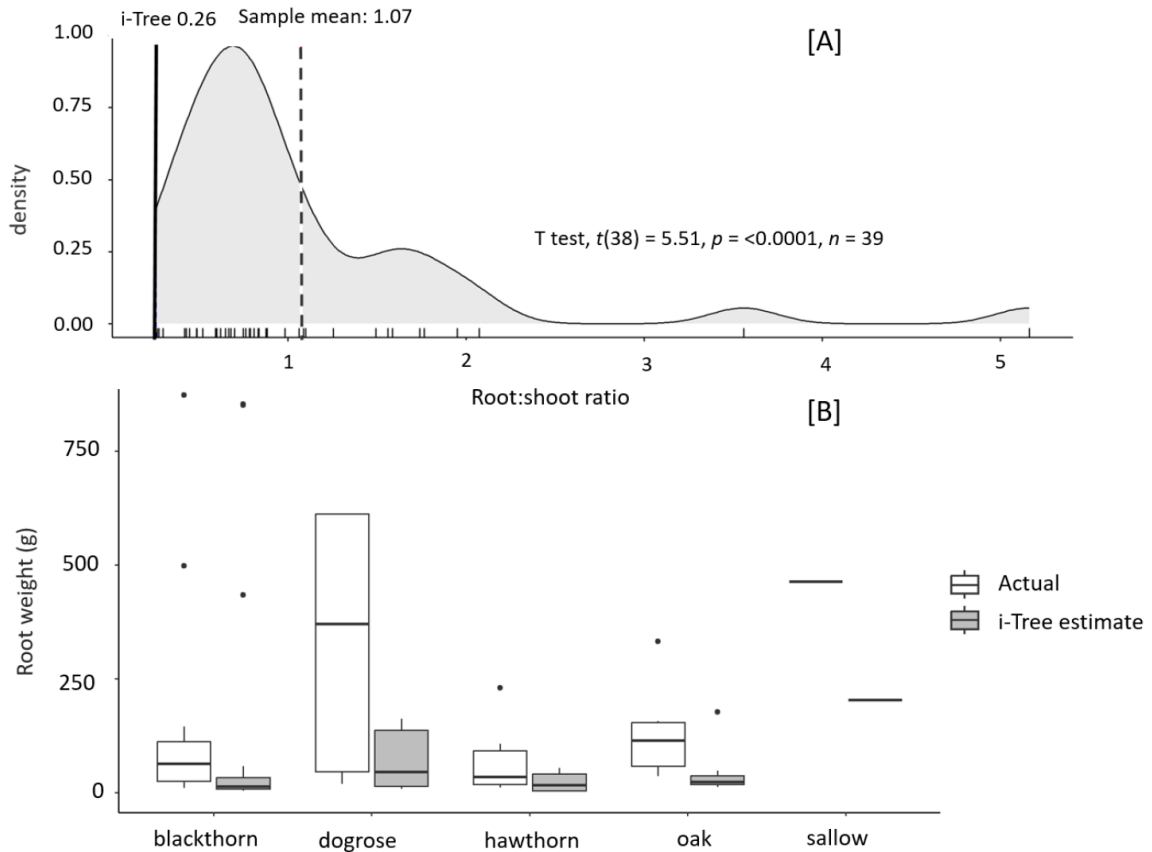


Figure 2.3: A comparison between the i-Tree estimates and the actual values of the destructive samples. Panel [A] exhibits the root:shoot ratio of the destructive samples, with $n = 39$. The solid line illustrates the i-Tree Eco predicted root:shoot ratio, which was 0.26, while the dotted line depicts the sample mean root:shoot ratio, which was 1.07. Panel [B] displays a comparison of the total belowground fresh weight (BGB, black bars) to the i-Tree prediction of belowground biomass (BGB, grey bars) for five different species. The number of samples (n) for each species is provided in parentheses: blackthorn (*Prunus spinosa*, $n = 16$), dog rose (*Rosa canina*, $n = 5$), hawthorn (*Crataegus* spp., $n = 6$), oak (*Quercus* spp., $n = 11$), and willow (*Salix* spp., $n = 1$).

2.4 Discussion

This study highlights the importance of species-specific allometric equations in ensuring reliable biomass estimation. We evaluated the use of i-Tree to estimate the biomass of scrubland species by comparing field-based measurements with the output generated by this

approach. While i-Tree has species-specific data for *Pinus sylvestris*, eliminating the need for a proxy, it lacked such specific equations for all the other tree species in our study. For eight of the species, genus-related equations had to be employed, and the remaining six species were absent entirely from the i-Tree database.

The use of generalised allometric equations can lead to inaccurate biomass estimates as they fail to account for species-specific variations that arise from environmental pressures and plant phenotypes. Our study presents a weak allometric relationship (Figure 2.2), which aligns with prior research, suggesting that species-specific equations offer better accuracy than genus-specific ones (Nogueira, 2018; Zhu, 2016). Indeed, several studies have emphasised the importance of applying species-specific allometry for trees that have unique growth forms and are poorly represented in the literature (Abich et al, 2019; Basuki et al, 2009; Chave et al, 2014; Ketterings et al, 2001; Litton & Boone Kauffman, 2008). As a result, the use of generalised allometric equations may underestimate the true biomass of certain species. Therefore, developing species-specific allometric equations is crucial for accurately estimating biomass and carbon stocks.

In utilizing the i-Tree model for estimating scrubland tree biomass, tree height poses a challenge. The i-Tree model necessitates measuring the diameter at breast height (dbh) at approximately 1.37 m aboveground, although it defines a tree as woody vegetation > 30.50 cm (height) and > 1.0 cm (dbh) in the i-Tree Field Guide (2021). Our study revealed that 42.53% tree sample population had heights less than 1.37 m, with an average height of 0.70 m (± 0.22 SD). The i-Tree Eco manual proposes alternative techniques like dendrometers or laser rangefinders to estimate dbh for smaller trees but cautions that they may introduce some error. When dbh measurement is not feasible, the manual suggests using other metrics, such

as tree height, crown dimensions or default biomass values for various tree species (i-Tree Field Guide, 2021). Since we could not measure dbh, we assessed the diameter at the base, which might lead to an overestimation of aboveground biomass, even though the i-Tree tool can adjust the diameter measurement point.

2.4.1 Allometric equations used to determine aboveground carbon storage

The i-Tree model utilises a correlation between diameter at breast height (dbh) and height to estimate aboveground biomass (Cifuentes Jara et al, 2015; Paul et al, 2016). Our study suggests that woodland trees do not exhibit the same linear dbh/height relationship as rewilded scrubland trees (Figure 2.2). The moderate positive correlation between dbh and h observed in single-stemmed trees above the browse line could be attributed to the absence of herbivore pressure, allowing for more efficient resource allocation to vertical growth and, thus, a positive allometric relationship (Mayer, 2017). However, the weaker positive correlation between dbh and h in single-stem trees below the browse line suggests a different growth pattern, with less efficient resource allocation to vertical growth and more to defence against herbivores or pathogens. The absence of a strong significant correlation between dbh and h in woodland trees below the browse line indicates a possible change in growth patterns. Unlike blackthorn and hawthorn which have a naturally thorny strategy, oak trees do not naturally grow thorns. However, they have been known to exhibit thorny traits when subjected to herbivore pressures - similar to that of oak savannas reported in Grove and Rackham (2001). The trees produce thorns and allocate tissue to defend against browsing (Perkovich et al, 2021), leading to a population of smaller trees below 2.5 meters until browsing pressure is

limited or defence mechanisms allow growth above the browse line (Vera 2000). The medium-sized trees (15-30 cm dbh) that comprised 90.81% of scrubland species in the Southern Block (Fig. 4) may be a result of the adaptation of the tree to browsing pressure, which Grove and Rackham (2001) suggest can take time to mature into a large-sized woodland. The eight-year delay in introducing livestock could have altered the dynamics of natural regeneration and succession, leading to different biomass accumulation patterns in trees established before, versus after, the livestock's arrival. Our study emphasises the importance of understanding growth patterns in response to herbivore pressure and highlights the need for accurate models to predict carbon storage potential in woodland ecosystems. Further investigations are required to confirm these findings and develop allometric relations for smaller woody plants to better comprehend their carbon storage potential.

2.4.2 Belowground carbon storage

Estimating belowground biomass (BGB) of trees is challenging, as it requires excavation of a much larger area than is typically feasible. In our study, BGB measurements were restricted to three times the canopy area of the tree, despite the root structures often extending beyond this boundary, leading to probable underestimation of BGB. Nevertheless, our preliminary results indicate a larger proportion of BGB than aboveground biomass (AGB), with a root:shoot ratio of 1.07. This ratio is higher than those reported for scrubland (0.32) by Mokany et al. (2006), and temperate hedgerows (0.94) by Axe et al. (2017). However, the large variation in root:shoot ratio within shrubland highlights the need for more extensive, species-specific studies to accurately assess the BGB of this ecosystem. Improving our understanding of

belowground biomass allocation is important for predicting ecosystem carbon storage and cycling, as well as for management and conservation of woodland ecosystems.

The higher root:shoot ratio observed in our preliminary results may be attributed to the smaller size of trees, as this ratio typically decreases with an increase in shoot biomass (Mokany et al., 2006). Environmental pressures such as herbivory may also play a role, as recent studies have shown that aboveground herbivory can stimulate the reallocation of non-structural carbohydrates to root storage in oak (*Quercus spp.*) trees (Orians et al, 2011; Perkovich & Ward, 2021). A more extensive dataset is needed to understand how these factors influence the root:shoot ratio of shrubland ecosystems.

2.5 Conclusion

This research evaluated the applicability of the i-Tree approach for estimating biomass and carbon storage of scrubland species within the rewilded Knepp Estate. While the i-Tree model has been effective in closed-canopy systems and urban treescapes, its limitations become evident in herbivore-driven landscapes.

Despite its widespread use in the industry, our findings demonstrate that this approach is inadequate for accounting for the complexity of aboveground woody plant attributes such as number of stems and belowground biomass, which can be influenced by herbivory. This study presents the first allometry-derived field inventory of scrubland for a rewilded landscape, highlighting the need to revise carbon lookup tables in standard models such as i-Tree to include species-specific biomass from destructive samples and a revised sampling protocol. We found that biomass allocation patterns vary depending on the external pressures

of the woody plant, with no evidence of a relationship between height and dbh for scrubland species below 2.5 m. Thus, existing carbon lookup tables for woodland species growing in forestry conditions cannot be applied to scrubland species using industry-standard methods such as i-Tree Eco.

Our results suggest that landscape-scale rewilding projects can have potential contributions to both biodiversity gains and climate change mitigation. A more comprehensive biomass inventory study is needed to accurately account for carbon storage potential in future 'rewilding' projects. This knowledge gap has been identified previously by Ockendon et al. (2018). Our results underscore the necessity for an updated carbon accounting method in rewilded landscapes and offer a foundation for subsequent investigations.

2.5.1 Acknowledgements

I am grateful to Operation Wallacea for supporting this work as part of its Wildlife Research Programme.

2.5.2 Peer review

The peer review history for this article is available at <https://www.webofscience.com/api/gateway/wos/peer-review/10.1002/2688-8319.12301>.

2.5.3 Date availability statement

All data supporting the findings of this study are openly available in the Dryad Digital Repository, as detailed in Burrell et al. (2023). This dataset includes comprehensive measurements of the height and dbh of scrubland vegetation at Knepp Estate, along with the above- and below-ground weights obtained from destructive sampling.

2.6 Reference List

- Abich, A., Mucheye, T., Tebikew, M., Gebremariam, Y. & Alemu, A. (2019) Species-specific allometric equations for improving aboveground biomass estimates of dry deciduous woodland ecosystems. *Journal of Forestry Research*, 30(5), 1619-1632.
- Axe, M. S., Grange, I. D. & Conway, J. S. (2017) Carbon storage in hedge biomass—A case study of actively managed hedges in England. *Agriculture, Ecosystems & Environment*, 250, 81-88.
- Bannister, N. R. & Watt, T. A. (1995) Effects of Cutting on the Growth of *Crataegus monogyna*(Hawthorn) in Hedges. *Journal of Environmental Management*, 45(4), 395-410.
- Basuki, T., Van Laake, P., Skidmore, A., Hussin, Y. J. F. e. & management (2009) Allometric equations for estimating the above-ground biomass in tropical lowland Dipterocarp forests, 257(8), 1684-1694.
- Bernhardt, E. S., Palmer, M. A., Allan, J. D., Alexander, G., Barnas, K., Brooks, S., Carr, J., Clayton, S., Dahm, C., Follstad-Shah, J., Galat, D., Gloss, S., Goodwin, P., Hart, D., Hassett, B., Jenkinson, R., Katz, S., Kondolf, G. M., Lake, P. S., Lave, R., Meyer, J. L., O'Donnell, T. K., Pagano, L., Powell, B. & Sudduth, O. (2005) Synthesizing U.S. river restoration efforts. *Science*, 308(5722), 636-637.
- Biermann, C. & Anderson, R. M. (2017) Conservation, biopolitics, and the governance of life and death, 11(10), e12329.
- Bonan, G. B. J. s. (2008) Forests and climate change: forcings, feedbacks, and the climate benefits of forests, 320(5882), 1444-1449.
- Broughton, R. K., Bullock, J. M., George, C., Hill, R. A., Hinsley, S. A., Maziarz, M., Melin, M., Mountford, J. O., Sparks, T. H. & Pywell, R. F. (2021) Long-term woodland restoration on lowland farmland through passive rewilding. *Plos one*, 16(6), e0252466.
- Brown, S. (1997) Estimating Biomass and Biomass Change of Tropical Forests: A Primer. *Food and Agriculture Organization of the United Nations*, 134.
- Burrell, N., Jeffers, E., Macias-Fauria, M., & Willis, K. (2023). Data from: The inadequacy of current carbon storage assessment methods for rewilding: A Knepp Estate case study. *Dryad Digital Repository* <https://doi.org/10.5061/dryad.76hdr7t3>
- Bytnerowicz, A., Omasa, K. & Paoletti, E. (2007) Integrated effects of air pollution and climate change on forests: A northern hemisphere perspective. *Environmental Pollution*, 147(3), 438-445.
- Ceaşu, S., Hofmann, M., Navarro, L. M., Carver, S., Verburg, P. H. & Pereira, H. M. J. C. B. (2015) Mapping opportunities and challenges for rewilding in Europe, 29(4), 1017-1027.
- Centre for Ecology and Hydrology (2004). *PLANTATT - Attributes of British and Irish Plants - Spreadsheet*. Huntingdon: Centre for Ecology and Hydrology.
- Cerqueira, Y., Navarro, L. M., Maes, J., Marta-Pedroso, C., Pradinho Honrado, J. & Pereira, H. M. (2015) Ecosystem Services: The Opportunities of Rewilding in Europe, in Pereira, H. M. &

- Navarro, L. M. (eds), *Rewilding European Landscapes*. Cham: Springer International Publishing, 47-64.
- Chave, J., Andalo, C., Brown, S., Cairns, M. A., Chambers, J. Q., Eamus, D., Fölster, H., Fromard, F., Higuchi, N. & Kira, T. J. O. (2005) Tree allometry and improved estimation of carbon stocks and balance in tropical forests, 145, 87-99.
- Chave, J., Réjou-Méchain, M., Búrquez, A., Chidumayo, E., Colgan, M. S., Delitti, W. B., Duque, A., Eid, T., Fearnside, P. M. & Goodman, R. C. J. G. c. b. (2014) Improved allometric models to estimate the aboveground biomass of tropical trees, 20(10), 3177-3190.
- Churski, M., Charles-Dominique, T., Bubnicki, J. W., Jędrzejewska, B., Kuijper, D. P. & Cromsigt, J. P. (2022) Herbivore-induced branching increases sapling survival in temperate forest canopy gaps. *Journal of Ecology*.
- Cifuentes Jara, M., Henry, M., Réjou-Méchain, M., Wayson, C., Zapata-Cuartas, M., Piotto, D., Alice Guier, F., Castañeda Lombis, H., Castellanos López, E., Cuenca Lara, R., Cueva Rojas, K., Del Águila Pasquel, J., Duque Montoya, Á., Fernández Vega, J., Jiménez Galo, A., López, O. R., Marklund, L. G., Michel Fuentes, J. M., Milla, F., Návar Chaidez, J. J., Ortiz Malavassi, E., Pérez, J., Ramírez Zea, C., Rangel García, L., Rubilar Pons, R., Saint-André, L., Sanquetta, C., Scott, C. & Westfall, J. (2015) Guidelines for documenting and reporting tree allometric equations. *Annals of Forest Science*, 72(6), 763-768.
- Corlett, T. R. (2016) Restoration, Reintroduction, and Rewilding in a Changing World. *Trends in Ecology & Evolution*, 31(6), 453-462.
- Crawley, M. J. (2012) *The R Book*. Wiley.
- Dale, M. J. J. U. m. (2013) Evaluation of methods for quantifying carbon storage of urban trees in New Zealand.
- Department for Environment, F. R. A. (2021) *The England Trees Action Plan 2021-2024*. UK:
- Di Sacco, A., Hardwick, K. A., Blakesley, D., Brancalion, P. H. S., Breman, E., Cecilio Rebola, L., Chomba, S., Dixon, K., Elliott, S., Ruyonga, G., Shaw, K., Smith, P., Smith, R. J. & Antonelli, A. (2021) Ten golden rules for reforestation to optimize carbon sequestration, biodiversity recovery and livelihood benefits. *Global Change Biology*, 27(7), 1328-1348.
- Doick, K., Handley, P., Ashwood, F., Monteiro, M. V., Frediani, K. & Rogers, K. (2017) Valuing Edinburgh's Urban Trees: An update to the 2011 i-Tree Eco survey-a report of Edinburgh City Council and Forestry Commission Scotland. Forest Research, Farnham.
- Fernández, N., Navarro, L. M. & Pereira, H. M. (2017) Rewilding: A Call for Boosting Ecological Complexity in Conservation. *Conservation Letters*, 10(3), 276-278.
- Garrido, P., Edenius, L., Mikusiński, G., Skarin, A., Jansson, A. & Thulin, C. G. (2021) Experimental rewilding may restore abandoned wood-pastures if policy allows. *Ambio*, 50(1), 101-112.
- Gill, R. M. & Fuller, R. J. J. I. (2007) The effects of deer browsing on woodland structure and songbirds in lowland Britain, 149, 119-127.

- Globalometree (2017) *Globalometree: Assessing volume, biomass and carbon stocks of trees and forests*, 2017. Available online: <http://www.globalometree.org/> [Accessed February 2023].
- Grove, A. T. & Rackham, O. (2001). *The Nature of Mediterranean Europe. An Ecological History*.
- Harden, G. J. (1990) *Flora of New South Wales*, 4UNSW Press.
- Hodder, K. H., Newton, A. C., Cantarello, E. & Perrella, L. (2014) Does landscape-scale conservation management enhance the provision of ecosystem services? *International Journal of Biodiversity Science, Ecosystem Services & Management*, 10(1), 71-83.
- Hutchings, T., Lawrence, V. & Brunt, A. (2012) Estimating the ecosystem services value of Edinburgh's trees. *The Research Agency of Forest Commission*, 45.
- i-Tree (2021) *i-Tree Eco User's Manual*, 2021. Available online: https://www.itreetools.org/documents/275/EcoV6_UsersManual.2021.09.22.pdf [Accessed March 2023].
- Jepson, P. J. E. (2016) A rewilding agenda for Europe: creating a network of experimental reserves, 39(2).
- Johnson, O. (2004) *Collins tree guide* Harper Collins Publishers.
- Keesstra, S., Nunes, J., Novara, A., Finger, D., Avelar, D., Kalantari, Z. & Cerdà, A. (2018) The superior effect of nature based solutions in land management for enhancing ecosystem services. *Science of the Total Environment*, 610-611, 997-1009.
- Ketterings, Q. M., Coe, R., van Noordwijk, M., Palm, C. A. J. F. E. & management (2001) Reducing uncertainty in the use of allometric biomass equations for predicting above-ground tree biomass in mixed secondary forests, 146(1-3), 199-209.
- Litton, C. M. & Boone Kauffman, J. J. B. (2008) Allometric models for predicting aboveground biomass in two widespread woody plants in Hawaii, 40(3), 313-320.
- Ma, J., Li, X., Baoquan, J., Liu, X., Li, T., Zhang, W., Liu, W. J. U. F. & Greening, U. (2021) Spatial variation analysis of urban forest vegetation carbon storage and sequestration in built-up areas of Beijing based on i-Tree Eco and Kriging, 66, 127413.
- Manual, i.-T. (2020) US Forest Service. i-Tree Eco User's Manual v.6.0.
- Matthews, R. (2017) 11. Forest carbon and biomass policy. *Forest Research Impact Case Studies*, 85.
- Matthews, R. W. & Mackie, E. D. (2006) *Forest mensuration: a handbook for practitioners* Forestry Commission.
- Mayer, S., Smith, J., & Johnson, R (2017) Effects of Grazing Pressure on the Allometric Relationship between Diameter at Breast Height and Height in Trees: A study on Trees growing Without Grazing Pressure. *Forest Ecology and Management*, 389, 198-204.
- Meli, P., Holl, K. D., Rey Benayas, J. M., Jones, H. P., Jones, P. C., Montoya, D. & Moreno Mateos, D. J. P. o. (2017) A global review of past land use, climate, and active vs. passive restoration effects on forest recovery, 12(2), e0171368.

- Mikołajczak, K. M., Jones, N., Sandom, C. J., Wynne-Jones, S., Beardsall, A., Burgelman, S., Ellam, L., Wheeler, H. C. J. P. & Nature (2022) Rewilding—The farmers' perspective. Perceptions and attitudinal support for rewilding among the English farming community, 4(6), 1435-1449.
- Mokany, K., Raison, R. J. & Prokushkin, A. S. J. G. c. b. (2006) Critical analysis of root: shoot ratios in terrestrial biomes, 12(1), 84-96.
- Monteiro, M. V., Handley, P. & Doick, K. J. (2019) An insight to the current state and sustainability of urban forests across Great Britain based on i-Tree Eco surveys. *Forestry: An International Journal of Forest Research*, 93(1), 107-123.
- Morani, A., Nowak, D., Hirabayashi, S., Guidolotti, G., Medori, M., Muzzini, V., Fares, S., Mugnozza, G. S. & Calfapietra, C. J. E. P. (2014) Comparing i-Tree modeled ozone deposition with field measurements in a periurban Mediterranean forest, 195, 202-209.
- Naundrup, P. J. & Svenning, J.-C. J. P. o. (2015) A geographic assessment of the global scope for rewilding with wild-living horses (*Equus ferus*), 10(7), e0132359.
- Navarro, L. M. & Pereira, H. M. (2015) Rewilding abandoned landscapes in Europe, *Rewilding European Landscapes* Springer International Publishing Cham, 3-23.
- Ngomanda, A., Obiang, N. L. E., Lebamba, J., Mavouroulou, Q. M., Gomat, H., Mankou, G. S., Loumeto, J., Iponga, D. M., Ditsouga, F. K., Koumba, R. Z. J. F. E. & Management (2014) Site-specific versus pantropical allometric equations: which option to estimate the biomass of a moist central African forest?, 312, 1-9.
- Nogueira, E. M. e. a. (2018) Genus- and species-specific allometric equations for estimating aboveground biomass in a tropical moist forest in Brazil. *Journal of Forestry Research*, 29(1), 261-269.
- Nowak, D. J. & Crane, D. E. J. E. p. (2002) Carbon storage and sequestration by urban trees in the USA, 116(3), 381-389.
- Nowak, D. J. (2019) Understanding i-Tree: Summary of programs and methods. *Understanding I-Tree: Summary of Programs and Methods*.
- Nowak, D. J. J. C. s. U. F. E. R. o. t. C. U. F. C. P. (1994) Atmospheric carbon dioxide reduction by Chicago's urban forest, 83-94.
- Nowak, D. J., Crane, D. E., Stevens, J. C., Hoehn, R. E., Walton, J. T. & Bond, J. (2008) A ground-based method of assessing urban forest structure and ecosystem services. *Arboriculture and Urban Forestry*, 34(6), 347-358.
- Nowak, D. J., Maco, S. & Binkley, M. J. A. C. (2018) i-Tree: Global tools to assess tree benefits and risks to improve forest management, 51(4), 10-13.
- Ockendon, N., Thomas, D. H. L., Cortina, J., Adams, W. M., Aykroyd, T., Barov, B., Boitani, L., Bonn, A., Branquinho, C., Brombacher, M., Burrell, C., Carver, S., Crick, H. Q. P., Duguay, B., Everett, S., Fokkens, B., Fuller, R. J., Gibbons, D. W., Gokhleshvili, R., Griffin, C., Halley, D. J., Hotham, P., Hughes, F. M. R., Karamanlidis, A. A., McOwen, C. J., Miles, L., Mitchell, R., Rands, M. R. W., Roberts, J., Sandom, C. J., Spencer, J. W., ten Broeke, E., Tew, E. R., Thomas, C. D., Timoshyna, A., Unsworth, R. K. F., Warrington, S. & Sutherland, W. J. (2018)

One hundred priority questions for landscape restoration in Europe. *Biological Conservation*, 221, 198-208.

Orians, C. M., Thorn, A. & Gómez, S. (2011) Herbivore-induced resource sequestration in plants: why bother? *Oecologia*, 167(1), 1-9.

Pati, P. K., Kaushik, P., Khan, M., Khare, P. J. T., *Forests & People* (2022) Allometric equations for biomass and carbon stock estimation of small diameter woody species from tropical dry deciduous forests: Support to REDD+, 9, 100289.

Paul, K. I., Roxburgh, S. H., Chave, J., England, J. R., Zerihun, A., Specht, A., Lewis, T., Bennett, L. T., Baker, T. G., Adams, M. A., Huxtable, D., Montagu, K. D., Falster, D. S., Feller, M., Sochacki, S., Ritson, P., Bastin, G., Bartle, J., Wildy, D., Hobbs, T., Larmour, J., Waterworth, R., Stewart, H. T. L., Jonson, J., Forrester, D. I., Applegate, G., Mendham, D., Bradford, M., O'Grady, A., Green, D., Sudmeyer, R., Rance, S. J., Turner, J., Barton, C., Wenk, E. H., Grove, T., Attiwill, P. M., Pinkard, E., Butler, D., Brooksbank, K., Spencer, B., Snowdon, P., O'Brien, N., Battaglia, M., Cameron, D. M., Hamilton, S., McAuthur, G. & Sinclair, J. (2016) Testing the generality of above-ground biomass allometry across plant functional types at the continent scale. *Global Change Biology*, 22(6), 2106-2124.

Pereira, H. M., Navarro, L. M., Martins, I. S. J. A. R. o. E. & *Resources* (2012) Global biodiversity change: the bad, the good, and the unknown, 37, 25-50.

Perkovich, C. & Ward, D. (2021) Aboveground herbivory causes belowground changes in twelve oak *Quercus* species: a phylogenetic analysis of root biomass and non-structural carbohydrate storage. *Oikos*, 130(10), 1797-1812.

Perkovich, C., Ward, D. J. E. & *Evolution* (2021) Herbivore-induced defenses are not under phylogenetic constraints in the genus *Quercus* (oak): Phylogenetic patterns of growth, defense, and storage, 11(10), 5187-5203.

Picard, N., Saint-André, L. & Henry, M. (2012) Manual for building tree volume and biomass allometric equations: from field measurement to prediction. *Manual for Building Tree Volume and Biomass Allometric Equations: From Field Measurement to Prediction*.

Qian, W., Zhang, Z. & Ping, W. J. J. o. L. R. (2019) An Assessment of Ecosystem Services of Urban Green Spaces Based on i-Tree, 11(1).

Randle, T. & Jenkins, T. (2011) The construction of lookup tables for estimating changes in carbon stocks in forestry projects. *A background document for users of the Forestry Commissions's Woodland Carbon Code*.

Raum, S., Hand, K., Hall, C., Edwards, D., O'brien, L., Doick, K. J. L. & Planning, U. (2019) Achieving impact from ecosystem assessment and valuation of urban greenspace: The case of i-Tree Eco in Great Britain, 190, 103590.

Rewilding-Britain (2020) Reforesting Britain - Why natural regeneration should be our default approach to woodland expansion.

Sandom, C., Wynne-Jones, S., Pettorelli, N., Durant, S. & Du Toit, J. J. R. (2019) Rewilding a country: Britain as a study case, 222-247.

- Seddon, P. J., Griffiths, C. J., Soorae, P. S. & Armstrong, D. P. J. S. (2014) Reversing defaunation: restoring species in a changing world, 345(6195), 406-412.
- Snowdon, P., Eamus, D., Gibbons, P., Khanna, P., Keith, H., Raison, J. & Kirschbaum, M. (2000) Synthesis of allometrics, review of root biomass and design of future woody biomass sampling strategies. *Synthesis of Allometrics, Review of Root Biomass and Design of Future Woody Biomass Sampling Strategies*.
- Stutter, M. I., Chardon, W. J. & Kronvang, B. (2012) Riparian buffer strips as a multifunctional management tool in agricultural landscapes: Introduction. *Journal of Environmental Quality*, 41(2), 297-303.
- Team, R. (2022) *RStudio: Integrated Development Environment for R*. Boston, MA. Available online: <http://www.rstudio.com/> [Accessed January 2023].
- Tree, I. (2017) The Knepp wildland project. *Biodiversity*, 18(4), 206-209.
- Tree, I. (2018) *Wilding: The return of nature to a British farm* Pan Macmillan.
- Van Uytvanck, J., Van Noyen, A., Milotic, T., Decler, K. & Hoffmann, M. J. J. f. N. C. (2010) Woodland regeneration on grazed former arable land: A question of tolerance, defence or protection?, 18(3), 206-214.
- Vera, F. J. T. I. c. A., flanders, s. i. & the Netherlads (2000) Giving the land back to nature: Nature development in the Netherlands.
- Vorster, A. G., Evangelista, P. H., Stovall, A. E., Ex, S. J. C. B. & Management (2020) Variability and uncertainty in forest biomass estimates from the tree to landscape scale: the role of allometric equations, 15, 1-20.
- Wickham, H. (2016) *ggplot2: Elegant Graphics for Data Analysis* Springer-Verlag New York.
- Zhu, Q. e. a. (2016) Comparison of genus- and species-specific allometric equations for estimating aboveground biomass of subtropical trees. *Forest Ecology and Management*, 361, 411-421.

2.7 Supplementary Materials

Table S2.1: Landcover classes observed in the Southern Block of the Knepp rewilding project in 2021, illustrating the vegetation cover that has emerged due to the rewilding efforts. Classes chosen for i-Tree sampling are marked with asterisks.

Sallow Dominated*	Closed canopy sallow (<i>Salix sp.</i>)
Open Sallow Scrubland*	Open grown sallow (<i>Salix sp.</i>)

Browsed Sallow*	Cattle, ponies, and deer browse the sallow (<i>Salix sp.</i>) as a result the height is kept at browse height (<2.5 m). Sallow (<i>Salix sp.</i>) dominates this landscape.
Bramble	Arable reversion or grassland with patches of bramble (<i>Rubus fruticosus</i>). Dominated by bramble (>50% coverage), interspersed with other woody plant species.
Bramble with Maiden trees	Dominated by bramble (<i>Rubus fruticosus</i>) but with more frequent numbers of sallow (<i>Salix sp.</i>), oak (<i>Quercus robur</i>) and other trees.
Arable reversion to grassland	Areas that were left to be colonised by plants from stubble – last harvest.
Permanent pasture	Land dominated by grasses (>80% coverage).
Improved Grassland	Areas that have been seeded specifically for higher yielding lays.
Injurious weeds topped grassland	The areas around the Knepp boundary that are topped with an agricultural mower.
Open Thorn Scrub*	Patch-like structures of hawthorn (<i>Crataegus monogyna</i>), dog rose (<i>Rosa canina</i>), bramble (<i>Rubus fruticosus</i>), blackthorn (<i>Prunus spinosa</i>) – showing no real dominance of any particular species of thorn. There can be oaks (<i>Quercus sp.</i>) birch (<i>Betula sp.</i>), sallow (<i>Salix sp.</i>) protected by these patches.
Plantations, woodland*	Areas that have been planted by trees, including mixed woodland, eucalypt (<i>Eucalyptus sp.</i>) and conifers.
Alder dominated	Areas dominated by alder (<i>Alnus sp.</i>).

Table S2.2: Destructive samples (n=39) of individual trees and shrubs sourced from the Southern Block of the Knepp rewilding project. Listed samples include their common name, measured aboveground biomass (AGB), and belowground biomass

(BGB). i-Tree predictions of BGB are derived from the actual AGB weight, using a factor of 0.26 to represent the anticipated root:shoot ratio.

ID number	species	AGB (g)	BGB (g)	i-Tree 0.26
EMB023	blackthorn	1668.35	498.66	433.771
EMB039	blackthorn	223.51	145.29	58.1126
EMB041	blackthorn	95.98	65.33	24.9548
EMB045	blackthorn	44.78	92.92	11.6428
EMB048	blackthorn	3274.68	903.83	851.4168
EMB070	blackthorn	3282.97	873.1	853.5722
EMD091	dogrose	622.57	612.21	161.8682
EMD126	dogrose	172.05	612.21	44.733
EMD128	dogrose	528.02	369.8	137.2852
EMO033	oak	46.29	72.32	12.0354
EMO100	oak	680.46	332.71	176.9196
EMO102	oak	56.1	45.42	14.586
EMO107	oak	186.09	155.9	48.3834
ESB007	blackthorn	18.66	19.84	4.8516
ESB021	blackthorn	44.22	33.78	11.4972
ESB031	blackthorn	24.66	10.57	6.4116
ESB032	blackthorn	17.05	25.46	4.433
ESB062	blackthorn	19.54	100.87	5.0804
ESB066	blackthorn	31.63	24.93	8.2238
ESD025	dogrose	52.81	46.38	13.7306
ESH036	hawthorn	29.99	22.45	7.7974
ESH040	hawthorn	178.57	107.27	46.4282
ESH044	hawthorn	94.87	46.18	24.6662
ESH084	hawthorn	208.895	229.845	54.3127
ESH085	hawthorn	10.44	16.56	2.7144
ESO011	oak	89.26	70.1	23.2076
ESO067	oak	87.58	152.445	22.7708
PMB025	blackthorn	66.41	34.66	17.2666
PMB143	blackthorn	31.51	61.48	8.1926
PMD013	dogrose	30.48	18.95	7.9248
PMO013	oak	158.56	140.35	41.2256
PMO017	oak	81.39	36.54	21.1614
PMS007	sallow	779.75	462.92	202.735
PSB018	blackthorn	95.09	79.24	24.7234
PSB020	blackthorn	59.27	24.89	15.4102
PSH007	hawthorn	6.11	10.79	1.5886
PSO012	oak	59.15	39.5	15.379
PSO019	oak	105.27	114.49	27.3702
PSO020	oak	125.065	157.08	32.5169

Chapter 3: Quantifying Carbon Storage in Rewilded Scrubland: Developing Allometric Equations through Destructive Sampling

Nancy C. Burrell¹, Marc Macias-Fauria², Elizabeth Jeffers¹, Katherine J. Willis¹

¹Department of Biology, University of Oxford, Oxford, UK

²Scott Polar Research Institute, Department of Geography, University of Cambridge, Cambridge, UK

Author contribution statement: Nancy C. Burrell led the study's conceptualisation, methodology, data analysis, and drafting, serving as project lead. Kathy J. Willis and Elizabeth S. Jeffers provided supervision, contributed to methodology design, and edited the manuscript. Marc Macias-Fauria validated the equations, offered additional supervision, and reviewed the final draft.

To be submitted for publication.

3.0 Abstract

Scrubland plants provide habitat for many species and support higher levels of productivity in times of stress. However, their carbon storage potential, particularly in temperate regions like the UK, remains understudied. Existing carbon accounting methods, calibrated using closed-canopy woodland systems and agroforestry models, fail to account for the complex growth patterns of scrub. Unlike single-stemmed forest trees, scrub species often have multi-stemmed structures that occupy space more densely and allocate a greater proportion of biomass belowground. Herbivory has also been shown to significantly influence these patterns by driving increased root investment for resilience (Perkovich & Ward, 2021). Observed root:shoot ratios have revealed in previous work that scrub species may allocate more biomass to roots than current models predict, underscoring the need for revised frameworks (Axe et al., 2017; Mokany et al., 2006). Lack of understanding of these factors represents a significant knowledge gap in the determination of carbon storage of scrubland species. This study aimed to address these gaps by developing taxon-specific allometric equations for five dominant scrub taxa at the rewilded Knepp Estate, incorporating height, canopy area, tree diameter, and a browsing metric. These models showed strong predictive accuracy ($R^2 = 0.63\text{--}0.95$) for above- and belowground biomass. The output offers a new quantitative method to calculate carbon offsets associated with temperate scrub ecosystems, highlighting their carbon storage potential and advocating for their inclusion in global carbon assessment strategies.

Key words: allometry, biomass allocation, root:shoot ratio, rewilding, scrubland, carbon stock

3.1 Introduction

The ecological benefits of rewilded scrubland, such as enhanced biodiversity, habitat restoration, and ecosystem resilience, are well-documented (Mikolajczak et al., 2022; Sandom et al., 2019; Cerqueira et al., 2015). Herbivores play a pivotal role in shaping these landscapes, promoting diverse habitats through browsing and grazing dynamics (Schmitz et al., 2023; Bakker & Svenning, 2018; Tree, 2018; Vera, 2000; Sandom et al., 2013). However, despite these well-established ecological values, the carbon storage potential of rewilded scrubland remains significantly understudied (Malhi et al., 2022; Sandhage-Hofmann et al., 2021; Berzaghi et al., 2023).

While woodland growth and agroforestry systems have received substantial attention for their carbon sequestration potential (Griscom et al., 2017; Bastin et al., 2019; Buotte et al., 2020; Saatchi et al., 2011), this has led to an over-reliance on models calibrated for closed-canopy forests and single-stem tree systems. These models fail to account for the unique growth forms and biomass allocation strategies of scrub species, which often exhibit multi-stemmed structures and allocate a higher proportion of biomass to roots (Perkovich & Ward, 2021; Wiley et al., 2017). As a result, scrubland ecosystems have been largely overlooked in carbon accounting frameworks, despite their potential contributions to carbon sequestration, particularly in regions undergoing rewilding (Mercer & Gregg, 2023; Burrell et al., 2024).

This research gap is particularly pronounced in the UK, where no published data currently quantifies the carbon stored in rewilded scrubland ecosystems (see Chapter 2). This lack of baseline data makes it difficult to assess the potential for these landscapes to contribute to carbon capture on a meaningful scale. Addressing this gap is essential not only for improving

the accuracy of carbon storage estimates but also for integrating scrublands into natural capital frameworks and conservation strategies, which are increasingly focused on mitigating climate change (La Notte., 2024; Nelson et al., 2009).

Previous work to understand the carbon storage potential of closed canopy woodland (Brown & Lugo, 1984; Chave et al., 2005; Picard et al., 2012) has typically made estimations based on biomass equations computed from destructive sampling. This approach uses measurable variables such as tree height (h) and diameter at breast height (dbh) to estimate biomass (Parresol, 1999) and has been used for both Tropical and Temperate woodland. For example, Chave et al. (2005) developed widely used allometric equations for tropical forests, incorporating variables such as wood density, dbh and height to infer biomass. In the UK, the main method for estimating temperate woodland carbon storage is the Woodland Carbon Code (WCC), devised in 2011 by the UK Forestry Commission (Randle & Jenkins, 2011). This method involves the use of carbon lookup tables derived from samples obtained from predominantly closed-canopy forestry plantations (Forestry Commission, 2011). The belowground biomass estimates are based on root:shoot ratios (Cairns et al., 1997; Jackson et al., 1996).

While these methods are well-established for estimating carbon storage in open woodlands with large trees, forestry plantations, and closed-canopy forests (Zianis et al., 2005; Jenkins et al., 2003; Brown et al., 1997; Chave et al., 2005), they are less suited for assessing carbon storage in more open landscapes and, particularly, in woody shrubs (as discussed in Chapter 2; Burrell et al., 2024). This limitation arises because these shrubs often have smaller, multi-stemmed, and irregularly shaped trunks that differ significantly from the typical structure of plantation trees.

Several studies have attempted to estimate carbon storage for woody scrubs in various biomes by using allometric models to estimate both above-ground and below-ground biomass. For example, Siddiq et al. (2021) developed models to predict the aboveground and belowground biomass for scrub species like *Acacia modesta* and *Olea ferruginea* in subtropical scrub forests in Pakistan. Another example is provided by Kühn et al. (2023), who investigated root trait variation in the Cape Floristic Region, demonstrating that shrub roots increase in size, particularly in length, as an adaptation to drought resistance and resource conservation in arid environments. One of the key findings from these studies is that the carbon storage capacity of scrubland ecosystems, particularly when taking into account belowground biomass, is often underestimated. For instance, the roots of woody species, particularly in semi-arid ecosystems, where many plants need to develop systems to access water and nutrients deep below ground, showed higher carbon storage potential than their aboveground parts (Saddiq et al., 2021; Schenk & Jackson, 2002; Schenk, 2005). Indeed, in such areas, some studies demonstrated that belowground biomass (BGB) can store substantial amounts of carbon, even surpassing aboveground biomass (AGB) in some cases (Erkin et al., 2023; Ranjan et al., 2022; Cairns et al., 1997; Jackson et al., 1996). Such examples highlight the importance of tailored allometric models to fully capture the carbon dynamics of scrubland ecosystems. This is because scrublands can often exhibit several carbon-intensive processes that enhance their role as carbon sinks. One notable characteristic, for example, is the adaptation of woody plants in scrublands to browsing pressure. When browsing animals are present, research has shown that plants often respond by producing new shoots above ground and increased root growth below ground as a survival mechanism. For example, Churski et al. (2022) explored how herbivore browsing in temperate forest canopy gaps in Białowieża Forest in Poland/Belarus induced the growth of multiple branches in saplings, increasing their lateral spread and

structural complexity, and promoting root growth to increase the plant's stability and acquisition of resources. Smit et al. (2015) found that herbivory in the Oostvaardersplassen nature reserve in the Netherlands led to a shift in resource allocation from aboveground biomass (AGB) to belowground biomass (BGB), as the plants invested more in their root systems to recover from browsing stress.

The same response is found in trees and shrubs subjected to forms of human management that, essentially, mimic the actions of browsing animals. For example, Axe et al. (2017) found that woody species in hedgerows in England which had been mechanically trimmed responded by allocating significant biomass to the root system, contributing to both the health of the plants and the carbon storage capacity of the hedgerow. Similarly, under controlled laboratory conditions, Perkovich and Ward (2021) found that mimicking herbivory by pruning different species of oak (*Quercus spp.*) triggered substantial root growth.

The reallocation of a woody plant's resources into root growth under herbivory (and similarly under human trimming and coppicing) is significant because belowground biomass, particularly root systems, plays a critical role in long-term carbon storage. Roots tend to have slower decomposition rates compared to aboveground plant matter, leading to more stable carbon storage (Jackson et al., 1996; Jobbágy and Jackson, 2000). Scrubland ecosystems, despite their modest aboveground appearance, may play a more significant role in carbon sequestration than previously assumed (Stephenson et al., 2014; Lutz et al., 2018; Slik et al., 2013) due to their substantial belowground carbon storage capacity, underscoring their importance in global carbon sequestration efforts.

What emerges from the research discussed above is a significant knowledge gap regarding the relative allocation of aboveground (AGB) and belowground biomass (BGB) in rewilded

and grazed landscapes containing scrubland species. Existing carbon storage models, designed for closed-canopy forests and single-stem systems, fail to capture the unique growth dynamics of scrub species, which often allocate a higher proportion of biomass below ground in response to environmental stressors like herbivory or pruning (Perkovich & Ward, 2021; Axe et al., 2017). In the UK, this gap is particularly pronounced, with no baseline data quantifying carbon storage in rewilded scrublands, despite their ecological and climate mitigation potential (Schmitz et al., 2023; Burrell et al., 2024).

The aim of this research was to address this gap by developing scrub-specific allometric equations using data from the rewilded scrubland at the Knepp Estate. A novel destructive sampling methodology is employed to directly measure AGB and BGB and determine their relationship under different browsing intensities. This approach builds on techniques used in other biomes (Saddiq et al., 2021) but adapts them to temperate scrub systems influenced by herbivory. By filling this gap, the study improves the accuracy of carbon storage estimates for scrub ecosystems, highlighting their overlooked potential as carbon sinks and supporting their integration into natural capital frameworks and climate mitigation strategies.

3.2 Materials and Methods

Five key taxa (hawthorn (*Crataegus spp.*), dog rose (*Rosa canina*), blackthorn (*Prunus spinosa*), oak (*Quercus spp.*), and willow (*Salix spp.*)) that dominate the rewilded vegetation composition in the temperate landscape of Knepp Wildland were examined. To achieve this, I addressed three interlinked methods:

1. Determination of the above and below ground biomass of 5 dominant woody scrubland taxa growing on the Knepp Estate.
2. Development of a scrub-specific allometric-based model for the above- and below-ground biomass within a rewilded landscape.
3. Improve understanding of the impact of browsing on the biomass allocation of rewilding scrubland.

3.2.1 Site Location and Sample Selection

The research was conducted in the "Southern Block" of the Knepp Estate, located in West Sussex, UK (coordinates: 50.975781°N, 0.344819°W) (Figure 3.1). The estate transitioned from traditional farming to rewilding initiatives beginning in 2001 (Tree, 2018). Prior to this shift, the Knepp Estate operated under a mixed farming system, focusing primarily on intensive arable and dairy production. The cessation of farming activities in the Southern Block between 2001 and 2006 initiated a fallow period, allowing natural vegetation to regenerate (Tree, 2018). The arable fields were simply left 'open', as stubble, after their last harvest, providing receptive ground for the seed rain from surrounding hedgerows and trees. The natural regeneration here, compared to other areas of the Estate (the Middle and Northern Blocks) that were under permanent grassland (which tends to repress the colonisation of woody shrubs), has been swift and prolific, resulting in an open wood pasture system with

regenerating scrub species such as *Prunus spinosa*, *Salix spp.*, *Quercus spp.*, *Crataegus spp.*, and *Rubus spp.* (Tree, 2018; Burrell et al., 2024).

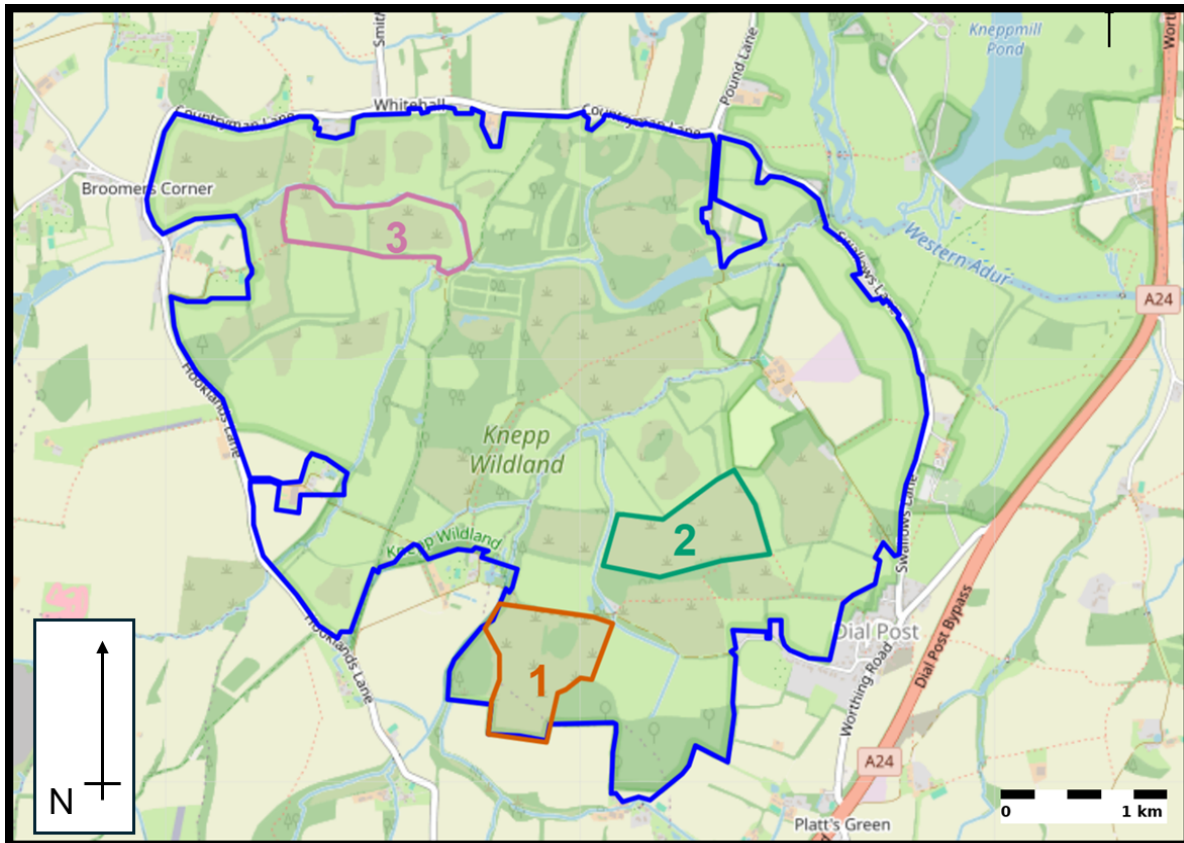


Figure 3.1: The Southern Block of the Knepp Estate (50.975781°N, 0.344819°W), showing the three possible sampling site locations (1-3) that were selected based on their heterogeneous land-cover classification. The blue area is the Southern

It was not until 2009 that large herbivores, including old English longhorn cattle (*Bos primigenius taurus*), Exmoor ponies (*Equus ferus caballus*), fallow deer (*Dama dama*), and Tamworth pigs (*Sus scrofa domesticus*), were introduced into the Southern Block to manage the vegetation (Bunzel-Druke, 2001, Tree, 2018). The hiatus of several years without significant herbivory (just very low numbers of rabbits (*Oryctolagus cuniculus*) and roe deer (*Capreolus capreolus*)) gave the emerging woody shrubs and saplings a chance to establish and invest in their defences before the introduction of the large browsers (Tree, 2018). Red deer (*Cervus*

elaphus) were introduced later, in 2013, when it was judged the scrubland vegetation was robust enough for some additional heavy browsers.

For this study, a 13-hectare plot within the Southern Block was randomly selected from three potential areas (plot 1–3) chosen for their heterogeneous land cover types (see Chapter 2). These plots were designated to examine the effects of browsing on biomass distribution. The selection of plot 1 was done randomly using the 'sample' function in R (R Core Team, 2024).

The sampling strategy aimed to capture the spatial diversity of land cover types and adequately represent different tree/shrub sizes as well as two different browsing conditions (exposed – freestanding, growing away from bramble (*Rubus fruticosus*), and protected – growing within a bramble patch). Within the selected site, the five dominant scrub taxa at the Knepp Estate (Ryland, 2015; Burrell et al., 2024)—oak (*Quercus spp.*), willow (*Salix spp.*), hawthorn (*Crataegus spp.*), blackthorn (*Prunus spinosa*), and dog rose (*Rosa canina*)—were selected from a range of heights to minimise bias in biomass estimates. Species identification was conducted using PlantATT (Centre for Ecology and Hydrology, 2004) and the Collins Tree Guide (Johnson, 2004). Hereafter, these species will be referred to as *Quercus spp.*, *Salix spp.*, *Crataegus spp.*, *Prunus spinosa*, and *Rosa canina*, or by their common names: oak, willow, hawthorn, blackthorn, and dog rose.

Willow is represented by a complex of two species and their hybrid, with the hybrid *Salix × reichardtii* being the most common, followed by the frequent parent *Salix cinerea* subsp. *oleifolia*, and the less abundant parent *Salix caprea* subsp. *caprea*. Oak is predominantly represented by the locally dominant *Quercus robur*, with occasional individuals of the hybrid *Quercus × rosacea*; while *Quercus petraea* was not recorded, it is possible they were planted historically at Knepp. Dog rose is primarily *Rosa canina s.s.*, although other species like *Rosa stylosa* and *Rosa*

arvensis were not observed during this survey. Hawthorn is identified as *Crataegus monogyna* s.s., and while *Crataegus laevigata* and other taxa may have been introduced in farmland hedgerows, they were absent from the study area. Blackthorn, identified as *Prunus spinosa*, completes the composition. All species identifications were verified by M.J. Crawley (2024).

In this study, scrubland is defined following Harden (1990) as areas dominated by shrubs, which are woody plants that typically do not exceed 5 m in height when single-stemmed or 8 m when multi-stemmed. Many shrubs within this category are thorny and subject to browsing by animals (Harden, 1990).

3.2.2. Individual Tree /Shrub Selection and Sample Collection Process

The collection phase occurred during the dormant periods from 2021 to 2024, when deciduous trees were leafless, and the young shoots had matured. The dormant season, which spanned from October to April, provided an ideal time for sampling before leaf emergence. Individuals were sampled without leaves in order to cause minimum disturbance to nesting wildlife.

A total of 3,300 scrub individuals were identified within study plot 1 (Figure 3.2A), from which 270 were randomly selected for destructive sampling (Figure 3.2B). The size classification was categorised into three distinct height classes: small (< 75 cm), medium (75 – 210 cm), and large (> 210 cm). This classification was informed by a preliminary size profile conducted at the sample site during the random tree collection phase. This was done to insure a representative distribution of scrub sizes for the destructive sampling population. For large "exposed" oak (*Quercus spp.*), random selection could not be performed due to the lower frequency of such individuals, given the age of the rewilding project (<20 years).



Figure 3.2: The left panel shows the 3,300 possible individual scrub taxa, including Blackthorn (*Prunus spinosa*), Dog rose (*Rosa canina*), Hawthorn (*Crataegus monogyna*), Sallow (*Salix* spp.), and Oak (*Quercus* spp.). The right panel displays the randomly selected samples to be destructively sampled for each taxon chosen from the initial pool under the specified browsing conditions.

3.2.3 Destructive sampling

Destructive sampling involves the direct measurement of plant material by extracting entire plants or representative samples from various components (Thomas and Martin, 2012; Eamus et al., 2000). This method provides detailed insights into carbon content and biomass distribution, yielding accurate estimates of carbon storage (Picard et al., 2012). Destructive sampling is the foundation upon which allometric models are built, allowing simple, scalable measurements—such as diameter, height, and canopy area—to predict total biomass (Chave et al., 2005). However, because destructive sampling is time-intensive and labour-demanding, studies often limit the number of samples to balance accuracy with feasibility. For instance, Axe et al. (2017) conducted destructive sampling on 15 hedgerow trees to develop allometric equations. Similarly, Huynh et al. (2021) destructively sampled 30 *Acacia mangium* trees to establish biomass models. This study significantly advances this approach by conducting an unprecedented number of destructive samples ($n = 270$) across multiple taxa ($n = 5$), providing a robust dataset to develop accurate and taxa-specific equations for rewilded scrub ecosystems. Furthermore, it allows for the examination of spatial carbon distribution within a landscape (Chave et al., 2005). The destructive sampling fieldwork was carried out following Walker et al., (2016) and the ICRAF 'Guidelines for establishing regional allometric equations for biomass estimation through destructive sampling' (2011).

3.2.4 Field sampling

Each selected tree/shrub was assigned a unique identification number (ID) and a specific protocol was followed (see Figure 3.3). This involved clearing the area around the individual of existing vegetation to prevent contamination from non-sample material. Crown diameter

(CD) was measured in two perpendicular directions, and the average crown diameter and canopy area (CA, cm²) were calculated using the equation previously used by Huynh et al., (2021):

$$CA = \frac{\pi g^2}{4} \text{ where, } g \text{ is average crown girth (cm)}$$

[1]

Above-ground height (cm) was recorded as part of this study, alongside diameter at breast height (dbh), which is a standard metric for estimating tree biomass (Ngomanda et al., 2014). This measurement is widely used in forest systems because it is relatively easy to obtain and strongly correlates with overall biomass in mature, single-stemmed forest trees (Picard & Henry, 2012). However, applying this method to scrub, which often have multi-stemmed growth forms and shorter heights, presents challenges. In forest systems, dbh is measured at a height of 1.37 m, yet 90.74% of the scrub sampled in this study were shorter than this threshold, making traditional dbh measurements impractical. To address this, I measured stem diameter at the base, following the guidelines outlined in the i-Tree Eco manual (2020), which permits diameter measurements at ground level when the standard dbh height is not applicable.

For individuals with multiple stems, I followed the multi-stem measurement protocol outlined in the i-Tree Eco Manual (2020). According to this guideline, stems branching above ground are considered part of the same tree, and up to six of the largest stems should be measured separately at ground level. However, in cases where trees had more than six stems—accounting for 56% of the sample population—I measured all stems. If the pith union

was below ground, each stem was treated as an individual tree. For multi-stemmed trees, the combined girth at the base was calculated using the following formula:

$$\sqrt{(g1^2 + g2^2 + g3^2 + \dots)}$$

[2]

To maintain clarity, I use the term diameter at base height (dbh) as a comparative measurement for other allometric equations. For trees shorter than 1.5 meters (56% of the sample population), the girth measurement was taken at the base of the tree. Within the context of this study, “dbh” specifically refers to the tree’s girth measured either at its base or at breast height, depending on the size of the tree.

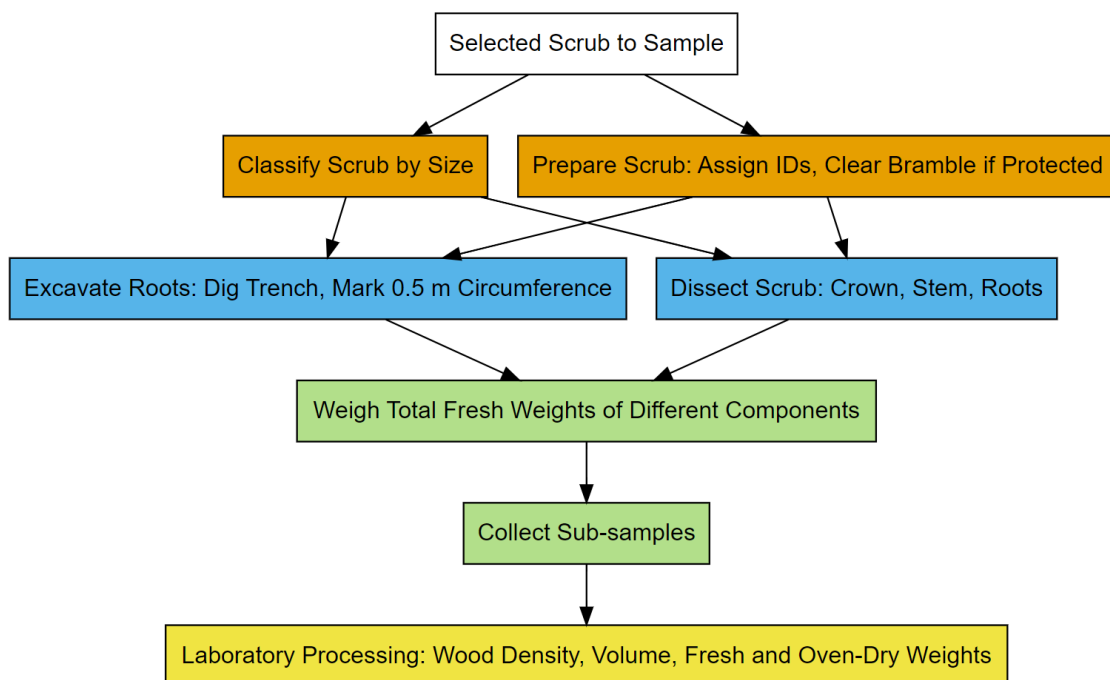


Figure 3.3: Methodology undertaken to sample aboveground biomass and belowground biomass of different scrub species.

Each tree or shrub was extracted and divided into three main components: crown, stem, and root ball, with the crown separated at the live crown base (the point where the lowest live branch begins). Root biomass sampling was standardised using a fixed-area method (Huynh et al., 2021), involving excavation within a 0.5 m radius and down to a depth of 0.5 m around each tree (Figure 3.4C). All roots within this area were collected, washed, and sorted by diameter into small (<2 mm), medium (2–10 mm), and large (>10 mm) categories (Figure 3.5B). Roots were carefully cleaned using an air pressure hose to remove soil while preserving the bark.

It is important to note that canopy projection was unconstrained, representing the full aerial spread of the tree or shrub, while root biomass was sampled within a fixed excavation area. This discrepancy between the unconstrained canopy and the constrained sampling area and depth for roots should be considered when interpreting root mass data and discussing root:shoot ratios.

After excavation, each component (crown, stem, and root ball) was weighed using either a digital crane scale with 0.02 kg precision (Figure 3.5D) or a precision balance scale with 0.005 g precision (Figure 3.5C), depending on the size of the shrub or tree (Table 3.1). Subsamples were taken from each section, including three from the above-ground portion and three from the roots, along with an age ring from the root collar for dendrochronological analysis. Chainsaw cuts were measured to estimate any sawdust loss (Figure 3.5C). Figure 3.3 describes the sample preparation and measurement process.

For larger trees that could not be transported, both above-ground and below-ground components were weighed on-site using a digital crane scale with 0.02 kg precision.

Subsamples from each part were taken, labelled, and transported to the lab for further analysis. This methodology is exemplified by Picard et al. (2012). For trees in protected areas, a mini-digger (Figure 3.6A) was used to clear *Rubus fruticosus* (bramble) from the sampling area before excavation, following the same destructive sampling protocol used for "exposed" trees (Figure 3.3).

To determine the dry biomass weight, fresh subsamples were first weighed using a precision balance (Table 3.1), then placed in paper bags (Figure 3.5A) and dried at 105°C until they reached a constant weight, typically after 72 hours (Figure 3.4B) (Picard et al., 2012). The dried subsamples were weighed immediately after removal from the oven to prevent moisture absorption from affecting the final weight. Both aboveground (AGB) and belowground (BGB) biomass weights were recorded in grams.

Wood density (ρ) was calculated for both above- and belowground components following standard methods of water displacement (Saranpää., 2003; Kallarackal & Ramirez, 2024). The volume (cm^3) of each subsample was derived from the displaced water weight, assuming water density as 1 g/cm^3 . After complete saturation in water, and the dry mass of the subsamples was obtained using the oven-drying method at a temperature of $105 \pm 5^\circ \text{C}$. The density value was determined by:

$$\text{Density}(\text{g}/\text{cm}^3) = \text{Dry Mass (g)} / \text{Volume (cm}^3)$$

Table 3.1: Description of different scales, balances, and equipment used in the field and laboratory.

<i>Digital crane scale</i>	500 kg (0.02 kg precision)	This scale is suitable for measuring the medium and large trees. The sample scrub was placed on a tarpaulin which was hooked onto the mini-digger bucket and suspended with the mounted scale.
<i>Digital balance</i>	10 kg (0.005 kg precision)	Used to weigh smaller scrub-trees and the fresh and dry weights of the sub-samples. Measurements were taken in a covered area to ensure that the wind did not affect the digital reading.
<i>Pressure hose</i>	500 L	Used to help excavate the roots and to clean off excess soil from the samples.
<i>Mini digger</i>		Used for digging trenches and to excavate scrub taxa.



Figure 3.4: Destructive sampling process in the field and in the laboratory [A] combination of the mini digger and the compressed air to extract a scrub tree; [B] samples in paper bags in ovens; [C] trench dug 0.5 m deep to extract the root ball of a larger tree.

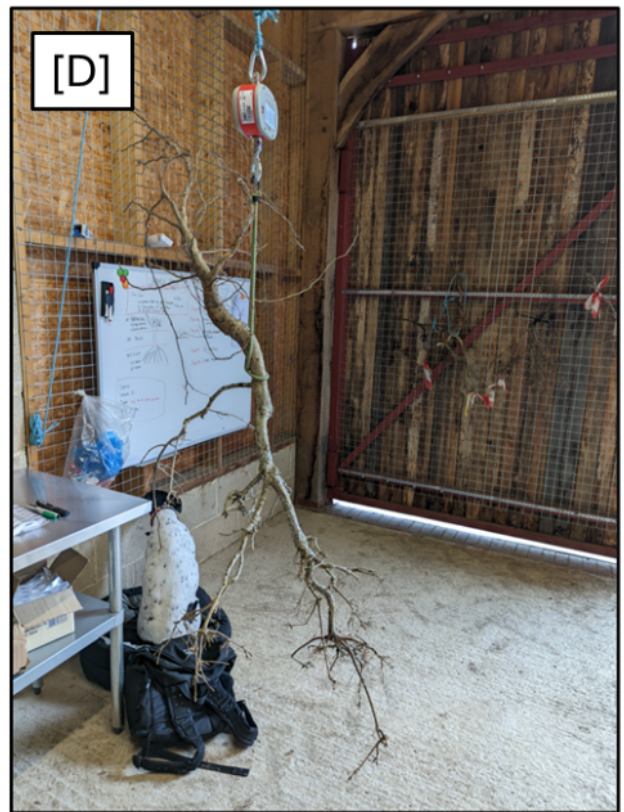


Figure 3.5: Laboratory measurements and processes of destructively sampled scrub trees [A] processed samples in paper bags ready for oven drying; [B] size categorisation of root classes based on diameter; [C] precision balance scales used to weigh samples, including the excess saw dust created during the processing (displayed here); [D] digital crane scale used to weigh the total weight of the scrub tree.

3.2.5. Allometric model development and statistical analysis

Various easily measurable variables, including height (cm), diameter at breast height (dbh) (cm), and canopy area (cm²), were evaluated for their predictive ability in estimating biomass. The best-performing models for each taxon were selected based on their AIC values (Table 3.4 and Table S3.1). These models use a maximum equation that includes height, canopy area, dbh, and condition (whether the scrub was “exposed” or “protected” from browsing) (Table 3.4; Figure 3.10). This contrasts with traditional allometric models, which often rely on dbh, height, and wood specific gravity (WSG) or density (ρ) as primary predictors (Ngomanda et al., 2014; Chave et al., 2005; Pati et al., 2022). In scrub ecosystems, focusing on canopy area and height is especially relevant due to the multi-stemmed and complex growth forms of scrub species, where alone may not adequately capture biomass (Nyamukuru et al., 2023; Vorster et al., 2020). Advancements in remote sensing technology highlight the practical importance of canopy area and height in particular, as these variables are more readily captured through drone technology (see Chapter 5).

In development of my allometric model, I employed equations that follow a log-linear allometric form, commonly used in forestry and ecology to estimate tree biomass and carbon stocks (Chave et al., 2005). This structure is based on power-law scaling, a concept derived from biological principles and applied to plant vascular systems (West et al., 1999). Power-law scaling expresses the biomass component (W) (aboveground, belowground or total biomass) as a function of variables like height (h), diameter at breast height (d) and basal area (A), and the coefficients ($\beta_0, \beta_1, \beta_2, \beta_3 \dots \beta_{15}$) are derived from empirical data using regression analysis, often obtained via destructive sampling (Zianis and Mencuccini, 2004). The condition variable x_c adjusts the intercept based on browsing exposure, allowing a single model to account for

both exposed and protected conditions. Each coefficient is a fitted parameter optimised for the specific taxon and biomass component using regression analysis. Density was also tested as a potential predictor of biomass but yielded no significant interactions during the initial exploratory analysis (see 4.X Supplementary Materials, Table S3.3). The stepwise selection process was then applied to a maximum model ($\log(\text{biomass}) \sim \text{condition} * \log(\text{height}) * \log(\text{canopy area}) * \log(\text{dbh})$) to identify the most relevant terms. The structure of the maximum model is as follows:

$$\log(W) = \beta_0 + \beta_1 \cdot x_c + \beta_2 \cdot \log(h) + \beta_3 \cdot \log(d) + \beta_4 \cdot \log(A) + \beta_5 \cdot (x_c \cdot \log(h)) + \beta_6 \cdot (x_c \cdot \log(d)) + \beta_7 \cdot (x_c \cdot \log(A)) + \beta_8 \cdot (\log(h) \cdot \log(d)) + \beta_9 \cdot (\log(h) \cdot \log(A)) + \beta_{10} \cdot (\log(d) \cdot \log(A)) + \beta_{11} \cdot (x_c \cdot \log(h) \cdot \log(d)) + \beta_{12} \cdot (x_c \cdot \log(h) \cdot \log(A)) + \beta_{13} \cdot (x_c \cdot \log(d) \cdot \log(A)) + \beta_{14} \cdot (\log(h) \cdot \log(d) \cdot \log(A)) + \beta_{15} \cdot (x_c \cdot \log(h) \cdot \log(d) \cdot \log(A))$$

[3]

where x_c is a binary term representing the browsing condition (0 for exposed, 1 for protected).

In this model:

- β_0 is the intercept.
- β_1 adjusts for differences between exposed and protected environments, adding to β_0 for the protected condition.
- β_2 , β_3 , and β_4 represent the main effects of height (h), dbh (d), and canopy area (A), respectively.
- β_5 , β_6 , and β_7 capture interactions between condition and each predictor.
- β_8 , β_9 , and β_{10} represent pairwise interactions among predictors.
- β_{11} , β_{12} , and β_{13} capture three-way interactions involving condition.
- β_{14} represents the three-way interaction of height, dbh, and canopy area.

- β_{15} captures the four-way interaction of condition, height, dbh, and canopy area.

In exponential terms, *Equation [3]* can be represented separately for exposed and protected conditions:

Exposed (where $x_c = 0$):

$$W = e^{B_0} \cdot h^{B_2} \cdot d^{B_3} \cdot A^{B_4} \cdot (h \cdot d)^{B_8} \cdot (h \cdot A)^{B_{10}} \cdot (d \cdot A)^{B_{10}} \cdot (h \cdot d \cdot A)^{B_{14}}$$

[4]

Protected (where $x_c = 1$):

$$W = e^{B_0+B_1} \cdot h^{B_2+B_5} \cdot d^{B_3+B_6} \cdot A^{B_4+B_7} \cdot (h \cdot d)^{B_8+B_{11}} \cdot (h \cdot A)^{B_9+B_{12}} \cdot (d \cdot A)^{B_{10}+B_{13}} \cdot (h \cdot d \cdot A)^{B_{14}+B_{15}}$$

[5]

This approach reflects how power-law scaling can adapt to changing environmental conditions (West et al., 1999).

To develop these equations, I used R software (R Core Team, 2024), employing the "caret" package for data partitioning and the "lm()" function for model fitting within the "stats" package. Model refinement was conducted using the AIC-based "step()" function, applied across all biomass types for each taxon using the maximum equation [3] as the base to identify the most relevant predictors (Table 3.4).

The performance of both aboveground, belowground and total biomass models was evaluated using the coefficient of determination (R^2) and the residual sum of squares (RSS), with model selection based on the lowest Akaike Information Criterion (AIC) value. In this study, p-values for interaction terms were calculated for the null hypothesis $H_0: b = 0$, rather than $H_0: b = 1$, focusing on testing the presence of an effect rather than deviation from an expected value. This distinction is important to interpret the results correctly and should be noted when evaluating the significance of the interactions presented in the results Table 3.3. Finally, I employed MANCOVA to evaluate the model's coefficients and significance and to compare models.

To gain a deeper understanding of the impact of browsing, the root:shoot (R:S) ratio was calculated for each taxon under both browsing conditions—“exposed” and “protected”. The data were then divided into two height categories: trees taller than 2.5 m and those shorter than 2.5 m, which correspond to above and below the browse line, respectively. This threshold for the browse line is widely accepted among researchers (e.g., Van Uytvanck et al., 2010).

3.3 Results

The allometric equations were developed using the 270 scrub trees, including roots and shoots, that I extracted from Site 1 (Figure 3.2, Table 3.2). These represented five taxa: blackthorn (*Prunus spinosa*, n = 55), dog rose (*Rosa canina*, n = 55), hawthorn (*Crataegus monogyna*, n = 56), oak (*Quercus robur*, n = 49), and willow (*Salix cinerea*, n = 55). Trees were sampled under two browsing conditions (“exposed” to browsing and “protected” from browsing) and across three size classes—small (<75 cm), medium (75–210 cm), and large (>210

cm)—determined through a preliminary study of scrub trees at Site 1 (Figure 3.6). This approach ensured a representative distribution of scrub sizes (height) for the destructive sampling population (Figure 3.7). Blackthorn (*Prunus spinosa*), hawthorn (*Crataegus monogyna*), and oak (*Quercus robur*) are predominantly concentrated in the smaller height classes (<75 cm), with oak showing the most pronounced skew towards shorter individuals (Figure 3.7). In contrast, dog rose (*Rosa canina*) and willow (*Salix cinerea*) display broader height distributions, with a higher proportion of individuals in the intermediate (75 - 210 cm) and larger height ranges.

Table 3.2: Number of samples extracted per scrub taxa according to their size class and exposure to browsing. Small <75 cm; medium 75 – 210 cm; large >210 cm.

Taxon	Exposed			protected		
	small	medium	large	small	medium	large
Blackthorn	9	7	13	12	6	8
dog rose	6	11	9	9	14	6
hawthorn	10	9	11	15	7	4
oak	NA	5	16	10	12	6
sallow	8	7	12	10	12	6

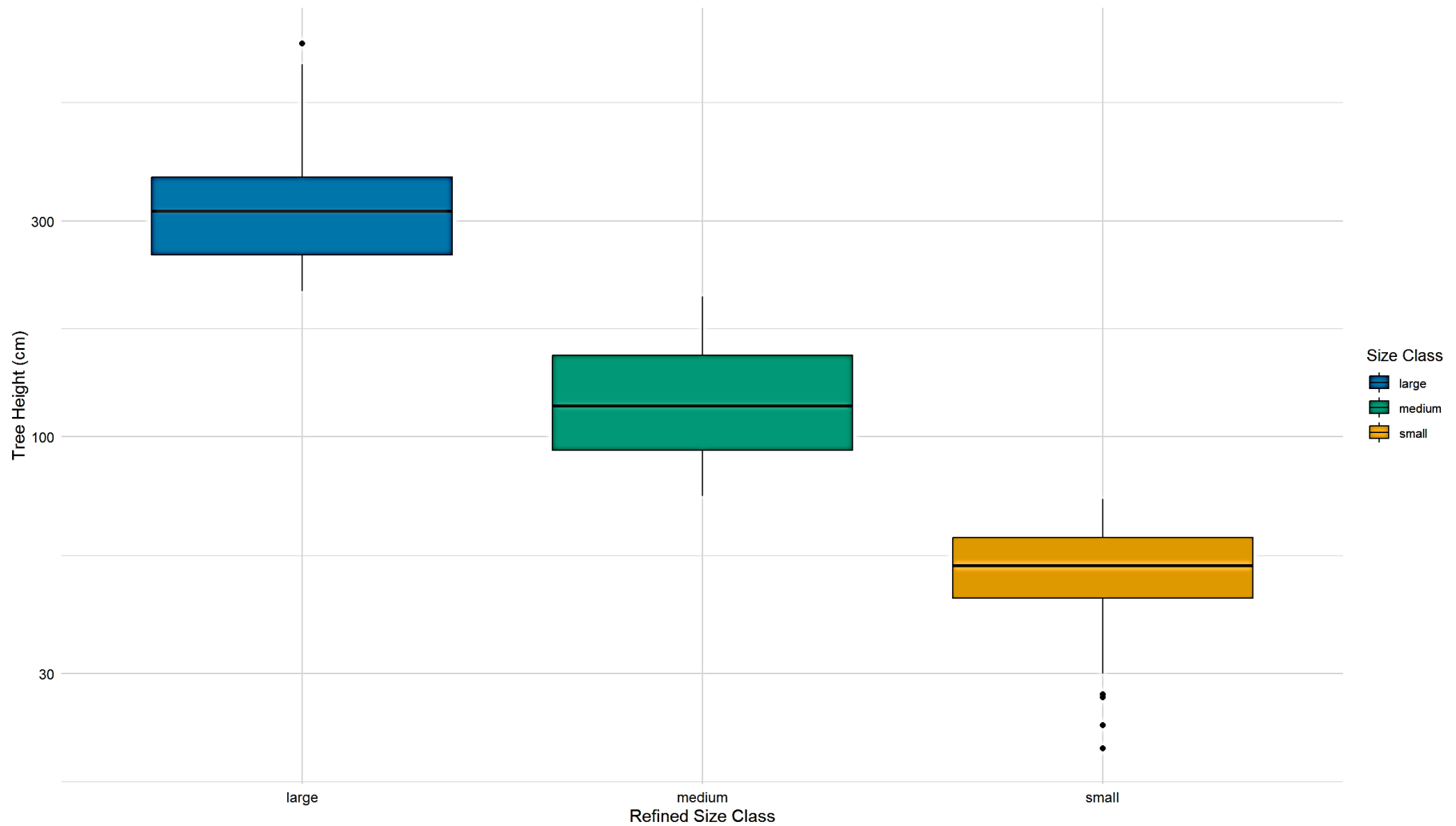


Figure 3.6: Distribution of tree sizes by refined tree height (cm), the preliminary population of scrub trees (Figure S3.6A) was analysed for summary statistics (min, max and mean values) to determine height classes for the destructive sampling of scrub (displayed in Figure 3.7).

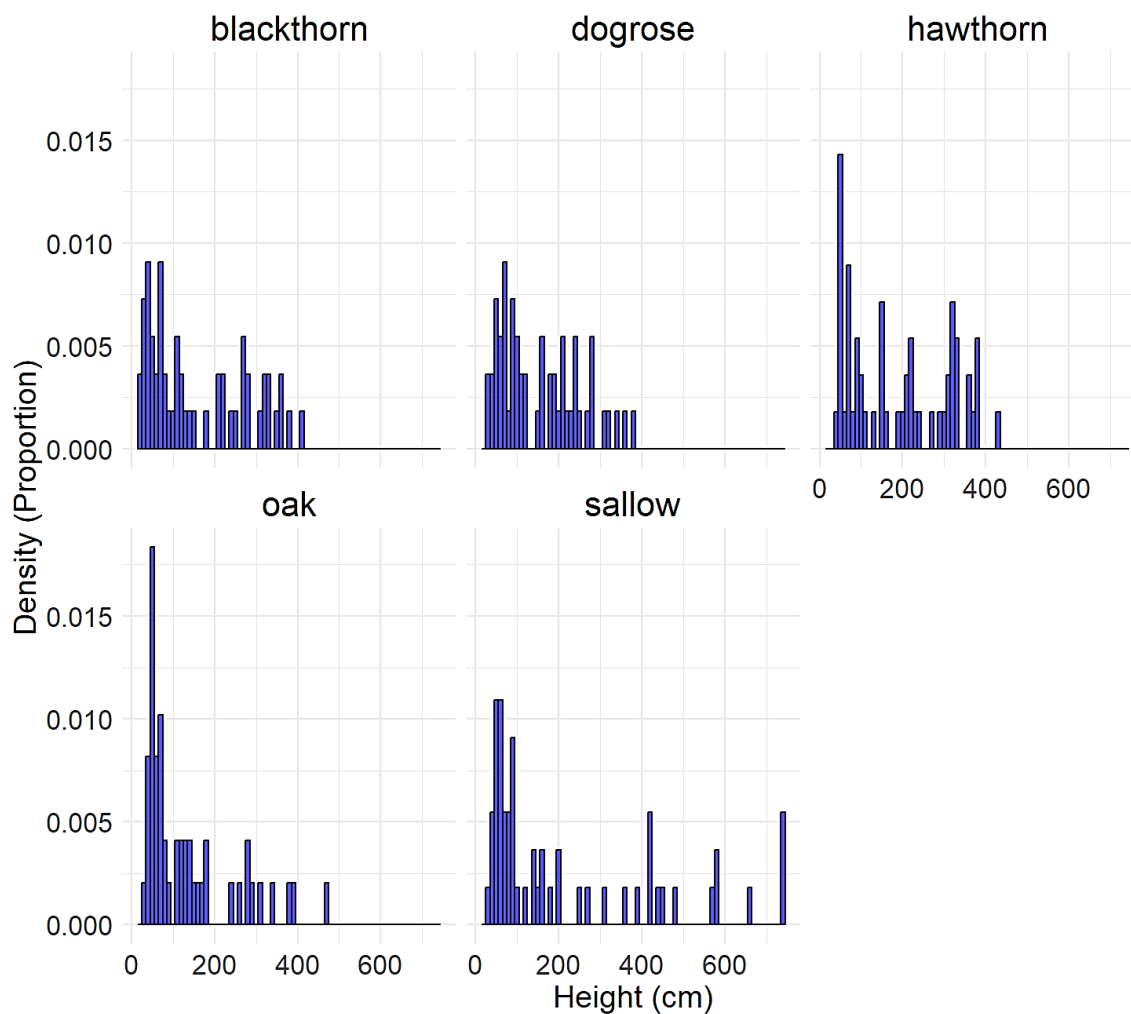


Figure 3.7: Height distribution (density as proportion) of five scrub species sampled for allometric equation development: blackthorn (*Prunus spinosa*), dog rose (*Rosa canina*), hawthorn (*Crataegus monogyna*), oak (*Quercus spp.*), and willow (*Salix spp.*). Density values represent the proportion of individuals within each height class.

3.3.1 Model outputs

The following results from my analyses to determine the relationship between specific taxa characteristics (e.g. height, dbh and canopy area) and above and below ground biomass are recorded in full in Table 3.3A for single predictor variables and Table 3.3B for interactions

between the predictor variables and the condition (“protected” or “exposed” from browsing) and presented in Figure 3.8.

Height and canopy area are significant predictors of both AGB and BGB in oak (*Quercus spp.*), with canopy effects particularly pronounced under protected conditions. Diameter at breast height (dbh) also influences total biomass (TB), while R:S decreases with tree height and under protected conditions. In blackthorn (*Prunus spinosa*), height, dbh, and canopy area exhibit strong predictive relationships with AGB, BGB, and TB, with protected trees showing higher BGB influenced by dbh. Height and canopy area also significantly influence R:S, with higher values in exposed conditions. For dog rose (*Rosa canina*), height and canopy area are consistent predictors of AGB, BGB, and TB, but canopy effects are more pronounced in protected conditions, while R:S ratios are significantly influenced by height and canopy area, with protected trees exhibiting slightly lower ratios. In hawthorn (*Crataegus spp.*), height, dbh, and canopy area strongly predict AGB, BGB, and TB, with no significant interactions related to browsing conditions, while R:S ratios also show consistent associations with height, dbh, and canopy area, but condition effects remain insignificant. For willow (*Salix spp.*), height, dbh, and canopy area are reliable predictors of AGB, BGB, and TB, while density (ρ) exhibits a significant negative association with BGB (-3.9822 ± 1.8672 , $p = 0.0379$) and TB (-4.9142 ± 2.1046 , $p = 0.0236$) (Table S3.3). R:S ratios are inversely related to height, dbh, and canopy area.

Table 3.3A: The response variables (aboveground biomass (AGB), belowground biomass (BGB), total biomass and root:shoot ratio) for each taxon (blackthorn, dog rose, hawthorn, oak, willow) as a function of single predictor variables (height, dbh and canopy area) on the log scale. Estimates, Standard Error (S.E) and p-values recorded.

Response Variable	Taxon	Height			DBH			Canopy Area		
		estimate	SE	p-value	estimate	SE	p-value	estimate	SE	p-value
AGB	Blackthorn	2.49	0.21	<2e-16	1.43	0.42	<0.01	1.10	0.11	<2e-16
BGB	Blackthorn	1.67	0.18	<0.001	1.25	0.29	<0.001	0.79	0.08	<0.001
Total	Blackthorn	2.26	0.20	<0.001	1.42	0.38	<0.001	1.02	0.10	<0.001
R:S Ratio	Blackthorn	-0.82	0.17	<0.001	-0.18	0.24	<0.1	-0.30	0.09	<0.001
AGB	Dog Rose	1.88	0.22	<0.001	NA	NA	NA	1.23	0.10	<2e-16
BGB	Dog Rose	1.35	0.18	<0.001	NA	NA	NA	0.88	0.07	<0.001
Total	Dog Rose	1.77	0.19	<0.001	NA	NA	NA	1.01	0.09	<2e-16
R:S Ratio	Dog Rose	-0.68	0.09	<0.001	NA	NA	NA	-0.46	0.06	<0.001
AGB	Hawthorn	2.44	0.19	<2e-16	2.27	0.28	<0.001	1.43	0.08	<2e-16
BGB	Hawthorn	1.69	0.17	<0.001	1.78	0.19	<0.001	0.97	0.08	<2e-16
Total	Hawthorn	2.18	0.18	<2e-16	2.14	0.24	<0.001	1.27	0.08	<2e-16
R:S Ratio	Hawthorn	-0.75	0.09	<0.001	-0.48	0.13	<0.001	-0.45	0.04	<0.001
AGB	Oak	1.59	0.16	<0.001	1.16	0.28	<0.001	0.76	0.07	<0.001
BGB	Oak	1.25	0.16	<0.001	0.83	0.26	<0.01	0.65	0.06	<0.001
Total	Oak	1.44	0.15	<0.001	1.00	0.26	<0.001	0.71	0.06	<0.001
R:S Ratio	Oak	-0.33	0.12	<0.01	-0.33	0.14	<0.05	-0.11	0.06	<0.1
AGB	Sallow	1.68	0.18	<0.001	2.16	0.17	<2e-16	1.15	0.09	<2e-16
BGB	Sallow	1.18	0.17	<0.001	1.59	0.17	<0.001	0.86	0.09	<0.001
Total	Sallow	1.50	0.17	<0.001	1.96	0.16	<0.001	1.04	0.09	<2e-16
R:S Ratio	Sallow	-0.49	0.08	<0.001	-0.57	0.10	<0.001	-0.30	0.05	<0.001

Table 3.3B: The response variables (aboveground biomass (AGB), belowground biomass (BGB), total biomass and root:shoot ratio) for each taxon (blackthorn, dog rose, hawthorn, oak, willow) as a function of condition of browsing (exposed or protected) in relation to single predictor variables (height, dbh and canopy). Interactive term, Standard Error (S.E) and p-values recorded.

Response Variable	Taxon	Height			DBH			Canopy Area		
		interaction	SE	p-value	interaction	SE	p-value	interaction	SE	p-value
AGB	Blackthorn	0.55	0.43	0.20	-0.82	1.06	0.44	-0.31	0.22	0.17
BGB	Blackthorn	0.81	0.33	0.02	0.09	0.37	0.81	0.23	0.17	0.20
Total	Blackthorn	0.87	0.32	0.01	0.00	0.35	0.99	0.24	0.16	0.15
R:S Ratio	Blackthorn	-0.76	0.37	0.04	-0.88	0.60	0.15	-0.16	0.17	0.36
AGB	Dog Rose	0.18	0.33	0.59	NA	NA	NA	0.29	0.14	0.05
BGB	Dog Rose	-0.35	0.32	0.29	NA	NA	NA	-0.05	0.12	0.65
Total	Dog Rose	0.03	0.31	0.91	NA	NA	NA	0.16	0.12	0.20
R:S Ratio	Dog Rose	-0.53	0.30	0.08	NA	NA	NA	-0.35	0.12	0.01
AGB	Hawthorn	0.09	0.41	0.83	0.46	0.55	0.40	0.11	0.17	0.51
BGB	Hawthorn	0.14	0.33	0.68	0.34	0.38	0.37	0.21	0.15	0.19
Total	Hawthorn	0.22	0.38	0.56	0.47	0.47	0.32	0.22	0.16	0.17
R:S Ratio	Hawthorn	-0.05	0.20	0.81	-0.12	0.25	0.63	-0.10	0.09	0.30
AGB	Oak	0.95	0.45	0.04	1.10	0.52	0.04	0.66	0.16	<0.0001
BGB	Oak	0.49	0.48	0.32	0.64	0.50	0.21	0.19	0.16	0.25
Total	Oak	0.79	0.42	0.07	0.91	0.50	0.07	0.45	0.14	<0.0001
R:S Ratio	Oak	-0.46	0.35	0.20	-0.46	0.28	0.10	-0.47	0.14	0.002
AGB	Sallow	0.89	0.34	0.01	-0.09	0.37	0.82	0.23	0.17	0.19
BGB	Sallow	0.81	0.33	0.02	0.09	0.37	0.81	0.23	0.17	0.20
Total	Sallow	0.87	0.32	0.01	0.00	0.35	0.99	0.24	0.16	0.15
R:S Ratio	Sallow	-0.53	0.30	0.08	-0.12	0.25	0.63	-0.002	0.11	0.99

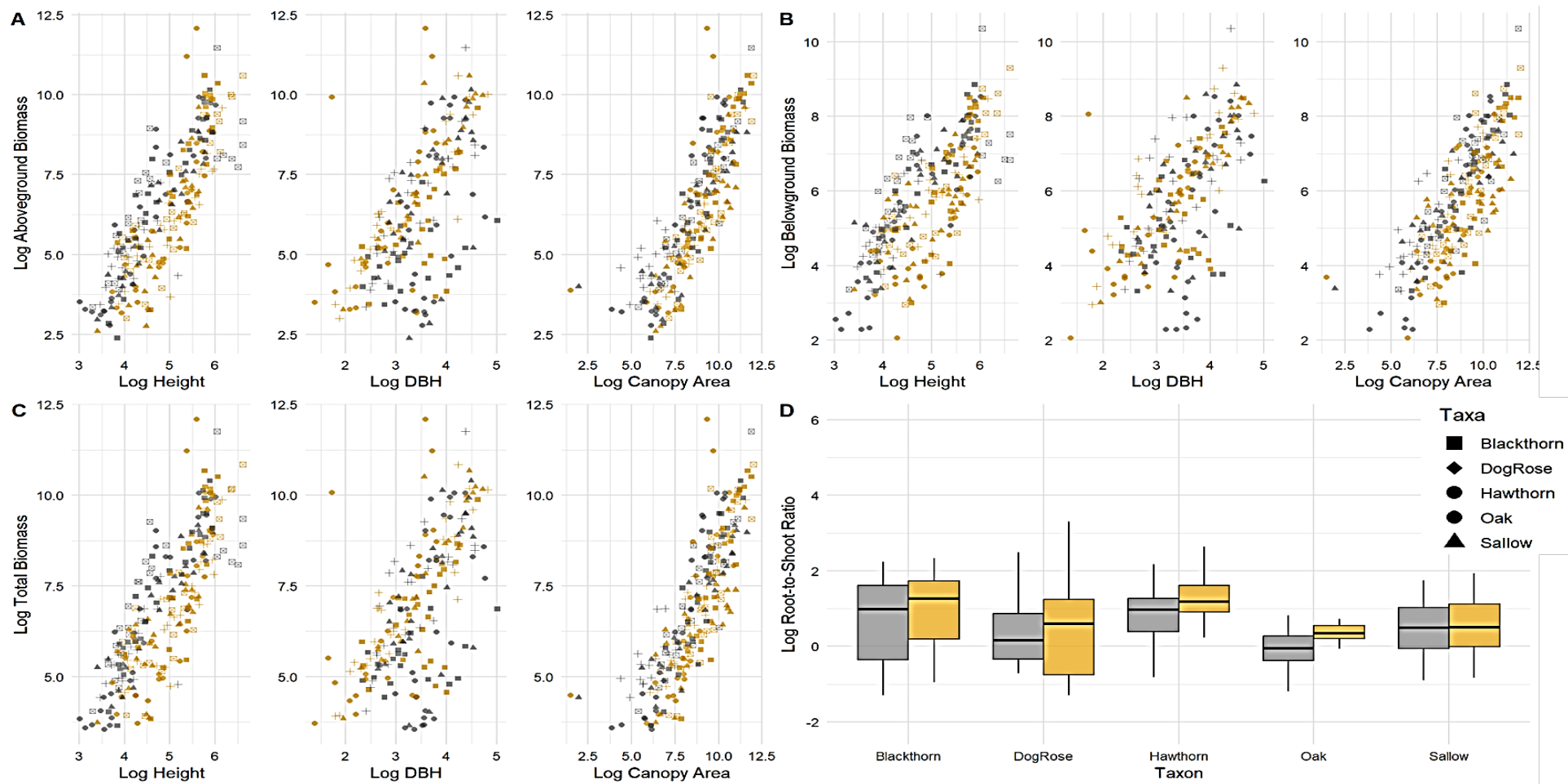


Figure 3.8: Relationships between predictor variables (log height, log dbh, and log canopy area) and three biomass components (A) log aboveground biomass, (B) log belowground biomass, and (C) log total biomass across five taxa (blackthorn, dog rose, hawthorn, oak, and sallow) and two conditions (exposed in grey and protected in yellow). Symbols represent different taxa: blackthorn (square), dog rose (diamond), hawthorn (triangle), oak (circle), and sallow (cross). (D) Box-and-whisker plots of log root:shoot ratio by taxon and condition.

3.4.2 Variation in Root:Shoot Ratio in Relation to Browse Line

The analysis of root:shoot ratios (R:S) indicated that trees below the browse line (2.5 m) had higher ratios (mean = 1.06, SE = 0.13) compared to those above the browse line (mean = 0.31, SE = 0.03) (Figure 3.9A), with a statistically significant difference ($p < 0.001$). Blackthorn showed a mean ratio of 0.91 (SE = 0.14) below and 0.18 (SE = 0.02) above. Dog rose had ratios of 1.36 (SE = 0.22) below and 0.27 (SE = 0.07) above. Hawthorn followed with 0.68 (SE = 0.11) below and 0.23 (SE = 0.02) above. Oak and willow also showed higher ratios below, with means of 1.11 (SE = 0.10) and 0.96 (SE = 0.10), respectively, compared to 0.54 (SE = 0.07) and 0.34 (SE = 0.04) above. The range of ratio was also much greater in the below browse line category (R:S 0.012 – 8.98) compared to above (0.025 – 0.88) (Figure 3.9B).

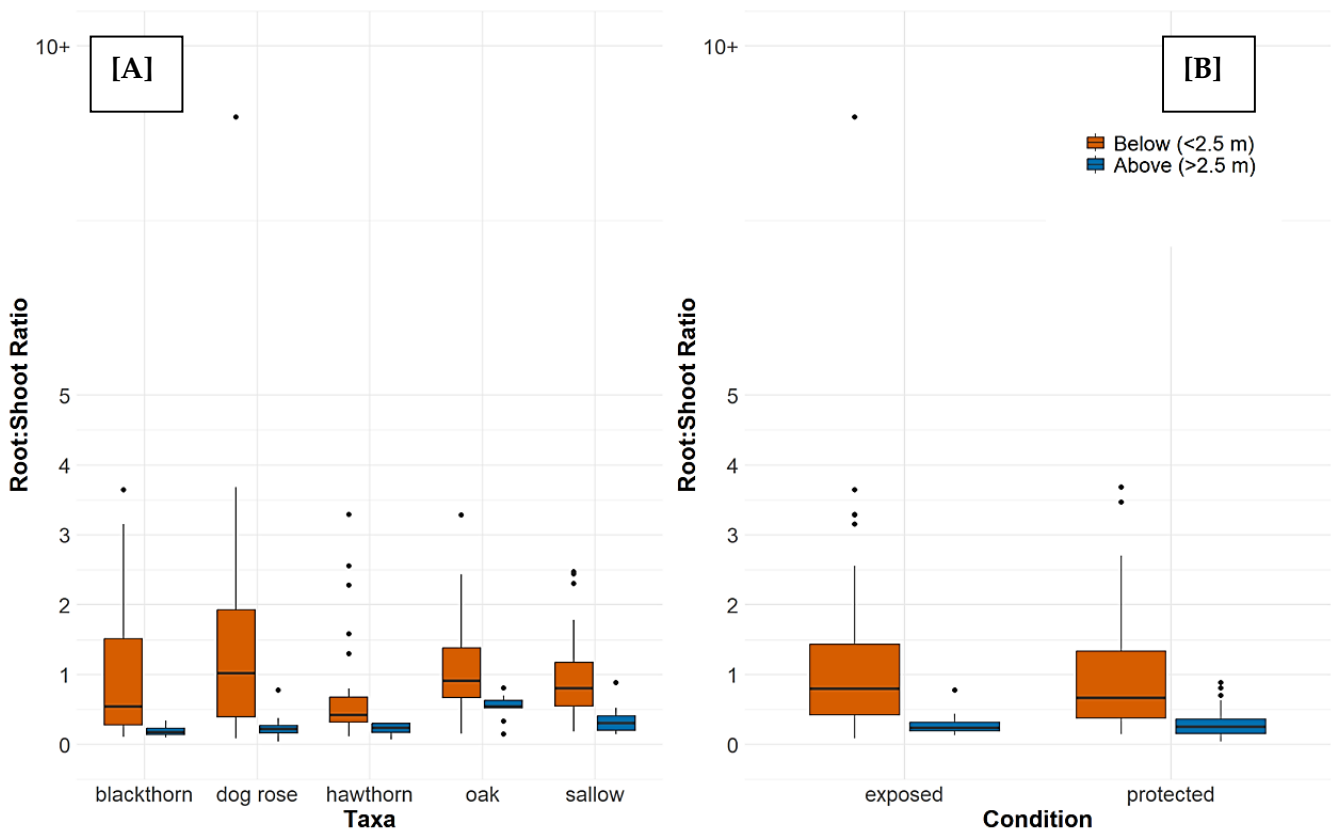


Figure 3.9: root:shoot ratio for various scrub taxa (blackthorn, dog rose, hawthorn, oak, and willow) and their relationship with the browse line (below and above 2.5 metres) and condition (exposed and protected).

3.3.3 Allometric equations

The allometric equations to describe the relationship between biomass (AGB or BGB) and key aboveground characteristics (e.g. height, dbh or canopy area) for each taxon under each condition (exposed or protected) (Table 3.4; Figure 3.10) were optimised using stepwise AIC selection (Table 3.4, see Table S3.1 for full results), incorporating browsing condition (“exposed” or “protected”) and field measurements (dbh, height, and canopy area) (Table 3.4). On average, the models explained 88% of the variability in AGB ($R^2 = 0.81\text{--}0.94$, $RSS = 8.05\text{--}66.78$), 80% of the variability in BGB ($R^2 = 0.63\text{--}0.92$, $RSS = 10.48\text{--}36.88$), and 85% of the variability TB ($R^2 = 0.80\text{--}0.95$, $RSS = 6.42\text{--}53.51$). Most taxa-specific models incorporated browsing condition, except for blackthorn AGB ($R^2 = 0.81$, $RSS = 66.78$) and willow BGB ($R^2 = 0.73$, $RSS = 36.88$).

Table 3.4: Summary of linear regression models used to predict biomass components (W) (aboveground biomass (AGB), belowground biomass (BGB), and total biomass (Total)) across five taxa (blackthorn, dog rose, hawthorn, oak, and willow). Each model incorporates predictor variables—height (h), diameter at Breast Height (d), and canopy area (A)—as well as interactions with browsing condition (xc) where specified. The models include combinations of main effects and interactions, up to a maximum model structure with all possible interaction terms (Equation 1). Model performance is evaluated using the coefficient of determination (R^2), residual sum of squares (RSS), and Akaike Information Criterion (AIC). Taxon specific biomass coefficient values (β_0 – β_{15}) can be found in Table 3.5.

Taxon	Model	R^2	RSS	AIC
Blackthorn	$\log(W_{AGB}) = \beta_0 + \beta_2 \cdot \log(h) + \beta_3 \cdot \log(d) + \beta_4 \cdot \log(A)$	0.81	66.78	174.71
	$\log(W_{BGB}) = \beta_0 + \beta_1 \cdot x_c + \beta_2 \cdot \log(h) + \beta_3 \cdot \log(d) + \beta_4 \cdot \log(A) + \dots + \beta_{15} \cdot (x_c \cdot \log(h) \cdot \log(d) \cdot \log(A))$	0.92	14.14	114.88
	$\log(W_{Total}) = \beta_0 + \beta_1 \cdot x_c + \beta_2 \cdot \log(h) + \beta_3 \cdot \log(d) + \beta_4 \cdot \log(A)$	0.82	53.51	164.76
Dog rose	$\log(W_{AGB}) = \beta_0 + \beta_1 \cdot x_c + \beta_2 \cdot \log(h) + \beta_4 \cdot \log(A)$	0.83	32.10	136.46
	$\log(W_{BGB}) = \beta_0 + \beta_1 \cdot x_c + \beta_2 \cdot \log(h) + \beta_4 \cdot \log(A)$	0.63	30.61	133.85

	$\text{Log}(W_{Total}) = \beta_0 + \beta_1 \cdot x_c + \beta_2 \cdot \log(h) + \beta_4 \cdot \log(A)$	0.80	26.57	126.07
Hawthorn	$\log(W_{AGB}) = \beta_0 + \beta_1 \cdot x_c + \beta_2 \cdot \log(h) + \beta_3 \cdot \log(d) + \beta_4 \cdot \log(A) + \dots + \beta_{15} \cdot (x_c \cdot \log(h) \cdot \log(d) \cdot \log(A))$	0.94	14.02	114.89
	$\log(W_{BGB}) = \beta_0 + \beta_1 \cdot x_c + \beta_2 \cdot \log(h) + \beta_3 \cdot \log(d) + \beta_4 \cdot \log(A) + \dots + \beta_{15} \cdot (x_c \cdot \log(h) \cdot \log(d) \cdot \log(A))$	0.92	10.48	98.91
	$\text{Log}(W_{Total}) = \beta_0 + \beta_1 \cdot x_c + \beta_2 \cdot \log(h) + \beta_3 \cdot \log(d) + \beta_4 \cdot \log(A) + \dots + \beta_{15} \cdot (x_c \cdot \log(h) \cdot \log(d) \cdot \log(A))$	0.95	10.57	99.38
Oak	$\log(W_{AGB}) = \beta_0 + \beta_1 \cdot x_c + \beta_2 \cdot \log(h) + \beta_3 \cdot \log(d) + \beta_4 \cdot \log(A) + \dots + \beta_{15} \cdot (x_c \cdot \log(h) \cdot \log(d) \cdot \log(A))$	0.91	8.05	84.38
	$\log(W_{BGB}) = \beta_0 + \beta_1 \cdot x_c + \beta_2 \cdot \log(h) + \beta_3 \cdot \log(d) + \beta_4 \cdot \log(A)$	0.80	13.82	87.23
	$\text{Log}(W_{Total}) = \beta_0 + \beta_1 \cdot x_c + \beta_2 \cdot \log(h) + \beta_3 \cdot \log(d) + \beta_4 \cdot \log(A) + \dots + \beta_{15} \cdot (x_c \cdot \log(h) \cdot \log(d) \cdot \log(A))$	0.92	6.42	73.93
Sallow	$\log(W_{AGB}) = \beta_0 + \beta_1 \cdot x_c + \beta_2 \cdot \log(h) + \beta_3 \cdot \log(d) + \beta_4 \cdot \log(A) + \dots + \beta_{15} \cdot (x_c \cdot \log(h) \cdot \log(d) \cdot \log(A))$	0.93	14.10	113.70
	$\log(W_{BGB}) = \beta_0 + \beta_2 \cdot \log(h) + \beta_3 \cdot \log(d) + \beta_4 \cdot \log(A)$	0.73	36.88	139.70
	$\text{Log}(W_{Total}) = \beta_0 + \beta_1 \cdot x_c + \beta_2 \cdot \log(h) + \beta_3 \cdot \log(d) + \beta_4 \cdot \log(A) + \dots + \beta_{15} \cdot (x_c \cdot \log(h) \cdot \log(d) \cdot \log(A))$	0.91	15.54	118.77

Table 3.5: Coefficient values β for models predicting aboveground biomass (AGB), belowground biomass (BGB), and total biomass (Total) for five scrub taxa (blackthorn, dog rose, hawthorn, oak, and willow). Each coefficient β corresponds to a predictor or interaction term in the model, where W represents the biomass component, β_0 is the intercept, and β_1 through β_{15} are coefficients for predictor variables and their interactions. Predictor terms include log (height) (tree height), log (dbh) (diameter at breast height), log (canopy area) (canopy area), and the browsing condition factor (conditionprotected), along with their interactions. Coefficients are ordered from the intercept (β_0) to the highest-order interaction term, “conditionprotected:log_height:log_dbh:log_canopy_area” (β_{15}). NA values indicate terms that were not included in the final model for that specific taxon and biomass component. The full table of coefficients with Standard Error (SE) and T-Value can be found in Table S3.2.

Taxon	W	β_0	β_1	β_2	β_3	β_4	β_5	β_6	β_7	β_8	β_9	β_{10}	β_{11}	β_{12}	β_{13}	β_{14}	β_{15}
Blackthorn	AGB	-5.98	2.01	0.37	0.09	NA	NA	NA	NA	NA	NA	NA	NA	NA	NA	NA	NA
	BGB	52.56	40.82	-12.72	-16.28	-3.69	-11.58	-12.55	3.88	-4.59	1.03	1.35	1.19	-0.31	-0.40	NA	NA
	Total	71.90	48.88	-19.33	-20.44	-5.96	-9.49	-18.28	5.47	-6.43	1.86	1.81	4.01	1.2	2.11	-0.5	-0.4
Dog rose	AGB	-4.67	-0.71	1.84	NA	0.25	NA	NA	NA	NA	NA	NA	NA	NA	NA	NA	NA
	BGB	0.55	-0.66	0.58	NA	0.31	NA	NA	NA	NA	NA	NA	NA	NA	NA	NA	NA
	Total	-1.53	-0.65	1.22	NA	0.30	NA	NA	NA	NA	NA	NA	NA	NA	NA	NA	NA
Hawthorn	AGB	-18.87	85.16	4.07	-0.18	1.85	-16.62	-13.77	0.00	-10.03	-0.27	0.14	2.71	1.84	1.79	-0.02	-0.33
	BGB	-18.53	118.98	8.85	2.12	-0.42	-28.34	-27.43	-1.64	-10.63	-0.36	0.50	6.62	2.51	2.43	0.04	-0.58
	Total	-4.92	86.19	3.12	-2.44	-0.49	-18.50	-16.02	0.03	-8.97	0.00	0.64	3.55	1.82	1.70	-0.07	-0.35
Oak	AGB	-141.73	141.52	37.44	46.30	22.63	-38.13	-47.23	-11.86	-21.60	-5.80	-7.34	12.20	5.78	7.30	1.88	-1.88
	BGB	-1.55	-0.84	0.28	0.27	0.68	NA	NA	NA	NA	NA	NA	NA	NA	NA	NA	NA
	Total	-109.23	113.48	29.12	36.34	17.77	-28.02	-38.45	-9.35	-18.43	-4.53	-5.76	9.28	4.56	6.18	1.49	-1.51

Taxon	W	β_0	β_1	β_2	β_3	β_4	β_5	β_6	β_7	β_8	β_9	β_{10}	β_{11}	β_{12}	β_{13}	β_{14}	β_{15}
Sallow	AGB	-26.09	-9.71	10.43	3.71	1.55	-5.63	13.12	-2.14	2.98	-0.73	0.10	-0.09	0.14	-2.04	0.14	0.15
	BGB	-1.25	NA	-0.04	0.89	0.52	NA	NA	NA	NA	NA	NA	NA	NA	NA	NA	NA
	Total	-32.79	5.20	11.71	7.11	2.23	-7.97	6.28	-2.72	1.46	-0.84	-0.22	0.99	0.38	-1.32	0.19	0.04

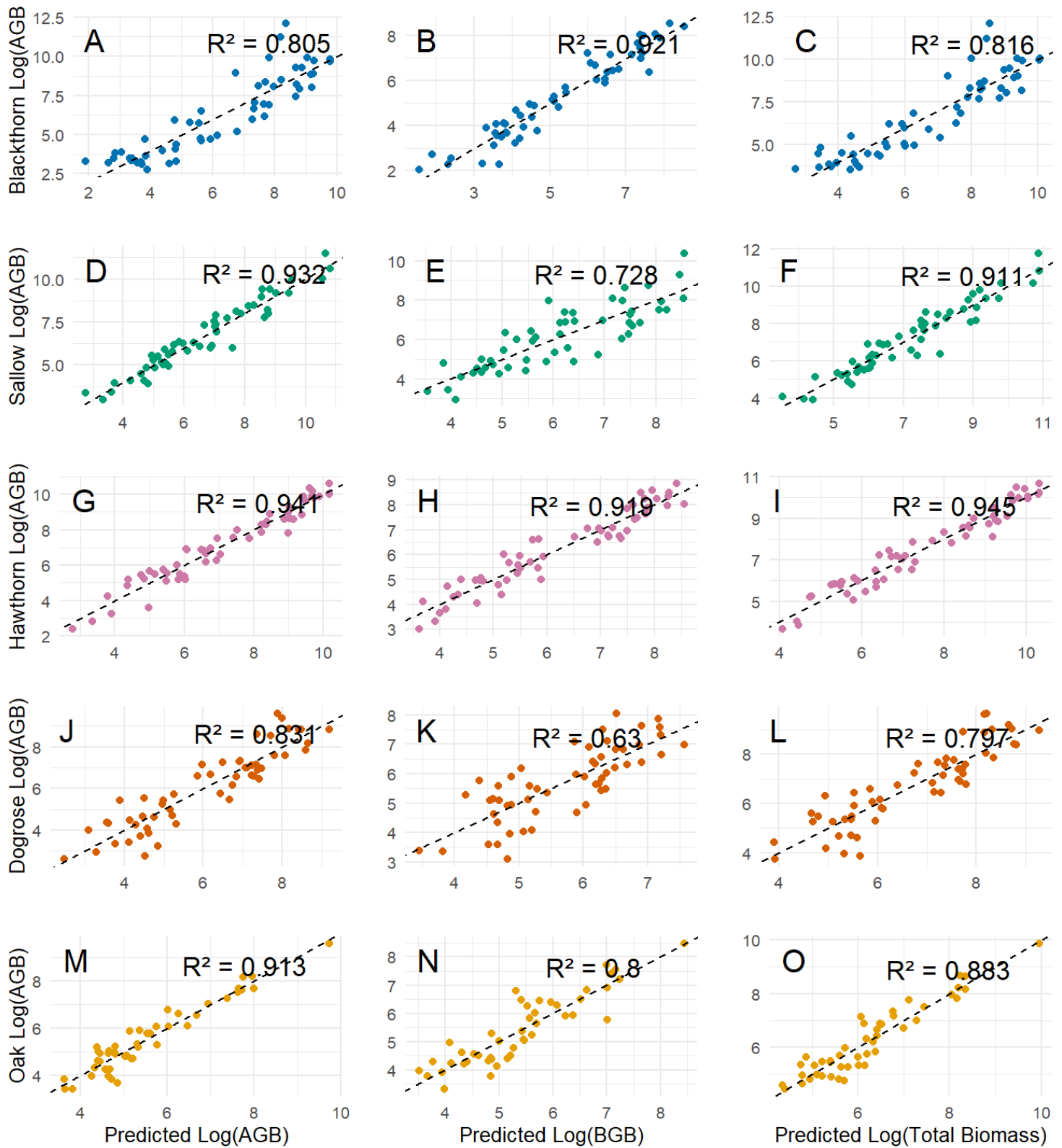


Figure 3.10: Predicted versus actual log-transformed biomass components for five taxa (blackthorn, sallow, hawthorn, dog rose, and oak), showing aboveground biomass (AGB), belowground biomass (BGB), and total biomass (Total Biomass) in panels A–O. Each panel represents a separate model for each biomass component across different taxa, with R^2 values indicating model fit. Points are coloured by taxa: Blackthorn (A–C, blue), Sallow (D–F, green), Hawthorn (G–I, pink), Dog Rose (J–L, orange), and Oak (M–O, yellow). Equations used for each model are displayed in table 3.2.

3.4 Discussion

3.4.1. Scrub-specific allometric equations and explanation

This study represents a significant advancement in biomass estimation by developing taxon-specific allometric equations derived from a dataset of 270 scrub individuals across five taxa (Table 3.2). This uniquely large sample size far exceeds the norm for similar studies (e.g. Axe et al., 2017, Virgulino-Júnior et al., 2020; Chen et al., 2024), providing robust and reliable estimates for aboveground biomass (AGB), belowground biomass (BGB), and total biomass (TB) in scrub vegetation. The performance of these equations is notable, with R^2 values ranging from 0.81 – 0.94 for AGB, 0.63 to 0.91 for BGB and 0.80 – 0.95 for TB, reflecting strong predictive capabilities (Table 3.4, Figure 3.8). This is a significant advance in biomass estimation for scrub ecosystems, a vegetation type that has been overlooked or underestimated in previous biomass models (Litton & Boon Kauffman, 2008; Zeng et al., 2010; Burrell et al., 2024).

Results from my analyses examining wood density (ρ) and its relationship with key characteristics (e.g., height, dbh, and canopy area) showed that wood density (ρ) was not a reliable predictor of biomass (AGB or BGB) in either protected or exposed scrub trees (Table S3.3). This is likely due to significant morphological variability induced by browsing. Given that browsing alters growth forms and regrowth patterns, my results suggest that biomass of shrubland taxa are better captured by canopy area and height rather than wood density (Chave et al., 2005; Enquist et al., 1999; Forrester et al., 2017). However, a significant negative relationship between wood density (ρ) and biomass was observed in *Salix spp.* (Table S3.3) suggesting that this taxon has a growth strategy that deviates from typical shrub responses to browsing.

While many studies have shown that shrubs tend to increase wood density under browsing pressure to enhance structural resilience (Jacobsen et al., 2007; Wheeler et al., 2007), my findings suggest that *Salix spp.* appears to adopt a different approach. Instead of investing in denser wood, *Salix spp.* seems to prioritise rapid growth by producing multiple, less dense stems (King et al., 2006; Chave et al., 2009; Chua & Potts, 2018). This growth form likely reflects *Salix spp.*'s adaptation to its environment, where its ability to quickly replace lost biomass and maximise resource capture is more advantageous than structural reinforcement (Castillo-Figueroa et al., 2023). Unlike the pattern seen in many shrubs, which allocate more resources to wood fibres for strength in resource-limited conditions (Martínez-Cabrera et al., 2009; Ziemińska et al., 2015; Poorter et al., 2008; Chave et al., 2009), these results could suggest that *Salix spp.* focuses on rapid biomass recovery and resilience through growth.

More generally, my findings indicate that the unique structural characteristics of scrub vegetation emphasise the need for scrub-specific allometric models tailored to these systems. Unlike plantation forests, which typically feature tall and uniform trees, scrub species grow in heterogeneous environments with substantial variation in height and canopy structure (Broughton et al., 2021; Navarro & Pereira, 2015). These species are often multi-stemmed and exhibit significant adaptations to environmental stressors, such as exposure to herbivory, resulting in irregular canopy shapes and increased biomass allocation to root systems (Kooch et al., 2024; Churski et al., 2022; Burrell et al., 2024; Perkovich & Ward, 2021). For example, oak (*Quercus spp.*) showed a strong relationship between canopy area and aboveground biomass and total biomass (Table 3.3A), with significant interactions under protected conditions (Table 3.3B). These results suggest that relief from browsing pressure enables oaks to allocate more resources to canopy development, enhancing their aboveground biomass accumulation.

This finding aligns with the "thorn is the mother of the oak" hypothesis (Vera, 2000), which posits that oak saplings benefit from the initial protection provided by thorny shrubs such as bramble (*Rubus fruticosus*). Such facilitative interactions allow oaks to prioritise canopy expansion once browsing pressures are alleviated, as reflected in the enhanced biomass of protected trees in this study. Previous research further supports this mechanism, showing that thorny shrubs improve soil conditions through leaf litter, reduce water stress, and buffer against temperature extremes, thereby fostering oak establishment and growth (Rousset & Lepart, 2000; Gómez-Aparicio et al., 2004; Callaway, 1995).

Conversely, blackthorn (*Prunus spinosa*) exhibited significantly higher belowground biomass (BGB) in protected trees, driven by diameter at base height (Table 3.3). This increase in BGB could be attributed to its clonal propagation strategy through root suckering (Leinemann et al., 2014; Brown et al., 2022). In the absence of browsing pressure, blackthorn appears to allocate more resources to root expansion, enabling the production of new suckers and contributing to its dense, clonal growth habit (Facciolati et al., 2024).

Dog rose (*Rosa canina*), however, exhibited a contrasting pattern, with lower aboveground biomass (AGB) in protected conditions, influenced by canopy area (Table 3.3). This result could be reflecting its competition with bramble (*Rubus fruticosus*). Bramble's rapid canopy expansion and shading could be limiting the light availability and growing space, suppressing the less competitive species like dog rose (Balandier et al., 2013; Tutin, 1964; Schnitzler & Borlea, 1998). Unlike blackthorn and oak, which possess traits enabling them to withstand competition or even benefit from facilitative interactions, dog rose may be particularly vulnerable to the resource-limiting effects of bramble.

These results highlight the variability in biomass predictors across taxa (Table 3.3), shaped by taxa-specific adaptations to stressors like browsing (Ngomanda et al., 2014; Chave et al., 2005). They emphasise the need for taxon-specific models (Table 3.4) to accurately capture growth patterns and responses to environmental stress, particularly in complex, multi-stemmed systems like scrub vegetation (Jucker et al., 2017; Picard et al., 2012).

The root:shoot (R:S) ratios observed reveal that scrub species allocate a substantially higher proportion of biomass to belowground components (BGB) (Figure 3.8D) than predicted by current carbon models. This aligns with my previous work (Chapter 2 – Burrell et al., 2024) highlighting the limitations of standardised approaches to estimating belowground biomass, such as the Woodland Carbon Code (WCC) model, which assumes a generalised R:S value of 0.26 (Nowak, 2019). For instance, applying this standardised approach to oak and dog rose in this study would have underestimated their BGB by more than four times the actual values (oak exposed R:S = 1.18 ± 0.67 SD; dog rose exposed R:S = 1.22 ± 1.66 SD; dog rose protected R:S = 1.15 ± 1.09 SD) (Figure 3.8D)). Such discrepancies highlight the urgent need for models that reflect the structural and ecological complexities of scrub vegetation.

This study reinforces the distinct carbon allocation dynamics of scrub ecosystems, setting them apart from plantation forests. Scrub species, with their higher R:S ratios, likely play a significant role in enhancing soil organic carbon stocks through organic matter accumulation, improved soil structure, and increased microbial activity—processes vital for carbon sequestration (Hamilton et al., 2008; Sun et al., 2017). The predictive accuracy of the models developed in this study (Figure 3.8, Table 3.4) is particularly crucial in rewilding contexts, where scrublands are often overlooked in carbon accounting frameworks (Matthews, 2017; Mercer et al., 2023). Estimates from other studies further illustrate that currently these systems

are being underestimated, with reported R:S values for scrubland ranging from 0.32 (Mokany et al., 2006) to 0.94 (Axe et al., 2017). Integrating taxon- and condition-specific R:S ratios into frameworks like the WCC will yield more accurate estimates of biomass and carbon storage, strengthening conservation and carbon offset strategies. Accounting for the higher belowground biomass allocation observed in scrub taxa, particularly in stress-prone landscapes, will improve the predictive power and applicability of these models (Ngomanda et al., 2014; Chave et al., 2005).

3.4.2. Impact of Browsing on Biomass Allocation

The allometric models developed in this study also demonstrate the significant role of browsing in shaping biomass allocation in scrub trees. Incorporating "exposed" and "protected" categories improved model performance, providing critical insights into how browsing pressure influences biomass distribution. In general, browsing increased belowground biomass (BGB) allocation, highlighting the need to consider browsing condition in allometric equations. For example, oak (*Quercus* spp.) exhibited a significantly lower root:shoot (R:S) ratio in protected trees compared to exposed trees (Table 3.3B). Similarly, hawthorn (*Crataegus* spp.) and dog rose (*Rosa canina*) displayed lower R:S ratios in protected trees than in exposed ones (Table 3.3B; Figure 3.8D). These results suggest that browsing prompts many scrub taxa to allocate more biomass to roots, likely as a strategy for resilience, defence, and recovery (Perkovich & Ward, 2021; Langley et al., 2002).

This pattern aligns with findings from other grazed and browsed landscapes (e.g., Dalglish & Hartnett, 2006; Qian et al., 2017), although it has not been widely documented in rewilded systems. Herbivory is known to drive increased root biomass investment as compensation for

canopy loss (Axe et al., 2020). Notably, blackthorn (*Prunus spinosa*) and willow (*Salix spp.*) showed differing responses (Table 3.4): blackthorn's aboveground biomass (AGB) was unaffected by browsing, likely due to its robust regrowth capacity and thorny morphology, which deter herbivory and maintain consistent aboveground biomass (Facciolati et al., 2024). However, blackthorn BGB was significantly higher in protected trees (Table 3.3B), suggesting that root biomass allocation is more responsive to reduced browsing pressure.

Willow, with its multi-stemmed growth strategy as a defence against browsing (Dormann & Skarpe, 2002), showed a significant browsing effect on AGB but not on BGB (Table 3.3B). This consistent root allocation may reflect the species' adaptation to water-saturated environments, where roots stabilise growth and enhance nutrient uptake (Kuzovkina & Quigley, 2005). Furthermore, *Salix spp.* are well-adapted to degraded soils, demonstrating fast growth, tolerance to flooding, and the ability to resprout after harvesting (Pietrzykowski et al., 2021; Kuzovkina & Quigley, 2004). These traits may explain the lack of statistical significance in this BGB model, as they promote stability and consistency in root biomass allocation regardless of environmental pressures.

Using the browse line (>2.5 m) as a metric instead of browsing condition highlighted significant differences in root-to-shoot (R:S) ratios for both willow and blackthorn (Figure 3.9). For both species, R:S ratios were notably higher below the browse line compared to above it, emphasising the impact of browsing pressure on their growth allocation patterns. These findings align with research by Facciolati et al. (2024), which showed that long-term browsing pressure by red deer (*Cervus elaphus*) drives structural adaptations in blackthorn. Browsed individuals developed increased thorn density and assumed a dwarf, shrubby growth form, whereas unbrowsed plants grew taller and tree-like.

The browse line results in this study better reflect biomass allocation patterns than those derived from the browsing proxy (bramble condition), aligning more closely with the findings of Facciolati et al. (2024) and Perkovich and Ward (2021). The bramble proxy, while useful, does not directly measure herbivore density or browsing intensity, limiting its ability to capture the complexity of biomass allocation. This limitation may partly explain the insignificant effects observed for blackthorn AGB and willow BGB, which could reflect noise in the dataset.

Significant BGB investment was also observed in other scrub taxa below the browse line, independent of browsing condition (Figure 3.9). This suggests an adaptive strategy among smaller individuals to withstand persistent herbivory. Among the species studied, dog rose (*Rosa canina*) and oak (*Quercus spp.*) exhibited the highest mean R:S ratios below the browse line (Figure 3.9). Dog rose, despite its thorny defences reducing browsing pressure (Salek et al., 2019; Coverdale et al., 2018), displayed a high R:S ratio, possibly reflecting a strategy to invest heavily in root biomass for rapid recovery and regrowth, even with minimal aboveground disturbance (Skarpe & Hester, 2008). Similarly, oak's elevated R:S mirrors observations by Rackham (1996) in sheep-browsed landscapes in Crete, where intense browsing pressure led to increased root investment as a survival strategy. This adaptive allocation enhances resilience in heavily disturbed environments, indicating that oaks consistently reallocate resources to roots as a defence against herbivory.

This highlights the importance of root biomass in ensuring long-term resilience and suggests that scrub trees adapt their growth strategies in response to environmental pressures in more complex ways than previously understood.

3.5 Conclusion

This study highlights the importance of developing taxa-specific allometric equations for accurately estimating biomass in scrub ecosystems. I assembled a database of 270 scrub individuals, including roots, across the five dominant scrub taxa to create these allometric equations. These equations, which can be used in conjunction with the taxa-specific carbon values estimated in Chapter 4, will enable assessments of other rewilding projects and help estimate the carbon storage potential of scrubland taxa on rewilded landscapes. The scrub- and taxa-specific models developed here for aboveground, belowground and total biomass, demonstrate a robust predictive performance, filling significant gaps in the carbon accounting of rewilded landscapes.

My findings also indicate that there is more biomass below ground than previously estimated, challenging previous models that failed to account for the complex structural traits of scrub vegetation on browsed landscape, including its higher proportion of belowground biomass.

My research therefore suggests that rewilding and its associated development of scrubland has the potential to store significant amounts of carbon and provide other ecosystem services.

This evidence provides further support that the growing recognition of rewilding and scrubland regeneration can be important contributors to carbon sequestration, particularly in the context of global initiatives such as the UN's REDD+ programme, which seeks to mitigate climate change through forest carbon stock enhancement (REDD+, www.redd.unfccc.int – Accessed on 18 Sep. 2024). The inclusion of scrublands in such frameworks could significantly enhance global carbon assessments by recognising the biomass and carbon sequestration potential of these ecosystems.

3.6 Reference list

- Ali, A., Xu, M.S., Zhao, Y.T., Zhang, Q.Q., Zhou, L.L., Yang, X.D., Yan, E.R., 2015. Allometric biomass equations for shrub and small tree species in subtropical China. *Silva Fenn.* 49 (4) <https://doi.org/10.14214/sf.1275>.
- Alliende, M.C., 1986. *Growth and reproduction in a dioecious tree, Salix cinera* (Doctoral dissertation, University College of North Wales).
- Axe, M.S., Grange, I.D. and Conway, J.S., 2017. Carbon storage in hedge biomass—A case study of actively managed hedges in England. *Agriculture, ecosystems & environment*, 250, pp.81-88.
- Bakker, E.S. and Svenning, J.C., 2018. Trophic rewilding: impact on ecosystems under global change. *Philosophical Transactions of the Royal Society B: Biological Sciences*, 373(1761), p.20170432.
- Bakker, E.S., Gill, J.L., Johnson, C.N., Vera, F.W., Sandom, C.J., Asner, G.P. and Svenning, J.C., 2016. Combining paleo-data and modern exclosure experiments to assess the impact of megafauna extinctions on woody vegetation. *Proceedings of the National Academy of Sciences*, 113(4), pp.847-855.
- Balandier, P., Collet, C., Miller, J.H., Reynolds, P.E. and Zedaker, S.M., 2006. Designing forest vegetation management strategies based on the mechanisms and dynamics of crop tree competition by neighbouring vegetation. *Forestry*, 79(1), pp.3-27.
- Balandier, P., Marquier, A., Casella, E., Kiewitt, A., Coll, L., Wehrlen, L. and Harmer, R., 2013. Architecture, cover and light interception by bramble (*Rubus fruticosus*): a common understorey weed in temperate forests. *Forestry*, 86(1), pp.39-46.
- Bardgett, R.D., Mommer, L. and De Vries, F.T., 2014. Going underground: root traits as drivers of ecosystem processes. *Trends in ecology & evolution*, 29(12), pp.692-699.
- Bar-On, Y.M., Phillips, R. and Milo, R., 2018. The biomass distribution on Earth. *Proceedings of the National Academy of Sciences*, 115(25), pp.6506-6511.
- Bastin, J.F., Finegold, Y., Garcia, C., Mollicone, D., Rezende, M., Routh, D., Zohner, C.M. and Crowther, T.W., 2019. The global tree restoration potential. *Science*, 365(6448), pp.76-79.
- Berzaghi, F., Bretagnolle, F., Durand-Bessart, C. and Blake, S., 2023. Megaherbivores modify forest structure and increase carbon stocks through multiple pathways. *Proceedings of the National Academy of Sciences*, 120(5), p.e2201832120.
- Biermann, C. and Anderson, R.M., 2017. Conservation, biopolitics, and the governance of life and death. *Geography Compass*, 11(10), p.e12329.
- Brooker, R.W. and Callaghan, T.V., 1998. The balance between positive and negative plant interactions and its relationship to environmental gradients: a model. *Oikos*, pp.196-207.

- Broughton, R. K., Bullock, J. M., George, C., Hill, R. A., Hinsley, S. A., Maziarz, M., Melin, M., Mountford, J. O., Sparks, T. H., & Pywell, R. F. (2021). Long-term woodland restoration on lowland farmland through passive rewilding. *PLoS One*, 16(6), e0252466.
- Brown, J.A., Montgomery, W.I. and Provan, J., 2022. Strong spatial structuring of clonal genetic diversity within blackthorn (*Prunus spinosa*) hedgerows and woodlands. *Tree Genetics & Genomes*, 18(1), p.5.
- Brown, S. (1997). Estimating biomass and biomass change of tropical forests: A primer (p. 134). Food and Agriculture Organization of the United Nations
- Brown, S. and Lugo, A.E., 1984. Biomass of tropical forests: a new estimate based on forest volumes. *Science*, 223(4642), pp.1290-1293.6.
- Bullock, J.M., Aronson, J., Newton, A.C., Pywell, R.F. and Rey-Benayas, J.M., 2011. Restoration of ecosystem services and biodiversity: conflicts and opportunities. *Trends in ecology & evolution*, 26(10), pp.541-549.
- Bunzel-Drüke, M., 2001. Ecological substitutes for wild horse (*Equus ferus* Boddaert, 1785= *E. przewalskii* Poljakov, 1881) and aurochs (*Bos primigenius* Bojanus, 1827). *Natur-und Kulturlandschaft*, 4(9).
- Buotte, P.C., Law, B.E., Ripple, W.J. and Berner, L.T., 2020. Carbon sequestration and biodiversity co-benefits of preserving forests in the western United States. *Ecological Applications*, 30(2), p.e02039.
- Burrell, N.C., Jeffers, E.S., Macias-Fauria, M. and Willis, K.J., 2024. The inadequacy of current carbon storage assessment methods for rewilding: A Knepp Estate case study. *Ecological Solutions and Evidence*, 5(1), p.e12301.
- Cairns, M.A., Brown, S., Helmer, E.H. and Baumgardner, G.A., 1997. Root biomass allocation in the world's upland forests. *Oecologia*, 111, pp.1-11.
- Callaway, R.M., 1995. Positive interactions among plants. *The botanical review*, 61, pp.306-349.
- Castillo-Figueroa, D., González-Melo, A. and Posada, J.M., 2023. Wood density is related to aboveground biomass and productivity along a successional gradient in upper Andean tropical forests. *Frontiers in Plant Science*, 14, p.1276424.
- Cerqueira, Y., Navarro, L.M., Maes, J., Marta-Pedroso, C., Pradinho Honrado, J. and Pereira, H.M., 2015. Ecosystem services: the opportunities of rewilding in Europe. *Rewilding European Landscapes*, pp.47-64.
- Chave, J., Andalo, C., Brown, S., Cairns, M.A., Chambers, J.Q., Eamus, D., Fölster, H., Fromard, F., Higuchi, N., Kira, T. and Lescure, J.P., 2005. Tree allometry and improved estimation of carbon stocks and balance in tropical forests. *Oecologia*, 145, pp.87-99.
- Chave, J., Coomes, D., Jansen, S., Lewis, S.L., Swenson, N.G. and Zanne, A.E., 2009. Towards a worldwide wood economics spectrum. *Ecology letters*, 12(4), pp.351-366.
- Chen, J., Fang, X., Wu, A., Xiang, W., Lei, P. and Ouyang, S., 2024. Allometric equations for estimating biomass of natural shrubs and young trees of subtropical forests. *New Forests*, 55(1), pp.15-46.

- Chua, S.C. and Potts, M.D., 2018. The role of plant functional traits in understanding forest recovery in wet tropical secondary forests. *Science of the Total Environment*, 642, pp.1252-1262.
- Churski, M., Charles-Dominique, T., Bubnicki, J. W., Jędrzejewska, B., Kuijper, D. P., & Cromsigt, J. P. (2022). Herbivore-induced branching increases sapling survival in temperate forest canopy gaps. *Journal of Ecology*, 110, 1390–1402.
- Clough, B.J., Domke, G.M., MacFarlane, D.W., Radtke, P.J., Russell, M.B., Weiskittel, A. R., 2018. Testing a new component ratio method for predicting total tree aboveground and component biomass for widespread pine and hardwood species of eastern US. *For. Int. J. Forest Res.* 91 (5), 575–588. <https://doi.org/10.1093/forestry/cpy016>.
- Conti, G., Enrico, L., Casanoves, F., Díaz, S., 2013. Shrub biomass estimation in the semiarid Chaco forest: a contribution to the quantification of an underrated carbon stock. *Ann. For. Sci.* 70 (5), 515–524. <https://doi.org/10.1007/s13595-013-0285-9>.
- Coomes, D.A. and Allen, R.B., 2007. Effects of size, competition and altitude on tree growth. *Journal of Ecology*, 95(5), pp.1084-1097.
- Corlett, R.T., 2016. Restoration, reintroduction, and rewilding in a changing world. *Trends in ecology & evolution*, 31(6), pp.453-462.
- Coverdale, T.C., Goheen, J.R., Palmer, T.M. and Pringle, R.M., 2018. Good neighbors make good defenses: associational refuges reduce defense investment in African savanna plants. *Ecology*, 99(8), pp.1724-1736.
- Crawley, M.J., 2024. Species identifications verified. [Personal communication].
- Cromsigt, J.P., Te Beest, M., Kerley, G.I., Landman, M., Le Roux, E. and Smith, F.A., 2018. Trophic rewilding as a climate change mitigation strategy?. *Philosophical Transactions of the Royal Society B: Biological Sciences*, 373(1761), p.20170440.
- Dalgleish, H.J. and Hartnett, D.C., 2006. Below-ground bud banks increase along a precipitation gradient of the North American Great Plains: a test of the meristem limitation hypothesis. *New Phytologist*, 171(1), pp.81-89.
- Department for Environment, Food & Rural Affairs. (2021) *The Englandtrees action plan 2021–2024*. <https://www.gov.uk/government/publications/england-trees-action-plan-2021-to-2024:1>
- Dormann, C.F. and Skarpe, C., 2002. Flowering, growth and defence in the two sexes: consequences of herbivore exclusion for *Salix polaris*. *Functional Ecology*, pp.649-656.
- Eamus, D., Chen, X., Kelley, G. and Hutley, L.B., 2002. Root biomass and root fractal analyses of an open Eucalyptus forest in a savanna of north Australia. *Australian Journal of Botany*, 50(1), pp.31-41.
- Eamus, D., O'Grady, A.P. and Hutley, L., 2000. Dry season conditions determine wet season water use in the wet–tropical savannas of northern Australia. *Tree physiology*, 20(18), pp.1219-1226.

- Eldridge, D.J., et al. (2011). "Impacts of shrub encroachment on carbon storage in semi-arid ecosystems." *Ecology Letters*, 14(8), pp. 709-716.
- Enquist, B.J., West, G.B., Charnov, E.L. and Brown, J.H., 1999. Allometric scaling of production and life-history variation in vascular plants. *Nature*, 401(6756), pp.907-911.
- Erkin, F., Yue, D., Abdureyim, A., Huang, W. and Tayir, M., 2023. Link between the aboveground and belowground biomass allocation with growing of *Tamarix* sp. seedlings in the hinterland of Taklimakan Desert, China. *Plos one*, 18(8), p.e0289670.
- Facciolati, V., Zarek, M., Blonska, E., Lasota, J., Orman, O. and Ciach, M., 2024. To be browsed or not to be browsed: differences in nutritional characteristics of blackthorn *Prunus spinosa* subject to the long-term pressure of herbivores. *bioRxiv*, pp.2024-04.
- Feldpausch, T.R., Banin, L., Phillips, O.L., Baker, T.R., Lewis, S.L., Quesada, C.A., Affum-Baffoe, K., Arets, E.J., Berry, N.J., Bird, M. and Brondizio, E.S., 2011. Height-diameter allometry of tropical forest trees. *Biogeosciences*, 8(5), pp.1081-1106.
- Fernández, N., Navarro, L.M. and Pereira, H.M., 2017. Rewilding: a call for boosting ecological complexity in conservation. *Conservation Letters*, 10(3), pp.276-278.
- Fontana, M., Collin, A., Courchesne, F., Labrecque, M. and Bélanger, N., 2020. Root system architecture of *Salix miyabeana* "SX67" and relationships with aboveground biomass yields. *BioEnergy research*, 13, pp.183-196.
- Forrester, D.I., Benneter, A., Bouriaud, O. and Bauhus, J., 2017. Diversity and competition influence tree allometric relationships—Developing functions for mixed-species forests. *Journal of Ecology*, 105(3), pp.761-774.
- Gill, R.A. and Jackson, R.B., 2000. Global patterns of root turnover for terrestrial ecosystems. *The New Phytologist*, 147(1), pp.13-31.
- Goldberg, D. and Novoplansky, A., 1997. On the relative importance of competition in unproductive environments. *Journal of Ecology*, pp.409-418.
- Gómez-Aparicio, L., Zamora, R., Gómez, J.M., Hódar, J.A., Castro, J. and Baraza, E., 2004. Applying plant facilitation to forest restoration: a meta-analysis of the use of shrubs as nurse plants. *Ecological applications*, 14(4), pp.1128-1138.
- Griscom, B.W., Adams, J., Ellis, P.W., Houghton, R.A., Lomax, G., Miteva, D.A., Schlesinger, W.H., Shoch, D., Siikamäki, J.V., Smith, P. and Woodbury, P., 2017. Natural climate solutions. *Proceedings of the National Academy of Sciences*, 114(44), pp.11645-11650.
- Guo, Q., Chi, X., Xie, Z. and Tang, Z., 2017. Asymmetric competition for light varies across functional groups. *Journal of Plant Ecology*, 10(1), pp.74-80.
- Hamilton III, E.W., Frank, D.A., Hinchey, P.M. and Murray, T.R., 2008. Defoliation induces root exudation and triggers positive rhizospheric feedbacks in a temperate grassland. *Soil Biology and Biochemistry*, 40(11), pp.2865-2873.
- Harden, G. J. (1990). *Flora of New South Wales* (Vol. 4). UNSW Press.

- Harmer, R., Kerr, G., Stokes, V. and Connolly, T., 2017. The influence of thinning intensity and bramble control on ground flora development in a mixed broadleaved woodland. *Forestry: An International Journal of Forest Research*, 90(2), pp.247-257.
- Harmer, R., Kiewitt, A., Morgan, G. and Gill, R., 2010. Does the development of bramble (*Rubus fruticosus* L. agg.) facilitate the growth and establishment of tree seedlings in woodlands by reducing deer browsing damage?. *Forestry*, 83(1), pp.93-102.
- Henry, M., 2010. Carbon stocks and dynamics in Sub-Saharan Africa.
- Henry, M., Picard, N., Trotta, C., Manlay, R., Valentini, R., Bernoux, M., Saint-André, L., 2011. Estimating tree biomass of sub-Saharan African forests: a review of available allometric equations. *Silva Fenn.* 45 (3B) <https://doi.org/10.14214/sf.38>.
- Hester, A.J., Edenius, L., Buttenschøn, R.M. and Kuiters, A.T., 2000. Interactions between forests and herbivores: the role of controlled grazing experiments. *Forestry*, 73(4), pp.381-391.
- Hodder, K.H. and Bullock, J.M., 2009. Really Wild? Naturalistic grazing in modern landscapes. *British Wildlife*, 20(5), pp.37-43.
- Hodder, K.H., Newton, A.C., Cantarello, E. and Perrella, L., 2014. Does landscape-scale conservation management enhance the provision of ecosystem services?. *International Journal of Biodiversity Science, Ecosystem Services & Management*, 10(1), pp.71-83.
- Howison, R.A., Olff, H., van de Koppel, J. and Smit, C., 2017. Biotically driven vegetation mosaics in grazing ecosystems: the battle between bioturbation and biocompaction. *Ecological Monographs*, 87(3), pp.363-378.
- Huynh, T., Lee, D.J., Applegate, G. and Lewis, T., 2021. Field methods for above and belowground biomass estimation in plantation forests. *MethodsX*, 8, p.101192.
- i-Tree Eco Manual (2020) US Forest Service. i-Tree Eco User's Manual v.6.0.
- Jackson, R.B., et al. (1996). "A global analysis of root distributions for terrestrial biomes." *Oecologia*, 108(3), pp. 389-411.
- Jacobsen, A.L., Pratt, R.B., Ewers, F.W. and Davis, S.D., 2007. Cavitation resistance among 26 chaparral species of southern California. *Ecological Monographs*, 77(1), pp.99-115.
- Jenkins, J.C., Chojnacky, D.C., Heath, L.S. and Birdsey, R.A., 2003. National-scale biomass estimators for United States tree species. *Forest science*, 49(1), pp.12-35.
- Jepson, P., 2016. A rewilding agenda for Europe: creating a network of experimental reserves. *Ecography*, 39(2).
- Jobbágy, E.G., and Jackson, R.B. (2000). "The vertical distribution of soil organic carbon and its relation to climate and vegetation." *Ecological Applications*, 10(2), pp. 423-436.
- Daryanto, S., Eldridge, D.J. (2010). "Plant and soil surface responses to shrub removal and grazing in a shrub-encroached woodland." *Journal of Environmental Management*, 91, pp. 2639-2648.
- Johnson, O., 2004. *Collins tree guide* (pp. 464-pp).
- Josh Donlan, C., Berger, J., Bock, C.E., Bock, J.H., Burney, D.A., Estes, J.A., Foreman, D., Martin, P.S., Roemer, G.W., Smith, F.A. and Soulé, M.E., 2006. Pleistocene rewilding: an

optimistic agenda for twenty-first century conservation. *The American Naturalist*, 168(5), pp.660-681.

Jucker, T., Caspersen, J., Chave, J., Antin, C., Barbier, N., Bongers, F., Dalponte, M., van Ewijk, K.Y., Forrester, D.I., Haeni, M. and Higgins, S.I., 2017. Allometric equations for integrating remote sensing imagery into forest monitoring programmes. *Global change biology*, 23(1), pp.177-190.

Kallarackal, J., Ramírez, F. (2024). Wood and Wood Density. In: *Wood Density*. Springer, Cham. https://doi.org/10.1007/978-3-031-61030-1_2

Kaštovská, E., Mastný, J. and Konvička, M., 2024. Rewilding by large ungulates contributes to organic carbon storage in soils. *Journal of Environmental Management*, 355, p.120430.

Keesstra, S., Nunes, J., Novara, A., Finger, D., Avelar, D., Kalantari, Z. and Cerdà, A., 2018. The superior effect of nature based solutions in land management for enhancing ecosystem services. *Science of the Total Environment*, 610, pp.997-1009.

King, D.A., 2003. Allocation of above-ground growth is related to light in temperate deciduous saplings. *Functional Ecology*, 17(4), pp.482-488.

King, D.A., Davies, S.J., Tan, S. and Noor, N.S.M., 2006. The role of wood density and stem support costs in the growth and mortality of tropical trees. *Journal of Ecology*, 94(3), pp.670-680.

Kooch, Y. and Sohrabzadeh, Z., 2024. Soil functional indicators in a semi-arid environment change patchy under the influence of shrub species. *Applied Soil Ecology*, 201, p.105500.

Kühn, N., Tovar, C., Willis, K.J. and Macias-Fauria, M., 2023. Root trait variation along water gradients in the Cape Floristic Region. *Journal of Vegetation Science*, 34(3), p.e13194.

Kunstler, G., Falster, D., Coomes, D.A., Hui, F., Kooyman, R.M., Laughlin, D.C., Poorter, L., Vanderwel, M., Vieilledent, G., Wright, S.J. and Aiba, M., 2016. Plant functional traits have globally consistent effects on competition. *Nature*, 529(7585), pp.204-207.

Kuzovkina, Y.A. and Quigley, M.F., 2005. Willows beyond wetlands: uses of *Salix* L. species for environmental projects. *Water, Air, and Soil Pollution*, 162, pp.183-204.

La Notte, A., 2024. Greening finance and green financing need environmental metrics. The opportunities offered by natural capital accounts. *Journal of Sustainable Finance and Accounting*, 3, p.100013.

Langley, J., Drake, B. and Hungate, B., 2002. Extensive belowground carbon storage supports roots and mycorrhizae in regenerating scrub oaks. *Oecologia*, 131, pp.542-548.

Laurent, L., Mårell, A., Korboulewsky, N., Saïd, S. and Balandier, P., 2017. How does disturbance affect the intensity and importance of plant competition along resource gradients?. *Forest Ecology and management*, 391, pp.239-245.

Le Roux, E., Kerley, G.I. and Cromsigt, J.P., 2018. Megaherbivores modify trophic cascades triggered by fear of predation in an African savanna ecosystem. *Current Biology*, 28(15), pp.2493-2499.

- Leinemann, Ludger, Jörg Kleinschmit, Barbara Fussi, Bernhard Hosius, Oleksandra Kuchma, Wolfgang Arenhövel, Patrick Lemmen, Ralf Kätzel, Martin Rogge, and Reiner Finkeldey. "Genetic composition and differentiation of sloe (*Prunus spinosa* L.) populations in Germany with respect to the tracing of reproductive plant material." *Plant Systematics and Evolution* 300 (2014): 2115-2125.
- Levillain, J., Thongo M'Bou, A., Deleporte, P., Saint-André, L. and Jourdan, C., 2011. Is the simple auger coring method reliable for below-ground standing biomass estimation in Eucalyptus forest plantations?. *Annals of Botany*, 108(1), pp.221-230.
- Litton, C.M., Boone Kauffman, J., 2008. Allometric models for predicting aboveground biomass in two widespread woody plants in Hawaii. *Biotropica* 40 (3), 313–320. <https://doi.org/10.1111/j.1744-7429.2007.00383.x>.
- Lutz, J.A., Furniss, T.J., Johnson, D.J., Davies, S.J., Allen, D., Alonso, A., Anderson-Teixeira, K.J., Andrade, A., Baltzer, J., Becker, K.M. and Blomdahl, E.M., 2018. Global importance of large-diameter trees. *Global Ecology and Biogeography*, 27(7), pp.849-864.
- Maestre, F.T., et al. (2009). "Carbon storage in Mediterranean shrublands: a focus on belowground biomass." *Oecologia*, 161(4), pp. 735-747.
- Malhi, Y., Lander, T., le Roux, E., Stevens, N., Macias-Fauria, M., Wedding, L., Girardin, C., Kristensen, J.Å., Sandom, C.J., Evans, T.D. and Svenning, J.C., 2022. The role of large wild animals in climate change mitigation and adaptation. *Current Biology*, 32(4), pp.R181-R196.
- Martínez-Cabrera, H.I., Jones, C.S., Espino, S. and Schenk, H.J., 2009. Wood anatomy and wood density in shrubs: responses to varying aridity along transcontinental transects. *American journal of botany*, 96(8), pp.1388-1398.
- Matthews, R. (2017). 11. Forest carbon and biomass policy. *Forest Research Impact Case Studies*, p. 85.- Navarro & Pereira, 2015
- Mercer, L. and Gregg, R., 2023. Exploring the carbon sequestration potential of rewilding in the UK: Policy and data needs to support net zero.
- Mikołajczak, K.M., Jones, N., Sandom, C.J., Wynne-Jones, S., Beardsall, A., Burgelman, S., Ellam, L. and Wheeler, H.C., 2022. Rewilding—The farmers' perspective. Perceptions and attitudinal support for rewilding among the English farming community. *People and Nature*, 4(6), pp.1435-1449.
- Mokany, K., Raison, R.J. and Prokushkin, A.S., 2006. Critical analysis of root: shoot ratios in terrestrial biomes. *Global change biology*, 12(1), pp.84-96.
- Mortimer, S.R., Turner, A.J., Brown, V.K., Fuller, R.J., Good, J.E.G., Bell, S.A., Stevens, P.A., Norris, D., Bayfield, N.G. and Ward, L.K., 2000. The nature conservation value of scrub in Britain.
- Mugasha, W.A., Eid, T., Bollandsås, O.M., Malimbwi, R.E., Chamshama, S.A.O., Zahabu, E., Katani, J.Z., 2013. Allometric models for prediction of above- and belowground biomass of trees in the Miombo woodlands of Tanzania. *For. Ecol. Manage.* 310, 87–101. <https://doi.org/10.1016/j.foreco.2013.08.003>.

- Navarro, L.M. and Pereira, H.M., 2015. Rewilding abandoned landscapes in Europe. In *Rewilding european landscapes* (pp. 3-23). Cham: Springer International Publishing.
- Navarro, M.N.V., Jourdan, C., Sileye, T., Braconnier, S., Mialet-Serra, I., Saint-André, L., Dauzat, J., Nouvellon, Y., Epron, D., Bonnefond, J.M. and Berbigier, P., 2008. Fruit development, not GPP, drives seasonal variation in NPP in a tropical palm plantation. *Tree physiology*, 28(11), pp.1661-1674.
- Nelson, E., Mendoza, G., Regetz, J., Polasky, S., Tallis, H., Cameron, D., Chan, K.M., Daily, G.C., Goldstein, J., Kareiva, P.M. and Lonsdorf, E., 2009. Modeling multiple ecosystem services, biodiversity conservation, commodity production, and tradeoffs at landscape scales. *Frontiers in Ecology and the Environment*, 7(1), pp.4-11.
- Ngomanda, A., Obiang, N. L. E., Lebamba, J., Mavouroulou, Q. M., Gomat, H., Mankou, G. S., Loumeto, J., Iponga, D. M., Ditsouga, F. K., Koumba, R. Z., Bobé, K. H. B., Okouyi, C. M., Nyangadouma, R., Lépengué, N., Mbatchi, B., & Picard, N. (2014). Site-specific versus pantropical allometric equations: Which option to estimate the biomass of a moist central African forest? *Forest Ecology and Management*, 312, 1–9.
- Nowak, D. J. (2019) Understanding i-Tree: Summary of programs and methods. *Understanding I-Tree: Summary of Programs and Methods*.
- Nowak, D.J., 2020. Understanding i-Tree: Summary of programs and methods. *General Technical Report NRS-200. Madison, WI: US Department of Agriculture, Forest Service, Northern Research Station. 100 p., 200, pp.1-100.*
- Nyamukuru, A., Whitney, C., Tabuti, J.R., Esaete, J. and Low, M., 2023. Allometric models for aboveground biomass estimation of small trees and shrubs in African savanna ecosystems. *Trees, Forests and People*, 11, p.100377.
- Orians, C.M., Thorn, A. and Gómez, S., 2011. Herbivore-induced resource sequestration in plants: why bother?. *Oecologia*, 167, pp.1-9.
- Pan, Y., Birdsey, R.A., Fang, J., Houghton, R., Kauppi, P.E., Kurz, W.A., Phillips, O.L., Shvidenko, A., Lewis, S.L., Canadell, J.G. and Ciais, P., 2011. A large and persistent carbon sink in the world's forests. *science*, 333(6045), pp.988-993.
- Parresol, B.R., 1999. Assessing tree and stand biomass: a review with examples and critical comparisons. *Forest science*, 45(4), pp.573-593.
- Pati, P. K., Kaushik, P., Khan, M., & Khare, P. K. (2022). Allometric equations for biomass and carbon stock estimation of small diameter woody species from tropical dry deciduous forests: Support to REDD+. *Trees, Forests and People*, 9, 100289.
- Pedersen, P.B.M., Ejrnæs, R., Sandel, B. and Svenning, J.C., 2020. Trophic Rewilding Advancement in Anthropogenically Impacted Landscapes (TRAIL): A framework to link conventional conservation management and rewilding. *Ambio*, 49, pp.231-244.
- Pereira, H.M., Navarro, L.M. and Martins, I.S., 2012. Global biodiversity change: the bad, the good, and the unknown. *Annual review of environment and resources*, 37(1), pp.25-50.

Perkovich, C. and Ward, D., 2021. Herbivore-induced defenses are not under phylogenetic constraints in the genus *Quercus* (oak): Phylogenetic patterns of growth, defense, and storage. *Ecology and Evolution*, 11(10), pp.5187-5203.

Perkovich, C., & Ward, D. (2021a). Aboveground herbivory causes belowground changes in twelve oak *Quercus* species: a phylogenetic analysis of root biomass and non-structural carbohydrate storage. *Oikos*, 130(10), 1797–1812.

Pettorelli, N., Graham, N.A., Seddon, N., Maria da Cunha Bustamante, M., Lowton, M.J., Sutherland, W.J., Koldewey, H.J., Prentice, H.C. and Barlow, J., 2021. Time to integrate global climate change and biodiversity science-policy agendas. *Journal of Applied Ecology*, 58(11), pp.2384-2393.

Picard, N., Saint-André, L. and Henry, M., 2012. Manual for building tree volume and biomass allometric equations: from field measurement to prediction.

Pietrzykowski, M., Woś, B., Tylek, P., et al. (2021). Carbon sink potential and allocation in above- and below-ground biomass in willow coppice. *Journal of Forestry Research*, 32, 349–354. <https://doi.org/10.1007/s11676-019-01089-3>.

Poorter, L., Wright, S.J., Paz, H., Ackerly, D.D., Condit, R., Ibarra-Manríquez, G., Harms, K.E., Licona, J.C., Martinez-Ramos, M., Mazer, S.J. and Muller-Landau, H.C., 2008. Are functional traits good predictors of demographic rates? Evidence from five neotropical forests. *Ecology*, 89(7), pp.1908-1920.

Post, E., Kaarlejärvi, E., Macias-Fauria, M., Watts, D.A., Bøving, P.S., Cahoon, S.M., Higgins, R.C., John, C., Kerby, J.T., Pedersen, C. and Post, M., 2023. Large herbivore diversity slows sea ice-associated decline in arctic tundra diversity. *Science*, 380(6651), pp.1282-1287.

Post, E., Pedersen, C. and Watts, D.A., 2022. Large herbivores facilitate the persistence of rare taxa under tundra warming. *Scientific Reports*, 12(1), p.1292.

Pringle, R.M., Abraham, J.O., Anderson, T.M., Coverdale, T.C., Davies, A.B., Dutton, C.L., Gaylard, A., Goheen, J.R., Holdo, R.M., Hutchinson, M.C. and Kimuyu, D.M., 2023. Impacts of large herbivores on terrestrial ecosystems. *Current Biology*, 33(11), pp.R584-R610.

Qian, J., Wang, Z., Liu, Z. and Busso, C.A., 2017. Belowground bud bank responses to grazing intensity in the Inner-Mongolia steppe, China. *Land Degradation & Development*, 28(3), pp.822-832.

R Core Team (2024). *R: A language and environment for statistical computing*. Version 4.4.1. R Foundation for Statistical Computing, Vienna, Austria. Available at: <https://www.R-project.org/> (Accessed: 2 November 2024).

Rackham O. 1990. *Trees and woodland in the British landscape*, 2nd edn. London, UK: Dent.

Rackham, O. and Moody, J., 1996. *The making of the Cretan landscape*. Manchester University Press.

Randle, T., & Jenkins, T. (2011). The construction of lookup tables for estimating changes in carbon stocks in forestry projects. *A background document for users of the Forestry Commissions's Woodland Carbon Code*.

- Ranjan, A., Sinha, R., Singla-Pareek, S.L., Pareek, A. and Singh, A.K., 2022. Shaping the root system architecture in plants for adaptation to drought stress. *Physiologia plantarum*, 174(2), p.e13651.
- Rewilding-Britain. (2020). Reforesting Britain—Why natural regeneration should be our default approach to woodland expansion.
- Rincon-Madroñero, M., Sánchez-Zapata, J.A., Barber, X. and Barbosa, J.M., 2024. Long-term vegetation responses to climate depend on the distinctive roles of rewilding and traditional grazing systems. *Landscape Ecology*, 39(1), p.1.
- Rousset, O. and Lepart, J., 2000. Positive and negative interactions at different life stages of a colonizing species (*Quercus humilis*). *Journal of Ecology*, 88(3), pp.401-412.
- Roxburgh, S.H., Paul, K.I., Clifford, D., England, J.R. and Raison, R.J., 2015. Guidelines for constructing allometric models for the prediction of woody biomass: how many individuals to harvest?. *Ecosphere*, 6(3), pp.1-27.
- Rule, S., Brook, B.W., Haberle, S.G., Turney, C.S., Kershaw, A.P. and Johnson, C.N., 2012. The aftermath of megafaunal extinction: ecosystem transformation in Pleistocene Australia. *Science*, 335(6075), pp.1483-1486.
- Saatchi, S.S., Harris, N.L., Brown, S., Lefsky, M., Mitchard, E.T., Salas, W., Zutta, B.R., Buermann, W., Lewis, S.L., Hagen, S. and Petrova, S., 2011. Benchmark map of forest carbon stocks in tropical regions across three continents. *Proceedings of the national academy of sciences*, 108(24), pp.9899-9904.
- Salek, L., Harmacek, J., Jerabkova, L., Topacoglu, O. and Machar, I., 2019. Thorny shrubs limit the browsing pressure of large herbivores on tree regeneration in temperate lowland forested landscapes. *Sustainability*, 11(13), p.3578.
- Sandhage-Hofmann, A., Linstädter, A., Kindermann, L., Angombe, S. and Amelung, W., 2021. Conservation with elevated elephant densities sequesters carbon in soils despite losses of woody biomass. *Global Change Biology*, 27(19), pp.4601-4614.
- Sandom, C., Donlan, C.J., Svenning, J.C. and Hansen, D., 2013. Rewilding. *Key topics in conservation biology 2*, pp.430-451.
- Sandom, C.J., Dempsey, B., Bullock, D., Ely, A., Jepson, P., Jimenez-Wisler, S., Newton, A., Pettorelli, N. and Senior, R.A., 2019. Rewilding in the English uplands: Policy and practice. *Journal of Applied Ecology*, 56(2), pp.266-273.
- Saranpää, P., 2003. *Wood density and growth. Wood quality and its biological basis*, pp.87-117.
- Schenk, H.J. and Jackson, R.B., 2002. Rooting depths, lateral root spreads and below-ground/above-ground allometries of plants in water-limited ecosystems. *Journal of Ecology*, pp.480-494.
- Schenk, H.J. and Jackson, R.B., 2005. Mapping the global distribution of deep roots in relation to climate and soil characteristics. *Geoderma*, 126(1-2), pp.129-140.

- Schmitz, O.J., Sylvén, M., Atwood, T.B., Bakker, E.S., Berzaghi, F., Brodie, J.F., Cromsigt, J.P., Davies, A.B., Leroux, S.J., Schepers, F.J. and Smith, F.A., 2023. Trophic rewilding can expand natural climate solutions. *Nature Climate Change*, 13(4), pp.324-333.
- Schnitzler, A. and Borlea, F., 1998. Lessons from natural forests as keys for sustainable management and improvement of naturalness in managed broadleaved forests. *Forest Ecology and Management*, 109(1-3), pp.293-303.
- Seddon, P.J., Griffiths, C.J., Soorae, P.S. and Armstrong, D.P., 2014. Reversing defaunation: restoring species in a changing world. *Science*, 345(6195), pp.406-412.
- Serapiglia, M.J., Cameron, K.D., Stipanovic, A.J., Abrahamson, L.P., Volk, T.A. and Smart, L.B., 2013. Yield and woody biomass traits of novel shrub willow hybrids at two contrasting sites. *Bioenergy research*, 6, pp.533-546.
- Siddiq, Z., Hayyat, M.U., Khan, A.U., Mahmood, R., Shahzad, L., Ghaffar, R. and Cao, K.F., 2021. Models to estimate the above and below ground carbon stocks from a subtropical scrub forest of Pakistan. *Global Ecology and Conservation*, 27, p.e01539.
- Skarpe, C. and Hester, A.J., 2008. Plant traits, browsing and grazing herbivores, and vegetation dynamics. *Ecological Studies*, 195, p.217.
- Slik, J.F., Paoli, G., McGuire, K., Amaral, I., Barroso, J., Bastian, M., Blanc, L., Bongers, F., Boundja, P., Clark, C. and Collins, M., 2013. Large trees drive forest aboveground biomass variation in moist lowland forests across the tropics. *Global ecology and biogeography*, 22(12), pp.1261-1271.
- Smit, C., Ruifrok, J.L., van Klink, R. and Olf, H., 2015. Rewilding with large herbivores: The importance of grazing refuges for sapling establishment and wood-pasture formation. *Biological Conservation*, 182, pp.134-142.
- Smithwick, E.A., Lucash, M.S., McCormack, M.L. and Sivandran, G., 2014. Improving the representation of roots in terrestrial models. *Ecological Modelling*, 291, pp.193-204.
- Stephenson, N.L., Das, A.J., Condit, R., Russo, S.E., Baker, P.J., Beckman, N.G., Coomes, D.A., Lines, E.R., Morris, W.K., Rüger, N. and Álvarez, E., 2014. Rate of tree carbon accumulation increases continuously with tree size. *Nature*, 507(7490), pp.90-93.
- Sun, G., Zhu-Barker, X., Chen, D., Liu, L., Zhang, N., Shi, C., He, L. and Lei, Y., 2017. Responses of root exudation and nutrient cycling to grazing intensities and recovery practices in an alpine meadow: an implication for pasture management. *Plant and Soil*, 416, pp.515-525.
- Svenning, J.C., McGeoch, M.A., Normand, S., Ordonez, A. and Riede, F., 2024. Navigating ecological novelty towards planetary stewardship: challenges and opportunities in biodiversity dynamics in a transforming biosphere. *Philosophical Transactions of the Royal Society B*, 379(1902), p.20230008.
- Svenning, J.C., Pedersen, P.B., Donlan, C.J., Ejrnæs, R., Faurby, S., Galetti, M., Hansen, D.M., Sandel, B., Sandom, C.J., Terborgh, J.W. and Vera, F.W., 2016. Science for a wilder Anthropocene: Synthesis and future directions for trophic rewilding research. *Proceedings of the National Academy of Sciences*, 113(4), pp.898-906.

Thomas, S.C. and Martin, A.R., 2012. Carbon content of tree tissues: a synthesis. *Forests*, 3(2), pp.332-352.

Tree, I., 2018. *Wilding: The return of nature to a British farm*. Pan Macmillan.

Trepel, J., le Roux, E., Abraham, A.J., Buitenwerf, R., Kamp, J., Kristensen, J.A., Tietje, M., Lundgren, E.J. and Svenning, J.C., 2024. Meta-analysis shows that wild large herbivores shape ecosystem properties and promote spatial heterogeneity. *Nature Ecology & Evolution*, 8(4), pp.705-716.

Tutin, T.G. ed., 1964. *Flora Europaea: Plantaginaceae to Compositae (and Rubiaceae)* (Vol. 4). Cambridge university press.

van Gent, B.A.R.T., 2014. *Rewilding in Europe: Present and Future Policy Potential* (Doctoral dissertation, PhD Thesis: University College Dublin).

Van Uytvanck, J., Van Noyen, A., Milotic, T., Decler, K. & Hoffmann, M. J. J. f. N. C. (2010) Woodland regeneration on grazed former arable land: A question of tolerance, defence or protection?, 18(3), 206-214.

Vera, F.W.M. ed., 2000. *Grazing ecology and forest history*. CABI publishing.

Virgulino-Júnior, P.C.C., Carneiro, D.N., Nascimento Jr, W.R., Cougo, M.F. and Fernandes, M.E.B., 2020. Biomass and carbon estimation for scrub mangrove forests and examination of their allometric associated uncertainties. *PloS one*, 15(3), p.e0230008.

Vorster, A. G., Evangelista, P. H., Stovall, A. E., & Ex, S. (2020). Variability and uncertainty in forest biomass estimates from the tree to landscape scale: The role of allometric equations. *Carbon Balance and Management*, 15, 1–20.

Walker, S.M., Murray, L. and Tepe, T., 2016. Allometric equation evaluation guidance document. *Winrock International: Little Rock, AR, USA*.

Watson, J.E., Shanahan, D.F., Di Marco, M., Allan, J., Laurance, W.F., Sanderson, E.W., Mackey, B. and Venter, O., 2016. Catastrophic declines in wilderness areas undermine global environment targets. *Current Biology*, 26(21), pp.2929-2934.

Wheeler, E.A., Baas, P. and Rodgers, S., 2007. Variations in diot wood anatomy: a global analysis based on the Insidewood database. *Iawa Journal*, 28(3), pp.229-258.

Wiley, E., Casper, B.B. and Helliker, B.R., 2017. Recovery following defoliation involves shifts in allocation that favour storage and reproduction over radial growth in black oak. *Journal of Ecology*, 105(2), pp.412-424.

Zeng, H.Q., Liu, Q.J., Feng, Z.W., Ma, Z.Q., 2010. Biomass equations for four shrub species in subtropical China. *J. Forest Res.* 15 (2), 83–90. <https://doi.org/10.1007/s10310-009-0150-8>.

Zianis, D. and Mencuccini, M., 2004. On simplifying allometric analyses of forest biomass. *Forest ecology and management*, 187(2-3), pp.311-332.

Zianis, D., Muukkonen, P., Mäkipää, R. and Mencuccini, M., 2005. *Biomass and stem volume equations for tree species in Europe*. FI.

Ziemińska, K., Westoby, M. and Wright, I.J., 2015. Broad anatomical variation within a narrow wood density range—A study of twig wood across 69 Australian angiosperms. *PLoS One*, 10(4), p.e0124892.

3.7 Supplementary Material

Table S3.1: Summary of biomass models for above-ground biomass (AGB), below-ground biomass (BGB), and total biomass across different taxa. Models include combinations of log-transformed height, diameter at breast height (DBH), canopy area, condition, and their interactions. Model fit improves with additional predictors and interactions, indicated by higher R² and lower AIC values.

Biomass	Taxon	Model	R ²	RSS	AIC
AGB	hawthorn	log_above ~ log_height	0.75	60.12	168.9
AGB	hawthorn	log_above ~ log_height + log_dbh	0.82	42.22	149.54
AGB	hawthorn	log_above ~ log_height + log_dbh + log_canopy_area	0.9	23.19	118.58
AGB	hawthorn	log_above ~ log_height * log_dbh	0.84	38.89	147.02
AGB	hawthorn	log_above ~ condition + log_height + log_dbh + log_canopy_area	0.91	20.9	114.87
AGB	hawthorn	log_above ~ condition * log_height	0.77	55.03	167.95
AGB	hawthorn	log_above ~ condition * log_height * log_dbh	0.89	26.45	133.83
AGB	hawthorn	log_above ~ condition * log_height * log_dbh * log_canopy_area	0.94	14.02	114.89
BGB	hawthorn	log_below ~ log_height	0.67	43.61	150.92
BGB	hawthorn	log_below ~ log_height + log_dbh	0.8	25.52	121.84
BGB	hawthorn	log_below ~ log_height + log_dbh + log_canopy_area	0.85	19.61	109.36
BGB	hawthorn	log_below ~ log_height * log_dbh	0.81	24.22	120.98
BGB	hawthorn	log_below ~ condition + log_height + log_dbh + log_canopy_area	0.88	15.93	99.94
BGB	hawthorn	log_below ~ condition * log_height	0.73	35.23	142.96
BGB	hawthorn	log_below ~ condition * log_height * log_dbh	0.88	15.53	104.55

Biomass	Taxon	Model	R²	RSS	AIC
BGB	hawthorn	log_below ~ condition * log_height * log_dbh * log_canopy_area	0.92	10.48	98.91
Total	hawthorn	log_total ~ log_height	0.74	51.65	160.39
Total	hawthorn	log_total ~ log_height + log_dbh	0.84	31.68	133.74
Total	hawthorn	log_total ~ log_height + log_dbh + log_canopy_area	0.9	18.43	105.96
Total	hawthorn	log_total ~ log_height * log_dbh	0.85	28.96	130.81
Total	hawthorn	log_total ~ condition + log_height + log_dbh + log_canopy_area	0.92	15.91	99.88
Total	hawthorn	log_total ~ condition * log_height	0.77	45.14	156.85
Total	hawthorn	log_total ~ condition * log_height * log_dbh	0.9	19.14	116.02
Total	hawthorn	log_total ~ condition * log_height * log_dbh * log_canopy_area	0.95	10.57	99.38
AGB	blackthorn	log_above ~ log_height	0.73	92.29	188.19
AGB	blackthorn	log_above ~ log_height + log_dbh	0.78	74.25	178.44
AGB	blackthorn	log_above ~ log_height + log_dbh + log_canopy_area	0.81	66.78	174.71
AGB	blackthorn	log_above ~ log_height * log_dbh	0.78	74.14	180.36
AGB	blackthorn	log_above ~ condition + log_height + log_dbh + log_canopy_area	0.81	66.33	176.35
AGB	blackthorn	log_above ~ condition * log_height	0.78	75.86	181.6
AGB	blackthorn	log_above ~ condition * log_height * log_dbh	0.79	70.33	185.51
AGB	blackthorn	log_above ~ condition * log_height * log_dbh * log_canopy_area	0.86	49.08	182.09
BGB	blackthorn	log_below ~ log_height	0.63	66.58	170.56
BGB	blackthorn	log_below ~ log_height + log_dbh	0.74	46.5	153.17
BGB	blackthorn	log_below ~ log_height + log_dbh + log_canopy_area	0.79	37.4	143.41
BGB	blackthorn	log_below ~ log_height * log_dbh	0.75	45.13	153.55
BGB	blackthorn	log_below ~ condition + log_height + log_dbh + log_canopy_area	0.8	36.25	143.72
BGB	blackthorn	log_below ~ condition * log_height	0.73	48.52	157.47

Biomass	Taxon	Model	R ²	RSS	AIC
BGB	blackthorn	log_below ~ condition * log_height * log_dbh	0.79	38.01	152.28
BGB	blackthorn	log_below ~ condition * log_height * log_dbh * log_canopy_area	0.92	14.14	114.88
Total	blackthorn	log_total ~ log_height	0.71	83.5	182.78
Total	blackthorn	log_total ~ log_height + log_dbh	0.78	62.58	169.21
Total	blackthorn	log_total ~ log_height + log_dbh + log_canopy_area	0.82	53.61	162.85
Total	blackthorn	log_total ~ log_height * log_dbh	0.79	62.16	170.84
Total	blackthorn	log_total ~ condition + log_height + log_dbh + log_canopy_area	0.82	53.51	164.76
Total	blackthorn	log_total ~ condition * log_height	0.76	68.45	176.05
Total	blackthorn	log_total ~ condition * log_height * log_dbh	0.79	59.62	176.59
Total	blackthorn	log_total ~ condition * log_height * log_dbh * log_canopy_area	0.88	36.28	165.77
AGB	sallow	log_above ~ log_height	0.64	75.62	173.04
AGB	sallow	log_above ~ log_height + log_dbh	0.79	42.9	145.57
AGB	sallow	log_above ~ log_height + log_dbh + log_canopy_area	0.87	26.91	123.32
AGB	sallow	log_above ~ log_height * log_dbh	0.8	41.43	145.76
AGB	sallow	log_above ~ condition + log_height + log_dbh + log_canopy_area	0.88	25.27	122.04
AGB	sallow	log_above ~ condition * log_height	0.72	58.73	163.9
AGB	sallow	log_above ~ condition * log_height * log_dbh	0.85	31.6	139.67
AGB	sallow	log_above ~ condition * log_height * log_dbh * log_canopy_area	0.93	14.1	113.7
BGB	sallow	log_below ~ log_height	0.49	69.78	168.86
BGB	sallow	log_below ~ log_height + log_dbh	0.65	47.98	151.38
BGB	sallow	log_below ~ log_height + log_dbh + log_canopy_area	0.73	36.88	139.7
BGB	sallow	log_below ~ log_height * log_dbh	0.67	45	150.05
BGB	sallow	log_below ~ condition + log_height + log_dbh + log_canopy_area	0.74	35.72	140.05

Biomass	Taxon	Model	R ²	RSS	AIC
BGB	sallow	log_below ~ condition * log_height	0.58	57.13	162.46
BGB	sallow	log_below ~ condition * log_height * log_dbh	0.73	36.63	147.35
BGB	sallow	log_below ~ condition * log_height * log_dbh * log_canopy_area	0.81	26.08	145.69
Total	sallow	log_total ~ log_height	0.61	69.06	168.32
Total	sallow	log_total ~ log_height + log_dbh	0.77	40.22	142.22
Total	sallow	log_total ~ log_height + log_dbh + log_canopy_area	0.85	26.66	122.82
Total	sallow	log_total ~ log_height * log_dbh	0.78	38.47	141.9
Total	sallow	log_total ~ condition + log_height + log_dbh + log_canopy_area	0.86	25.33	122.17
Total	sallow	log_total ~ condition * log_height	0.69	53.68	159.22
Total	sallow	log_total ~ condition * log_height * log_dbh	0.83	29.42	135.95
Total	sallow	log_total ~ condition * log_height * log_dbh * log_canopy_area	0.91	15.54	118.77
AGB	oak	log_above ~ log_height	0.7	27.66	113.15
AGB	oak	log_above ~ log_height + log_dbh	0.7	27.33	114.6
AGB	oak	log_above ~ log_height + log_dbh + log_canopy_area	0.8	18.23	97.96
AGB	oak	log_above ~ log_height * log_dbh	0.74	23.85	110.32
AGB	oak	log_above ~ condition + log_height + log_dbh + log_canopy_area	0.85	14.12	88.22
AGB	oak	log_above ~ condition * log_height	0.75	23.07	108.79
AGB	oak	log_above ~ condition * log_height * log_dbh	0.78	19.88	109.94
AGB	oak	log_above ~ condition * log_height * log_dbh * log_canopy_area	0.91	8.05	84.38
BGB	oak	log_below ~ log_height	0.58	28.9	115.17
BGB	oak	log_below ~ log_height + log_dbh	0.58	28.9	117.17
BGB	oak	log_below ~ log_height + log_dbh + log_canopy_area	0.74	18.01	97.4
BGB	oak	log_below ~ log_height * log_dbh	0.6	27.51	116.89

Biomass	Taxon	Model	R ²	RSS	AIC
BGB	oak	log_below ~ condition + log_height + log_dbh + log_canopy_area	0.8	13.82	87.23
BGB	oak	log_below ~ condition * log_height	0.62	26.6	115.34
BGB	oak	log_below ~ condition * log_height * log_dbh	0.66	23.72	118.08
BGB	oak	log_below ~ condition * log_height * log_dbh * log_canopy_area	0.84	10.99	98.68
Total	oak	log_total ~ log_height	0.68	24.47	107.51
Total	oak	log_total ~ log_height + log_dbh	0.68	24.4	109.38
Total	oak	log_total ~ log_height + log_dbh + log_canopy_area	0.81	14.64	87.88
Total	oak	log_total ~ log_height * log_dbh	0.72	21.66	105.89
Total	oak	log_total ~ condition + log_height + log_dbh + log_canopy_area	0.87	10.33	73.84
Total	oak	log_total ~ condition * log_height	0.73	20.76	103.95
Total	oak	log_total ~ condition * log_height * log_dbh	0.77	17.7	104.62
Total	oak	log_total ~ condition * log_height * log_dbh * log_canopy_area	0.92	6.42	73.93
AGB	dog rose	log_above ~ log_height	0.78	41.73	146.9
AGB	dog rose	log_above ~ log_height + log_canopy_area	0.8	38.95	145.1
AGB	dog rose	log_above ~ log_height * log_canopy_area	0.81	35.54	142.07
AGB	dog rose	log_above ~ condition + log_height + log_canopy_area	0.83	32.1	136.46
AGB	dog rose	log_above ~ condition * log_height	0.82	34.73	140.8
AGB	dog rose	log_above ~ condition * log_height * log_canopy_area	0.85	28.43	137.79
BGB	dog rose	log_below ~ log_height	0.51	40.7	145.53
BGB	dog rose	log_below ~ log_height + log_canopy_area	0.56	36.55	141.61
BGB	dog rose	log_below ~ log_height * log_canopy_area	0.56	36.39	143.37
BGB	dog rose	log_below ~ condition + log_height + log_canopy_area	0.63	30.61	133.85
BGB	dog rose	log_below ~ condition * log_height	0.59	34.04	139.69

Biomass	Taxon	Model	R ²	RSS	AIC
BGB	dog rose	log_below ~ condition * log_height * log_canopy_area	0.64	29.78	140.34
Total	dog rose	log_total ~ log_height	0.72	36.38	139.35
Total	dog rose	log_total ~ log_height + log_canopy_area	0.75	32.28	134.77
Total	dog rose	log_total ~ log_height * log_canopy_area	0.77	30.02	132.78
Total	dog rose	log_total ~ condition + log_height + log_canopy_area	0.8	26.57	126.07
Total	dog rose	log_total ~ condition * log_height	0.77	30.72	134.06
Total	dog rose	log_total ~ condition * log_height * log_canopy_area	0.81	24.64	129.92

Table S3.2: The table presents the estimated coefficients for the maximum model $\log(\text{biomass}) \sim \text{condition} * \log(\text{height}) * \log(\text{canopy_area}) * \log(\text{dbh})$, fitted separately for each taxon and biomass type (AGB = Above-Ground Biomass, BGB = Below-Ground Biomass, TB = Total Biomass). Each row shows the taxon, biomass type, coefficient estimate (β), standard error (s.e.), t-value (t), along with the beta identifier (b0 to b15) corresponding to the intercept, main effects, and interaction terms. The intercept is b0, while the highest-order interaction term (b15) captures the combined effect of condition, height, canopy area, and dbh. p-values are excluded from this table as uninformative to these model comparisons. Each of the terms included in the various models (Table 3.4) were significant ($p < 0.05$) (see Tables 3.3a and b).

Taxon	Log(W)	estimate	s.e.	t_value	b
blackthorn	AGB	71.64	66.78	1.07	b0
blackthorn	AGB	43.70	81.77	0.53	b1
blackthorn	AGB	-20.82	18.32	-1.14	b2
blackthorn	AGB	-5.97	7.08	-0.84	b3
blackthorn	AGB	-19.59	18.46	-1.06	b4
blackthorn	AGB	-6.30	21.07	-0.30	b5
blackthorn	AGB	-6.32	9.11	-0.69	b6
blackthorn	AGB	2.06	1.86	1.10	b7
blackthorn	AGB	-18.25	24.59	-0.74	b8
blackthorn	AGB	5.65	4.98	1.13	b9

Taxon	Log(W)	estimate	s.e.	t_value	b
blackthorn	AGB	1.67	1.95	0.86	b10
blackthorn	AGB	0.91	2.21	0.41	b11
blackthorn	AGB	3.46	6.15	0.56	b12
blackthorn	AGB	2.20	2.76	0.80	b13
blackthorn	AGB	-0.52	0.50	-1.03	b14
blackthorn	AGB	-0.40	0.65	-0.61	b15
blackthorn	BGB	52.56	35.84	1.47	b0
blackthorn	BGB	40.82	43.89	0.93	b1
blackthorn	BGB	-12.72	9.83	-1.29	b2
blackthorn	BGB	-3.69	3.80	-0.97	b3
blackthorn	BGB	-16.28	9.91	-1.64	b4
blackthorn	BGB	-11.58	11.31	-1.02	b5
blackthorn	BGB	-4.59	4.89	-0.94	b6
blackthorn	BGB	1.03	1.00	1.03	b7
blackthorn	BGB	-12.55	13.20	-0.95	b8
blackthorn	BGB	3.88	2.67	1.45	b9
blackthorn	BGB	1.35	1.05	1.29	b10
blackthorn	BGB	1.32	1.18	1.12	b11
blackthorn	BGB	3.84	3.30	1.16	b12
blackthorn	BGB	1.19	1.48	0.81	b13
blackthorn	BGB	-0.31	0.27	-1.16	b14
blackthorn	BGB	-0.40	0.35	-1.14	b15
blackthorn	TB	71.90	57.42	1.25	b0
blackthorn	TB	48.88	70.30	0.70	b1
blackthorn	TB	-19.33	15.75	-1.23	b2
blackthorn	TB	-5.96	6.09	-0.98	b3
blackthorn	TB	-20.44	15.87	-1.29	b4
blackthorn	TB	-9.49	18.12	-0.52	b5
blackthorn	TB	-6.43	7.83	-0.82	b6
blackthorn	TB	1.86	1.60	1.16	b7
blackthorn	TB	-18.28	21.14	-0.86	b8

Taxon	Log(W)	estimate	s.e.	t_value	b
blackthorn	TB	5.47	4.28	1.28	b9
blackthorn	TB	1.81	1.68	1.08	b10
blackthorn	TB	1.20	1.90	0.63	b11
blackthorn	TB	4.01	5.29	0.76	b12
blackthorn	TB	2.11	2.37	0.89	b13
blackthorn	TB	-0.50	0.43	-1.15	b14
blackthorn	TB	-0.45	0.56	-0.80	b15
dogrose	AGB	-14.21	43.28	-0.33	b0
dogrose	AGB	3.83	62.71	0.06	b1
dogrose	AGB	4.29	10.23	0.42	b2
dogrose	AGB	1.00	5.75	0.17	b3
dogrose	AGB	3.22	16.36	0.20	b4
dogrose	AGB	0.03	13.71	0.00	b5
dogrose	AGB	-1.01	9.12	-0.11	b6
dogrose	AGB	-0.19	1.30	-0.15	b7
dogrose	AGB	5.32	27.05	0.20	b8
dogrose	AGB	-0.73	3.71	-0.20	b9
dogrose	AGB	-0.27	2.20	-0.12	b10
dogrose	AGB	0.01	1.81	0.00	b11
dogrose	AGB	-1.77	5.83	-0.30	b12
dogrose	AGB	-0.16	3.74	-0.04	b13
dogrose	AGB	0.06	0.47	0.12	b14
dogrose	AGB	0.14	0.72	0.20	b15
dogrose	BGB	30.50	42.40	0.72	b0
dogrose	BGB	-56.96	61.44	-0.93	b1
dogrose	BGB	-8.04	10.02	-0.80	b2
dogrose	BGB	-2.50	5.63	-0.44	b3
dogrose	BGB	-9.79	16.03	-0.61	b4
dogrose	BGB	14.24	13.44	1.06	b5
dogrose	BGB	5.64	8.93	0.63	b6
dogrose	BGB	0.81	1.27	0.64	b7

Taxon	Log(W)	estimate	s.e.	t_value	b
dogrose	BGB	29.63	26.50	1.12	b8
dogrose	BGB	3.00	3.63	0.83	b9
dogrose	BGB	0.81	2.15	0.37	b10
dogrose	BGB	-1.47	1.77	-0.83	b11
dogrose	BGB	-7.12	5.71	-1.25	b12
dogrose	BGB	-2.93	3.66	-0.80	b13
dogrose	BGB	-0.26	0.47	-0.56	b14
dogrose	BGB	0.72	0.70	1.02	b15
dogrose	TB	10.34	39.19	0.26	b0
dogrose	TB	-24.79	56.78	-0.44	b1
dogrose	TB	-2.49	9.26	-0.27	b2
dogrose	TB	-0.68	5.21	-0.13	b3
dogrose	TB	-3.59	14.81	-0.24	b4
dogrose	TB	6.88	12.42	0.55	b5
dogrose	TB	2.09	8.25	0.25	b6
dogrose	TB	0.34	1.18	0.29	b7
dogrose	TB	15.26	24.49	0.62	b8
dogrose	TB	1.31	3.36	0.39	b9
dogrose	TB	0.21	1.99	0.11	b10
dogrose	TB	-0.70	1.64	-0.43	b11
dogrose	TB	-3.94	5.28	-0.75	b12
dogrose	TB	-1.35	3.39	-0.40	b13
dogrose	TB	-0.11	0.43	-0.25	b14
dogrose	TB	0.39	0.65	0.60	b15
hawthorn	AGB	-18.87	53.22	-0.35	b0
hawthorn	AGB	85.16	94.81	0.90	b1
hawthorn	AGB	4.07	12.76	0.32	b2
hawthorn	AGB	1.85	5.85	0.32	b3
hawthorn	AGB	-0.18	13.73	-0.01	b4
hawthorn	AGB	-16.62	19.66	-0.85	b5
hawthorn	AGB	-10.03	10.59	-0.95	b6

Taxon	Log(W)	estimate	s.e.	t_value	b
hawthorn	AGB	-0.27	1.34	-0.20	b7
hawthorn	AGB	-13.77	27.00	-0.51	b8
hawthorn	AGB	0.00	3.18	0.00	b9
hawthorn	AGB	0.14	1.55	0.09	b10
hawthorn	AGB	1.84	2.11	0.87	b11
hawthorn	AGB	2.71	5.40	0.50	b12
hawthorn	AGB	1.79	3.02	0.59	b13
hawthorn	AGB	-0.02	0.34	-0.05	b14
hawthorn	AGB	-0.33	0.58	-0.56	b15
hawthorn	BGB	-18.53	46.02	-0.40	b0
hawthorn	BGB	118.98	81.99	1.45	b1
hawthorn	BGB	8.85	11.03	0.80	b2
hawthorn	BGB	-0.42	5.06	-0.08	b3
hawthorn	BGB	2.12	11.88	0.18	b4
hawthorn	BGB	-28.34	17.00	-1.67	b5
hawthorn	BGB	-10.63	9.16	-1.16	b6
hawthorn	BGB	-0.36	1.16	-0.31	b7
hawthorn	BGB	-27.43	23.35	-1.17	b8
hawthorn	BGB	-1.64	2.75	-0.60	b9
hawthorn	BGB	0.50	1.34	0.37	b10
hawthorn	BGB	2.51	1.83	1.37	b11
hawthorn	BGB	6.62	4.67	1.42	b12
hawthorn	BGB	2.43	2.61	0.93	b13
hawthorn	BGB	0.04	0.29	0.13	b14
hawthorn	BGB	-0.58	0.50	-1.16	b15
hawthorn	TB	-4.92	46.22	-0.11	b0
hawthorn	TB	86.19	82.35	1.05	b1
hawthorn	TB	3.12	11.08	0.28	b2
hawthorn	TB	-0.49	5.08	-0.10	b3
hawthorn	TB	-2.44	11.93	-0.20	b4
hawthorn	TB	-18.50	17.07	-1.08	b5

Taxon	Log(W)	estimate	s.e.	t_value	b
hawthorn	TB	-8.97	9.20	-0.97	b6
hawthorn	TB	0.00	1.17	0.00	b7
hawthorn	TB	-16.02	23.45	-0.68	b8
hawthorn	TB	0.03	2.76	0.01	b9
hawthorn	TB	0.64	1.35	0.47	b10
hawthorn	TB	1.82	1.84	0.99	b11
hawthorn	TB	3.55	4.69	0.76	b12
hawthorn	TB	1.70	2.62	0.65	b13
hawthorn	TB	-0.07	0.29	-0.23	b14
hawthorn	TB	-0.35	0.51	-0.70	b15
oak	AGB	-141.73	68.74	-2.06	b0
oak	AGB	141.52	74.66	1.90	b1
oak	AGB	37.44	17.71	2.11	b2
oak	AGB	22.63	10.89	2.08	b3
oak	AGB	46.30	19.81	2.34	b4
oak	AGB	-38.13	19.09	-2.00	b5
oak	AGB	-21.60	11.95	-1.81	b6
oak	AGB	-5.80	2.78	-2.09	b7
oak	AGB	-47.23	21.22	-2.23	b8
oak	AGB	-11.86	5.05	-2.35	b9
oak	AGB	-7.34	3.18	-2.31	b10
oak	AGB	5.78	2.88	2.00	b11
oak	AGB	12.20	5.37	2.27	b12
oak	AGB	7.30	3.44	2.12	b13
oak	AGB	1.88	0.80	2.34	b14
oak	AGB	-1.88	0.83	-2.28	b15
oak	BGB	-82.59	80.29	-1.03	b0
oak	BGB	84.34	87.21	0.97	b1
oak	BGB	21.69	20.69	1.05	b2
oak	BGB	13.64	12.72	1.07	b3
oak	BGB	27.54	23.14	1.19	b4

Taxon	Log(W)	estimate	s.e.	t_value	b
oak	BGB	-17.55	22.30	-0.79	b5
oak	BGB	-15.40	13.96	-1.10	b6
oak	BGB	-3.42	3.24	-1.06	b7
oak	BGB	-29.97	24.78	-1.21	b8
oak	BGB	-7.07	5.90	-1.20	b9
oak	BGB	-4.37	3.72	-1.18	b10
oak	BGB	3.37	3.37	1.00	b11
oak	BGB	6.38	6.28	1.02	b12
oak	BGB	5.20	4.02	1.29	b13
oak	BGB	1.13	0.94	1.21	b14
oak	BGB	-1.16	0.97	-1.20	b15
oak	TB	-109.23	61.35	-1.78	b0
oak	TB	113.48	66.64	1.70	b1
oak	TB	29.12	15.81	1.84	b2
oak	TB	17.77	9.72	1.83	b3
oak	TB	36.34	17.68	2.06	b4
oak	TB	-28.02	17.04	-1.64	b5
oak	TB	-18.43	10.66	-1.73	b6
oak	TB	-4.53	2.48	-1.83	b7
oak	TB	-38.45	18.94	-2.03	b8
oak	TB	-9.35	4.51	-2.07	b9
oak	TB	-5.76	2.84	-2.03	b10
oak	TB	4.56	2.57	1.77	b11
oak	TB	9.28	4.80	1.94	b12
oak	TB	6.18	3.07	2.01	b13
oak	TB	1.49	0.72	2.07	b14
oak	TB	-1.51	0.74	-2.04	b15
sallow	AGB	-26.09	24.21	-1.08	b0
sallow	AGB	-9.71	39.27	-0.25	b1
sallow	AGB	10.43	6.35	1.64	b2
sallow	AGB	1.55	2.85	0.54	b3

Taxon	Log(W)	estimate	s.e.	t_value	b
sallow	AGB	3.71	7.56	0.49	b4
sallow	AGB	-5.63	8.98	-0.63	b5
sallow	AGB	2.98	4.51	0.66	b6
sallow	AGB	-0.73	0.69	-1.05	b7
sallow	AGB	13.12	12.33	1.06	b8
sallow	AGB	-2.14	1.62	-1.32	b9
sallow	AGB	0.10	0.87	0.12	b10
sallow	AGB	0.14	0.99	0.14	b11
sallow	AGB	-0.09	2.45	-0.04	b12
sallow	AGB	-2.04	1.35	-1.51	b13
sallow	AGB	0.14	0.18	0.77	b14
sallow	AGB	0.15	0.26	0.58	b15
sallow	BGB	-39.66	32.93	-1.20	b0
sallow	BGB	24.91	53.41	0.47	b1
sallow	BGB	13.72	8.64	1.59	b2
sallow	BGB	2.41	3.88	0.62	b3
sallow	BGB	9.04	10.28	0.88	b4
sallow	BGB	-12.70	12.21	-1.04	b5
sallow	BGB	-0.19	6.13	-0.03	b6
sallow	BGB	-0.96	0.94	-1.03	b7
sallow	BGB	-0.35	16.77	-0.02	b8
sallow	BGB	-3.25	2.20	-1.48	b9
sallow	BGB	-0.29	1.19	-0.25	b10
sallow	BGB	0.81	1.34	0.60	b11
sallow	BGB	2.43	3.33	0.73	b12
sallow	BGB	-0.75	1.83	-0.41	b13
sallow	BGB	0.22	0.24	0.91	b14
sallow	BGB	-0.09	0.36	-0.26	b15
sallow	TB	-32.79	25.42	-1.29	b0
sallow	TB	5.20	41.23	0.13	b1
sallow	TB	11.71	6.67	1.76	b2

Taxon	Log(W)	estimate	s.e.	t_value	b
sallow	TB	2.23	2.99	0.74	b3
sallow	TB	7.11	7.93	0.90	b4
sallow	TB	-7.97	9.43	-0.85	b5
sallow	TB	1.46	4.73	0.31	b6
sallow	TB	-0.84	0.72	-1.16	b7
sallow	TB	6.28	12.95	0.49	b8
sallow	TB	-2.72	1.70	-1.60	b9
sallow	TB	-0.22	0.91	-0.25	b10
sallow	TB	0.38	1.04	0.37	b11
sallow	TB	0.99	2.57	0.39	b12
sallow	TB	-1.32	1.42	-0.93	b13
sallow	TB	0.19	0.18	1.02	b14
sallow	TB	0.04	0.28	0.14	b15

Table S3.3: Summary of model results for relationships between ecological variables and response variables across different taxa. The table provides coefficients (Estimate), standard errors (S.E.), t-values, and p-values for predictors such as log-transformed density, canopy area, height, and interactions involving these variables. Significant effects ($p < 0.05$) are highlighted for each taxon and response type.

Response	Taxon	Term	Estimate	S.E.	<i>t</i>	<i>P-value</i>
above	blackthorn	(Intercept)	-7.72	2.56	-3.02	0.00421165
total	blackthorn	(Intercept)	-5.47	2.29	-2.39	0.02121804
below	blackthorn	log(density)	-38.90	22.26	-1.75	0.08748869
below	blackthorn	log(density):conditionprotected	13.30	7.76	1.71	0.09349710
below	blackthorn	log(canopy_area)	0.63	0.38	1.65	0.10655590
above	blackthorn	log(height)	1.55	0.95	1.64	0.10903158
below	blackthorn	conditionprotected	-0.92	0.58	-1.57	0.12330241
total	blackthorn	log(canopy_area)	0.65	0.49	1.33	0.19001937
total	blackthorn	log(height)	1.08	0.85	1.28	0.20707562
above	blackthorn	log(canopy_area)	0.69	0.55	1.26	0.21501404
below	blackthorn	(Intercept)	-2.13	1.77	-1.20	0.23617611
below	blackthorn	log(density):log(height)	8.87	8.40	1.06	0.29695431
below	blackthorn	log(density):log(dbh)	6.91	7.52	0.92	0.36319179
total	blackthorn	log(dbh)	0.55	0.69	0.80	0.42920605
below	blackthorn	log(density):log(canopy_area)	-4.08	5.25	-0.78	0.44093041
below	blackthorn	log(height)	0.43	0.66	0.65	0.51597171
above	blackthorn	log(density):log(canopy_area)	-4.86	7.57	-0.64	0.52437837
total	blackthorn	log(density):conditionprotected	5.97	10.01	0.60	0.55435597
total	blackthorn	log(density):log(canopy_area)	-3.87	6.78	-0.57	0.57053884
above	blackthorn	log(density):log(dbh)	5.88	10.83	0.54	0.58993841
total	blackthorn	log(density):log(height)	5.60	10.85	0.52	0.60814399
above	blackthorn	conditionprotected	-0.42	0.84	-0.50	0.61990858
below	blackthorn	log(dbh)	0.27	0.54	0.50	0.62143185
above	blackthorn	log(density):conditionprotected	5.17	11.18	0.46	0.64577208
total	blackthorn	log(density):log(dbh)	4.16	9.70	0.43	0.66981718
above	blackthorn	log(dbh)	0.31	0.77	0.40	0.69165637
total	blackthorn	conditionprotected	-0.29	0.75	-0.38	0.70215092
total	blackthorn	log(density)	-10.46	28.73	-0.36	0.71745238
above	blackthorn	log(density):log(height)	3.74	12.11	0.31	0.75863450
above	blackthorn	log(density)	3.05	32.07	0.09	0.92476296
above	dogrose	log(height)	1.70	0.43	3.93	0.00043792
above	dogrose	(Intercept)	-4.36	1.20	-3.64	0.00099353
total	dogrose	log(height)	1.06	0.37	2.87	0.00732109
below	dogrose	log(dbh)	0.54	0.23	2.38	0.02349121
total	dogrose	conditionprotected	-0.67	0.31	-2.17	0.03755801
below	dogrose	log(canopy_area)	0.26	0.12	2.13	0.04088628

total	dogrose	log(canopy_area)	0.24	0.12	2.09	0.04510217
above	dogrose	conditionprotected	-0.66	0.36	-1.85	0.07416589
below	dogrose	conditionprotected	-0.54	0.32	-1.70	0.09900963
total	dogrose	log(dbh)	0.34	0.22	1.52	0.13874056
above	dogrose	log(canopy_area)	0.19	0.14	1.38	0.17637503
above	dogrose	log(dbh)	0.32	0.26	1.25	0.22044811
total	dogrose	(Intercept)	-1.19	1.02	-1.16	0.25467965
above	dogrose	log(density):log(dbh)	4.41	4.33	1.02	0.31609105
below	dogrose	log(height)	0.37	0.38	0.97	0.34021955
total	dogrose	log(density):log(dbh)	3.44	3.70	0.93	0.35946255
above	dogrose	log(density):log(canopy_area)	-2.55	2.85	-0.89	0.37845991
below	dogrose	log(density):conditionprotected	-2.98	4.33	-0.69	0.49625216
above	dogrose	log(density):log(height)	3.07	7.25	0.42	0.67465413
total	dogrose	log(density):log(canopy_area)	-0.94	2.44	-0.38	0.70295629
below	dogrose	(Intercept)	0.39	1.06	0.37	0.71488338
above	dogrose	log(density)	-5.42	15.31	-0.35	0.72558318
total	dogrose	log(density):conditionprotected	-1.46	4.19	-0.35	0.73031410
below	dogrose	log(density):log(dbh)	1.26	3.83	0.33	0.74497285
total	dogrose	log(density)	-3.63	13.09	-0.28	0.78366804
below	dogrose	log(density)	-3.47	13.55	-0.26	0.79939154
below	dogrose	log(density):log(canopy_area)	-0.37	2.52	-0.15	0.88531436
above	dogrose	log(density):conditionprotected	0.54	4.90	0.11	0.91270777
total	dogrose	log(density):log(height)	0.29	6.20	0.05	0.96359083
below	dogrose	log(density):log(height)	0.27	6.42	0.04	0.96609190
above	hawthorn	(Intercept)	-5.57	1.48	-3.77	0.00046663
total	hawthorn	(Intercept)	-4.67	1.29	-3.61	0.00077094
below	hawthorn	(Intercept)	-4.35	1.30	-3.35	0.00164455
total	hawthorn	log(canopy_area)	0.79	0.25	3.14	0.00301264
above	hawthorn	log(canopy_area)	0.85	0.29	2.96	0.00486754
below	hawthorn	log(canopy_area)	0.61	0.25	2.40	0.02072952
below	hawthorn	log(height)	0.66	0.36	1.83	0.07389403
total	hawthorn	log(dbh)	0.54	0.30	1.78	0.08174508
total	hawthorn	log(height)	0.62	0.36	1.72	0.09153228
below	hawthorn	conditionprotected	-0.46	0.28	-1.62	0.11281619
above	hawthorn	log(height)	0.65	0.41	1.58	0.12159898
below	hawthorn	log(dbh)	0.48	0.31	1.57	0.12440290
above	hawthorn	log(dbh)	0.52	0.35	1.49	0.14405977
total	hawthorn	conditionprotected	-0.34	0.28	-1.22	0.22780206
above	hawthorn	conditionprotected	-0.33	0.32	-1.03	0.30795912
above	hawthorn	log(density)	-13.69	14.01	-0.98	0.33371905
below	hawthorn	log(density):conditionprotected	-2.34	2.95	-0.79	0.43086541
below	hawthorn	log(density):log(height)	-2.73	3.99	-0.69	0.49637648
below	hawthorn	log(density)	7.94	12.34	0.64	0.52340714
below	hawthorn	log(density):log(dbh)	1.60	2.84	0.56	0.57546209
total	hawthorn	log(density):conditionprotected	-1.47	2.93	-0.50	0.61902585
total	hawthorn	log(density):log(dbh)	1.37	2.83	0.48	0.63072035

above	hawthorn	log(density):log(canopy_area)	1.29	3.01	0.43	0.67165437
total	hawthorn	log(density):log(height)	-1.29	3.97	-0.32	0.74720706
total	hawthorn	log(density)	-3.80	12.28	-0.31	0.75829712
above	hawthorn	log(density):log(dbh)	0.94	3.23	0.29	0.77163203
above	hawthorn	log(density):log(height)	-0.89	4.53	-0.20	0.84472645
total	hawthorn	log(density):log(canopy_area)	0.44	2.64	0.17	0.86888367
above	hawthorn	log(density):conditionprotected	-0.41	3.35	-0.12	0.90196917
below	hawthorn	log(density):log(canopy_area)	0.07	2.66	0.03	0.97888672
total	oak	log(canopy_area)	0.72	0.11	6.77	0.00000007
above	oak	log(canopy_area)	0.74	0.12	6.25	0.00000032
below	oak	log(canopy_area)	0.71	0.12	5.73	0.00000159
above	oak	(Intercept)	-3.14	0.65	-4.86	0.00002297
total	oak	conditionprotected	-0.77	0.25	-3.11	0.00365209
total	oak	(Intercept)	-1.70	0.58	-2.94	0.00572436
below	oak	conditionprotected	-0.85	0.29	-2.94	0.00576636
above	oak	conditionprotected	-0.72	0.28	-2.59	0.01362203
above	oak	log(density):log(canopy_area)	4.82	1.88	2.56	0.01473891
below	oak	(Intercept)	-1.61	0.67	-2.40	0.02173916
above	oak	log(dbh)	0.42	0.19	2.24	0.03143627
above	oak	log(density):log(height)	-9.99	5.07	-1.97	0.05650032
total	oak	log(dbh)	0.31	0.17	1.87	0.06965980
total	oak	log(density):log(canopy_area)	2.93	1.68	1.74	0.08964666
total	oak	log(height)	0.39	0.26	1.46	0.15230611
above	oak	log(height)	0.43	0.30	1.46	0.15315800
total	oak	log(density):log(height)	-5.97	4.53	-1.32	0.19593138
below	oak	log(density)	14.04	11.45	1.23	0.22810667
above	oak	log(density):log(dbh)	4.73	3.94	1.20	0.23812435
below	oak	log(dbh)	0.22	0.20	1.12	0.27199439
below	oak	log(height)	0.30	0.31	0.96	0.34531628
above	oak	log(density)	-9.00	10.99	-0.82	0.41823982
total	oak	log(density):log(dbh)	1.92	3.52	0.54	0.58979011
below	oak	log(density):log(dbh)	-2.11	4.11	-0.51	0.60993535
below	oak	log(density):log(height)	-2.67	5.28	-0.51	0.61642262
below	oak	log(density):log(canopy_area)	0.62	1.96	0.32	0.75268762
total	oak	log(density)	-2.98	9.83	-0.30	0.76343321
above	oak	log(density):conditionprotected	1.16	4.14	0.28	0.78133907
total	oak	log(density):conditionprotected	0.80	3.70	0.22	0.82951492
below	oak	log(density):conditionprotected	0.55	4.31	0.13	0.89990010
above	sallow	(Intercept)	-3.90	0.95	-4.09	0.00019209
above	sallow	log(canopy_area)	0.63	0.18	3.53	0.00101306
total	sallow	log(canopy_area)	0.55	0.18	3.09	0.00351451
total	sallow	(Intercept)	-2.51	0.96	-2.62	0.01220472
below	sallow	log(canopy_area)	0.51	0.22	2.34	0.02402341
above	sallow	conditionprotected	-0.81	0.36	-2.24	0.03066032
total	sallow	log(dbh)	0.74	0.34	2.18	0.03468268
above	sallow	log(dbh)	0.70	0.34	2.09	0.04273200

above	sallow	log(height)	0.59	0.28	2.07	0.04416909
total	sallow	conditionprotected	-0.68	0.36	-1.87	0.06814139
total	sallow	log(height)	0.52	0.29	1.83	0.07489362
above	sallow	log(density):conditionprotected	-3.90	2.27	-1.72	0.09343399
below	sallow	(Intercept)	-1.96	1.17	-1.68	0.10125195
below	sallow	log(dbh)	0.68	0.41	1.64	0.10769465
total	sallow	log(density):conditionprotected	-3.10	2.28	-1.36	0.18222255
below	sallow	conditionprotected	-0.59	0.44	-1.33	0.18935297
below	sallow	log(density)	-6.62	7.14	-0.93	0.35922820
total	sallow	log(density):log(height)	1.72	1.87	0.92	0.36405850
below	sallow	log(density):conditionprotected	-2.53	2.79	-0.91	0.36890240
below	sallow	log(height)	0.31	0.35	0.90	0.37241962
above	sallow	log(density):log(height)	1.67	1.86	0.90	0.37370395
total	sallow	log(density)	-5.18	5.85	-0.88	0.38129523
above	sallow	log(density)	-4.04	5.82	-0.69	0.49093158
below	sallow	log(density):log(dbh)	1.23	2.89	0.42	0.67371143
below	sallow	log(density):log(height)	0.87	2.29	0.38	0.70598562
total	sallow	log(density):log(canopy_area)	-0.43	1.26	-0.34	0.73371651
above	sallow	log(density):log(canopy_area)	-0.28	1.25	-0.22	0.82421550
above	sallow	log(density):log(dbh)	-0.39	2.36	-0.17	0.86779399
below	sallow	log(density):log(canopy_area)	-0.16	1.54	-0.10	0.91708146
total	sallow	log(density):log(dbh)	0.23	2.37	0.10	0.92359655

Chapter 4: Quantifying Carbon Content in Rewilded Scrublands: Challenging the '50% Rule' through Elemental Analysis

Nancy C. Burrell¹, Elizabeth Jeffers¹, Katherine J. Willis¹

¹Department of Biology, University of Oxford, Oxford, UK

Author contribution statement: Nancy C. Burrell led the study's conceptualisation, data analysis, and drafting, serving as project lead. Kathy J. Willis and Elizabeth S. Jeffers provided supervision, contributed to methodology design, and edited the manuscript.

To be submitted for publication.

4.0 Abstract

Rewilding initiatives are increasingly recognised for their benefits to biodiversity and ecosystem restoration. It is known that rewilded landscapes can enhance habitat complexity and species diversity. However, their potential to sequester carbon remains unclear. The current practice, based on the forestry plantation model, often assumes that 50% of a tree's dry biomass is carbon, but this generalisation is not based on empirical data for scrub species typical of rewilded areas where environmental conditions are very different and the impact of browsing herbivores affects growth and structure. This lack of specific knowledge makes it difficult to accurately assess the carbon storage capacity of these landscapes, potentially leading to overestimations or underestimations of their role in climate change mitigation. A more precise understanding of the carbon content in scrub species currently represents a significant knowledge gap. In this study, I use elemental analysis to measure the carbon content in various scrub species under different environmental conditions with the aim to determine whether the 50% rule also holds true for scrubland species; critical data to refine carbon stock estimates and better inform the carbon storage potential of rewilding projects.

Key words: elemental analysis, carbon content, 50% rule biomass; rewilding, root:shoot ratio, scrubland

4.1 Introduction

The potential carbon storage associated with reforestation is considered an important part of global carbon mitigation budgets for reducing greenhouse gas emissions to achieve Net Zero (IPCC, 2019; Strassburg et al., 2020; Mappin et al., 2022; Bastin et al., 2019). The most recent IPCC report spotlights the ability of trees to capture atmospheric carbon and store it within their biomass (European Environment Agency, 2022) and this has provided the impetus of global initiatives such as the Bonn Challenge, the Trillion Tree Campaign, and the United Nations Decade on Ecosystem Restoration, to set ambitious targets for landscape reforestation and associated offsetting of greenhouse gas emissions (Brancalion et al., 2024). However there remains the key challenge of robustly quantifying this capacity of trees for capturing CO₂, thus contributing to reaching the objectives delineated in the Paris Agreement (United Nations, 2015).

Previous research has shown that quantification of carbon content in living trees varies significantly across different species and environmental conditions. For instance, studies have reported that wood carbon content ranges from 41.9% to 60.7%, varying significantly among species and biomes such as tropical, subtropical, and temperate regions (Thomas & Martin, 2012; He et al., 2018).

The carbon content in trees is influenced by a variety of factors including the species, the age of the tree, geographical location, and environmental stressors (Mildrexler et al., 2020; Bardule et al., 2021; Lines et al., 2010). As such, determining the species-specific carbon content in different woody environments is complex (Lamlom & Savidge, 2003; Martin & Thomas, 2011; Thomas & Malczewski, 2007) and, as a result, the use of detailed species-specific carbon

fractions in calculating woody carbon storage remains uncommon. Instead, the prevailing practice is to rely on carbon stock assumptions, based on a few common species, which lack chemical analysis to determine quantitatively their carbon content (Bhatti et al. 2022; Rutishauser et al., 2013; Phillips et al., 2016; Hauck et al., 2023).

A widely adopted method in frameworks such as i-Tree Eco (i-Tree, 2021) and the Woodland Carbon Code (Forestry Commission, 2014) is to estimate carbon content based on the assumption that 50% of a tree's dry biomass is carbon (Jenkins et al., 2011). Dry biomass is calculated using an allometric equation based on height (h), density (ρ) and diameter at breast height (dbh) (Chave et al., 2014). However, the origin and validity of this “rule-of-thumb” estimation have been questioned. Some researchers argue that this assumption is not supported by robust data and can lead to errors of 5-8% in carbon stock assessments (Martin & Thomas, 2011). This discrepancy arises because allometric equations only quantify total biomass and do not directly measure carbon content (nowak et al., 2014; Chave et al., 2005; Pati et al., 2022; Vorster et al., 2020). For example, trees in the forestry plantation model, planted close together to encourage straight trunks as they compete for light, may reach height faster than open-grown trees but their wood is likely to be less dense, resulting in lower carbon storage capacity (Bohn & Huth, 2017; Poorter et al., 2012). Similarly, the chemical and structural changes exhibited by trees and woody shrubs under herbivory in a rewilding scenario—such as increased levels of tannins (Feeny, 1976; Bryant et al., 1983), bifurcation of stems and branches, growth of thorns to repel browsers (Karban & Baldwin, 2007; Gowda, 1996), and protective growth to heal tissue damage (Coetsee et al., 2019)—may result in different levels of carbon storage than the prevailing 50% carbon/biomass rule predicts. At the same time, their root systems are likely to be larger, responding to herbivory pressures, than

the below-ground biomass predicted by standard above-ground measurements (Burrell et al., 2024). Additionally, the structure, composition, wood density, and below-ground biomass of trees affected by harsh environmental conditions such as drought and wind can differ from those of trees grown in the forestry plantation model, potentially altering the carbon-to-biomass ratio (West et al., 2001; Rosell et al., 2016). As a result, applying a generalised biomass-to-carbon conversion across diverse woodland environments is thought to lead to significant inaccuracies in carbon stock estimates (Thomas & Martin, 2012; Saner et al., 2012; Melson et al., 2011).

Even more problematic is the fact that the foundation upon which the 50% C content assumption is based (Matthews 1993) is the Woodland Carbon Code dataset (Natural England, 2024; Timber Development UK, 2024). This dataset encompasses only 23 taxa, with 40% of these based on a single representative tree sample, indicating a worrying lack of statistically significant sample size. Even within taxa like oak (*Quercus* spp.), significant variations of up to 10% in carbon content have been observed (Martin & Thomas, 2011).

Admittedly, the Intergovernmental Panel on Climate Change (IPCC) and a few selective studies use alternative biomass-carbon conversion factors that take into account different environments when estimating carbon stocks (IPCC, 2006). For example, a study on Silky oak (*Grevillea robusta*) in Thailand found that the adjusted 47% carbon content assumed by the IPCC estimates was an accurate representation for that species in that tropical savanna environment (Laosuwan et al., 2023). However, studies from different ecozones suggest that the IPCC's biomass-carbon conversion factor might also be oversimplified since it does not take sufficiently into account how the biomass-carbon content relationship may differ by species. Its calculations are based on very few samples and tend to generalise across tree

species—often pooling tree species with insufficient replicates (Martin & Thomas, 2011). For instance, a study on the IPCC's conversion factors for major tree species in Latvia revealed a notable 5.1% underestimation in carbon stocks using the default IPCC carbon content values (Bardule et al., 2021), and research conducted by Martin & Thomas (2011) on the carbon content of Panamanian rainforests found substantial variability among species, which frequently led to lower carbon estimates than typically expected. In the study by Liepins et al. (2017), the three deciduous tree species examined in Latvia were birch (*Betula spp.*), aspen (*Populus tremula*), and black alder (*Alnus glutinosa*). The study found that IPCC values overestimated the carbon content of these species. These findings highlight the urgent need for a more sophisticated and detailed woodland carbon accounting methodology, reflecting the complexities of actual carbon content in trees.

Elemental analysis via dry combustion has proven pivotal in highlighting the inadequacy of the 50% carbon assumption rule (Thomas & Martin, 2012; Lamlo et al., 2003; Thomas & Malczewski, 2007). This method accurately determines the species-specific carbon content of trees, revealing considerable variations across ecosystems. However, it is not yet widely used. Despite the fact that there have been significant advancements in biomass quantification through innovative methods such as the use of Unmanned Aerial Vehicles (UAV) for volume estimates (Reef & Gordon, 2024; Alonzo et al., 2020) and allometric equations (Verly et al., 2023; Liu et al., 2023; Tian et al., 2023; Bouvet et al., 2018; Zhang et al., 2020) there is still a significant gap in converting biomass to accurate carbon stock figures. This is perhaps because of the cost and time required to measure the elemental chemistry over large enough samples. Macro-scale data is, however, needed in order to test whether the 50% biomass calculation can, indeed, be used as a proxy for carbon content, or whether it is a blunt instrument, and

further measurements of carbon concentration are required that take into account different species and environmental conditions.

Another issue with the current methods for determining carbon stock is the lack of representation of the diverse environments in which trees grow. For example, the WCC's carbon stock data is tailored exclusively to forestry plantations (Matthews, 1993). The IPCC reports use calculations based on mature forest stands in temperate regions (IPCC, 2019). Similarly, models like i-Tree Eco (Nowak et al., 2008), used extensively by urban planners, calculate urban tree carbon stocks using data from forestry plantations, assuming that trees in cities store similar amounts of carbon as those in managed forests. These assumptions overlook the significant differences in growth conditions and carbon storage capabilities between these environments.

In the past decade, there has been increasing recognition that natural regeneration of trees and shrubs in landscapes can play a pivotal role in climate change mitigation strategies, along with other benefits for biodiversity and human well-being (Griscom et al., 2017; Biermann & Anderson, 2017; Corlett, 2016; Fernández et al., 2017; Jepson, 2016; Keesstra et al., 2018; Rewilding Britain, 2020). Among these approaches, rewilding stands out by prioritising natural regeneration processes, often facilitated / modulated by the activities of large herbivores (Mikołajczak et al., 2022; Sandom et al., 2019). Contrary to the prevailing belief that large animals predominantly cause a reduction in woody biomass through browsing (Gill & Fuller, 2007), evidence suggests that, within ecologically balanced systems and at appropriate population densities, herbivory can significantly enhance the carbon sequestration capacity of the landscape (Berzaghi et al., 2022; Doughty et al., 2016; Sitters et al., 2020). Recent research underscores the beneficial impact of medium-to-large herbivores on carbon storage (Schmitz,

2023), attributing enhancements to several mechanisms. These include seed dispersal, which aids in the proliferation of carbon-rich wood species (Enquist et al., 2020; Villar & Medici, 2021; Bardgett & Wardle, 2003), the reduction of plant competition through selective feeding (Gordon & Prins, 2008), increases in soil fertility and ecosystem metabolism (Van der Graaf & Bakker, 2005), browsing-induced plant responses that lead to a reallocation of biomass (Perkovich & Ward, 2021), and the creation of plant defences, such as thorns, which is a carbon-intensive process (Facciolati et al., 2024; Balaji & Jambagi., 2024; Skarpe & Hester, 2008; Hanley et al., 2007). Additionally, modifications to the ecosystem's functional strategy towards increased carbon assimilation have been observed (Malhi et al., 2022). Furthermore, the presence of these herbivores is linked to improved soil nutrient availability and enhanced storage of organic carbon within the soil matrix (Sobral et al., 2017; Osuri et al., 2016; Culot et al., 2017). The type of scrubland that often emerges as a consequence of rewilding initiatives represents a focal point of this study, underscoring the critical role of rewilding in augmenting the carbon storage potential of these landscapes.

But what is the carbon storage potential of a rewilded landscape? Given that it is exposed to browsing pressure, contains mainly small, multiple-stemmed shrubs, and may store much of its biomass belowground in response to herbivory, the 'traditional' WCC datasets for estimating such carbon storage cannot be applied as discussed in Burrell et al. (2024) (Chapter 2). The aim of this research was, therefore, to quantify the carbon content across five distinct scrub species typically found on rewilded landscapes in the UK and across temperate Europe, using the Knepp estate the model field site. Elemental analysis of representative samples from aboveground components—branches and trunk—as well as belowground parts—roots—allowed me to investigate whether the conventional assumption that 50% of dry weight

comprises carbon holds true for scrubland species. Additionally, I investigated the influence of herbivory on the carbon content both within and across these species.

4.2 Materials and Methods

4.2.1 Site location

This study was conducted at the rewilding project at the Knepp Estate in West Sussex and specifically within the 'Southern Block' (50.975781°N, 0.344819°W) - an area characterised by large areas of thorny scrub. The estate began transitioning from intensive arable and dairy farming to rewilding in 2001 (Tree, 2018). Between 2001 and 2006 the Southern Block, which was mostly arable, was taken out of production in stages, starting with the least productive fields. The fields were simply left 'open' after their last harvest, facilitating natural colonisation. Unlike the other two areas of the Estate – the Northern and Middle Blocks – there was initially no available funding to ringfence the area to allow the introduction of free-roaming animals, one of the main criteria of trophic rewilding (Tree, 2018). By default, this provided an extended fallow period which further facilitated natural vegetation regeneration. In 2009, funding was eventually granted by Higher Level Stewardship to fence the Southern Block, and large herbivores - old English longhorn cattle (*Bos primigenius taurus*), Exmoor ponies (*Equus ferus caballus*), fallow deer (*Dama dama*) and Tamworth pigs (*Sus scrofa domesticus*) were introduced. Red deer (*Cervus elaphus*) were added in 2013. Since the inception of the rewilding project, the Southern Block has undergone substantial ecological transformation, resulting in much scrubbier and more complex mosaic of vegetation responses than the more homogenous, grassland-dominated Middle and Southern Blocks - at least, thus far (Tree & Burrell, 2023). The current dominant vegetation of the Southern Block

consists of open wood pasture systems with regenerating scrub species such as *Prunus spinosa*, *Salix spp.*, *Quercus spp.* (*Quercus robur* and *Quercus petraea*), *Crataegus spp.* (*Crataegus monogyna* and *Crataegus laevigata*), and *Rubus fruticosus*. (Ryland, 2015).

4.2.2 Destructive Sampling

As described in chapter 3, a total of 270 trees were randomly selected from a single study site, itself chosen at random from three potential locations characterised by diverse land cover types. Trees were selected based on size, taxa—oak (*Quercus spp.*), hawthorn (*Crataegus spp.*), blackthorn (*Prunus spinosa*), dog rose (*Rosa canina*), and willow (*Salix spp.*)—and browsing condition, classified as either “protected” by bramble or “exposed” to browsing. Tree taxa were identified using PlantATT (Centre for Ecology and Hydrology, 2004) and the Collins Tree Guide (Johnson, 2004).

To minimise bias in biomass estimates, scrub trees were grouped into three height size classes: small (<75 cm), medium (75–210 cm), and large (>210 cm). Sampling was conducted during the dormant season (April to October, 2021–2024) when deciduous trees were leafless.

A total of 201 sub-samples were collected from 34 selected trees across five taxa (Table 4.3), both under herbivory-exposed and protected conditions, from the 270 trees that were destructively sampled (roots and all) (See Chapter 3). Each representative tree provided six samples—three aboveground and three belowground. Thirty-four scrub species were selected for the carbon analysis with at least one tree selected per category (Table 4.4). This analysis was conducted concurrently with the tree extraction process throughout the study period. Each scrub tree was entirely removed and divided into three main components: crown, stem, and root ball. The crown was separated from the stem at the base of the live crown, defined

as the point on the main trunk where the lowest live branch with foliage began. For the root system, all parts below 1 cm from the soil surface were categorised as roots. To standardise below-ground biomass (BGB) measurements, excavation was performed within a radius of 0.5 m and to a depth of 0.5 m around each tree, following a protocol similar to Hunyh et al. (2021). Roots were carefully cleaned using an air pressure hose to remove soil while preserving the bark. Roots were then classified by diameter as small (<2 mm), medium (2–10 mm), or large (>10 mm). Branches were similarly categorised by diameter: small (<4 cm), medium (4–7 cm), and large (>7 cm).

After excavation and preparation, all components—crown, stem, and roots—were weighed using a digital balance (Bonviosin 0.01 g). Samples from each category were then dried at 100°C until their weight stabilised, all within 72 hours (Houghton et al., 2009). The dry weights of both above-ground biomass (AGB) and BGB were subsequently recorded. Wood density (ρ) was calculated for above- and below-ground components using water displacement to determine sample volume (cm^3) and oven-drying at $105 \pm 5^\circ\text{C}$ for dry mass, following Archimedes principle (Saranpää, 2003; Kallarackal & Ramirez, 2024).

4.2.3 Elemental Analysis

The 201 sub-samples from the 34 randomly selected trees (Table 4.1) were processed at the Pennine Analytical Laboratory, where they were ground into a homogeneous powder using a Retsch SM 100 grinder. The powdered samples were then analysed for non-volatile carbon content using a FlashSmart Elemental Analyser (Thermo Fisher Scientific, Waltham, MA, USA) (Chevalier et al., 2017), with calibration and measurements performed in duplicate for accuracy. Results were recorded as carbon percentages. The total carbon content in tree tissues

comprises both non-volatile and volatile fractions (Bardule et al., 2021; Thomas & Martin, 2012). However, consistent with previous studies (Bardule et al., 2021), our analysis focused solely on the non-volatile fraction due to the oven-drying pre-treatment of samples before elemental analysis.

Table 4.1: Number of representative trees per category used for elemental analysis, including taxa, size and exposure to/protection from herbivory. Each tree is made up of six representative sub-samples – three from aboveground tree parts and three from the roots.

Taxon	Exposed			Protected		
	<i>Small</i>	<i>Medium</i>	<i>Large</i>	<i>Small</i>	<i>Medium</i>	<i>Large</i>
Oak (<i>Quercus spp.</i>)	1	1	N/A	1	1	1
Hawthorn (<i>Crataegus spp.</i>)	4	1	1	1	1	1
Blackthorn (<i>Prunus spinosa</i>)	1	1	1	1	1	1
Sallow (<i>Salix spp.</i>)	1	1	2	1	1	1
Dog Rose (<i>Rosa canina</i>)	1	2	1	1	1	1

4.2.4 Data handling

Statistical analysis and graph creation were performed in R (R Core Team, 2024), using the ggplot2 package (Wickham, 2016). Descriptive statistics were used to summarise the mean and variance of carbon content for each taxon. A Wilcoxon signed-rank test was used to compare carbon content between root and aboveground parts due to non-normality of the

data. This non-parametric test is suitable for paired samples with non-normal distributions (Jones et al., 2022). Pearson correlation and linear regression was used to assess the relationship between tree age and carbon content in roots and shoots (Zar, 1999; Field, 2013). Interaction analyses were conducted to explore combined effects of exposure and taxa, as well as exposure and sample part (roots vs. aboveground). Due to the limited sample size for each taxon (Table 4.1), statistical analysis could not be performed as the small sample sizes would not provide sufficient power to detect meaningful differences or ensure reliable estimates of variance.

4.3 Results

4.3.1. Carbon content of studied taxa

The observed carbon content mean for all the scrub taxa was 43.66% ($\pm 3.33\%$) (Figure 4.1). Results for the five taxa are as follows: blackthorn (*Prunus spinosa*) 43.68% ($\pm 4.24\%$), hawthorn (*Crataegus spp.*) 44.28% ($\pm 1.91\%$), willow (*Salix spp.*) 42.96% ($\pm 4.12\%$), oak (*Quercus spp.*) 42.65% ($\pm 2.92\%$), and dog rose (*Rosa canina*) 44.21% ($\pm 3.19\%$) (Figure 4.2).

There was significant variation in carbon content within individual trees (measured using six above- and below-ground samples). The average standard deviation for each tree was 2.68%, with a minimum standard deviation of 0.59% (*Rosa canina*) and a maximum of 9.15% (*Prunus spinosa*).

There was also a large variation in carbon content across taxa, which was compounded by the low number of sample trees per taxon (Figure 4.2). *Salix spp.* exhibited the largest variation (SD = 4.12%, n = 7), followed by *Rosa canina* (SD = 3.19%, n = 7) and *Quercus spp.* (SD = 2.92%, n = 5). Further statistical relevance will require a larger sample size.

Finally, the correlation and regression analyses revealed no significant relationship between tree age (3–19 years) and carbon content in either roots or shoots. The correlation coefficients were negligible (roots: $r = -0.04$; shoots: $r = -0.03$), and the regression slopes were not statistically significant ($n = 27$, roots: $p = 0.841$, $t = -0.201$; shoots: $p = 0.866$, $t = -0.170$).

Until a larger, taxa-specific scrub tree dataset can be generated, we recommend using the average carbon content of all scrub trees displayed in Figure 4.3 (44% for AGB and 43% for BGB).

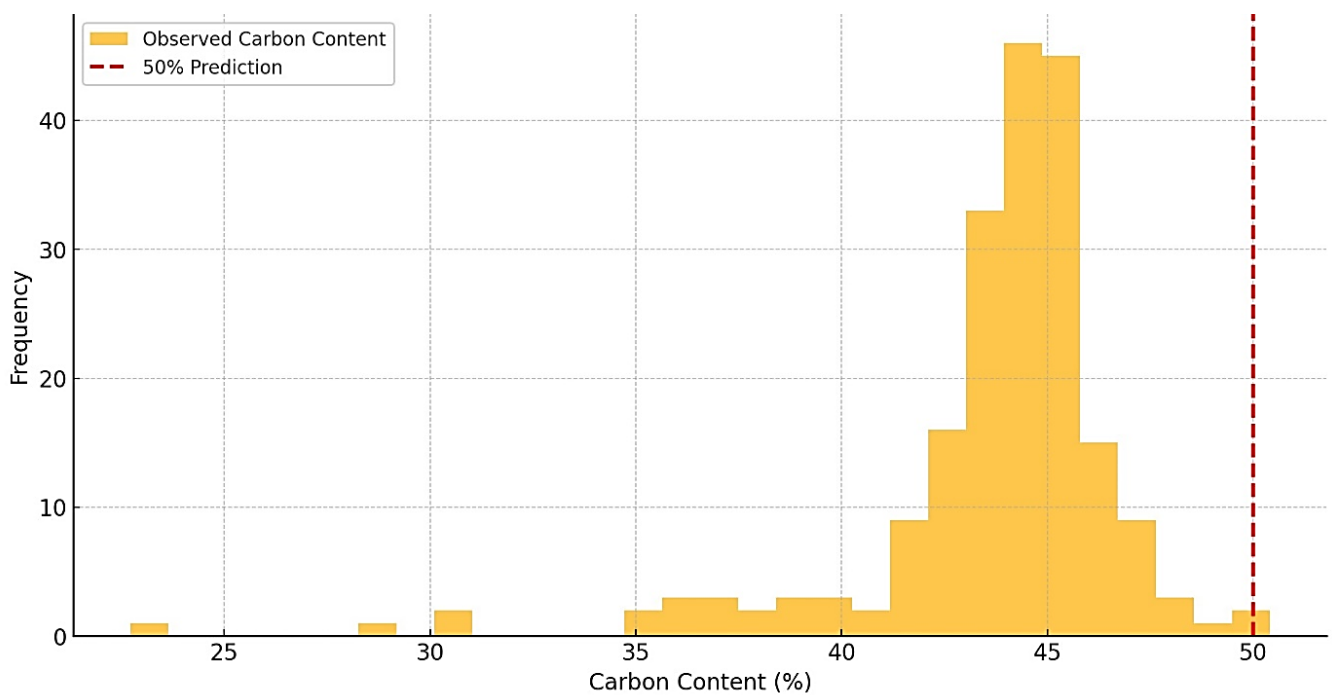


Figure 4.1: Distribution of observed carbon content (%) compared to the 50% assumption value (red dotted line) for five tree taxa: blackthorn (*Prunus spinosa*) $n=36$, dog rose (*Rosa canina*) $n=42$, hawthorn (*Crataegus spp.*) $n=54$, willow (*Salix spp.*) $n=39$ and oak (*Quercus spp.*) $n=30$.

4.3.2. Carbon Content in Aboveground vs. Belowground Parts by Taxon

The overall scrub mean carbon content was 42.51% ($\pm 2.34\%$) in root samples and 44.78% ($\pm 1.06\%$) in aboveground parts, showing a statistically significant difference. The Shapiro-Wilk test revealed significant deviations from normality in both the root ($n = 34$, $W = 0.80$, $p < 0.0001$) and shoot ($n = 34$, $W = 0.82$, $p < 0.0001$) datasets. Consequently, the non-parametric Wilcoxon signed-rank test ($V = 42.5$, $p < 0.0001$) confirmed that aboveground parts had a significantly higher mean carbon content compared to roots.

All scrub tree taxa exhibited higher carbon content in aboveground parts compared to belowground parts. In blackthorn (*Prunus spinosa*), aboveground carbon content was slightly higher ($45.69\% \pm 2.85\%$) than belowground ($43.34\% \pm 3.12\%$). Sallow (*Salix* spp.) showed a similar trend, with aboveground carbon content at $45.35\% \pm 2.74\%$ and belowground at $41.88\% \pm 3.64\%$. Hawthorn (*Crataegus* spp.) also followed this pattern, with aboveground parts averaging $45.13\% \pm 2.92\%$ and belowground parts at $43.21\% \pm 3.14\%$.

Both oak (*Quercus* spp.) and dog rose (*Rosa canina*) exhibited higher carbon content aboveground, with oak having $44.73\% \pm 3.65\%$ aboveground and $41.23\% \pm 3.92\%$ belowground, and dog rose at $44.91\% \pm 3.50\%$ aboveground compared to $43.44\% \pm 4.10\%$ belowground (Figure 4.3).

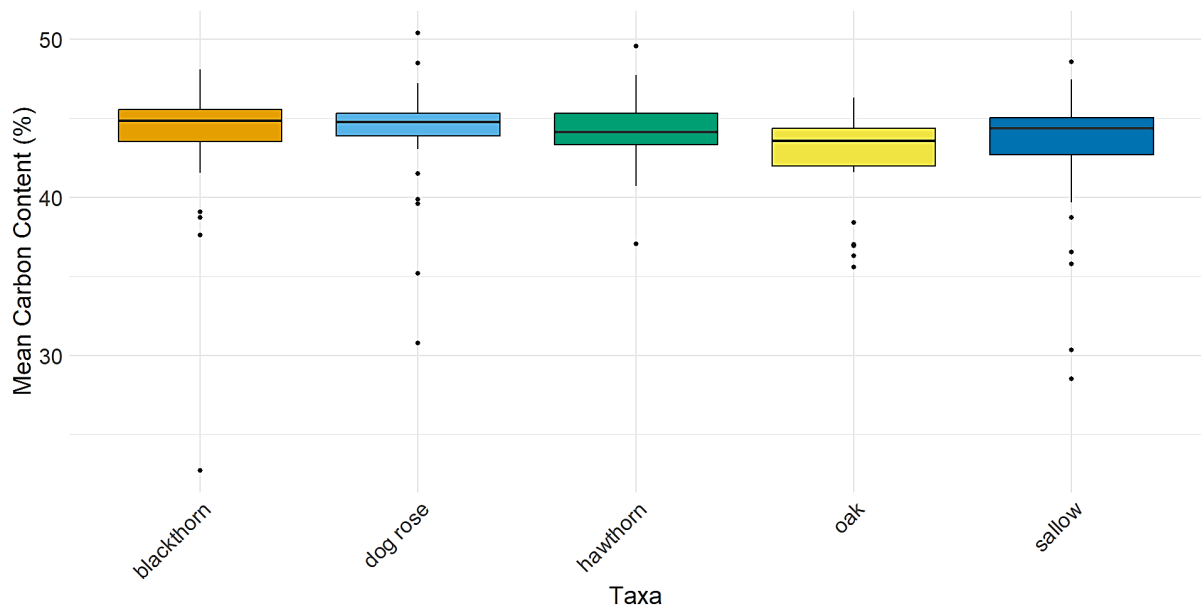


Figure 4.2: Variation in carbon content (%) across five different tree taxa: blackthorn (*Prunus spinosa*) n=36, dog rose (*Rosa canina*) n=42, hawthorn (*Crataegus* spp.) n=54, sallow (*Salix* spp.) n=39 and oak (*Quercus* spp.) n=30.

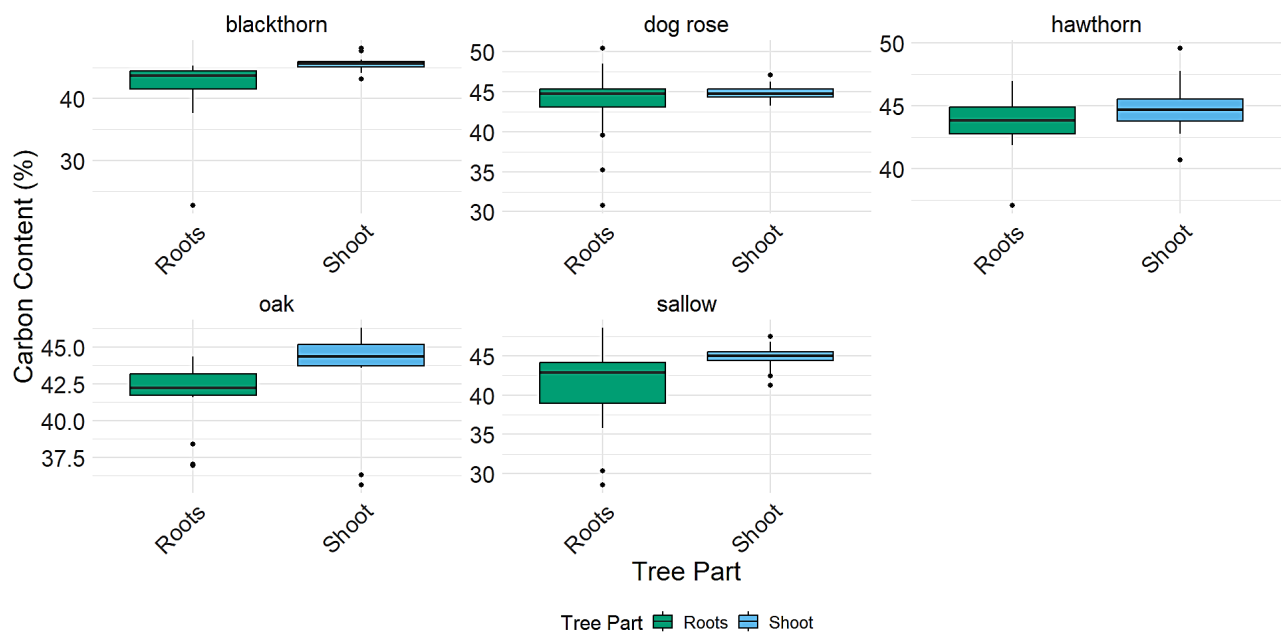


Figure 4.3: The carbon content (%) in aboveground (shoot) and belowground (root) parts for five tree taxa: blackthorn (*Prunus spinosa*), dog rose (*Rosa canina*), hawthorn (*Crataegus* spp.), oak (*Quercus* spp.), and sallow (*Salix* spp.).

4.3.3. Relationship between tree height and taxon-specific carbon content

There was a slight variation in carbon content distribution across different size groups: large (> 210 cm), medium (75 – 210 cm), and small (< 75 cm). Large trees exhibited the highest mean carbon content (mean: 44.9% \pm 2.03%), followed by medium (mean: 43.8% \pm 3.49%) and small (mean: 43.5% \pm 3.71%) trees, with the highest variability observed in the small size group (Figure 4.4A).

The variation in carbon content (C%) across size groups within species revealed distinct trends (Figure 4.4B). In blackthorn (*Prunus spinosa*), carbon content decreased slightly with size, averaging 44.18% \pm 2.58% in large trees, 44.04% \pm 2.78% in medium trees, and 42.83% \pm 6.45% in small trees. Dog rose (*Rosa canina*) exhibited a similar trend, with carbon content decreasing from 44.91% \pm 3.50% in large trees to 43.46% \pm 3.43% in medium trees and 43.46% \pm 3.24% in small trees.

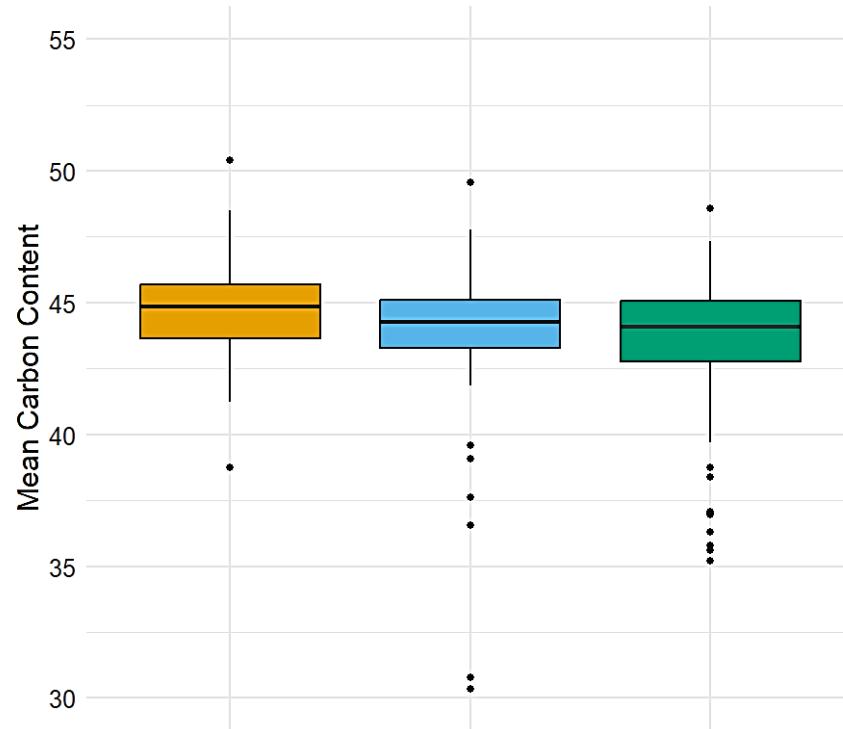
Hawthorn (*Crataegus* spp.) displayed higher carbon content in medium-sized trees (45.13% \pm 2.92%) compared to large (44.28% \pm 2.91%) and small (43.21% \pm 3.14%) trees. Sallow (*Salix* spp.) showed considerable variation among small trees (mean: 45.35% \pm 2.74%), which had a higher average carbon content than medium-sized trees (42.96% \pm 4.12%). Oak (*Quercus* spp.) demonstrated a decreasing trend in carbon content from large trees (44.73% \pm 3.65%) to small trees (42.65% \pm 3.92%), with medium trees showing a slightly higher carbon content (43.23% \pm 3.62%) than small ones.

The Pearson correlation between mean carbon content and density is $r = -0.067$ with a $p=0.719$ (Table S4.1 and Figure S4.1).

4.3.4 Exposure Impact on Carbon Content

The independent t-test shows no significant difference in carbon content between exposed ($n = 19$) and protected ($n = 14$) browsing conditions (aboveground: $t = -0.36$, $p=0.72$; belowground: $t=-0.51$, $p=0.62$). Blackthorn (*Prunus spinosa*) and oak (*Quercus spp.*) exhibited higher root carbon content under protected conditions, increasing from $40.11\% \pm 7.01\%$ to $43.43\% \pm 2.01\%$ (+3.32%) and from $40.88\% \pm 3.09\%$ to $42.27\% \pm 1.69\%$ (+1.39%), respectively. In contrast, willow (*Salix spp.*) showed a slight decrease, from $41.15\% \pm 4.87\%$ to $40.30\% \pm 6.25\%$ (-0.85%). Dog rose (*Rosa canina*) showed below-ground carbon content increasing from $43.5\% \pm 4.8\%$ (exposed) to $44.6\% \pm 2.1\%$ (protected), while hawthorn (*Crataegus spp.*) showed a slight decrease, from $44.0\% \pm 1.7\%$ (exposed) to $43.5\% \pm 1.2\%$ (protected). Above-ground carbon content was consistent across taxa, with minor variations between exposed and protected conditions. Blackthorn (*Prunus spinosa*) had values of $46.0\% \pm 1.2\%$ (exposed) and $45.2\% \pm 1.0\%$ (protected). Dog rose (*Rosa canina*) exhibited values of $44.8\% \pm 1.4\%$ (exposed) and $44.6\% \pm 1.4\%$ (protected). Hawthorn (*Crataegus spp.*) ranged from $45.2\% \pm 1.1\%$ (exposed) to $45.7\% \pm 0.8\%$ (protected). *Quercus spp.* showed slightly lower values, with $44.7\% \pm 0.9\%$ (exposed) and $44.4\% \pm 0.6\%$ (protected). *Salix spp.* remained stable, with $45.6\% \pm 0.8\%$ (exposed) and $45.5\% \pm 0.7\%$ (protected).

[A]



[B]

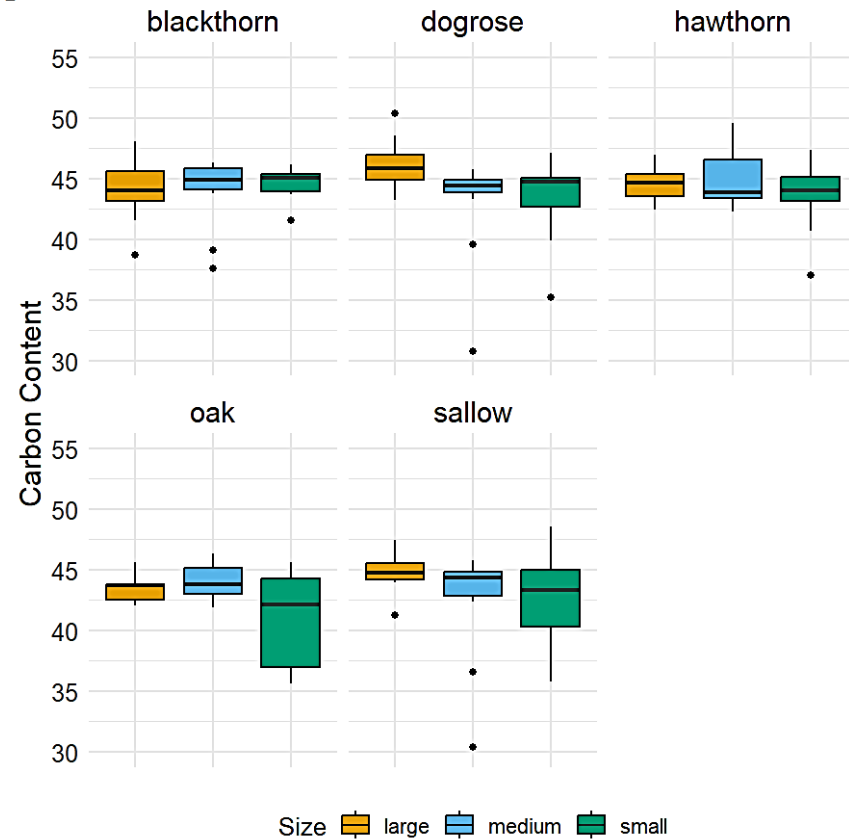


Figure 4.4: The mean carbon content in relation to tree size and taxa. [A]: Mean carbon content by tree size (large: >150 cm, medium <150 cm >50 cm, small: <50 cm). [B]: Mean carbon content by taxon (blackthorn (*Prunus spinosa*), dog rose (*Rosa canina*), hawthorn (*Crataegus* spp.), oak (*Quercus* spp.), willow (*Salix* spp.)) and size categories. Each taxon is further divided into size categories (large, medium, small).

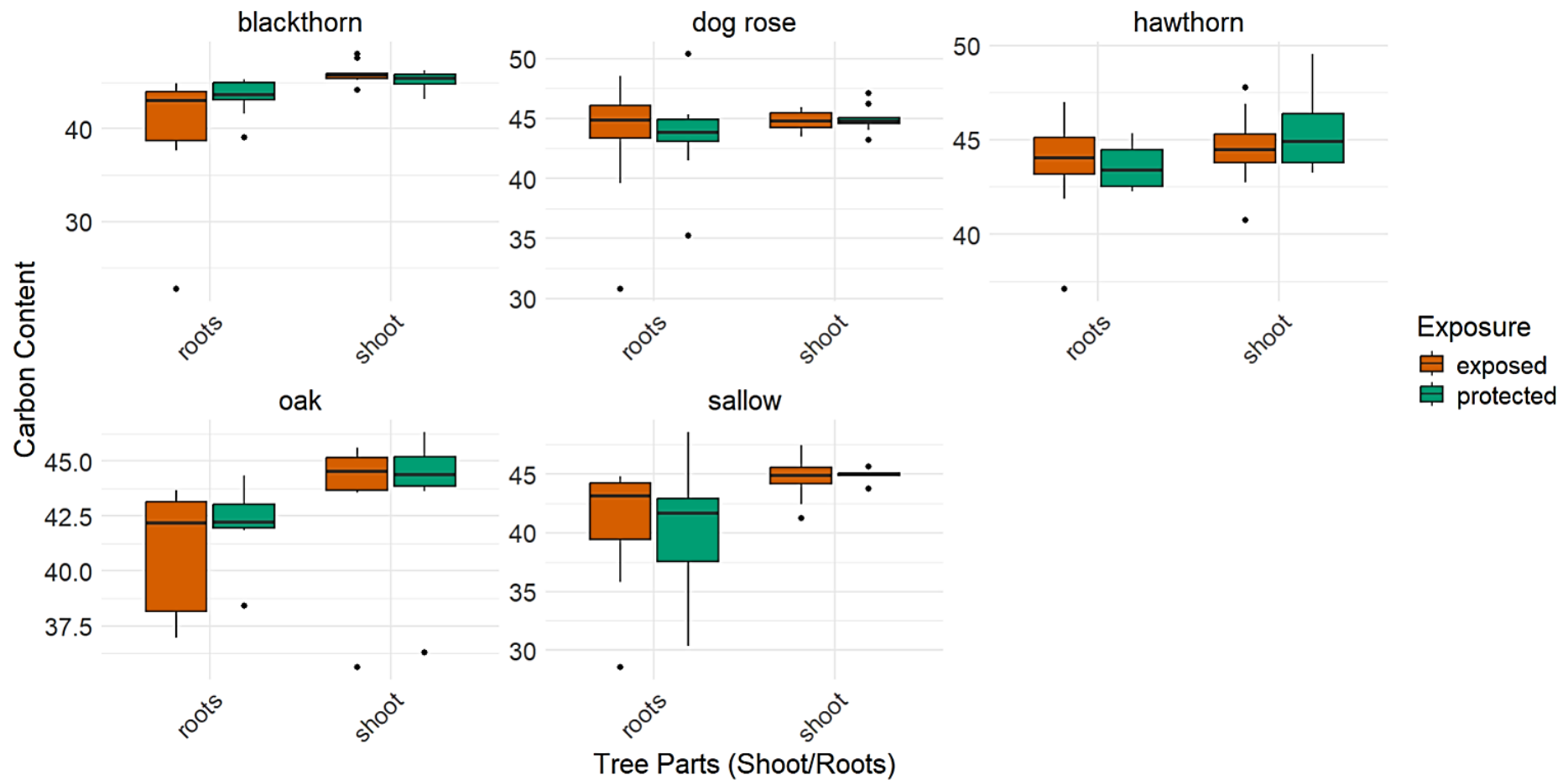


Figure 4.5: Mean carbon content, divided by tree part (shoot or root) of the five taxa (blackthorn (*Prunus spinosa*), dog rose (*Rosa canina*), hawthorn (*Crataegus* spp.), oak (*Quercus* spp.), willow (*Salix* spp.)). Each taxon is further divided into exposure categories: exposed (not found within a bramble patch) and protected (found within a bramble patch).

4.4 Discussion

The results of this study suggest that the common assumption that 50% of a tree's dry mass is carbon (Jenkins et al., 2011) is not applicable to shrub tree species in rewilded landscapes. My findings highlight the importance of using taxa-specific carbon content values rather than relying on this generalised assumption. Elemental analysis of 201 samples from 34 individual trees, conducted via dry combustion, revealed that none of the samples aligned with the 50% benchmark. Instead, most taxa exhibited carbon content values between 43% and 45%. Although some studies support the 50% rule for certain tree species (Malhi et al., 2004; Brown & Lugo, 1984; Petrokofsky et al., 2012), our findings indicate significant variations in carbon content between taxa (Figure 4.4). In naturally regenerating scrub trees, the carbon content was consistently below the 50% rule, aligning with findings from other studies (Bardule et al., 2021; Lamloom et al., 2003; Gao et al., 2016; Ying et al., 2019) (Figure 4.1).

These findings align with previous studies reporting significant variation in carbon content across tree species and local conditions. For example, Thomas and Martin (2012) found that stem wood carbon content in temperate forests varied widely among species, ranging from 43.4% to 55.6%, challenging the 50% assumption. Similarly, Lamloom and Savidge (2003) observed carbon content in kiln-dried hardwood species ranging from 46.27% to 49.97%, and in conifers from 47.21% to 55.20%, indicating variability due to species traits and environmental factors. Additionally, Martin et al. (2018) demonstrated that soil fertility and climate can influence carbon content, even within related taxa, underscoring the need for localised carbon estimates. More generally, relying on the generalised 50% rule can lead to inaccurate carbon stock valuations, over-estimating the amount of carbon stored across the landscape. My findings suggest that the average carbon content across five temperate scrub

taxa in my study centres around 44% for the aboveground biomass (AGB) and 43% for the belowground biomass (BGB) (Figure 4.1). While this central tendency is notable, the considerable spread within taxa indicates that further research is needed to validate whether this value is generalisable. However, given these findings I propose that the 44% and 43% figures should serve as provisional guidelines for temperate scrub trees until more data are available to demonstrate that this estimate captures the variability across all species and environments. This aligns with previous studies (Martin et al., 2018; Thomas & Martin, 2012; Ma et al., 2018), which recommend using more precise taxa-specific or context-specific carbon values wherever possible.

4.4.1. Factors Contributing to Lower Carbon Content in Scrub Trees

Reflecting on the factors that might contribute to the lower carbon content observed in scrub tree species on the Knepp Estate, one key consideration is their relatively small size and minimal timber volume. Timber volume, which refers to the amount of usable wood material within a tree—typically measured by the size of its trunk and main branches—is a common metric in forestry and carbon assessments (Matthews, 2017; Mackie & Matthews, 2008). Scrub trees, with their thinner trunks and less developed branches, generally have much lower timber volume compared to larger, timber-producing species (Jenkins et al., 2011). As a result, their carbon storage potential is often regarded as negligible relative to high-timber-volume trees (Matthews, 2017). Age may also be an important factor influencing carbon content. The scrub trees sampled from the rewilding project are relatively young, with all trees being less than twenty years old. My results show a clear trend where larger scrub trees exhibit higher mean carbon content ($44.73\% \pm 2.02\%$) compared to medium-sized trees ($43.54\% \pm 3.48\%$) and small trees ($43.07\% \pm 3.71\%$) (Figure 4.4). This pattern suggests that as scrub trees grow and

mature, their carbon content increases, potentially reflecting changes in wood composition or density associated with age.

Another factor is the common belief that juvenile wood contains a higher proportion of lignin, a carbon-rich compound that contributes to higher carbon content, supporting structural stability during early growth phases (Bembenek et al., 2015; Zobel & Sprague, 2012; Thomas & Martin, 2012; Lamloom & Savidge, 2003). Research by Bembenek et al. (2015), for example, found that in Scots pine (*Pinus sylvestris*), juvenile wood exhibited slightly higher carbon content (48.15%) than mature wood (46.94%), attributed to its higher lignin and earlywood content. However, in my study, this trend was not observed; instead, the young wood (<20 years old) samples showed lower-than-expected carbon content. This may reflect natural variability rather than an issue with the combustion-based analysis method, which effectively retains lignin (degraded between 200–500°C; Brebu & Vasile, 2009; Nassar & Mackay, 1984) and other stable carbon compounds. This suggests that differences in carbon content across taxa are likely due to taxa-specific carbon allocation patterns or environmental factors, rather than any loss during processing (Thermo Fisher, 2023; Chevalier et al., 2017).

Finally, environmental stressors, such as browsing, can influence plant strategies, vegetation recruitment, and photosynthesis rates, potentially leading to lower overall carbon storage in areas with herbivores compared to herbivore-free zones (Tanentzap et al., 2023; Jia et al., 2018; Tanentzap and Coomes, 2012). Furthermore, physiological differences in carbon allocation and storage across taxa, along with growth rates that affect the balance between structural and non-structural carbohydrates in biomass, also contribute to variations in carbon storage (Young et al., 2011; Poorter et al., 2012).

Currently, taxa- and species-specific carbon values have been assigned to oak (*Quercus spp.*) through studies such as Castaño-Santamaría and Bravo (2012) and Thomas and Martin (2012). Castaño-Santamaría and Bravo (2012) examined carbon concentration (%C) and basic density in sessile oak (*Quercus petraea*) (45.49%–46.86%) and Pyrenean oak (*Quercus pyrenaica*) (45.58%–45.82%) in NW Spain, revealing significant variation across woody tissues (bark, sapwood, heartwood) and between species. These findings highlight the necessity of using tissue- and species-specific carbon values to improve estimation accuracy, potentially explaining the variability observed in my study (Figures 4.2 and 4.3). Similarly, Thomas and Martin (2012) reported a mean carbon content of 48.8% for temperate and boreal oak species, focusing on *Quercus rubra* (northern red oak). At Knepp, however, the mean carbon content for scrub oak (*Quercus robur* and *Quercus petraea*) was 42.64% ($\pm 2.43\%$), notably lower than the values reported in these studies. This discrepancy underscores the importance of accounting for both taxa-specific traits and environmental factors in carbon content assessments.

For other tree taxa studied in this research—sallow (*Salix spp.*), dog rose (*Rosa canina*), hawthorn (*Crataegus spp.*), and blackthorn (*Prunus spinosa*)—there are limited or no references to taxa-specific carbon content values. Most studies either overlook these species or generalise their carbon values. For example, in studies involving willow (*Salix spp.*), generalised values are often used instead of taxa-specific data. Masi et al. (2021) applied generalised carbon content values to broadleaf species, including willow (*Salix spp.*), using average values from the European Forest Biomass dataset, which provides an average carbon content of 48%. At Knepp, the mean carbon content for willow (*Salix spp.*) scrub was found to be 43.1% ($\pm 3.37\%$), much lower than previously reported values. This supports the notion that when estimating the carbon content, the local environmental conditions should be considered.

4.4.2. Carbon content variation by tree part across taxa

Taxa-specific responses to herbivory were observed (Figure 4.3). Blackthorn (*Prunus spinosa*), oak (*Quercus* spp.), and willow (*Salix* spp.) exhibited higher root carbon content under protected conditions. This suggests that browsing may reduce below-ground carbon allocation in these species. In contrast, dog rose (*Rosa canina*) and hawthorn (*Crataegus* spp.) showed minimal differences in root carbon content between exposed and protected conditions (Figure 4.5), indicating that these taxa may be less sensitive to browsing impacts on their below-ground carbon reserves.

Recent studies suggest that plants often reallocate biomass to roots under stress conditions such as browsing (Perkovich & Ward, 2021; Axe et al., 2017; Burrell et al., 2024). My findings indicate that carbon content in above-ground parts (mean: $44.77\% \pm 1.84\%$) may be higher than in roots (mean: $42.53\% \pm 4.05\%$) (Figure 4.3) potentially linked to active defence mechanisms. The evolutionary arms race between plants and herbivores has led to a variety of plant defences, including the production of chemical compounds (Mithöfer & Boland, 2012; Sánchez-Sánchez & Morquecho-Contreras, 2017), nutrient reallocation (Pérez-de-Lis et al., 2017; Perkovich & Ward, 2021; Wiley et al., 2017), and the formation of callouses and tannins (Haukioja et al., 2002; Hjältén et al., 2006; Herms & Mattson, 1992) to deter herbivores (Barbehenn & Constabel, 2011). These defences likely contribute to the higher carbon content observed in the aboveground parts of the scrub trees.

While my study found no significant effect of browsing exposure on overall carbon content in aboveground or belowground tree parts, it highlights the complex interactions between herbivory and plant carbon dynamics. The observed patterns suggest that browsing may

trigger specific defensive responses in aboveground biomass, leading to increased carbon content, while also promoting biomass reallocation to roots (see Chapter 3). Further research on the specificity of browsing and its long-term impacts is needed to better understand these processes and their implications for carbon storage in rewilding projects.

4.5 Conclusion

This study evaluated the 50% dry biomass carbon rule for estimating carbon stocks in rewilded scrubland at Knepp Estate. While effective in some woodland and forest systems, our findings suggest this assumption may overestimate carbon content in complex, herbivore-affected shrub landscapes like Knepp. With mean carbon contents of approximately 44% (AGB) and 43% (BGB), our data reveal significant variation across taxa and root:shoot ratios, highlighting the limitations of a one-size-fits-all approach. These results stress the need for further work to determine accurate, representative carbon values tailored to scrub ecosystems.

By demonstrating the influence of taxa-specific and environmental factors, this study underscores the importance of detailed carbon measurements for reliable carbon assessments in rewilded landscapes. Without these, current models risk poorly estimating the carbon storage potential of scrublands. Expanding on these findings with larger sample sizes will improve our understanding of scrubland carbon dynamics, enabling more precise rewilding strategies for carbon sequestration.

In summary, this research contributes to the development of a rewilding-specific carbon model by providing scrub-specific carbon data. These findings will strengthen the allometric equations developed in Chapter 3, enhancing the accuracy of carbon storage estimates and supporting informed conservation and management efforts.

4.6 References

- Alonzo, M., Dial, R.J., Schulz, B.K., Andersen, H.E., Lewis-Clark, E., Cook, B.D. and Morton, D.C., 2020. Mapping tall shrub biomass in Alaska at landscape scale using structure-from-motion photogrammetry and lidar. *Remote Sensing of Environment*, 245, p.111841.
- Axe, M.S., Grange, I.D. and Conway, J.S., 2017. Carbon storage in hedge biomass—A case study of actively managed hedges in England. *Agriculture, ecosystems & environment*, 250, pp.81-88.
- Balaji, B.N. and Jambagi, S.R., 2024. Structural Defences in Plants against Herbivores-A Review. *Indian Journal of Entomology*, pp.1-9.
- Barbehenn, R.V. and Constabel, C.P., 2011. Tannins in plant–herbivore interactions. *Phytochemistry*, 72(13), pp.1551-1565.
- Bardgett, R.D. and Wardle, D.A., 2003. Herbivore-mediated linkages between aboveground and belowground communities. *Ecology*, 84(9), pp.2258-2268.
- Bārdule, A., Liepiņš, J., Liepiņš, K., Stola, J., Butlers, A. and Lazdiņš, A., 2021. Variation in carbon content among the major tree species in hemiboreal forests in Latvia. *Forests*, 12(9), p.1292.
- Bastin, J.F., Finegold, Y., Garcia, C., Mollicone, D., Rezende, M., Routh, D., Zohner, C.M. and Crowther, T.W., 2019. The global tree restoration potential. *Science*, 365(6448), pp.76-79.
- Bembenek, M., Giefing, D.F., Jelonek, T., Karaszewski, Z., Kruszyk, R., Tomczak, A., Woszczyk, M.I.C.H.A.Ü. and Mederski, P.S., 2015. Carbon content in juvenile and mature wood of Scots pine (*Pinus sylvestris* L.). *Balt. For*, 21, pp.279-284.
- Berzaghi, F., Chami, R., Cosimano, T. and Fullenkamp, C., 2022. Financing conservation by valuing carbon services produced by wild animals. *Proceedings of the National Academy of Sciences*, 119(22), p.e2120426119.
- Bhatti, S., Ahmad, S.R., Asif, M. and Farooqi, I.U.H., 2023. Estimation of aboveground carbon stock using Sentinel-2A data and Random Forest algorithm in scrub forests of the Salt Range, Pakistan. *Forestry*, 96(1), pp.104-120.
- Biermann, C. and Anderson, R.M., 2017. Conservation, biopolitics, and the governance of life and death. *Geography Compass*, 11(10), p.e12329.
- Bohn, F.J. and Huth, A., 2017. The importance of forest structure to biodiversity–productivity relationships. *Royal Society open science*, 4(1), p.160521.
- Bouvet, A., Mermoz, S., Le Toan, T., Villard, L., Mathieu, R., Naidoo, L. and Asner, G.P., 2018. An above-ground biomass map of African savannahs and woodlands at 25 m resolution derived from ALOS PALSAR. *Remote sensing of environment*, 206, pp.156-173.
- Brancalion, P.H., Balmford, A., Wheeler, C.E., Rodrigues, R.R., Strassburg, B.B. and Swinfield, T., 2024. A call to develop carbon credits for second-growth forests. *Nature Ecology & Evolution*, pp.1-2.

- Brebu, M. and Vasile, C., 2010. Thermal degradation of lignin—a review. *Cellulose Chemistry & Technology*, 44(9), p.353.
- Brown, S. and Lugo, A.E., 1984. Biomass of tropical forests: a new estimate based on forest volumes. *Science*, 223(4642), pp.1290-1293.6.
- Bryant, J.P., Chapin III, F.S. and Klein, D.R., 1983. Carbon/nutrient balance of boreal plants in relation to vertebrate herbivory. *Oikos*, pp.357-368.
- Burrell, N.C., Jeffers, E.S., Macias-Fauria, M. and Willis, K.J., 2024. The inadequacy of current carbon storage assessment methods for rewilding: A Knepp Estate case study. *Ecological Solutions and Evidence*, 5(1), p.e12301.
- Castaño-Santamaría, J. and Bravo, F., 2012. Variation in carbon concentration and basic density along stems of sessile oak (*Quercus petraea* (Matt.) Liebl.) and Pyrenean oak (*Quercus pyrenaica* Willd.) in the Cantabrian Range (NW Spain). *Annals of Forest Science*, 69, pp.663-672.
- Centre for Ecology and Hydrology (2004). *PLANTATT - Attributes of British and Irish Plants - Spreadsheet*. Huntingdon: Centre for Ecology and Hydrology.
- Čermák, J., Kučera, J., Bauerle, W.L., Phillips, N. and Hinckley, T.M., 2007. Tree water storage and its diurnal dynamics related to sap flow and changes in stem volume in old-growth Douglas-fir trees. *Tree physiology*, 27(2), pp.181-198.
- Chave, J., Andalo, C., Brown, S., Cairns, M.A., Chambers, J.Q., Eamus, D., Fölster, H., Fromard, F., Higuchi, N., Kira, T. and Lescure, J.P., 2005. Tree allometry and improved estimation of carbon stocks and balance in tropical forests. *Oecologia*, 145, pp.87-99.
- Chave, J., Condit, R., Aguilar, S., Hernandez, A., Lao, S. and Perez, R., 2004. Error propagation and scaling for tropical forest biomass estimates. *Philosophical Transactions of the Royal Society of London. Series B: Biological Sciences*, 359(1443), pp.409-420.
- Chevalier, D., Leone, F., Krotz, L., and Giazzi, G. 2017. *Elemental Analysis: Nitrogen and carbon determination of soils and plants with a single reactor*. Courtaboeuf, France: Thermo Fisher Scientific. Available at: [<https://www.thermofisher.com/uk/en/home/industrial/spectroscopy-elemental-isotope-analysis/trace-elemental-analysis/organic-elemental-analysis-oea.html#menu5>] (Accessed: 3 June 2024).
- Coetsee, C., Fornara, D., Veldtman, A. and Wigley, B., 2019. Indirect effects of browsing herbivores in savannas. *Savanna Woody Plants and Large Herbivores*, pp.613-641.
- Corlett, R.T., 2016. Plant diversity in a changing world: status, trends, and conservation needs. *Plant diversity*, 38(1), pp.10-16.
- Crawley, M. J. (2012). *The R Book*. 2nd Edition. Wiley.
- Culot, L., Bello, C., Batista, J.L.F., Do Couto, H.T.Z. and Galetti, M., 2017. Synergistic effects of seed disperser and predator loss on recruitment success and long-term consequences for carbon stocks in tropical rainforests. *Scientific Reports*, 7(1), p.7662.

- de Vries, W., Solberg, S., Dobbertin, M., Sterba, H., Laubhahn, D., Reinds, G.J., Nabuurs, G.J., Gundersen, P. and Sutton, M.A., 2008. Ecologically implausible carbon response? *Nature*, 451(7180), pp.E1-E3.
- Doughty, C.E., Wolf, A., Morueta-Holme, N., Jørgensen, P.M., Sandel, B., Violle, C., Boyle, B., Kraft, N.J., Peet, R.K., Enquist, B.J. and Svenning, J.C., 2016. Megafauna extinction, tree species range reduction, and carbon storage in Amazonian forests. *Ecography*, 39(2), pp.194-203.
- Enquist, B.J., Abraham, A.J., Harfoot, M.B., Malhi, Y. and Doughty, C.E., 2020. The megabiota are disproportionately important for biosphere functioning. *Nature communications*, 11(1), p.699.
- European Environment Agency (2022). State of Nature in the EU: Results from reporting under the nature directives 2013-2018. EEA Report No 10/2020. Available at: <https://www.eea.europa.eu/publications/state-of-nature-in-the-eu-2020> (Accessed: 4 June 2024).
- Facciolati, V., Zarek, M., Blonska, E., Lasota, J., Orman, O. and Ciach, M., 2024. To be browsed or not to be browsed: differences in nutritional characteristics of blackthorn *Prunus spinosa* subject to the long-term pressure of herbivores. *bioRxiv*, pp.2024-04.
- Feeny, P., 1976. Plant apparency and chemical defense. In *Biochemical interaction between plants and insects* (pp. 1-40). Boston, MA: Springer US.
- Feldpausch, T.R., Lloyd, J., Lewis, S.L., Brienen, R.J., Gloor, M., Monteagudo Mendoza, A., Lopez-Gonzalez, G., Banin, L., Abu Salim, K., Affum-Baffoe, K. and Alexiades, M., 2012. Tree height integrated into pantropical forest biomass estimates. *Biogeosciences*, 9(8), pp.3381-3403.
- Fernández, N., Navarro, L.M. and Pereira, H.M., 2017. Rewilding: a call for boosting ecological complexity in conservation. *Conservation Letters*, 10(3), pp.276-278.
- Field, A., 2013. *Discovering statistics using IBM SPSS statistics*.
- Forestry Commission. (2014). *The Woodland Carbon Code: The UK Standard for Woodland Creation Projects*. Forestry Commission.
- Franceschi, V. R., Krokene, P., Christiansen, E., & Krekling, T. (2005). Anatomical and chemical defenses of conifer bark against bark beetles and other pests. *New Phytologist*, 167(2), 353-375.
- Gao, B., Taylor, A.R., Chen, H.Y. and Wang, J., 2016. Variation in total and volatile carbon concentration among the major tree species of the boreal forest. *Forest Ecology and Management*, 375, pp.191-199.
- Gill, R.M. and Fuller, R.J., 2007. The effects of deer browsing on woodland structure and songbirds in lowland Britain. *Ibis*, 149, pp.119-127.
- Gordon, I.J. and Prins, H.H., 2008. *The ecology of browsing and grazing* (No. 195). Berlin:: Springer.
- Gowda, J.H., 1996. Spines of *Acacia tortilis*: what do they defend and how?. *Oikos*, pp.279-284.

- Griscom, B.W., Adams, J., Ellis, P.W., Houghton, R.A., Lomax, G., Miteva, D.A., Schlesinger, W.H., Shoch, D., Siikamäki, J.V., Smith, P. and Woodbury, P., 2017. Natural climate solutions. *Proceedings of the National Academy of Sciences*, 114(44), pp.11645-11650.
- Hamilton, J.G., Zangerl, A.R., DeLucia, E.H. and Berenbaum, M.R., 2001. The carbon–nutrient balance hypothesis: its rise and fall. *Ecology letters*, 4(1), pp.86-95.
- Hanley, M.E., Lamont, B.B., Fairbanks, M.M. and Rafferty, C.M., 2007. Plant structural traits and their role in anti-herbivore defence. *Perspectives in Plant Ecology, Evolution and Systematics*, 8(4), pp.157-178.
- Harmon, M.E., Franklin, J.F., Swanson, F.J., Sollins, P., Gregory, S.V., Lattin, J.D., Anderson, N.H., Cline, S.P., Aumen, N.G., Sedell, J.R. and Lienkaemper, G.W., 2004. Ecology of coarse woody debris in temperate ecosystems. *Advances in ecological research*, 34, pp.59-234.
- Hauck, M., Csapek, G. and Dulamsuren, C., 2023. The significance of large old trees and tree cavities for forest carbon estimates. *Forest Ecology and Management*, 546, p.121319.
- Haukioja, E., Ossipov, V. and Lempa, K., 2002. Interactive effects of leaf maturation and phenolics on consumption and growth of a geometrid moth. *Entomologia Experimentalis et Applicata*, 104(1), pp.125-136.
- He, H., Zhang, C., Zhao, X., Fousseni, F., Wang, J., Dai, H., Yang, S. and Zuo, Q., 2018. Allometric biomass equations for 12 tree species in coniferous and broadleaved mixed forests, Northeastern China. *PloS one*, 13(1), p.e0186226..
- Herms, D.A. and Mattson, W.J., 1992. The dilemma of plants: to grow or defend. *The quarterly review of biology*, 67(3), pp.283-335.
- Hjältén, J., Lindau, A., Wennström, A., Blomberg, P., Witzell, J., Hurry, V. and Ericson, L., 2007. Unintentional changes of defence traits in GM trees can influence plant–herbivore interactions. *Basic and Applied Ecology*, 8(5), pp.434-443.
- Houghton, T.P., Stevens, D.M., Pryfogle, P.A., Wright, C.T. and Radtke, C.W., 2009. The effect of drying temperature on the composition of biomass. *Applied biochemistry and biotechnology*, 153, pp.4-10.
- IPCC (2019). *Climate Change and Land: an IPCC special report on climate change, desertification, land degradation, sustainable land management, food security, and greenhouse gas fluxes in terrestrial ecosystems*. Available at: <https://www.ipcc.ch/report/srccl/> (Accessed: 4 June 2024).
- i-Tree. (2021). *i-Tree Eco (version 6.0)* [Computer software]. USDA Forest Service. Available from <https://www.itreetools.org>.
- Jenkins, T.A., Mackie, E.D., Matthews, R.W., Miller, G., Randle, T.J. and White, M.E., 2011. *FC woodland carbon code: Carbon assessment protocol*. Forestry Commission, Edinburgh.
- Jepson, P., 2016. A rewilding agenda for Europe: creating a network of experimental reserves. *Ecography*, 39(2).
- Jia, S., Wang, X., Yuan, Z., Lin, F., Ye, J., Hao, Z. and Luskin, M.S., 2018. Global signal of top-down control of terrestrial plant communities by herbivores. *Proceedings of the National*

- Academy of Sciences, 115(24), pp.6237-6242. Koricheva, J., 2002. The carbon-nutrient balance hypothesis is dead; long live the carbon-nutrient balance hypothesis?. *Oikos*, 98(3), pp.537-539.
- Jones, E., Harden, S. and Crawley, M.J., 2022. *The R book*. John Wiley & Sons.
- Kallarackal, J., Ramírez, F. (2024). Wood and Wood Density. In: Wood Density. Springer, Cham. https://doi.org/10.1007/978-3-031-61030-1_2
- Karban, R. and Baldwin, I.T., 2007. *Induced responses to herbivory*. University of Chicago Press.
- Keesstra, S., Nunes, J., Novara, A., Finger, D., Avelar, D., Kalantari, Z. and Cerdà, A., 2018. The superior effect of nature based solutions in land management for enhancing ecosystem services. *Science of the Total Environment*, 610, pp.997-1009.
- Lamloom, S.H. and Savidge, R.A., 2003. A reassessment of carbon content in wood: variation within and between 41 North American species. *Biomass and Bioenergy*, 25(4), pp.381-388.
- Langenheim, J. H., 2003. *Plant resins: chemistry, evolution, ecology, and ethnobotany*. Timber Press.
- Laosuwan, T., Uttaruk, Y., Sangpradid, S., Butthep, C. and Leammanee, S., 2023. The Carbon Sequestration Potential of Silky Oak (*Grevillea robusta* A. Cunn. ex R. Br.), a High-Value Economic Wood in Thailand. *Forests*, 14(9), p.1824.
- Liepiņš, J., Lazdiņš, A. and Liepiņš, K., 2018. Equations for estimating above-and belowground biomass of Norway spruce, Scots pine, birch spp. and European aspen in Latvia. *Scandinavian Journal of Forest Research*, 33(1), pp.58-70.
- Liepiņš, J., Liepiņš, K. and Lazdiņš, A., 2021. Equations for estimating the above-and belowground biomass of grey alder (*Alnus incana* (L.) Moench.) and common alder (*Alnus glutinosa* L.) in Latvia. *Scandinavian Journal of Forest Research*, 36(5), pp.389-400.
- Lines, E.R., Coomes, D.A. and Purves, D.W., 2010. Influences of forest structure, climate and species composition on tree mortality across the eastern US. *PloS one*, 5(10), p.e13212.
- Litton, C. M., Raich, J. W., & Ryan, M. G. (2007). Carbon allocation in forest ecosystems. *Global Change Biology*, 13(10), 2089-2109.
- Liu, B., Bu, W. and Zang, R., 2023. Improved allometric models to estimate the aboveground biomass of younger secondary tropical forests. *Global Ecology and Conservation*, 41, p.e02359.
- Ma, S., He, F., Tian, D., Zou, D., Yan, Z., Yang, Y., Zhou, T., Huang, K., Shen, H. and Fang, J., 2018. Variations and determinants of carbon content in plants: a global synthesis. *Biogeosciences*, 15(3), pp.693-702.
- Ma, Z., Chen, H.Y., Bork, E.W., Carlyle, C.N. and Chang, S.X., 2020. Carbon accumulation in agroforestry systems is affected by tree species diversity, age and regional climate: A global meta-analysis. *Global ecology and biogeography*, 29(10), pp.1817-1828.
- Mackie, E.D and R.W. Matthews (2008) *Timber Measurement*. Forestry Commission, Edinburgh. 70pp. ISBN: 978-0-85538-749-5.

- Malhi, Y. and Phillips, O.L., 2004. Tropical forests and global atmospheric change: a synthesis. *Philosophical Transactions of the Royal Society of London. Series B: Biological Sciences*, 359(1443), pp.549-555.
- Malhi, Y., Lander, T., le Roux, E., Stevens, N., Macias-Fauria, M., Wedding, L., Girardin, C., Kristensen, J.Å., Sandom, C.J., Evans, T.D. and Svenning, J.C., 2022. The role of large wild animals in climate change mitigation and adaptation. *Current Biology*, 32(4), pp.R181-R196.
- Mappin, B., Ward, A., Hughes, L., Watson, J.E., Cosier, P. and Possingham, H.P., 2022. The costs and benefits of restoring a continent's terrestrial ecosystems. *Journal of Applied Ecology*, 59(2), pp.408-419.
- Martin, A.R. and Thomas, S.C., 2011. A reassessment of carbon content in tropical trees. *PloS one*, 6(8), p.e23533.
- Martin, A.R., Doraisami, M. and Thomas, S.C., 2018. Global patterns in wood carbon concentration across the world's trees and forests. *Nature Geoscience*, 11(12), pp.915-920.
- Masi, E.B., Segoni, S. and Tofani, V., 2021. Root reinforcement in slope stability models: a review. *Geosciences*, 11(5), p.212.
- Matthews, G., 1993. The carbon content of trees (No. 4, pp. iv+21).
- Matthews, R. (2017). 11. Forest carbon and biomass policy. *Forest Research Impact Case Studies*, p. 85
- Melson, S.L., Harmon, M.E., Fried, J.S. and Domingo, J.B., 2011. Estimates of live-tree carbon stores in the Pacific Northwest are sensitive to model selection. *Carbon Balance and Management*, 6, pp.1-16.
- Mikołajczak, K.M., Jones, N., Sandom, C.J., Wynne-Jones, S., Beardsall, A., Burgelman, S., Ellam, L. and Wheeler, H.C., 2022. Rewilding—The farmers' perspective. Perceptions and attitudinal support for rewilding among the English farming community. *People and Nature*, 4(6), pp.1435-1449.
- Mildrexler, D.J., Berner, L.T., Law, B.E., Birdsey, R.A. and Moomaw, W.R., 2020. Large trees dominate carbon storage in forests east of the cascade crest in the United States Pacific Northwest. *Frontiers in Forests and Global Change*, 3, p.594274.
- Misra, R.K., Turnbull, C.R.A., Cromer, R.N., Gibbons, A.K. and LaSala, A.V., 1998. Below-and above-ground growth of *Eucalyptus nitens* in a young plantation: I. Biomass. *Forest Ecology and Management*, 106(2-3), pp.283-293.
- Mitchard, E.T., Feldpausch, T.R., Brienen, R.J., Lopez-Gonzalez, G., Monteagudo, A., Baker, T.R., Lewis, S.L., Lloyd, J., Quesada, C.A., Gloor, M. and Ter Steege, H., 2014. Markedly divergent estimates of Amazon forest carbon density from ground plots and satellites. *Global ecology and biogeography*, 23(8), pp.935-946.
- Mithöfer, A. and Boland, W., 2012. Plant defense against herbivores: chemical aspects. *Annual review of plant biology*, 63(1), pp.431-450.52.

Mokany, K., McCarthy, J.K., Falster, D.S., Gallagher, R.V., Harwood, T.D., Kooyman, R. and Westoby, M., 2022. Patterns and drivers of plant diversity across Australia. *Ecography*, 2022(11), p.e06426.44.

Moundounga Mavouroulou, Q., Ngomanda, A., Engone Obiang, N.L., Lebamba, J., Gomat, H., Mankou, G.S., Loumeto, J., Midoko Iponga, D., Kossi Ditsouga, F., Zinga Koumba, R. and Botsika Bobé, K.H., 2014. How to improve allometric equations to estimate forest biomass stocks? Some hints from a central African forest. *Canadian Journal of Forest Research*, 44(7), pp.685-691.

Nassar, M.M. and MacKay, G.D.M., 1984. Mechanism of thermal decomposition of lignin. *Wood and Fiber Science*, pp.441-453.

Natural England (2024). Natural England publishes major new report on carbon storage and sequestration by habitat. Available at: <https://naturalengland.blog.gov.uk> (Accessed: 4 June 2024).

Negi, J. D. S., et al. (2003). Carbon allocation in forest ecosystems: some challenges in understanding the complex system. Springer.

Ngomanda, A., Obiang, N. L. E., Lebamba, J., Mavouroulou, Q. M., Gomat, H., Mankou, G. S., Loumeto, J., Iponga, D. M., Ditsouga, F. K., Koumba, R. Z., Bobé, K. H. B., Okouyi, C. M., Nyangadouma, R., Lépengué, N., Mbatchi, B., & Picard, N. (2014). Site-specific versus pantropical allometric equations: Which option to estimate the biomass of a moist central African forest? *Forest Ecology and Management*, 312, 1–9.

Nowak, D. J., Crane, D. E., Stevens, J. C., Hoehn, R. E., Walton, J. T. & Bond, J. (2008) A ground-based method of assessing urban forest structure and ecosystem services. *Arboriculture and Urban Forestry*, 34(6), 347-358.

Osuri, A.M., Ratnam, J., Varma, V., Alvarez-Loayza, P., Hurtado Astaiza, J., Bradford, M., Fletcher, C., Ndoundou-Hockemba, M., Jansen, P.A., Kenfack, D. and Marshall, A.R., 2016. Contrasting effects of defaunation on aboveground carbon storage across the global tropics. *Nature communications*, 7(1), p.11351.

Pati, P.K., Kaushik, P., Khan, M.L. and Khare, P.K., 2022. Allometric equations for biomass and carbon stock estimation of small diameter woody species from tropical dry deciduous forests: Support to REDD+. *Trees, Forests and People*, 9, p.100289.

Pérez-de-Lis, G., Olano, J.M., Rozas, V., Rossi, S., Vázquez-Ruiz, R.A. and García-González, I., 2017. Environmental conditions and vascular cambium regulate carbon allocation to xylem growth in deciduous oaks. *Functional Ecology*, 31(3), pp.592-603.

Perkovich, C. and Ward, D., 2021. Aboveground herbivory causes belowground changes in twelve oak *Quercus* species: a phylogenetic analysis of root biomass and non-structural carbohydrate storage. *Oikos*, 130(10), pp.1797-1812.

Perkovich, C. and Ward, D., 2021. Herbivore-induced defenses are not under phylogenetic constraints in the genus *Quercus* (oak): Phylogenetic patterns of growth, defense, and storage. *Ecology and Evolution*, 11(10), pp.5187-5203.

- Petrokofsky, G., Kanamaru, H., Achard, F., Goetz, S.J., Joosten, H., Holmgren, P., Lehtonen, A., Menton, M.C., Pullin, A.S. and Wattenbach, M., 2012. Comparison of methods for measuring and assessing carbon stocks and carbon stock changes in terrestrial carbon pools. How do the accuracy and precision of current methods compare? A systematic review protocol. *Environmental Evidence*, 1, pp.1-21.
- Phillips, J., Duque, A., Scott, C., Wayson, C., Galindo, G., Cabrera, E., Chave, J., Pena, M., Alvarez, E., Cardenas, D. and Duivenvoorden, J., 2016. Live aboveground carbon stocks in natural forests of Colombia. *Forest Ecology and Management*, 374, pp.119-128.
- Poorter, H., Niklas, K.J., Reich, P.B., Oleksyn, J., Poot, P. and Mommer, L., 2012. Biomass allocation to leaves, stems and roots: meta-analyses of interspecific variation and environmental control. *New Phytologist*, 193(1), pp.30-50.
- Reef, R. and Gordon, C., 2024. Allometric Equations for Aboveground Biomass Estimation of Temperate Mangroves Using Uncrewed Aerial Vehicles. *Journal of Coastal Research*.
- Rewilding Britain. (2020). New network to spearhead rapid rewilding in Britain. <https://www.rewildingbritain.org.uk/blog/new-network-to-spearhead-rapid-rewilding-across-britain>
- Rosell, J.A., 2016. Bark thickness across the angiosperms: more than just fire. *New Phytologist*, 211(1), pp.90-102.
- RStudio Team (2022). RStudio: Integrated Development for R. RStudio, PBC, Boston, MA.
- Rutishauser, E., Noor'an, F., Laumonier, Y., Halperin, J., Hergoualc'h, K. and Verchot, L., 2013. Generic allometric models including height best estimate forest biomass and carbon stocks in Indonesia. *Forest Ecology and Management*, 307, pp.219-225.
- Ryland, K., 2015. KNEPP CASTLE ESTATE WILDLANDS PROJECT TRANSECT SURVEY 2015. *Constraints*, 2(2).
- Sánchez-Sánchez, H. and Morquecho-Contreras, A., 2017. Chemical plant defense against herbivores. In *Herbivores*. IntechOpen.
- Sandom, C. and Wynne-Jones, S., 2019. Rewilding a country: Britain as a study case. *Rewilding*, pp.222-247.
- Saner, P., Loh, Y.Y., Ong, R.C. and Hector, A., 2012. Carbon stocks and fluxes in tropical lowland dipterocarp rainforests in Sabah, Malaysian Borneo. *PloS one*, 7(1), p.e29642.
- Santantonio, D., Hermann, R.K. and Overton, W.S., 1977. Root biomass studies in forest ecosystems.
- Saranpää, P., 2003. *Wood density and growth. Wood quality and its biological basis*, pp.87-117.
- Schmitz, O.J., Sylvén, M., Atwood, T.B., Bakker, E.S., Berzaghi, F., Brodie, J.F., Cromsigt, J.P., Davies, A.B., Leroux, S.J., Schepers, F.J. and Smith, F.A., 2023. Trophic rewilding can expand natural climate solutions. *Nature Climate Change*, 13(4), pp.324-333.
- Schutz, A.E.N., Bond, W.J. and Cramer, M.D., 2009. Juggling carbon: allocation patterns of a dominant tree in a fire-prone savanna. *Oecologia*, 160, pp.235-246.

- Sitters, J., Kimuyu, D.M., Young, T.P., Claeys, P. and Olde Venterink, H., 2020. Negative effects of cattle on soil carbon and nutrient pools reversed by megaherbivores. *Nature Sustainability*, 3(5), pp.360-366.
- Skarpe, C. and Hester, A.J., 2008. Plant traits, browsing and grazing herbivores, and vegetation dynamics. *Ecological Studies*, 195, p.217.
- Snowdon, P., Raison, J., Keith, H., Montagu, K., Bi, H., Ritson, P., Grierson, P., Adams, M., Burrows, W. and Eamus, D., 2001. Protocol for sampling tree and stand biomass.
- Sobral, M., Silvius, K.M., Overman, H., Oliveira, L.F., Raab, T.K. and Fragoso, J.M., 2017. Mammal diversity influences the carbon cycle through trophic interactions in the Amazon. *Nature ecology & evolution*, 1(11), pp.1670-1676.
- Stephenson, N.L., Das, A.J., Condit, R., Russo, S.E., Baker, P.J., Beckman, N.G., Coomes, D.A., Lines, E.R., Morris, W.K., Rüger, N. and Álvarez, E., 2014. Rate of tree carbon accumulation increases continuously with tree size. *Nature*, 507(7490), pp.90-93.
- Strassburg, B.B., Iribarrem, A., Beyer, H.L., Cordeiro, C.L., Crouzeilles, R., Jakovac, C.C., Braga Junqueira, A., Lacerda, E., Latawiec, A.E., Balmford, A. and Brooks, T.M., 2020. Global priority areas for ecosystem restoration. *Nature*, 586(7831), pp.724-729.
- Tanentzap, A.J. and Coomes, D.A., 2012. Carbon storage in terrestrial ecosystems: do browsing and grazing herbivores matter?. *Biological Reviews*, 87(1), pp.72-94.
- Tanentzap, A.J., Daykin, G., Fennell, T., Hearne, E., Wilkinson, M., Carey, P.D., Woodcock, B.A. and Heard, M.S., 2023. Trade-offs between passive and trophic rewilding for biodiversity and ecosystem functioning. *Biological Conservation*, 281, p.110005.
- Thermo Fisher Scientific, 2023. *FlashSmart Elemental Analyzer: Supporting quantitative elemental analysis in biological samples*. Available at: <https://www.thermofisher.com>.
- Thomas, S.C. and Malczewski, G., 2007. Wood carbon content of tree species in Eastern China: Interspecific variability and the importance of the volatile fraction. *Journal of Environmental Management*, 85(3), pp.659-662.
- Thomas, S.C. and Martin, A.R., 2012. Carbon content of tree tissues: a synthesis. *Forests*, 3(2), pp.332-352.
- Tian, L., Wu, X., Tao, Y., Li, M., Qian, C., Liao, L. and Fu, W., 2023. Review of remote sensing-based methods for forest aboveground biomass estimation: Progress, challenges, and prospects. *Forests*, 14(6), p.1086.
- Timber Development UK (2024). 2024 Embodied Carbon Data for Timber Products. Available at: <https://timberdevelopment.uk> (Accessed: 4 June 2024).
- Tree, I., 2023. *The book of wilding: a practical guide to rewilding, big and small*. Bloomsbury Publishing.
- Ueda, M., & Shibata, H. (2010). Seasonal changes in the carbon dynamics of trees. *Journal of Plant Research*, 123(2), 165-175.

- United Nations (2015). Transforming our world: the 2030 Agenda for Sustainable Development. Available at: <https://sdgs.un.org/2030agenda> (Accessed: 4 June 2024).
- Van der Graaf, A.J., Stahl, J. and Bakker, J.P., 2005. Compensatory growth of *Festuca rubra* after grazing: can migratory herbivores increase their own harvest during staging?. *Functional Ecology*, pp.961-969.
- Van Uytvanck, J., Van Noyen, A., Milotic, T., Declerck, K. and Hoffmann, M., 2010. Woodland regeneration on grazed former arable land: A question of tolerance, defence or protection?. *Journal for Nature Conservation*, 18(3), pp.206-214.
- Verly, O.M., Leite, R.V., da Silva Tavares-Junior, I., da Rocha, S.J.S.S., Leite, H.G., Gleriani, J.M., Rufino, M.P.M.X., de Fatima Silva, V., Torres, C.M.M.E., Plata-Rueda, A. and e Castro, B.M.D.C., 2023. Atlantic forest woody carbon stock estimation for different successional stages using Sentinel-2 data. *Ecological Indicators*, 146, p.109870.
- Villar, N. and Medici, E.P., 2021. Large wild herbivores slow down the rapid decline of plant diversity in a tropical forest biodiversity hotspot. *Journal of Applied Ecology*, 58(11), pp.2361-2370.
- Vorster, A.G., Evangelista, P.H., Stovall, A.E. and Ex, S., 2020. Variability and uncertainty in forest biomass estimates from the tree to landscape scale: the role of allometric equations. *Carbon Balance and Management*, 15, pp.1-20.
- West, G.B., Brown, J.H. and Enquist, B.J., 2001. A general model for ontogenetic growth. *Nature*, 413(6856), pp.628-631.
- Wickham, H. (2016). *ggplot2: Elegant Graphics for Data Analysis*. Springer-Verlag New York.
- Wiley, E., Hoch, G. and Landhäusser, S.M., 2017. Dying piece by piece: carbohydrate dynamics in aspen (*Populus tremuloides*) seedlings under severe carbon stress. *Journal of Experimental Botany*, 68(18), pp.5221-5232.
- Ying, J., Weng, Y., Oswald, B.P. and Zhang, H., 2019. Variation in carbon concentrations and allocations among *Larix olgensis* populations growing in three field environments. *Annals of forest science*, 76, pp.1-14.11. Thomas & Martin, 2012
- Young, B., Liang, J. and Chapin III, F.S., 2011. Effects of species and tree size diversity on recruitment in the Alaskan boreal forest: a geospatial approach. *Forest ecology and management*, 262(8), pp.1608-1617. 28.
- Zar, J.H., 1999. *Biostatistical analysis*. ed. *Princeton-Hall, New Jersey*.
- Zhang, J., Zhang, J., Mattson, K. and Finley, K., 2020. Effect of silviculture on carbon pools during development of a ponderosa pine plantation. *Forests*, 11(9), p.997.
- Zobel, B.J. and Sprague, J.R., 2012. *Juvenile wood in forest trees*. Springer Science & Business Media.

4.7 Supplementary Materials

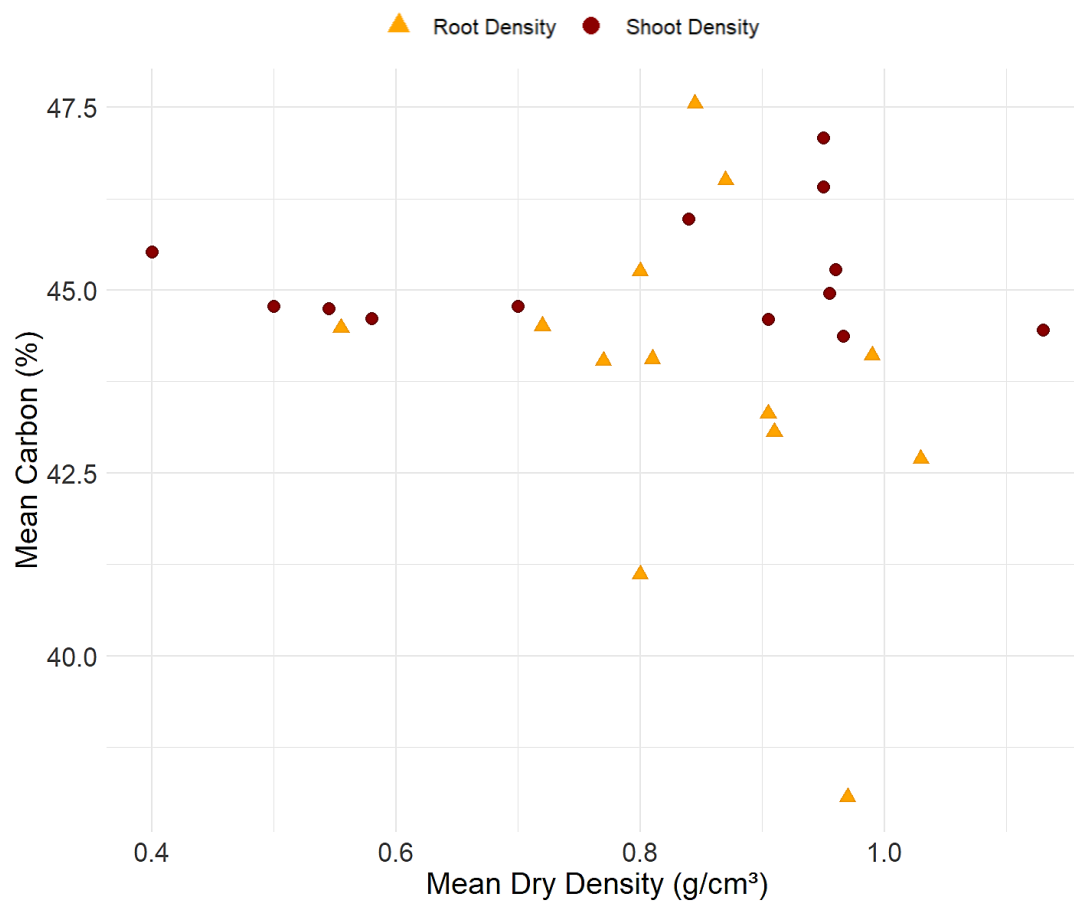


Figure S4.1: relationship between mean carbon content (%) and mean dry density (g/cm^3) for aboveground (shoots) and belowground (roots) biomass. Red circles represent shoot density versus carbon, while orange triangles represent root density versus carbon.

Table S4.1: Linear regression analysis results for the relationships between mean carbon content (%) and mean dry density (g/cm^3) for shoots and roots. The table includes the slope, intercept, R-squared value, p-value, and standard error (s.e.) for each variable pair. Results indicate weak correlations, with no statistically significant relationships at the 0.05 level.

Variable Pair	Slope	Intercept	R-squared	P-value	s.e.
Shoot Density vs Carbon	0.037404719	-0.892017238	0.018715138	0.655845435	0.081664082
Root Density vs Carbon	-0.017147257	1.594410052	0.103285615	0.284288902	0.015233702

Chapter 5: Integrating Structure from Motion and 5-Band Imaging to Estimate Above- and Belowground Biomass in a Rewilded Scrubland Ecosystem

Nancy C. Burrell¹, Katherine J. Willis¹, Marcus Spiegel³, Jeff Kerby², Marc Macias-Fauria²

¹Department of Biology, University of Oxford, Oxford, UK

²Scott Polar Research Institute, Department of Geography, University of Cambridge, Cambridge, UK

³School of Geography and the Environment, University of Oxford, Oxford, UK

Author contribution statement: Nancy C. Burrell led the study's conceptualisation, methodology, data analysis, and drafting, serving as the project lead. Marc Macias-Fauria provided supervision, contributed to the design of the methodology and conceptualisation, supported data collection, and offered feedback and edits on the manuscript. Marcus Spiegel designed the flight path and assisted with conducting the drone missions. Jeff Kerby advised on the generation of a height model and the R GIS code for extracting multispectral imaging. Kathy J. Willis provided supervision and contributed to manuscript editing.

To be submitted for publication.

5.0 Abstract

Scrublands are undervalued in carbon accounting due to the lack of scalable tools for estimating their biomass and carbon storage potential. This study addresses this gap by integrating UAV RGB-based photogrammetry with a Structure-from-Motion workflow and multispectral imaging with taxon- and condition-specific allometric equations. Conducted at the Knepp Wildland Estate, this research aims to demonstrate the potential for using this approach to estimate aboveground and belowground biomass for five dominant scrub taxa across a 13-hectare plot. Results demonstrated that Structure-from-Motion derived metrics such as canopy height and canopy area correlated strongly with field measurements, while spectral data improved taxonomic classification. Combined with scrub-specific allometric models, these methods therefore have the potential to yield accurate estimates of total biomass and carbon storage, remotely valuing the nascent rewilded scrublands in terms of carbon storage. By establishing a scalable, non-destructive framework for biomass modelling at a landscape scale, this novel approach enables for the first time scrublands to be properly valued alongside woodlands in global carbon accounting and ecosystem service assessments.

Key words: Structure-from-Motion, multispectral imaging, allometry, carbon stock, rewilding, scrubland taxa

5.1 Introduction

Accurate forest and woodland biomass estimation plays a pivotal role in understanding key ecological processes, including carbon sequestration (Chapin et al., 2006; Pan et al., 2011; Saatchi et al., 2015), habitats for biodiversity (Parmenter & MacMahon, 1983; Chave et al., 2014; Poorter et al., 2015), and the provision of other ecosystem services (Jankju, 2013; Ballantyne & Pickering, 2015; Bastin et al., 2019; Sullivan et al., 2017). Measuring scrub biomass is critical to monitor rewilding's scrubland productivity (Chai et al., 2021; Gomez-Aparicio et al., 2004) and is therefore vital for assessing its ecological functions and evaluating its ecosystem carbon storage (Yu et al., 2010; Fonseca & Bompastor Ramos., 2012; Catchpole & Wheeler, 1992).

Scrub creation through rewilding is thought to have significant potential to contribute to global carbon storage (Kaštovská et al., 2024; Cerqueira et al., 2015; Schmitz et al., 2023). Scrublands cover approximately 13% of the world's terrestrial surface, representing a substantial portion of global biomass, especially in comparison to forests (31%) and plantation woodlands (3%) (FAO, 2020). However, unlike forests and woodlands, there is currently a lack of reliable tools to estimate scrubland biomass at larger scales (Chai et al., 2021; Liu et al., 2024). Moreover, existing carbon flux data for these successional habitats, such as scrub and scattered forests, are not yet of sufficient quality to be included in Greenhouse Gas inventories or other net zero pathways (Mercer & Gregg, 2023). Addressing this gap requires the development of advanced methodologies that account for the complexity of scrubland ecosystems in terms of their shape and scale.

Moreover, with the urgency of meeting the 1.5°C pathway outlined in the Paris Agreement (IPCC, 2022; Friedlingstein et al., 2022), monitoring underrepresented ecosystems like scrublands could play a crucial role. In addition, developing scalable solutions for these ecosystems is essential to ensure scientifically robust monitoring of rewilding projects, enabling environmental targets established at the project's outset, to align with evolving social-ecological goals (to Bühne et al., 2022).

Although localised advances in biomass estimations have been made through improved allometric equations (see Chapter 3), scaling these efforts to capture landscape-level biomass and carbon storage remains a challenge (to Buhne et al., 2022; Pettorelli et al., 2018; Torres et al., 2018). Traditional field-based methods for biomass estimation, such as measuring diameter at breast height (dbh), canopy area and plant height, are labour-intensive and have been shown to face serious challenges when used to estimate landscape-scale biomass, especially in scrubland ecosystems where vegetation structures are highly variable (to Buhne et al., 2022; Brown, 2002; Wulder et al., 2008; Burrell et al., 2024; Maraseni et al., 2005) (see also chapter 2 and 3). This is because, unlike plantation forests where trees have predictable morphologies, scrublands consist of dense, often thorny, and impenetrable vegetation, complicating direct measurements (Perkovich & Ward, 2022; Salek et al., 2019). These complexities and heterogeneity, along with fluctuating environmental conditions, make traditional methods impractical for capturing biomass distribution (Laliberte et al., 2004; Liu et al., 2024).

In rewilded scrubland ecosystems, the challenge is further amplified by the browsing activity of large herbivores which significantly alters vegetation structure and biomass allocation (Perkovich & Ward, 2022; Burrell et al., 2024). Herbivory leads to irregular growth patterns

and non-uniform biomass distribution, factors that traditional allometric models often fail to account for (Vesk & Westoby, 2001; Pringle et al., 2014).

To address the limitations of conventional field surveys, many previous studies have demonstrated that remote sensing can provide an opportunity to scale allometric models to landscape levels (Roy & Ravan, 1996; Liu et al., 2024). In particular it has been shown that spatially continuous observations at landscape scales and beyond, can enable the capture of the structural diversity of scrub ecosystems (Siewert & Olofsson, 2021; Liu et al., 2024). For example, satellite remote sensing has been widely used to track shrub cover (Fraser et al., 2016; Ju & Masek, 2016; McManus et al., 2012; Pastick et al., 2018), disturbance dynamics (Chuvieco et al., 2020), primary productivity (Juntilla et al., 2021) and even vegetation shifts over time within a rewilding project (to Buhn et al., 2022). However, these observations are often at a coarse resolution (30-500 m pixel size), making it difficult to assess the heterogeneity (Pettorelli & Schulte to Buhne, 2023; Alonzo et al., 2020; Zandler et al., 2015b; Fraser et al., 2016) and the impact of browsing required for biomass modelling at the scrub level.

Recent technological advances in unmanned aerial vehicles (UAVs) present a promising solution for biomass estimation, offering flexible, cost-effective platforms for monitoring vegetation structure. Light Detection and Ranging (LiDAR) has long been recognised as a robust tool for quantifying vegetation structure and biomass, especially for capturing highly accurate 3D information across large areas (Goetz & Dubayah, 2011; Greaves et al., 2015). LiDAR's ability to penetrate dense canopy cover makes it particularly useful in forested environments, providing detailed insights into tree height, canopy structure, and vegetation density (Zolkos et al., 2013). However, the historically high cost and limited accessibility of LiDAR systems constrain their widespread use (Trier et al., 2018; Tóth & Józskóv, 2016).

Structure-from-Motion (SfM) photogrammetry combined with UAV-based multispectral imagery has emerged as a cost-effective alternative to LiDAR for mapping vegetation structure. SfM generates detailed 3D models at a fraction of LiDAR's cost by using overlapping images captured from multiple angles (Dandois & Ellis, 2013). This technique is particularly effective for estimating aboveground biomass in scrublands, capturing the structural complexity needed to model taxa- and condition-specific factors, such as exposure to herbivory (Assmann et al., 2020; Siewert & Olofsson, 2020). UAVs equipped with consumer-grade cameras enable high image overlap and centimetre-scale resolution when flown at low altitudes, providing accurate biomass estimates comparable to LiDAR in open environments (Thomson et al., 2021; Cunliffe et al., 2016).

Recent studies show minimal accuracy differences between biomass estimates from SfM and LiDAR, with SfM sometimes producing denser point clouds (up to 10 times) than LiDAR (Alonzo et al., 2020; Cunliffe et al., 2020; Fraser et al., 2016). While SfM struggles in tall and closed canopy areas due to limited canopy penetration, recent studies have demonstrated that it excels in open scrub environments where it can accurately detect smaller scrub species (Juan-Ovejero et al., 2023; Alonzo et al., 2020). These smaller species contribute more to carbon storage than previously estimated, due to higher root:shoot ratios (Chapter 2; Chapter 3; Burrell et al., 2024).

To date, SfM photogrammetry combined with multi-band imagery has been effectively used in several studies to estimate biomass. For example, Dandois & Ellis (2013) applied this method in temperate forests, achieving high-resolution 3D models of vegetation structure and biomass. Their results demonstrated that SfM captured fine-scale variations in canopy structure, with biomass estimates showing strong correlations with field measurements,

particularly in open environments where vegetation was less dense. Similarly, Puliti et al. (2020) applied SfM in boreal forests to enhance biomass model precision. Their study combined UAV-based SfM data with multispectral imagery and random forest models to improve species-specific biomass estimates. The combination of spectral and structural data significantly increased the accuracy of biomass predictions compared to traditional models based solely on LiDAR or field data. These approaches not only improve workflow efficiency by allowing larger sample sizes to be gathered at lower costs compared to traditional field-based methods (Dandois & Ellis, 2013; Cunliffe et al., 2016) but also enhance species profiling through machine learning techniques such as random forest classification (Puliti et al., 2020). Moreover, these methods allow more precise scaling of biomass estimates from ground-based measurements and allometric equations to larger landscapes (Liu et al., 2024).

The overarching aims of this study were two-fold. First, building on these previous studies, to use Structure-from-Motion (SfM) photogrammetry combined with multispectral imagery for classifying scrub at the taxon level and estimating aboveground biomass. Second, using outputs from chapter 3 and 4, combined with the SfM results, to remotely quantify the above- and below-ground carbon storage capacity of scrub vegetation within the study area.

In this study, I applied taxa- and condition-specific allometric equations for above- and belowground biomass from Chapter 3, along with scrub-specific carbon content values from Chapter 4 to a SfM model that estimates both above- and belowground biomass. I used 5-band multispectral data to develop taxa-specific spectral signatures, enabling canopy identification at the taxa level within the model.

5.2 Materials and methods

5.2.1. Study site

The research was conducted within a 13-hectare study plot in the "Southern Block" of the Knepp rewilding estate, West Sussex, UK (50.975781°N, 0.344819°W) (Figure 5.1). This study plot was randomly selected from three designated sub-areas (Plots 1-3), each representing diverse land cover types to best reflect the variety found across the rewilding estate. Plot 1 was chosen using the 'sample' function in R (R Core Team, 2024) and is the same location where destructive sampling of scrub was conducted in Chapters 3 and 4.

Vegetation within the study plot is classified as open wood pasture, with regenerating scrub species such as blackthorn (*Prunus spinosa*), willow (*Salix* spp.), oak (*Quercus* spp. both *Quercus robur* and *Quercus petraea*), hawthorn (*Crataegus* spp. both *Crataegus monogyna* and *Crataegus laevigata*), dog rose (*Rosa canina*), and bramble (*Rubus fruticosus*) (Tree, 2018; to Bühne et al., 2022). Canopy coverage varies, featuring dense patches of willow (*Salix* spp.) and blackthorn (*Prunus spinosa*) interspersed with mixed open scrub and bramble (*Rubus fruticosus*; see Chapter 2 for detailed land cover classifications).

The study plot has been exposed to herbivory since 2009, following an eight-year fallow period after the Knepp rewilding estate's transition from conventional arable and dairy farming (Tree, 2018). Large herbivores, including old English longhorn cattle (*Bos primigenius taurus*), Exmoor ponies (*Equus ferus caballus*), fallow deer (*Dama dama*), and Tamworth pigs (*Sus scrofa domesticus*), were introduced to help stimulate vegetation. Prior to this, only small numbers of rabbits (*Oryctolagus cuniculus*) and roe deer (*Capreolus capreolus*) inhabited the area, allowing woody shrubs and saplings to establish and develop defences. Red deer (*Cervus*

elaphus) were introduced in 2013 when the scrubland was deemed robust enough to sustain additional heavy browsers (Tree, 2018).

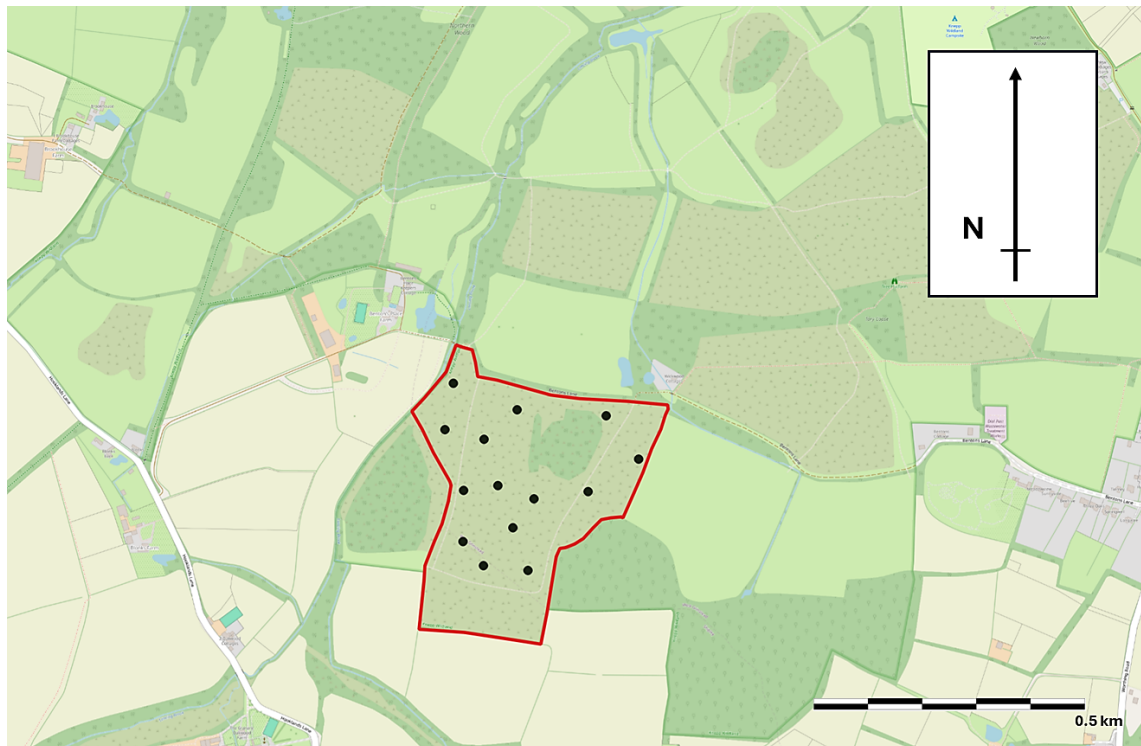


Figure 5.1: Study site 3 (red line) within the Southern Block of Knepp Wildland (50.975781°N, 0.344819°W). Black dots represent the 14 ground control points (GCPs) used for georeferencing.

5.2.2 UAV surveys

5.2.2.1 RGB very high-resolution mapping for Structure-from-Motion

On 9th February 2022, I conducted a very high-resolution UAV mapping survey to derive a precise 3D reconstruction of the vegetation using Structure-from-Motion (SfM) photogrammetry (Table 5.1). A DJI Mavic 2 Pro (DJI, Shenzhen, China) quadcopter with a 20 MP RGB camera was used, and flights were planned with the DJI Ground Station Pro app. The mission was flown twice—once for nadir imagery and once at a 20-degree angle following Cunliffe et al. (2020). The UAV flew at a nominal altitude of 50 m with 75% image overlap,

capturing images at ~1 cm ground resolution. The "Capture Mode" was set to hover and capture at each waypoint for sharper images.

5.2.2.2 multispectral 5-band camera

Six flights were conducted monthly from February to July 2022 using a MicaSense RedEdge-MX 5-band multispectral camera (AgEagle Aerial Systems Inc., Wichita, KS, USA) to monitor phenological changes in scrub vegetation over a six-month timeframe. Adopting a methodology similar to that outlined by Assmann et al. (2018), this system integrates a five-band camera capable of capturing reflectance data across multiple spectral wavelengths. The RedEdge-MX camera features a durable metallic casing and records images in five specific spectral bands: red (668 nm centre, 14 nm bandwidth), green (560 nm centre, 27 nm bandwidth), blue (475 nm centre, 32 nm bandwidth), red edge (717 nm centre, 12 nm bandwidth), and near-infrared (NIR) (842 nm centre, 57 nm bandwidth). The flights were conducted at a nominal altitude of 80 metres.

A 10 × 10 cm calibration reflectance panel (CRP) was used for radiometric calibration before and after each flight. The CRP, pre-calibrated by MicaSense (MicaSense, 2023), has a uniform reflectance of approximately 50% across the five RedEdge-MX spectral bands. Photos of the CRP were taken from 1 metre above the panel to ensure accurate calibration. The CRP, with an embedded barcode, was automatically recognised during image processing in Agisoft Metashape (v2.2.0), streamlining the reflectance correction process. Additionally, the camera was equipped with a Downwelling Light Sensor (DLS), mounted on the top of the UAV and oriented toward the sky. The DLS records ambient light conditions during the flight, which is critical for adjusting the imagery based on changes in lighting conditions throughout the mission (Iqbal et al., 2018).

In all flights (RGB and multispectral), we placed fourteen 60 cm x 60 cm ground control markers at key locations (Figure 5.1), distributed evenly across the study site, which were visible from the UAV to aid in photogrammetric modelling. These markers were precisely geolocated using an RTK-GNSS survey instrument (Emlid Reach+, Emlid, Hong Kong) with centimetre-level accuracy.

5.2.3. Imagery processing

5.2.3.1 Structure-from-Motion

The RGB UAV imagery was processed using Agisoft Metashape Professional (v.2.2.0) with a structure-from-motion (SfM) workflow, as outlined by Over et al. (2021). All images from nadir and oblique flights were imported and georeferenced to the WGS84 UTM 30N. The photo alignment, set to the highest quality with a 60,000 key point limit and unlimited tie points, resulted in sparse point clouds of over 2.1 million tie points per survey. To ensure only high-quality images were used for further processing, an image quality estimation was performed. Images with a quality index below 0.6 were disabled to maintain high processing standards. The "Align Photos" tool was used for photo alignment, and when alignment issues occurred, the key point and tie point limits were adjusted to improve accuracy.

Ground control points (GCPs) were integrated for georeferencing and to minimise errors, followed by bundle adjustment for camera model optimisation (Over et al., 2021). GCP accuracy was set to 0.02 m for latitude and longitude, and 0.5 m for altitude. Markers were placed manually on the images, with corrections made to any misaligned points. Marker location accuracy was set at 0.02 m to reflect GNSS uncertainties, while marker projection and tie point accuracy were initially 0.5 pixels and 1 pixel, respectively. Low-quality tie points

were removed iteratively based on reconstruction uncertainty and reprojection error, refining camera parameters like focal length, principal point, and lens distortions. Post-optimisation, all surveys had unweighted reprojection errors under 0.21 pixels, an ideal threshold (Over et al., 2021). Depth maps were then generated, and dense point clouds were created using high-quality settings and mild depth filtering.

After GCP integration, camera optimization was performed to adjust camera parameters, including focal length and lens distortions, improving alignment accuracy. A dense point cloud was then generated using the "Build Dense Point Cloud" tool with high quality and aggressive depth filtering. Iterative cleaning was conducted to remove erroneous points that could negatively impact the Digital Elevation Model (DEM). Following the generation of the dense point cloud, a high-resolution Digital Surface Model (DSM) was created through the "Build DEM" function, that represented the contiguous surface of the resulting model (Over et al., 2021).

5.2.3.2 Multispectral orthomosaics

One orthomosaic was generated for each reflectance band from the 5 monthly flights done with the 5-band MicaSense RedEdge-MX camera. Here, I followed the protocol outlined by Wang et al., (2021), which is the same as for the RGB image processing (section 5.2.3.2) with the addition of the next steps: reflectance calibration was conducted using reflectance panels, and data from the RedEdge-MX's Downwelling Light Sensor (DLS) was integrated to account for varying light conditions during flight. Orthomosaics were generated from all five multispectral flights conducted between February and July 2022 (Table 5.1), providing detailed 2D models suitable for taxon identification through spectral analysis.

Table 5.1: Description of drone surveys and their photogrammetric models. The February survey included a dual-flight approach with a multispectral survey, capturing both nadir and oblique (20° from nadir) imagery. All other flights followed a standardised mission plan with set waypoints, though launch point variations led to slight differences in altitude and resolution. Automated camera triggering occasionally caused minor inconsistencies in image count. Each survey includes details on camera type, ground resolution, point density, total images, dense point cloud size, and RMS reprojection error.

Date	Camera type	no. of images	Ground resolution (cm/pixel)	point density (points/m ²)	no.dense point cloud	RMS reprojection error
09/02/2022	5-band	7910	5.36	86.9	23,852,487	0.172178
09/02/2022	RGB	1742	1.13	1950	495,046,992	0.145828
15/03/2022	5-band	10290	5.36	87	24,115,604	0.180036
05/03/2022	5-band	10955	5.41	85.4	22,046,804	0.190643
20/05/2022	5-band	10230	5.37	86.7	26,580,382	0.202987
15/06/2022	5-band	10320	5.52	82.2	26,935,507	0.192866
07/07/2022	5-band	10580	5.58	80.4	26,937,863	0.190613

5.2.4. Canopy features from SfM

We developed a biomass estimation model by extracting the variables - canopy area (cm²) and canopy height (cm) from the Structure-from-Motion (SfM) model described above.

5.2.4.1. Canopy height

A canopy height model (CHM) was calculated by first classifying ground points in the dense point cloud and then interpolating a surface model from these points to produce a digital terrain model (DTM). Both the DTM and DSM were exported as GeoTIFF files for further analysis.

In R (R Core Team, Version 4.4.1., 2024) using RStudio (v2024.09.), the DSM and DTM were used to calculate surface heights for scrub canopies. The difference between these two models

was computed to estimate canopy height, using the 'terra' package to subtract the DTM from the DSM (Wimberley., 2023).

5.2.4.2. Canopy area

Canopy areas were delineated using the Geo-SAM plugin in QGIS, which integrates the Segment Anything Model (SAM) (Zhao et al., 2023). The general workflow includes running an image encoder to identify all potential features within the image, and then using an interactive segmentation graphical user interface to guide individual segmentation of tree canopies (Zhao et al., 2023). Approximately 7,000 individual scrub canopies were identified across the study site, although resolution limitations meant that some smaller canopies were not captured. In this study, "scrub" refers to dense, shrubby vegetation with multiple woody stems and low to moderate height, often comprising native species adapted to harsh conditions and contributing to habitat complexity in open landscapes (Harden, 1990).

In areas with dense vegetation where canopies are difficult to distinguish from one another in drone imagery, ground-truthing was employed to refine canopy area estimates, particularly for species like blackthorn (*Prunus spinosa*), where manual trunk counts helped overcome limitations of the polygon-based tool. This hybrid approach provided a more comprehensive biomass estimate (Kirillov et al., 2023; Li et al., 2024).

5.2.4.3. Browsing protection

In the allometric model described in Chapter 3, bramble (*Rubus fruticosus*) cover was used as a proxy for browsing protection, with trees categorised as either protected (within bramble) or exposed (outside bramble cover). Bramble coverage was mapped using a supervised random forest classification in ArcGIS Pro (Esri, 2024), where training points for "bramble"

and “no bramble” classes were derived from an RGB drone orthomosaic of the study plot taken in February 2022 (Figure 5.2B).

To improve classification accuracy, the resulting bramble map was generalised by upscaling the data to a coarser resolution (e.g., 10 cm) to focus on substantial bramble patches, removing small, misclassified areas and conservatively biasing toward larger bramble clusters (Esri, 2024). The final output was a binary raster where areas covered by bramble were assigned a value of 1, while non-bramble areas received a value of 0. This binary classification allowed for automated identification of trees as either protected or exposed based on their proximity to bramble patches.

5.2.4.4. Data extraction

RStudio (v2024.09) was used for extracting raster values associated with segmented tree canopy polygons. The analysis relied on the ‘terra’ (Hijmans, 2020) and ‘exactextractr’ (Baston, 2021) packages to handle spatial data and extract the relevant metrics from the raster layers. First, canopy polygons were merged from two shapefiles using `vect()` and reprojected to a WGS84 UTM 30N coordinate reference system (CRS) to facilitate area measurements. The bramble shapefile was similarly processed and intersected with the canopy polygons to classify trees as “protected” or “exposed” based on proximity to bramble (*Rubus fruticosus*). This classification was achieved using the `intersect()` function, and the results were stored as binary values (1 for touching bramble, 0 for not) (Figure 5.2B). I then loaded the Canopy Height Model (CHM) raster into R (RStudio, v2024.09), ensuring it was also properly projected in WGS 84 UTM 30N. The maximum canopy height for each polygon was extracted using the `extract()` function from the raster package (Hijmans, 2018) (Figure 5.2A).

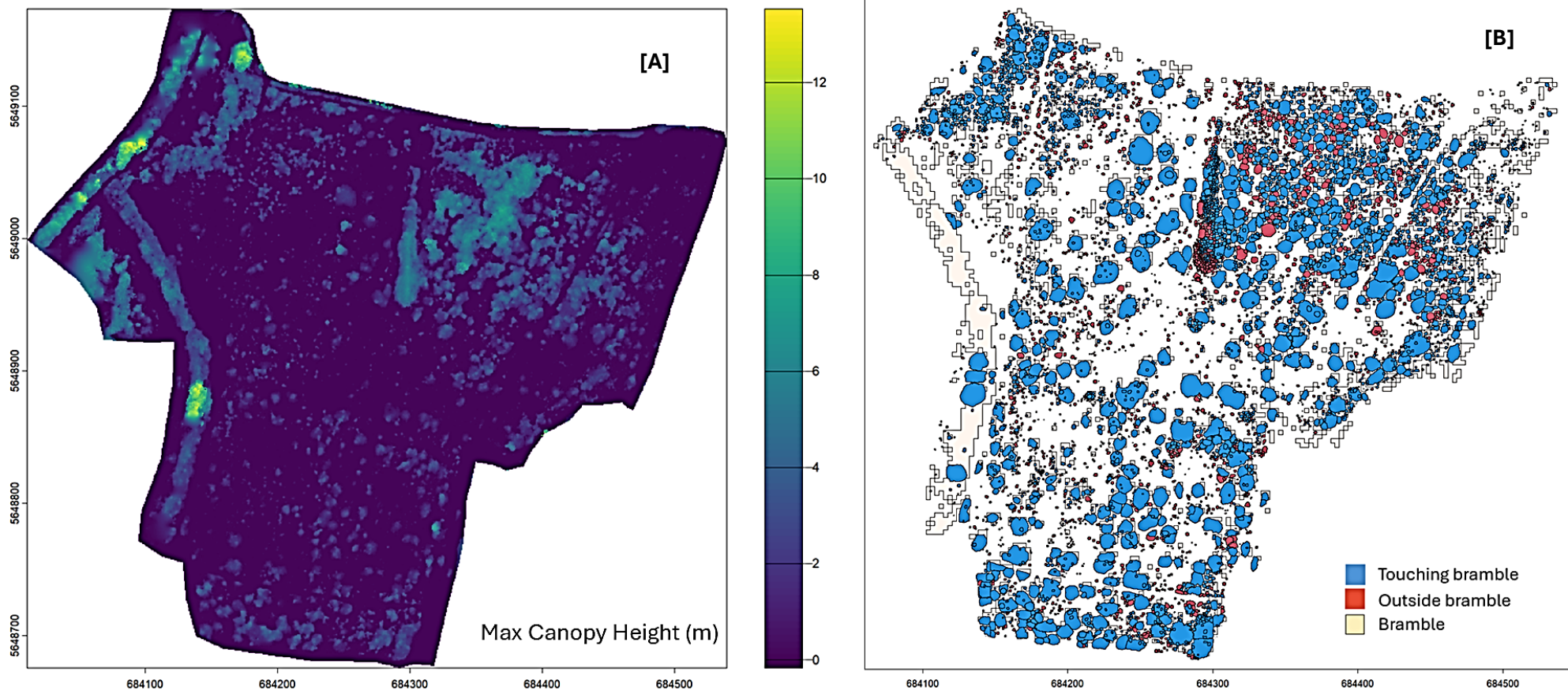


Figure 5.2: Spatial distribution of vegetation characteristics within the study area. Panel A shows the maximum canopy height (m) derived from SfM data, with taller canopies highlighted in brighter colours. Panel B visualises the spatial arrangement of canopy interactions, categorising areas as "touching bramble" (blue), "outside bramble" (red), and "bramble" (yellow).

5.2.5 Taxonomic classification of scrubland taxa from multispectral orthomosaics

The spectral composition for each canopy was calculated by extracting key statistical metrics—mean, standard deviation, median, skewness, and kurtosis—for each spectral band within the canopy polygons from each of the 5-Band monthly (Feb – Jul) multispectral orthomosaics. These metrics provided insights into seasonal changes within the canopy (Lausch et al., 2016; Ustin et al., 2009). The mean and standard deviation captured average reflectance and variability, while the median offered a robust measure less affected by outliers (Fassnacht et al., 2016). Skewness and kurtosis were used to assess the asymmetry and peakedness of the reflectance distributions, potentially revealing uneven growth in the canopy (Komsta and Novomestky, 2015; Jones and Vaughan, 2010; Asner and Vitousek, 2005). I used a combination of packages including “dplyr” (Wickham et al., 2020), “xgboost” (Chen & Guestrin, 2016), “caret” (Kuhn, 2008), and “moments” (Komsta and Novomestky, 2015). Below is a detailed description of the steps used in the analysis:

The dataset was divided into training and testing sets using a 70:30 random split, facilitated by the “caret” package (Kuhn, 2008). This split ensures that the model is evaluated on a separate portion of the data that it has not seen during training, improving the robustness of the performance metrics (Kuhn, 2013; Hastie, 2009). An XGBoost model was then trained using the XGBoost package (Chen & Guestrin, 2016). The model predicts the taxa based on various spectral band features from ground-truthed canopies across five taxa – oak (*Quercus* spp.) (n = 29), blackthorn (*Prunus spinosa*) (n = 27), hawthorn (*Crataegus monogyna*) (n = 38), willow (*Salix* spp.) (n = 31), dog rose (*Rosa canina*) (n = 27), and bramble (*Rubus fruticosus*) (n = 31). XGBoost was selected over other algorithms due to its higher predictive accuracy of tree species compared to other algorithms (Los et al., 2021).

The XGBoost model calculates the importance of each feature in determining the taxa using the “xgb.importance” function. This information is valuable for understanding which variables have the most influence on the model's predictions (Chen & Guestrin, 2016). The most important features are visualised using the xgb.plot.importance function from the same package. This step helps identify which spectral bands and canopy characteristics are most relevant to the classification task. Model performance is evaluated using accuracy metrics and a confusion matrix generated with the caret package (Kuhn, 2008). The top 20 variables identified from the feature importance analysis were selected for further use in the classification of taxa (presented in the Results section, Figure 5.4). The log loss metric and taxa-specific error rates were recorded for further performance evaluation.

5.2.6. Estimating carbon and biomass from allometric equations

I employed the log-linear allometric equations developed in Chapter 3, widely used in forestry and ecology to estimate carbon stocks (Chave et al., 2005) where biomass (W)—aboveground, belowground, or total—is modelled as a function of height (h), diameter at breast height (dbh), and canopy area (A), with coefficients (β) derived through regression analysis (Zianis and Mencuccini, 2004).

A condition variable (x_c) adjusted the intercept for browsing exposure, enabling a single model to account for both exposed and protected conditions. Stepwise selection was applied to a maximum model $\log(W) \sim x_c * \log(h) * \log(A) * \log(dbh)$ to identify the most relevant terms. The best-performing equations, determined using Akaike Information Criterion (AIC, Jones et al., 2022), were tailored to taxa and biomass type. Since (dbh) could not be estimated with

our UAV flight data (Lee et al., 2016), height and canopy area were used as predictors. The structure of the maximum model is as follows:

$$\log(W)=\beta_0+\beta_1 \cdot x_c+\beta_2 \cdot \log(h)+\beta_3 \cdot \log(A)+\beta_4 \cdot (x_c \cdot \log(h))+\beta_5 \cdot (x_c \cdot \log(A))+\beta_6 \cdot (\log(h) \cdot \log(A))+\beta_7 \cdot (x_c \cdot \log(h) \cdot \log(A))$$

[1]

where x_c is a binary term representing the browsing condition (0 for exposed, 1 for protected).

In this model:

- β_0 is the intercept.
- β_1 adjusts for differences between exposed and protected environments, adding to β_0 for the protected condition.
- β_2 and β_3 represent the main effects of height (h) and canopy area (A), respectively.
- β_4 and β_5 capture interactions between condition (x_c) and each predictor (h and A).
- β_6 represents the pairwise interactions between height (h) and canopy area (A).
- β_7 captures three-way interaction involving condition (x_c), height (h) and canopy area (A).

In exponential terms, *Equation [1]* can be represented separately for exposed and protected conditions:

Exposed (where $x_c = 0$):

$$W = e^{\beta_0} \cdot h^{\beta_2} \cdot A^{\beta_3} \cdot (h \cdot A)^{\beta_6}$$

[2]

Protected (where $x_c = 1$):

$$W = e^{B_0+B_1} \cdot h^{B_2+B_4} \cdot A^{B_3+B_5} \cdot (h \cdot A)^{B_6+B_7}$$

[3]

I developed these equations using R software (R Core Team, 2024), employing the "caret" package for data partitioning and the "lm()" function for model fitting. Model refinement, based on AIC, was performed with the "step()" function across all biomass types for each taxon, using the maximum equation [1] as the starting point (Table S5.1). Model performance was evaluated using the coefficient of determination (R^2) and residual sum of squares (RSS), with selection based on the lowest AIC value.

The allometric equations were applied to the scrub polygons identified in the Structure-from-Motion (SfM) model to estimate biomass across the study area. Biomass was converted to carbon content using scrub-specific carbon percentages: 44% for aboveground biomass (AGB) and 43% for belowground biomass (BGB). These percentages were applied to the estimated dry weight generated by the allometric equations and were derived from elemental analysis via dry combustion on a subset of scrub trees, as detailed in Chapter 4.

5.3 Results

5.3.1. Extracting predictor variables from the SfM model

The destructive samples ($n = 270$) had a mean canopy area of 17.24 cm² (median: 6.13 cm²), with a standard deviation of 26.85 cm², a minimum value of 4.52 cm², and a maximum of 162.11 cm² (Figure 5.6A). The predicted canopy area for the whole 13-hectare area had a mean

of 73.10 cm² (median: 22.50 cm²), with a standard deviation of 192.43 cm², a minimum of 100 cm², and a maximum of 2,788.41 cm² (Figure 5.6B).

For height, the destructive samples had a mean of 173 cm (median: 117 cm), a standard deviation of 141 cm, with a minimum of 20.5 cm and a maximum of 740 cm (Figure 5.6C). The predicted height for the whole 14-hectare area had a mean of 226 cm (median: 201 cm), a standard deviation of 160 cm, a minimum of 20.0 cm, and a maximum of 1,335 cm (Figure 5.6D). The abundance distributions for canopy area and height in the destructive field samples and UAV-predicted datasets reveal notable similarities, despite differences in scale and sampling intensity (Figure 5.6A – 6D). Both datasets show right-skewed distributions, with a predominance of smaller canopy areas and shorter heights across samples.

5.3.2. Taxonomic classification of scrub from multispectral orthomosaics

5.3.2.1 Model Performance

The confusion matrix summarises the classification performance of the XGBoost model across six taxa: blackthorn, bramble, dog rose, hawthorn, oak, and willow (Figure 5.3). The overall accuracy of the model was 58.49%, with a 95% confidence interval of (44.13%, 71.86%). The Kappa statistic was 0.5, indicating moderate agreement between predicted and actual classifications. The No Information Rate (NIR), is a baseline measure that represents the accuracy a model would achieve by randomly guessing or by always predicting the most frequent class in the dataset (Kuhn., 2013). In this case, the NIR is 20.75% meaning that my model performed significantly better than the NIR, with a P-value < 0.001, indicating that its accuracy was highly unlikely to be due to random chance and demonstrates meaningful

predictive power. Bramble had the highest sensitivity (proportion of correctly identified samples for each taxon; 0.90) and balanced accuracy (0.88), indicating strong performance for this taxon (Table 5.2). Blackthorn and dog rose had the lowest sensitivity scores (both 0.38). Sallow had a balanced accuracy of 0.73 and comparable sensitivity and specificity (proportion of correctly identified non-samples for each taxon) values. Hawthorn and oak exhibited balanced accuracy (the average of sensitivity and specificity for each taxon) scores above 0.78, reflecting reliable classification performance. The XGBoost model canopy ID estimates for the scrub taxa are displayed in Figure 5.5.

Table 5.2: Class-wise statistics derived from the confusion matrix for the XGBoost model, showing the performance metrics for each taxon (blackthorn, bramble, dog rose, hawthorn, oak, and sallow). The evaluated metrics: Sensitivity (proportion of correctly identified samples for each taxon), Specificity (proportion of correctly identified non-samples for each taxon), Positive Predictive Value (precision of predictions for each taxon), Negative Predictive Value (proportion of correctly excluded samples), and Balanced Accuracy (the average of Sensitivity and Specificity for each taxon).

Statistic	Blackthorn	Bramble	Dog rose	Hawthorn	Oak	Sallow
Sensitivity	0.38	0.89	0.38	0.64	0.63	0.56
Specificity	0.93	0.86	0.91	0.93	0.96	0.91
Pos Pred Value	0.50	0.57	0.43	0.70	0.71	0.56
Neg Pred Value	0.89	0.97	0.89	0.91	0.93	0.91
Balanced Accuracy	0.65	0.88	0.64	0.78	0.79	0.73

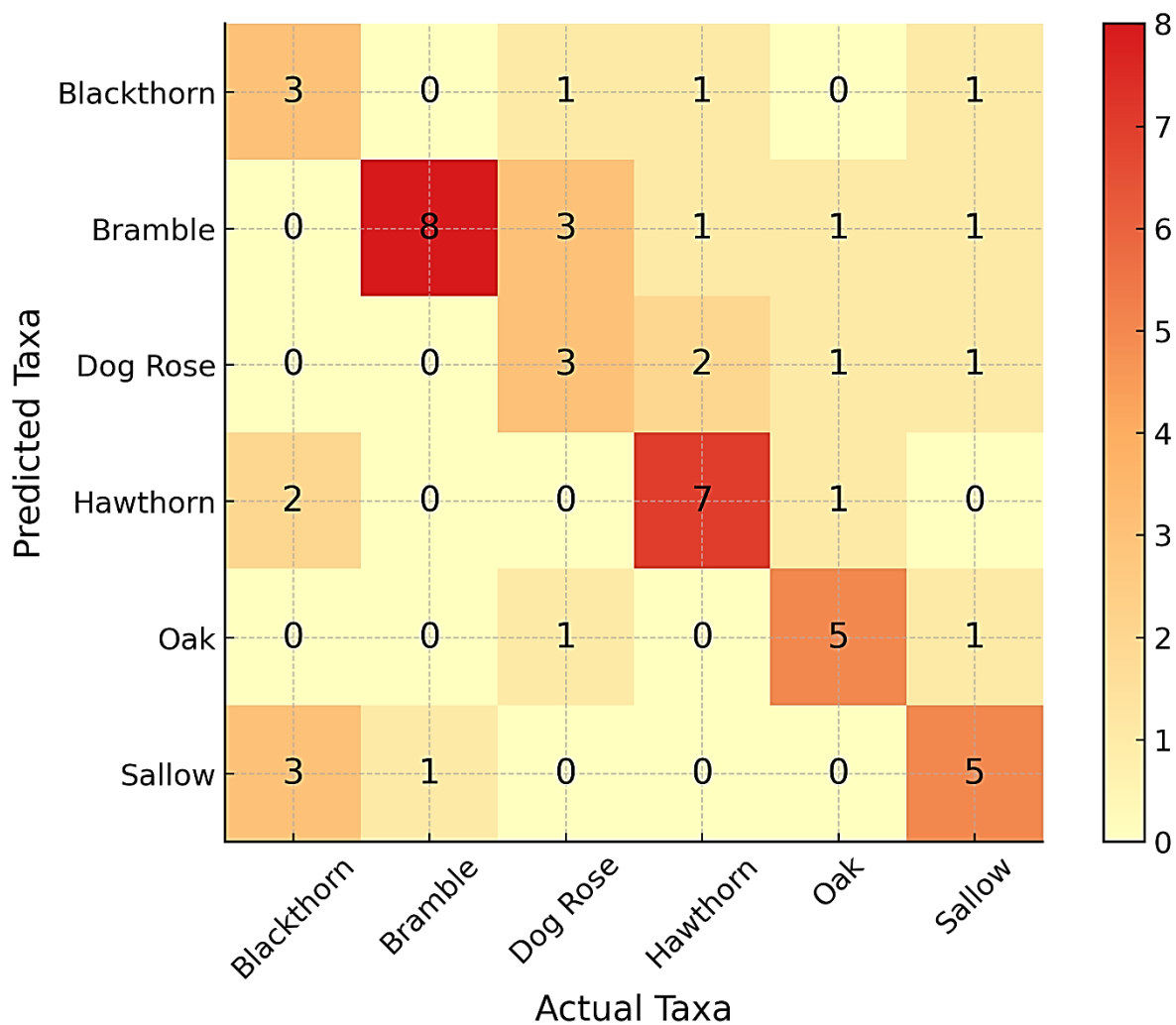


Figure 5.3: Confusion matrix illustrating the classification performance of the XGBoost model for six taxa: blackthorn, bramble, dog rose, hawthorn, oak, and willow. The rows represent the predicted taxa, and the columns represent the actual taxa. Diagonal cells indicate correct classifications, while off-diagonal cells represent misclassifications. The colour intensity corresponds to the number of samples, with darker shades (red) indicating higher counts. The heatmap represents the 30% evaluation dataset, separated from the training data using a 70:30 random split.

5.3.2.2 Covariate Importance Analysis

The feature June sd 5 had the highest Gain value (the relative contribution of the feature to improving the model's accuracy) of 0.056, making it the most important predictor in the model

(Table 5.3, Figure 5.4). This was followed by May sd 5 (Gain = 0.040) and July sd 5 (Gain = 0.038), ranking second and third, respectively. The fourth most important feature was May sd 5.4 (Gain = 0.036). The standard deviation (sd) metric appeared in 15 of the top 20 features (Table 5.3). Features based on the mean metric, such as Feb mean 2 and May mean 5, were less common. Median metrics appeared only twice, in April median 2 and April median 4 (Figure 5.4). Notably, features related to skewness and kurtosis were absent from the top 20 features, indicating they did not significantly contribute to the model's predictive performance.

Features from the months of June, May, and July dominated the list, while features from February, March, and April were present but had lower Gain values (Table 5.3). Band 5 was the most frequently represented spectral band (with frequency defined as the number of times the feature was used in splitting data across all decision trees in the model), followed by Bands 4 and 2. Bands 1 and 3 appeared less frequently. The feature May sd 5 had the highest Cover value of 0.040, indicating that it influenced the largest proportion of samples during tree splits. Other features with high Cover values (the proportion of samples affected by the feature during tree splits) included June sd 5 (0.034) and Feb sd 1 (0.026). In terms of Frequency, May sd 5 (0.0258) and Feb sd 1 (0.0227) were the most frequently used features in tree splits.

Table 5.3: The top 20 features ranked by their importance in the XGBoost model for taxa classification. The month from which the feature was derived, the statistical metric used (including standard deviation, mean, and median), the spectral band number associated with the feature, Gain (the relative contribution of the feature to improving the model's accuracy), Cover (the proportion of samples affected by the feature during tree splits), and Frequency (the number of times the feature was used in splitting data across all decision trees in the model).

Month	Metric	Band	Gain	Cover	Frequency
June	sd	5	0.056	0.034	0.022
May	sd	5	0.040	0.040	0.026
July	sd	5	0.038	0.032	0.025
May	sd	4	0.036	0.030	0.024
Feb	mean	2	0.026	0.020	0.016
March	sd	2	0.025	0.019	0.019
May	mean	5	0.024	0.019	0.018
June	sd	4	0.024	0.023	0.019
July	sd	4	0.024	0.020	0.019
Feb	sd	1	0.023	0.026	0.023
June	sd	1	0.023	0.024	0.021
July	sd	1	0.021	0.019	0.018
April	sd	5	0.021	0.020	0.020
June	sd	2	0.020	0.015	0.015
July	mean	3	0.020	0.018	0.013
April	median	2	0.019	0.018	0.017
May	sd	2	0.019	0.019	0.019
April	median	4	0.017	0.010	0.010
April	sd	4	0.016	0.018	0.020
March	sd	4	0.016	0.023	0.023

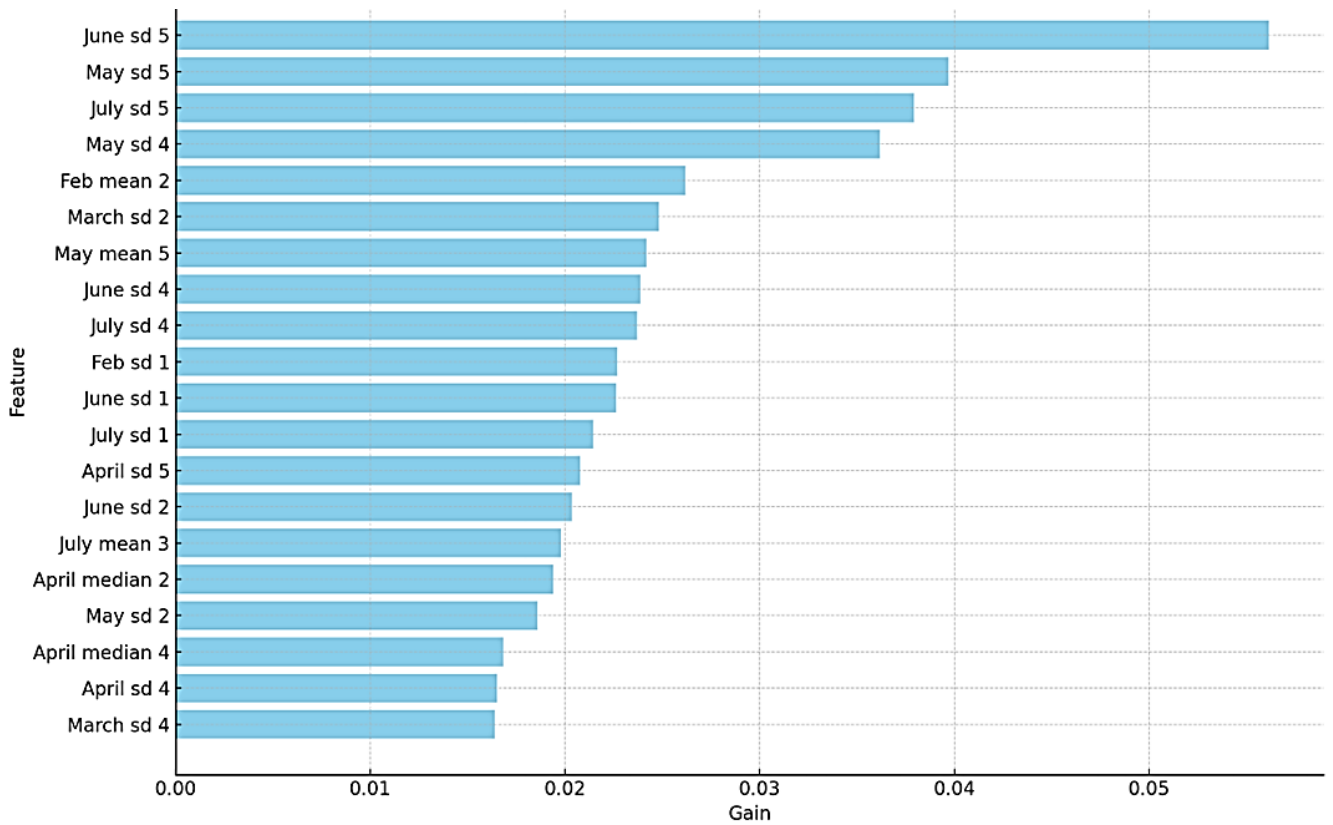


Figure 5.4: Top 20 features ranked by Gain (the relative contribution of the feature to improving the model's accuracy) in the XGBoost model for taxa classification.

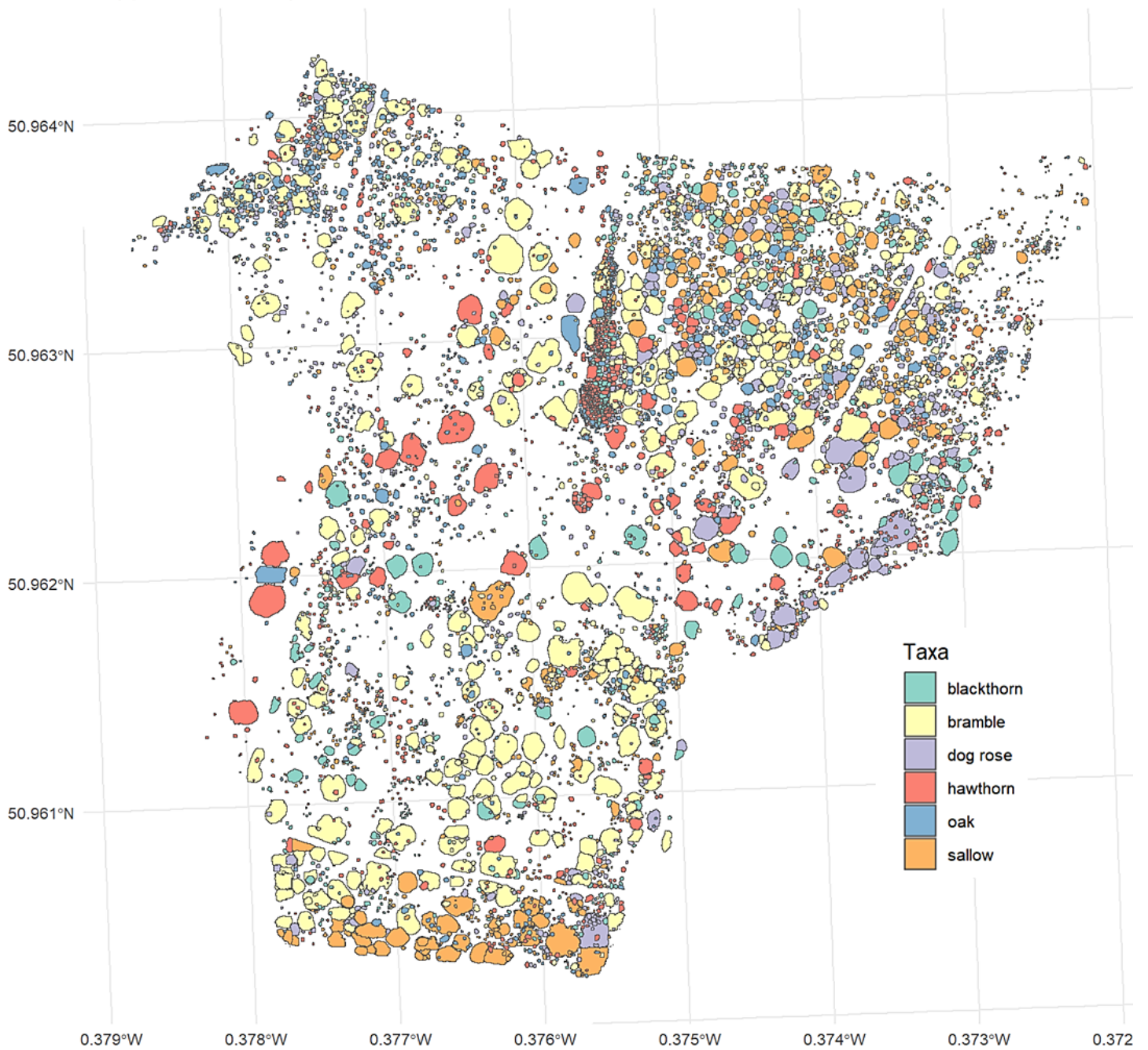


Figure 5.5: Spatial distribution of classified taxa across the study area based on XGBoost model predictions. Each polygon represents an individual canopy, color-coded by predicted taxon: blackthorn (green), bramble (yellow), dog rose (red), hawthorn (purple), oak (blue), and willow (orange).

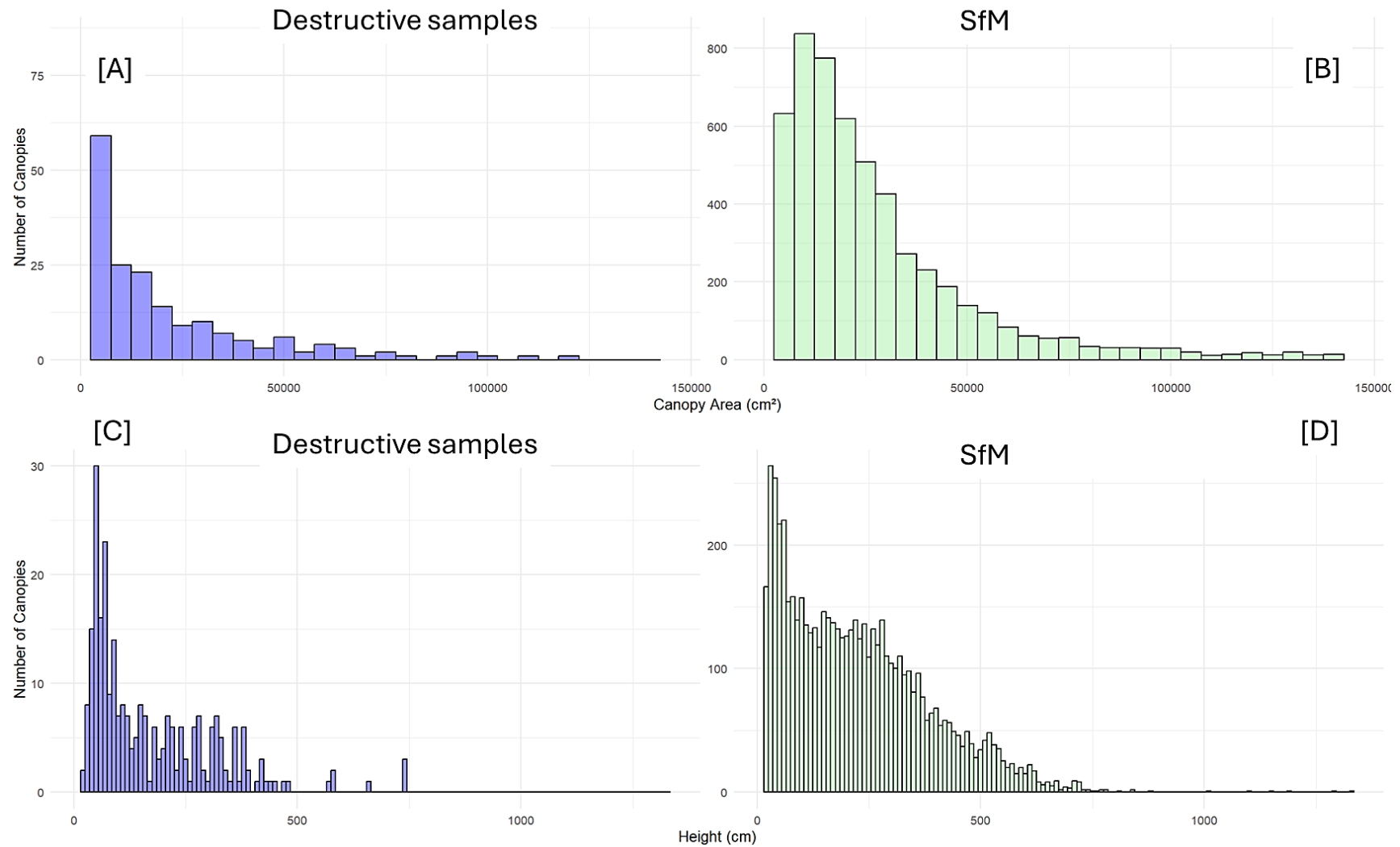


Figure 5.6: Distribution of canopy area and height for destructively sampled scrub and Structure-from-Motion (SfM) models. Panels [A] and [B] show the distribution of canopy area (cm²) for both models, while panels [C] and [D] display the distribution of canopy height (cm) for the same.

5.3.3 allometric equations

The allometric equations for each taxon and biomass type (AGB and BGB) (Table 5.4) were optimised using a stepwise AIC selection (Table S5.1). The models incorporated browsing condition (“exposed” or “protected”) and field measurements (height and canopy area) as predictors (Table 5.4). Overall, the models explained an average of 82% of the variability in AGB ($R^2 = 0.79-0.88$, $RSS = 19.71-62.75$) and 75% of the variability in BGB ($R^2 = 0.63-0.85$, $RSS = 18.94-42.12$).

Blackthorn had complex maximum models for both AGB ($R^2 = 0.82$, $RSS = 62.75$) and BGB ($R^2 = 0.83$, $RSS = 31.57$), incorporating all interaction terms between browsing condition, height, and canopy area. Dog rose AGB ($R^2 = 0.83$, $RSS = 32.10$) and BGB ($R^2 = 0.63$, $RSS = 30.61$) were predicted using simpler models without interaction terms. Hawthorn AGB ($R^2 = 0.88$, $RSS = 28.33$) relied on a main-effects model, while its BGB model ($R^2 = 0.85$, $RSS = 19.35$) included an additional interaction between height and canopy area (Table 5.4).

Sallow AGB ($R^2 = 0.87$, $RSS = 27.98$) included interaction terms with browsing condition, but its BGB model ($R^2 = 0.70$, $RSS = 42.14$) relied only on main effects. Finally, oak AGB ($R^2 = 0.79$, $RSS = 19.71$) was predicted using height and canopy area interactions, while its BGB model ($R^2 = 0.74$, $RSS = 18.94$) included browsing condition as a predictor.

5.3.4 Biomass and carbon estimates

The total aboveground biomass (AGB) and belowground biomass (BGB) for five taxa—hawthorn, blackthorn, dog rose, willow, and oak—were computed, and the results are

summarised in Table 5.5 and illustrated in Figure 5.7. Biomass totals are presented as kilograms per 13 hectares (kg/13 ha) (the size of the study site) and on a per hectare basis, while individual-level distributions of AGB and BGB are displayed on a log scale to capture variability.

Aboveground Biomass (AGB): Blackthorn had the highest total AGB ($25,804.22 \pm 208.78$ kg/13 ha), with a mean biomass of $1,984.94 \pm 16.06$ kg/ha and carbon storage of 873.37 ± 7.07 kg C/ha. Hawthorn followed with a total AGB of $10,983.43 \pm 55.13$ kg/13 ha (mean biomass of 844.88 ± 4.24 kg/ha, 371.75 ± 1.86 kg C/ha). Sallow ($7,091.48 \pm 18.17$ kg/13 ha, mean of 545.50 ± 1.40 kg/ha, 240.02 ± 0.61 kg C/ha), oak ($4,460.51 \pm 40.56$ kg/13 ha, mean of 343.12 ± 3.12 kg/ha, 151.97 ± 1.38 kg C/ha), and dog rose ($2,215.51 \pm 3.17$ kg/13 ha, mean of 170.42 ± 0.24 kg/ha, 75.33 ± 0.11 kg C/ha) demonstrated progressively lower AGB contributions. Figure 5.7 reflects this pattern, highlighting the dominance of blackthorn and hawthorn in aboveground biomass contributions compared to the other taxa.

Belowground Biomass (BGB): Sallow contributed the highest total BGB ($1,641.45 \pm 2.41$ kg/13 ha), corresponding to a mean of 126.27 ± 0.19 kg/ha and carbon storage of 54.29 ± 0.08 kg C/ha. Oak and hawthorn followed closely, with total BGB values of $1,610.67 \pm 6.94$ kg/13 ha (mean of 123.90 ± 0.53 kg/ha, 53.28 ± 0.23 kg C/ha) and $2,026.64 \pm 13.10$ kg/13 ha (mean of 155.90 ± 1.01 kg/ha, 67.03 ± 0.43 kg C/ha), respectively. Blackthorn had a total BGB of $1,434.93 \pm 7.06$ kg/13 ha (mean of 110.38 ± 0.54 kg/ha, 47.46 ± 0.23 kg C/ha), while dog rose exhibited the lowest BGB (549.98 ± 0.42 kg/13 ha), corresponding to a mean of 42.31 ± 0.03 kg/ha and carbon storage of 18.19 ± 0.01 kg C/ha. Figure 5.7 reflects this pattern, showing that sallow and oak have notable belowground biomass contributions relative to the other taxa.

Figure 5.7B illustrates the distributions of individual AGB and BGB values on a log scale, highlighting the variation within and among taxa. For AGB, blackthorn displayed the broadest range of biomass values, with a skew toward larger individual values. Hawthorn also showed substantial variability but with a more moderate range compared to blackthorn. Dog rose had the smallest range and median for AGB, with most values clustering at the lower end of the scale. Sallow and oak exhibited intermediate ranges for AGB, with relatively symmetric distributions.

For BGB, the patterns were more consistent across taxa, but variability was lower compared to AGB. Blackthorn and sallow demonstrated the widest range of BGB values, while dog rose exhibited the narrowest distribution. Median values for BGB were generally lower than for AGB across all taxa. Notably, the overlap of AGB and BGB distributions for each taxon highlights a stronger skew toward lower BGB values, particularly for dog rose and oak.

Table 5.4: Summary of linear regression models used to predict biomass components **W** (aboveground biomass (AGB) and belowground biomass (BGB)) across five taxa (blackthorn, dog rose, hawthorn, oak, and willow). Each model incorporates predictor variables—height **h** and canopy area **A**—as well as interactions with browsing condition (x_c) where specified. The models include combinations of main effects and interactions, up to a maximum model structure with all possible interaction terms (Equation 1). Model performance is evaluated using the coefficient of determination (R^2), residual sum of squares (RSS), and Akaike Information Criterion (AIC). Taxon specific biomass coefficient values ($\beta_0 - \beta_7$) are displayed, coefficients are ordered from the intercept (β_0) to the highest-order interaction term, “conditionprotected:log_height:log_canopy_area” (β_7). NA values indicate terms that were not included in the final model for that specific taxon and biomass component. The full table of coefficients with Standard Error (SE), T-Value and P-value can be found in Table S5.2.

Taxon	log (W)	model	β_0	β_1	β_2	β_3	β_4	β_5	β_6	β_7	R^2	RSS	AIC
Blackthorn	AGB	$\beta_0 + \beta_1 \cdot x_c + \beta_2 \cdot \log(h) + \beta_3 \cdot \log(A) + \beta_4 \cdot (x_c \cdot \log(h)) + \beta_5 \cdot (x_c \cdot \log(A)) + \beta_6 \cdot (\log(h) \cdot \log(A)) + \beta_7 \cdot (x_c \cdot \log(h) \cdot \log(A))$	1.280	8.800	-0.280	-0.080	-1.319	-1.757	0.182	0.278	0.819	62.75	181.34
	BGB	$\beta_0 + \beta_1 \cdot x_c + \beta_2 \cdot \log(h) + \beta_3 \cdot \log(A) + \beta_4 \cdot (x_c \cdot \log(h)) + \beta_5 \cdot (x_c \cdot \log(A)) + \beta_6 \cdot (\log(h) \cdot \log(A)) + \beta_7 \cdot (x_c \cdot \log(h) \cdot \log(A))$	-1.484	15.933	0.017	0.643	-2.675	-2.432	0.048	0.395	0.826	31.57	143.56
Dog rose	AGB	$\beta_0 + \beta_1 \cdot x_c + \beta_2 \cdot \log(h) + \beta_3 \cdot \log(A)$	-4.491	13.818	1.961	0.168	NA	NA	NA	NA	0.831	32.1	136.46
	BGB	$\beta_0 + \beta_1 \cdot x_c + \beta_2 \cdot \log(h) + \beta_3 \cdot \log(A)$	-2.290	7.795	1.251	0.542	NA	NA	NA	NA	0.63	30.61	133.85
Hawthorn	AGB	$\beta_0 + \beta_1 \cdot x_c + \beta_2 \cdot \log(h) + \beta_3 \cdot \log(A)$	-15.381	17.013	3.385	1.732	NA	NA	NA	NA	0.882	28.33	130.77
	BGB	$\beta_0 + \beta_1 \cdot x_c + \beta_2 \cdot \log(h) + \beta_3 \cdot \log(A) + \beta_6 \cdot (\log(h) \cdot \log(A))$	-3.098	6.067	1.383	0.304	NA	NA	-0.003	NA	0.853	19.351	117.41

Taxon	log (W)	model	β_0	β_1	β_2	β_3	β_4	β_5	β_6	β_7	R ²	RSS	AIC
Sallow	AGB	$\beta_0 + \beta_1 \cdot xc + \beta_2 \cdot \log(h) + \beta_3 \cdot \log(A) + \beta_6 \cdot (\log(h) \cdot \log(A)) + \beta_7 \cdot (xc \cdot \log(h) \cdot \log(A))$	-2.859	3.520	0.437	0.852	NA	NA	-0.001	0.153	0.87	27.98	136.92
	BGB	$\beta_0 + \beta_1 \cdot xc + \beta_2 \cdot \log(h) + \beta_3 \cdot \log(A)$	-2.697	0.840	0.661	0.915	NA	NA	NA	NA	0.699	42.14	151.43
Oak	AGB	$\beta_0 + \beta_2 \cdot \log(h) + \beta_3 \cdot \log(A) + \beta_6 \cdot (\log(h) \cdot \log(A))$	18.757	NA	-3.846	-2.814	NA	NA	0.754	NA	0.791	19.71	104.44
	BGB	$\beta_0 + \beta_1 \cdot xc + \beta_2 \cdot \log(h) + \beta_3 \cdot \log(A)$	13.017	-7.029	-2.866	-1.735	NA	NA	NA	NA	0.739	18.94	102.48

Table 5.5: Summary of total aboveground biomass (AGB) and belowground biomass (BGB) for each taxon across 13 hectares, along with their corresponding carbon estimates. The table includes total biomass (kg), carbon storage (kg), root-to-shoot ratios, and the minimum, maximum, and mean biomass values per individual (kg). Additionally, the per-hectare biomass and carbon values for both AGB and BGB are presented.

Taxon	<i>n</i>	Total kg/13 ha				agb (kg)			bgb (kg)			kg/hectares		Carbon/ha	
		AGB	BGB	AGB C	BGB C	min	max	mean	min	max	mean	AGB	BGB	AGB	BGB
Hawthorn	1144	10983.43	2026.64	4832.71	871.45	0.0179	1416.78	9.60	0.0063	363.08	1.77	844.88	155.90	371.75	67.03
blackthorn	769	25804.22	1434.93	11353.86	617.02	0.0013	3711.51	33.60	0.0039	116.75	1.87	1984.94	110.38	873.37	47.46
dog rose	1010	2215.51	549.98	974.83	236.49	0.0061	30.83	2.20	0.0247	3.31	0.55	170.42	42.31	74.99	18.19
sallow	1048	7091.48	1641.45	3120.25	705.82	0.0073	250.80	6.77	0.0216	27.37	1.57	545.50	126.27	240.02	54.29
oak	1120	4460.51	1610.67	1962.62	692.59	0.0303	1349.22	3.99	0.0500	25.58	1.44	343.12	123.90	150.97	53.28

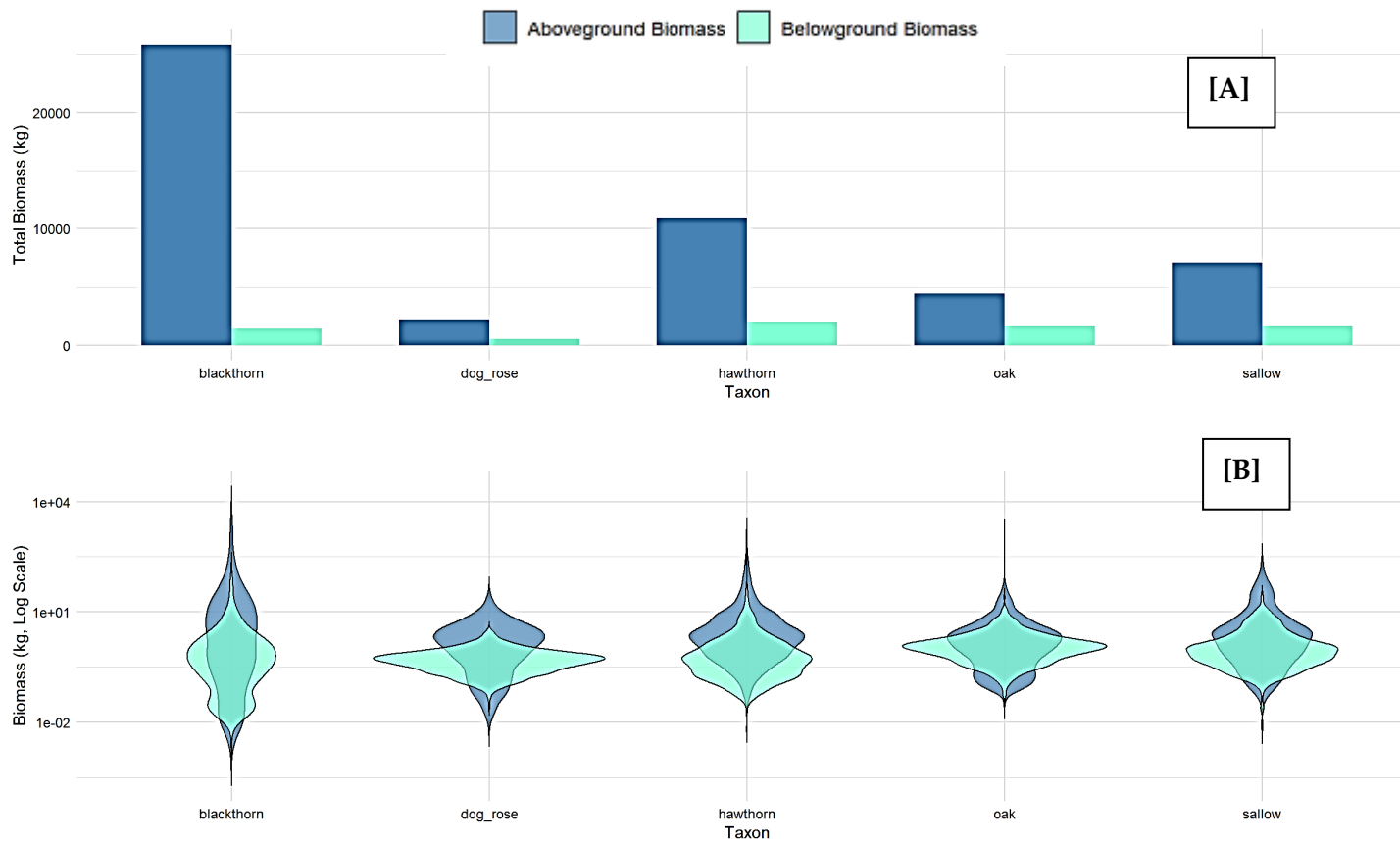


Figure 5.7: Total biomass and distribution of aboveground and belowground biomass across five taxa. **[A]** total aboveground biomass (blue) and belowground biomass (aqua) in kilograms (kg) per taxon, aggregated across 13 hectares. **[B]** the distribution of individual biomass values (log scale) for aboveground (blue) and belowground (aqua) biomass across taxa. Taxa include blackthorn, dog rose, hawthorn, oak, and sallow.

5.4 Discussion

This study successfully evaluated the integration of Structure-from-Motion (SfM) photogrammetry and multispectral imagery to classify scrub taxa and estimate their biomass, highlighting its potential for quantifying carbon storage in scrubland ecosystems. The results indicate that these methodologies can differentiate taxa while providing robust estimates of aboveground and belowground biomass, contributing to a scalable and replicable method of estimating scrub biomass for above and belowground.

5.4.1. Generating predictor variables through Structure from Motion (SfM)

Structure-from-Motion (SfM) photogrammetry using UAVs is a promising tool for vegetation studies, offering scalable and non-destructive data collection. In this study, the mean canopy area and height derived from SfM were higher than those from the destructive sampling (Chapter 3), likely because SfM was not constrained by tree size and included larger trees typically excluded in destructive methods for practical reasons. For instance, the destructive sample mean canopy area (17.24 cm²) was lower than the SfM-predicted mean (73.10 cm²), and the mean height derived from SfM (226 cm) exceeded that from destructive measurements (173 cm). These differences could be a reflection of the broader sampling scope achievable with SfM and its ability to represent a more comprehensive range of canopy structures.

While some studies have highlighted potential inaccuracies in UAV-based SfM, such as underestimations of tree height and volume (Kameyama and Sugiura, 2020) and the sensitivity of canopy height reconstruction to wind speed during data collection (Slade et al., 2024), this study did not find such discrepancies. The congruence observed in the overall

frequency distributions of canopy height and area between SfM and destructive methods (Figure 5.5), along with the similar shapes of these distributions, suggests that SfM accurately captures the variability and structural patterns of vegetation.

This finding aligns with previous research supporting the reliability of SfM for vegetation assessments. For example, Dandois and Ellis (2013) demonstrated SfM's capability for high spatial-resolution mapping of forest canopy structure, while Cunliffe et al. (2022) and Wallace et al. (2017) highlighted its effectiveness in estimating aboveground biomass using fine-grain volumetric models. Additionally, Vafidis et al. (2021) validated its use for mapping scrub vegetation cover in reserve management, and Orndahl et al. (2022) successfully applied SfM to estimate plant functional type cover, height, and biomass in tundra ecosystems. The similar height and canopy area frequency distributions observed in this study strongly suggest that SfM provided adequate representations of the site (Figure 5.6).

Incorporating browsing as a condition in allometric models is crucial yet often overlooked. There are now many research studies indicating that herbivory significantly affects biomass distribution, often increasing belowground allocation as a defence mechanism (Peláez et al., 2024; Perkovich & Ward, 2021; Hester et al., 2006). Yet, despite its importance, most existing models fail to account for browsing intensity or protection, creating a critical knowledge gap that undermines the ecological accuracy of biomass predictions. Addressing this gap is essential for refining allometric models in ecosystems shaped by herbivory. In this respect, results from my study are particularly important since by employing bramble cover as a proxy for browsing protection, and then identified using a supervised random forest classification from drone-derived RGB orthomosaics in ArcGIS pro (Esri, 2024), I was able to remotely classify scrub trees as either protected or exposed based on their proximity to bramble. In this

instance, drone-acquired data was therefore used to assess ecological variables like browsing protection, again making the information transferable and scalable across larger landscapes.

While the binary classification provided a broad indication of protection and was intentionally conservative—assigning a larger proportion of trees as protected—it potentially misrepresented the actual proportion of bramble cover. For example, taxa such as hawthorn and blackthorn showed disproportionately high representation in protected categories despite observed exposure within the field site. Nonetheless, the use of a coarser resolution in ArcGIS Pro (Figure 5.2B) for mapping bramble distribution proved advantageous for capturing this variable more accurately. The coarser resolution reduced noise from smaller misclassified patches and provided a clearer delineation of meaningful bramble clusters, better reflecting their ecological influence on browsing protection.

Despite potential limitations in misrepresenting finer-scale variability, the AIC results indicated that browsing condition significantly influenced biomass allocation in all taxa except for belowground oak (Table 5.4) demonstrating the utility of this variable. Results showed higher root:shoot (RS) ratios in exposed trees (see Chapter 3), consistent with the hypothesis that herbivory promotes belowground carbon allocation as a defence strategy (Perkovich & Ward, 2021).

By leveraging drone-based remote sensing, this method represents a significant advancement in biomass estimation, demonstrating its applicability for integrating remote sensing data into allometric modelling while explicitly accounting for browsing impacts. To date, most allometric models used in temperate ecosystems, such as those developed by Chave et al. (2005) and Jenkins et al. (2003), focus on environmental or structural variables like soil type, tree height, and canopy area but overlook the role of herbivory. The limited integration of

browsing is surprising given the extensive body of literature documenting its ecological effects (Perkovich & Ward, 2021; Rooke, 2003a; 2003b; Rooke et al., 2004a; 2004b; Rooke & Bergström, 2007; Gill, 1992).

However, the use of bramble as a proxy also has limitations, as it does not directly quantify browsing pressure or herbivore density, and in this study, it is produced as a binary variable. Future work could refine this approach by integrating direct measures of browsing, such as faecal pellet counts (Forsyth et al., 2007), remote sensing of vegetation damage (Spiegel et al., 2023), or herbivore exclusion experiments (Tanentzap et al., 2023). Nonetheless, the integration of browsing has been a key knowledge gap in allometric modelling and this work offers a critical step toward bridging that gap while demonstrating the potential of remote sensing technologies in ecological studies.

5.4.2. Multi-spectral imaging to identify scrub taxa

The XGBoost model's classification performance varied significantly across taxa, revealing both strengths and limitations in classifying scrub vegetation (Table 5.2). While the model demonstrated high specificity across all taxa, its sensitivity and balanced accuracy were more variable, particularly for taxa such as blackthorn (*Prunus spinosa*) and dog rose (*Rosa canina*). These results highlight its proficiency in excluding false positives but underscore challenges in reliably identifying certain taxa.

The lower sensitivity and balanced accuracy for blackthorn and dog rose are likely due to their distinct structural traits. Blackthorn's dense, thorny canopy and spectral similarity to other scrub taxa may have impeded accurate classification, as noted in previous studies documenting difficulties with species having overlapping spectral profiles (e.g., Shataee-

Joibary et al., 2007; Darvishsefat et al., 2009; Fassnacht et al., 2016). Similarly, dog rose's fragmented growth form, characterised by canopy gaps, may have introduced noise into the drone-derived metrics, an issue frequently cited in remote sensing workflows involving discontinuous vegetation structures (Baena et al., 2017; Hernandez-Santin et al., 2019; Takahashi Miyoshi et al., 2020; Lu & Weng, 2007).

These structural complexities likely contributed to the model's limitations, particularly its reduced ability to predict positive occurrences for these taxa compared to more robust classifications observed for species like oak (*Quercus robur*) and hawthorn (*Crataegus monogyna*).

Multispectral imagery features, particularly standard deviation metrics from red-edge and near-infrared bands (e.g., Bands 5, 4, and 2), were critical for distinguishing between taxa. Temporal windows in May, June, and July were identified as optimal for capturing phenological differences that enhance taxonomic differentiation (Table 5.3, Figure 5.4), likely due to increased spectral heterogeneity between taxa during this period, as observed in Grybas et al., (2021). However, even when leveraging temporal variability, the classification accuracy of blackthorn and dog rose was still low.

Although the model demonstrated limitations for certain taxa, its high specificity and balanced accuracy for oak, hawthorn, and willow affirm its utility in scrub vegetation classification. In the future, using a 10-band camera, which captures more spectral diversity than a 5-band system, can improve taxonomic differentiation and overcome challenges such as spectral overlap or morphological complexity (Liu et al., 2024). Furthermore, increasing the ground-truth dataset may address biases related to morphological variability, as recommended by Zhang et al. (2022).

5.4.3. Scrub biomass and carbon estimation

The allometric models demonstrated high levels of predictive power across taxa. Hawthorn (*Crataegus monogyna*) exhibited the highest predictive accuracy, with AGB and BGB models achieving R^2 values of 0.88 and 0.85, respectively, and low residual variability. Sallow (*Salix spp.*) and oak (*Quercus spp.*) displayed robust AGB predictions ($R^2 = 0.87$ and 0.80 , respectively), though their BGB models were slightly lower, with R^2 values of 0.70 for sallow and 0.74 for oak. The R^2 values observed across taxa are consistent with the range reported on allometric model studies on other forest ecosystems. For instance, research using allometric models to estimate biomass in tropical and temperate ecosystems often reports R^2 values between 0.6 and 0.9, depending on species, predictors, and site heterogeneity (Vorster et al., 2020; Chave et al., 2005; Jenkins et al., 2003). The lower R^2 value for the BGB model of dog rose ($R^2=0.63$) is notable and aligns with the general challenge of modelling belowground biomass, which is inherently more variable and difficult to measure (Cairns et al., 1997). Despite this, the dog rose model still falls within the range of allometric equations reported for other forested systems, highlighting its utility in biomass estimation.

The combined aboveground and belowground carbon storage for the Knepp scrubland, encompassing contributions from oak (*Quercus spp.*), blackthorn (*Prunus spinosa*), hawthorn (*Crataegus monogyna*), dog rose (*Rosa canina*), and sallow (*Salix spp.*), totals approximately 1950 kg C ha⁻¹ (AGB: 1710 kg C ha⁻¹; BGB: 240 kg C ha⁻¹) (Table 5.5). These values represent the minimum carbon storage potential for this scrubland ecosystem, as several factors likely contributed to underestimations.

Several methodological constraints limited the ability to fully capture the full biomass measurement. The use of destructive sampling techniques posed challenges, particularly for accurately estimating the root biomass. Deep or extensive root networks are difficult to extract, especially in dense soils, leading to their frequent underrepresentation in biomass studies (Mokany et al., 2006; Cairns et al., 1997). Furthermore, the polygon-SAM based techniques used for canopy identification likely resulted in the under-sampling or omission of smaller or overlapping canopies, further contributing to an underestimation of total biomass.

The total biomass value reported here also excludes foliage, a potentially significant contributor to biomass and carbon storage. For example, Saddiq et al. (2021) found that leaves in a subtropical scrub forest in Pakistan accounted for approximately 6.97 t C ha⁻¹, representing around 14% of the total carbon within that scrub environment. This omission is notable, as foliage plays a crucial role in carbon sequestration and nutrient cycling (Poorter et al., 2012), particularly in smaller scrub systems where leaf mass may constitute a significant proportion of total biomass.

One final point is that the majority of scrub measured at Knepp was less than 0.5 m in height (Figure 5.6D) and younger than 19 years, indicative of the early successional stage of this ecosystem. Comparisons with similar systems worldwide provide valuable context for understanding the carbon storage potential of Knepp's developing scrubland.

In Jhariya (2017), the carbon sequestration potential of shrubs in the Boramdeo Wildlife Sanctuary, India, found a total shrub biomass ranging from 6.82 to 15.71 t ha⁻¹, corresponding to carbon storage of 2.93 to 6.76 t ha⁻¹ across different fire regimes. In comparison, the nascent scrub at Knepp produced a carbon value of 1.95 t ha⁻¹. Similarly, Tomilla et al. (2024) reported mean total carbon values per shrub in Finland ranging from 18.5 ± 1.4 kg to 0.05 ± 0.02 kg,

aligning closely with Knepp's scrub, which exhibited an average biomass range of 1.21 kg (dog rose) to 15.61 kg (blackthorn). Ruiz-Peinado et al. (2013) also found comparable total biomass range values of 4.67 kg and 12.7 kg per shrub for two Mediterranean species, further corroborating the findings at Knepp.

Comparisons between Knepp's nascent scrubland and mature systems, such as Mediterranean habitats and hedgerows in the UK, underscore the potential of Knepp's developing scrub to evolve into a significant carbon sink. For instance, Pasalodos-Tato et al. (2015) reported that scrubland in Andalusia, Southern Spain, sequestered 16.73 Mg ha⁻¹ of carbon, with scrub trees averaging 12.1 m in height. Similarly, Axe et al. (2017) estimated aboveground biomass (AGB) of 42.0 tC ha⁻¹ and belowground biomass (BGB) of 38.2 tC ha⁻¹ for 3.5 m tall hedgerows in the UK. These higher biomass values reflect the advanced age, height and structural development of these systems compared to Knepp's younger scrub.

Interestingly, despite these differences, the structural morphology of these woody systems, shaped by factors such as browsing pressures (e.g. Rincon-Madroñero et al., 2024) or hedge trimming (Axe et al., 2017), is similar to the developing scrub at Knepp. These similarities include multi-stemmed structures, which result from adaptations to herbivory (Peláez et al., 2024; Rooke et al., 2004b; Chapter 3), as well as the dominance of thorny scrub species like blackthorn and hawthorn (Figure 5.5), which offer natural protection against browsing. Additionally, both systems demonstrate higher root:shoot ratios (Chapter 2, 3), reflecting adaptations to similar stressors such as browsing or limited resource availability, where plants allocate more biomass belowground to enhance stability, resilience, and nutrient acquisition (Perkovich & Ward, 2021). Other shared characteristics include dense, heterogeneous canopy

structures, and a propensity for clonal propagation, particularly in species such as blackthorn (Facciolati et al., 2024).

By measuring carbon storage during these early stages, this study also establishes a baseline for monitoring carbon sequestration over time. Such measurements are critical for understanding the long-term developmental trajectory of scrubland ecosystems and enable a more comprehensive evaluation of their ecosystem service contributions (Lindenmayer et al., 2012). Further validation of these similarities through comparative studies of mature and early-successional scrubland systems would strengthen the evidence for these shared dynamics and their implications for the future of scrubland regeneration within rewilding projects.

In terms of the carbon storage compared to other landscapes, although Knepp's young scrubland currently falls short of the carbon storage potential of mature scrublands (Pasalodos-Tato et al., 2015) or ancient hedgerows (Axe et al., 2017), the woody vegetation measured here represents only part of the ecosystem's carbon dynamics. Soils (Kaštovská et al., 2024; Tudge et al., 2023; Lal et al., 2021), wetlands (Law et al., 2017; Nummi et al., 2018), and grasslands, particularly those under grazing and browsing regimes (Rincon-Madroño et al., 2024; Frank et al., 1994; Hu et al., 2016), are recognised as critical carbon reservoirs with a significant role in carbon storage and sequestration. Recent findings at Knepp demonstrate soil sequestration rates of 3.3–4.8 tCO₂e/ha/year, with a midpoint estimate of 4.05 tCO₂e/ha/year, comparable to woodland carbon estimates (Knepp Wildland Carbon Project, 2024). Importantly, rewilding delivers a suite of essential ecosystem services beyond carbon storage, including promoting biodiversity (Svenning et al., 2019; Wang et al., 2023), improving soil health (Andriuzzi & Wall, 2018; Lal et al., 2021), regulating water (Harvey & Henshaw,

2023), and providing habitats for diverse species (Garrido et al., 2019; Svenning, 2020). A biodiversity and carbon co-crediting system offers a practical framework to integrate and value these ecosystem services (Tedersoo et al., 2023; The Wallacea Trust, 2023). By modelling the minimum carbon storage in the woody component of scrubland, this study provides a foundation for incorporating these broader benefits into rewilding strategies.

5.5 Conclusion

By focusing on the carbon dynamics of developing scrub at Knepp, this study emphasises the importance of early-stage monitoring to track and model carbon trajectories over time. These efforts not only contribute to assessments of scrubland in climate mitigation strategies but also provide a foundation for recognising and valuing the broader ecological benefits of rewilding landscapes. It also demonstrates the utility of using integrating Structure-from-Motion (SfM) photogrammetry and multispectral imagery for classifying scrub taxa and estimating biomass in browsed rewilded scrubland. By leveraging scalable, non-destructive methodologies, such as this, the potential is huge for measuring global scrublands. It provides robust methodologies to estimate aboveground and belowground biomass, laying a foundation for assessing carbon storage and broader ecosystem services in such structurally complex systems. The incorporation of browsing effects into allometric models also addresses a critical gap, enhancing ecological accuracy in biomass predictions. While the XGBoost model highlighted challenges in differentiating structurally similar taxa like blackthorn and dog rose, its overall high balanced accuracy, together with the high specificity for taxa such as hawthorn and oak underscores its potential for scrub vegetation classification. These findings not only support the role of developing scrublands in carbon sequestration but also establish a framework for integrating biodiversity and other ecosystem services into rewilding

strategies. By focusing on early-stage carbon dynamics, this research contributes to long-term monitoring and climate mitigation efforts in global landscapes.

5.6 References

- Ali, A., Xu, M.S., Zhao, Y.T., Zhang, Q.Q., Zhou, L.L., Yang, X.D. and Yan, E.R., 2015. Allometric biomass equations for shrub and small tree species in subtropical China. *Silva Fennica*, 49(4).
- Alonzo, M., Dial, R.J., Schulz, B.K., Andersen, H.E., Lewis-Clark, E., Cook, B.D. and Morton, D.C., 2020. Mapping tall shrub biomass in Alaska at landscape scale using structure-from-motion photogrammetry and lidar. *Remote Sensing of Environment*, 245, p.111841.
- Andriuzzi, W.S. and Wall, D.H., 2018. Soil biological responses to, and feedbacks on, trophic rewilding. *Philosophical Transactions of the Royal Society B: Biological Sciences*, 373(1761), p.20170448.
- Asner, G.P. and Vitousek, P.M., 2005. Remote analysis of biological invasion and biogeochemical change. *Proceedings of the National Academy of Sciences*, 102(12), pp.4383-4386.
- Assmann, J.J., Kerby, J.T., Cunliffe, A.M. and Myers-Smith, I.H., 2018. Vegetation monitoring using multispectral sensors—best practices and lessons learned from high latitudes. *Journal of Unmanned Vehicle Systems*, 7(1), pp.54-75.
- Axe, M.S., Grange, I.D. and Conway, J.S., 2017. Carbon storage in hedge biomass—A case study of actively managed hedges in England. *Agriculture, ecosystems & environment*, 250, pp.81-88.
- Baena, S., Moat, J., Whaley, O. and Boyd, D.S., 2017. Identifying species from the air: UAVs and the very high resolution challenge for plant conservation. *PloS one*, 12(11), p.e0188714.
- Bakker, E.S., Gill, J.L., Johnson, C.N., Vera, F.W., Sandom, C.J., Asner, G.P. and Svenning, J.C., 2016. Combining paleo-data and modern exclosure experiments to assess the impact of megafauna extinctions on woody vegetation. *Proceedings of the National Academy of Sciences*, 113(4), pp.847-855.
- Ballantyne, M. and Pickering, C.M., 2015. Shrub facilitation is an important driver of alpine plant community diversity and functional composition. *Biodiversity and Conservation*, 24, pp.1859-1875.
- Bastin, J.F., Finegold, Y., Garcia, C., Mollicone, D., Rezende, M., Routh, D., Zohner, C.M. and Crowther, T.W., 2019. The global tree restoration potential. *Science*, 365(6448), pp.76-79.
- Baston, D., 2021. exactextractr: Fast Extraction from Raster Datasets using Polygons. R package version 0.7. 2. CRAN. *R-project.org/package=exactextractr*.

- Boelman, N.T., Gough, L., Wingfield, J., Goetz, S., Asmus, A., Chmura, H.E., Krause, J.S., Perez, J.H., Sweet, S.K. and Guay, K.C., 2015. Greater shrub dominance alters breeding habitat and food resources for migratory songbirds in Alaskan arctic tundra. *Global Change Biology*, 21(4), pp.1508-1520.
- Boelman, N.T., Rocha, A.V. and Shaver, G.R., 2011. Understanding burn severity sensing in Arctic tundra: exploring vegetation indices, suboptimal assessment timing and the impact of increasing pixel size. *International Journal of Remote Sensing*, 32(22), pp.7033-7056.
- Brown, S., 2002. Measuring carbon in forests: current status and future challenges. *Environmental pollution*, 116(3), pp.363-372.
- Bull, J.W., Taylor, I., Biggs, E., Grub, H.M., Yearley, T., Waters, H. and Milner-Gulland, E.J., 2022. Analysis: the biodiversity footprint of the University of Oxford. *Nature*, 604(7906), pp.420-424.
- Cairns, M.A., Brown, S., Helmer, E.H. and Baumgardner, G.A., 1997. Root biomass allocation in the world's upland forests. *Oecologia*, 111, pp.1-11.
- Catchpole, W.R. and Wheeler, C.J., 1992. Estimating plant biomass: a review of techniques. *Australian Journal of Ecology*, 17(2), pp.121-131.
- Cerqueira, Y., Navarro, L.M., Maes, J., Marta-Pedroso, C., Pradinho Honrado, J. and Pereira, H.M., 2015. Ecosystem services: the opportunities of rewilding in Europe. *Rewilding European Landscapes*, pp.47-64.
- Chai, Y., Zhong, J., Zhao, J., Guo, J., Yue, M., Guo, Y., Wang, M. and Wan, P., 2021. Environment and plant traits explain shrub biomass allocation and species composition across ecoregions in North China. *Journal of Vegetation Science*, 32(6), p.e13080.
- Chapin, F.S., Matson, P.A., Mooney, H.A. and Vitousek, P.M., 2002. Principles of terrestrial ecosystem ecology.
- Chave, J., Andalo, C., Brown, S., Cairns, M.A., Chambers, J.Q., Eamus, D., Fölster, H., Fromard, F., Higuchi, N., Kira, T. and Lescure, J.P., 2005. Tree allometry and improved estimation of carbon stocks and balance in tropical forests. *Oecologia*, 145, pp.87-99.
- Côté, S.D., Rooney, T.P., Tremblay, J.P., Dussault, C. & Waller, D.M. (2004). Ecological impacts of deer overabundance. *Annual Review of Ecology, Evolution, and Systematics*, 35(1), pp. 113–147.
- Chave, J., Réjou-Méchain, M., Búrquez, A., Chidumayo, E., Colgan, M.S., Delitti, W.B., Duque, A., Eid, T., Fearnside, P.M., Goodman, R.C. and Henry, M., 2014. Improved allometric models to estimate the aboveground biomass of tropical trees. *Global change biology*, 20(10), pp.3177-3190.
- Chen, T. and Guestrin, C., 2016, August. Xgboost: A scalable tree boosting system. In *Proceedings of the 22nd acm sigkdd international conference on knowledge discovery and data mining* (pp. 785-794).

Chuvieco, E., Aguado, I., Salas, J., García, M., Yebra, M. and Oliva, P., 2020. Satellite remote sensing contributions to wildland fire science and management. *Current Forestry Reports*, 6, pp.81-96.

Coles, T. (2023). Identifying an agreed unit of biodiversity change for inclusion in a biodiversity definition. OBE-CEO rePLANET. Retrieved 2 December, 2024, from <https://www.replanet.org.uk/>

Cunliffe, A.M., Anderson, K., Boschetti, F., Brazier, R.E., Graham, H.A., Myers-Smith, I.H., Astor, T., Boer, M.M., Calvo, L.G., Clark, P.E. and Cramer, M.D., 2022. Global application of an unoccupied aerial vehicle photogrammetry protocol for predicting aboveground biomass in non-forest ecosystems. *Remote Sensing in Ecology and Conservation*, 8(1), pp.57-71.

Cunliffe, A.M., Brazier, R.E. and Anderson, K., 2016. Ultra-fine grain landscape-scale quantification of dryland vegetation structure with drone-acquired structure-from-motion photogrammetry. *Remote Sensing of Environment*, 183, pp.129-143.

Dandois, J.P. and Ellis, E.C., 2013. High spatial resolution three-dimensional mapping of vegetation spectral dynamics using computer vision. *Remote Sensing of Environment*, 136, pp.259-276.

Darvishsefat, A.A., Abbasi, M.O.Z.H.G.A.N. and Mohadjer, M.M., 2009. Investigation on the possibility of beech forest type mapping using Landsat ETM+ data (case study: Khyrood forest).

Esri, 2024. *Generalization of classified raster imagery*. ArcGIS Pro Documentation. Available at: <https://pro.arcgis.com/en/pro-app/latest/tool-reference/spatial-analyst/generalization-of-classified-raster-imagery.htm> [Accessed 23 October 2024].

Facciolati, V., Zarek, M., Blonska, E., Lasota, J., Orman, O. and Ciach, M., 2024. To be browsed or not to be browsed: differences in nutritional characteristics of blackthorn *Prunus spinosa* subject to the long-term pressure of herbivores. *bioRxiv*, pp.2024-04.

FAO. 2020. Global Forest Resources Assessment 2020 – Key findings. Rome. <https://doi.org/10.4060/ca8753en>

Fassnacht, F.E., Latifi, H., Stereńczak, K., Modzelewska, A., Lefsky, M., Waser, L.T., Straub, C. and Ghosh, A., 2016. Review of studies on tree species classification from remotely sensed data. *Remote sensing of environment*, 186, pp.64-87.

Fonseca, F., de Figueiredo, T. and Bompastor Ramos, M.A., 2012. Carbon storage in the Mediterranean upland shrub communities of Montesinho Natural Park, northeast of Portugal. *Agroforestry Systems*, 86, pp.463-475.

Forsyth, D.M., Barker, R.J., Morriss, G. and Scroggie, M.P., 2007. Modeling the relationship between fecal pellet indices and deer density. *The Journal of Wildlife Management*, 71(3), pp.964-970.

Fraser, R.H., Olthof, I., Lantz, T.C. and Schmitt, C., 2016. UAV photogrammetry for mapping vegetation in the low-Arctic. *Arctic Science*, 2(3), pp.79-102.

- Friedlingstein, P., O'sullivan, M., Jones, M.W., Andrew, R.M., Gregor, L., Hauck, J., Le Quéré, C., Luijkx, I.T., Olsen, A., Peters, G.P. and Peters, W., 2022. Global carbon budget 2022. *Earth System Science Data*, 14(11), pp.4811-4900.
- Garcia-Estringana, P., Alonso-Blázquez, N., Marques, M.J., Bienes, R., González-Andrés, F. and Alegre, J., 2013. Use of Mediterranean legume shrubs to control soil erosion and runoff in central Spain. A large-plot assessment under natural rainfall conducted during the stages of shrub establishment and subsequent colonisation. *Catena*, 102, pp.3-12.
- Garrido, P., Mårell, A., Öckinger, E., Skarin, A., Jansson, A. and Thulin, C.G., 2019. Experimental rewilding enhances grassland functional composition and pollinator habitat use. *Journal of Applied Ecology*, 56(4), pp.946-955.
- Gill, R.M.A., 1992. A review of damage by mammals in north temperate forests: 1. Deer. *Forestry: An International Journal of Forest Research*, 65(2), pp.145-169.
- Giller, K.E., Hijbeek, R., Andersson, J.A. and Sumberg, J., 2021. Regenerative agriculture: an agronomic perspective. *Outlook on agriculture*, 50(1), pp.13-25.
- Godlee, J.L., Ryan, C.M., Bauman, D., Bowers, S.J., Carreiras, J.M.B., Chisingui, A.V., Cromsigt, J.P.G.M., Druce, D.J., Finckh, M., Gonçalves, F.M., Holdo, R.M., Makungwa, S., McNicol, I.M., Mitchard, E.T.A., Muchawona, A., Revermann, R., Ribeiro, N.S., Siampale, A., Syampungani, S., Tchamba, J.J., Tripathi, H.G., Wallenfang, J., te Beest, M., Williams, M. and Dexter, K.G. (2021), Structural diversity and tree density drives variation in the biodiversity–ecosystem function relationship of woodlands and savannas. *New Phytol*, 232: 579-594. <https://doi.org/10.1111/nph.17639>
- Goetz, S. and Dubayah, R., 2011. Advances in remote sensing technology and implications for measuring and monitoring forest carbon stocks and change. *Carbon Management*, 2(3), pp.231-244.
- Gómez-Aparicio, L., Zamora, R., Gómez, J.M., Hódar, J.A., Castro, J. and Baraza, E., 2004. Applying plant facilitation to forest restoration: a meta-analysis of the use of shrubs as nurse plants. *Ecological applications*, 14(4), pp.1128-1138.
- Gosnell H, Gill N, Voyer M (2019) Transformational adaptation on the farm: Processes of change and persistence in transitions to 'climate-smart' regenerative agriculture. *Global Environ Change* 59(101965):1–13
- Grassi, G., House, J., Dentener, F., Federici, S., den Elzen, M. and Penman, J., 2017. The key role of forests in meeting climate targets requires science for credible mitigation. *Nature Climate Change*, 7(3), pp.220-226.
- Greaves, H.E., Vierling, L.A., Eitel, J.U., Boelman, N.T., Magney, T.S., Prager, C.M. and Griffin, K.L., 2015. Estimating aboveground biomass and leaf area of low-stature Arctic shrubs with terrestrial LiDAR. *Remote Sensing of Environment*, 164, pp.26-35.

- Griscom, B.W., Adams, J., Ellis, P.W., Houghton, R.A., Lomax, G., Miteva, D.A., Schlesinger, W.H., Shoch, D., Siikamäki, J.V., Smith, P. and Woodbury, P., 2017. Natural climate solutions. *Proceedings of the National Academy of Sciences*, 114(44), pp.11645-11650.
- Grybas, H. and Congalton, R.G., 2021. A comparison of multi-temporal RGB and multispectral UAS imagery for tree species classification in heterogeneous New Hampshire Forests. *Remote Sensing*, 13(13), p.2631.
- Hackwell, K. and Robinson, M., 2021. Protecting Our Natural Ecosystems' Carbon Sinks. *Forest & Bird*.
- Harden, G. J. (1990) *Flora of New South Wales*, 4UNSW Press.
- Harvey, G.L. and Henshaw, A.J., 2023. Rewilding and the water cycle. *Wiley Interdisciplinary Reviews: Water*, 10(6), p.e1686.
- Hastie, T., 2009. The elements of statistical learning: data mining, inference, and prediction.
- Hastie, T., Tibshirani, R., Friedman, J. and Franklin, J., 2005. The elements of statistical learning: data mining, inference and prediction. *The Mathematical Intelligencer*, 27(2), pp.83-85.
- Hernandez-Santin, L., Rudge, M.L., Bartolo, R.E. and Erskine, P.D., 2019. Identifying species and monitoring understorey from UAS-derived data: A literature review and future directions. *Drones*, 3(1), p.9.
- Hester, A.J., 2006. Impacts of large herbivores on plant community structure and dynamics. *Large herbivore ecology. Ecosystem dynamics and conservation*, pp.97-128.
- Hijmans, R.J., 2018. raster: Geographic data analysis and modeling. *R package version*, 2, p.8.
- Hijmans, R.J., 2020. terra: Spatial data analysis. *CRAN: Contributed Packages*.
- Huff, S., Ritchie, M. and Temesgen, H., 2017. Allometric equations for estimating aboveground biomass for common shrubs in northeastern California. *Forest Ecology and Management*, 398, pp.48-63.
- IPCC, 2019. *Climate Change and Land: an IPCC special report on climate change, desertification, land degradation, sustainable land management, food security, and greenhouse gas fluxes in terrestrial ecosystems*. Intergovernmental Panel on Climate Change, Geneva.
- IPCC, 2022. *Climate Change 2022: Impacts, Adaptation and Vulnerability*. Working Group II Contribution to the Sixth Assessment Report. Cambridge University Press, Cambridge.
- Iqbal, F., Lucieer, A. and Barry, K., 2018. Simplified radiometric calibration for UAS-mounted multispectral sensor. *European Journal of Remote Sensing*, 51(1), pp.301-313.
- Jankju, M., 2013. Role of nurse shrubs in restoration of an arid rangeland: Effects of microclimate on grass establishment. *Journal of Arid Environments*, 89, pp.103-109.
- Jenkins, J.C., Chojnacky, D.C., Heath, L.S. and Birdsey, R.A., 2003. National-scale biomass estimators for United States tree species. *Forest science*, 49(1), pp.12-35.

- Jhariya, M.K., 2017. Vegetation ecology and carbon sequestration potential of shrubs in tropics of Chhattisgarh, India. *Environmental monitoring and assessment*, 189, pp.1-15.
- Jones, E., Harden, S. and Crawley, M.J., 2022. *The R book*. John Wiley & Sons.
- Jones, H.G. and Vaughan, R.A., 2010. *Remote sensing of vegetation: principles, techniques, and applications*. Oxford University Press, USA.
- Ju, J. and Masek, J.G., 2016. The vegetation greenness trend in Canada and US Alaska from 1984–2012 Landsat data. *Remote Sensing of Environment*, 176, pp.1-16.
- Juan-Ovejero, R., Elghouat, A., Navarro, C.J., Reyes-Martín, M.P., Jiménez, M.N., Navarro, F.B., Alcaraz-Segura, D. and Castro, J., 2023. Estimation of aboveground biomass and carbon stocks of *Quercus ilex* L. saplings using UAV-derived RGB imagery. *Annals of Forest Science*, 80(1), p.44.
- Kameyama, S. and Sugiura, K., 2020. Estimating tree height and volume using unmanned aerial vehicle photography and SfM technology, with verification of result accuracy. *Drones*, 4(2), p.19.
- Kaštovská, E., Mastný, J. and Konvička, M., 2024. Rewilding by large ungulates contributes to organic carbon storage in soils. *Journal of Environmental Management*, 355, p.120430.
- Khan, A., Ahmad, A., Rahman, Z., Qureshi, R. and Muhammad, J., 2015. The assessment of carbon stocks in the oak scrub forest of Sheringal Valley Dir Kohistan. *Open Journal of Forestry*, 5(5), pp.510-517.
- Kirillov, A., Mintun, E., Ravi, N., Mao, H., Rolland, C., Gustafson, L., Xiao, T., Whitehead, S., Berg, A.C., Lo, W.Y. and Dollár, P., 2023. Segment anything. In *Proceedings of the IEEE/CVF International Conference on Computer Vision* (pp. 4015-4026).
- Knepp Estate, Arup & Nattergal Ltd., 2023. *Knepp Wildland Carbon Project*. Available at: <https://www.arup.com/globalassets/downloads/insights/knepp-wildland-carbon-project.pdf> [Accessed 1 Dec. 2024].
- Komsta, L. and Novomestky, F., 2015. Moments, cumulants, skewness, kurtosis and related tests. *R package version*, 14(1).
- Kuhn, M., 2008. Building predictive models in R using the caret package. *Journal of statistical software*, 28, pp.1-26.
- Kuhn, M., 2013. *Applied predictive modeling*.
- Lal, R., 2004. Soil carbon sequestration impacts on global climate change and food security. *science*, 304(5677), pp.1623-1627.
- Lal, R., Monger, C., Nave, L. and Smith, P., 2021. The role of soil in regulation of climate. *Philosophical Transactions of the Royal Society B*, 376(1834), p.20210084.

- Laliberte, A.S., Rango, A., Havstad, K.M., Paris, J.F., Beck, R.F., McNeely, R. and Gonzalez, A.L., 2004. Object-oriented image analysis for mapping shrub encroachment from 1937 to 2003 in southern New Mexico. *Remote sensing of Environment*, 93(1-2), pp.198-210.
- Larrea, M.L. and Werner, F.A., 2010. Response of vascular epiphyte diversity to different land-use intensities in a neotropical montane wet forest. *Forest Ecology and Management*, 260(11), pp.1950-1955.
- Lausch, A., Erasmi, S., King, D.J., Magdon, P. and Heurich, M., 2016. Understanding forest health with remote sensing-part I—a review of spectral traits, processes and remote-sensing characteristics. *Remote Sensing*, 8(12), p.1029.
- Law, A., Gaywood, M.J., Jones, K.C., Ramsay, P. and Willby, N.J., 2017. Using ecosystem engineers as tools in habitat restoration and rewilding: beaver and wetlands. *Science of the Total Environment*, 605, pp.1021-1030.
- Lee, J.H., Ko, Y. and McPherson, E.G., 2016. The feasibility of remotely sensed data to estimate urban tree dimensions and biomass. *Urban Forestry & Urban Greening*, 16, pp.208-220.
- Li, G., Li, C., Jia, G., Han, Z., Huang, Y. and Hu, W., 2024. Estimating the Vertical Distribution of Biomass in Subtropical Tree Species Using an Integrated Random Forest and Least Squares Machine Learning Mode. *Forests*, 15(6), p.992.
- Liaw, A. and Wiener, M., 2015. randomForest: Breiman and Cutler's random forests for classification and regression. *R package version*, 4(1.1).
- Liaw, A., 2002. Classification and regression by randomForest. *R news*.
- Lindenmayer, D.B., Likens, G.E., Andersen, A., Bowman, D., Bull, C.M., Burns, E., Dickman, C.R., Hoffmann, A.A., Keith, D.A., Liddell, M.J. and Lowe, A.J., 2012. Value of long-term ecological studies. *Austral Ecology*, 37(7), pp.745-757.
- Liu, H., 2024. Classification of tree species using UAV-based multi-spectral and multi-seasonal images: A multi-feature-based approach. *New Forests*, 55(1), pp.173-196.
- Liu, W., Wang, J., Hu, Y., Ma, T., Otgonbayar, M., Li, C., Li, Y. and Yang, J., 2024. Mapping Shrub Biomass at 10 m Resolution by Integrating Field Measurements, Unmanned Aerial Vehicles, and Multi-Source Satellite Observations. *Remote Sensing*, 16(16), p.3095.
- Łoś, H., Mendes, G.S., Cordeiro, D., Grosso, N., Costa, H., Benevides, P. and Caetano, M., 2021, July. Evaluation of XGBoost and LGBM performance in tree species classification with sentinel-2 data. In *2021 IEEE International Geoscience and Remote Sensing Symposium IGARSS* (pp. 5803-5806). IEEE.
- Lu, D. and Weng, Q., 2007. A survey of image classification methods and techniques for improving classification performance. *International journal of Remote sensing*, 28(5), pp.823-870.
- Maestre, F.T., Quero, J.L., Gotelli, N.J., Escudero, A., Ochoa, V., Delgado-Baquerizo, M., García-Gómez, M., Bowker, M.A., Soliveres, S., Escolar, C. and García-Palacios, P., 2012. Plant

species richness and ecosystem multifunctionality in global drylands. *Science*, 335(6065), pp.214-218.

Maraseni, T.N., Cockfield, G., Apan, A. and Mathers, N., 2005. Estimation of shrub biomass: development and evaluation of allometric models leading to innovative teaching methods. *International Journal of business and management education*.

McManus, K.M., Morton, D.C., Masek, J.G., Wang, D., Sexton, J.O., Nagol, J.R., Ropars, P. and Boudreau, S., 2012. Satellite-based evidence for shrub and graminoid tundra expansion in northern Quebec from 1986 to 2010. *Global Change Biology*, 18(7), pp.2313-2323.

Mehrabi, Z. and Naidoo, R., 2022. Shifting baselines and biodiversity success stories. *Nature*, 601(7894), pp.E17-E18.

Mercer, L. and Gregg, R., 2023. Exploring the carbon sequestration potential of rewilding in the UK: Policy and data needs to support net zero.

MicaSense, 2023. *RedEdge-P Multispectral Sensor*. [online] Available at: <https://www.micasense.com/rededge-p> [Accessed 25 October 2024].

Mitchard, E.T., 2018. The tropical forest carbon cycle and climate change. *Nature*, 559(7715), pp.527-534.

Mokany, K., Raison, R.J. and Prokushkin, A.S., 2006. Critical analysis of root: shoot ratios in terrestrial biomes. *Global change biology*, 12(1), pp.84-96.

Muukkonen, P. and Mäkipää, R., 2006. Biomass equations for European trees: addendum.

Myers, N., Mittermeier, R.A., Mittermeier, C.G., Da Fonseca, G.A. and Kent, J., 2000. Biodiversity hotspots for conservation priorities. *Nature*, 403(6772), pp.853-858.

Navarro, L.M. and Pereira, H.M., 2015. Rewilding abandoned landscapes in Europe. In *Rewilding european landscapes* (pp. 3-23). Cham: Springer International Publishing.

Nummi, P., Vehkaoja, M., Pumpanen, J. and Ojala, A., 2018. Beavers affect carbon biogeochemistry: both short-term and long-term processes are involved. *Mammal Review*, 48(4), pp.298-311.

Orndahl, K.M., Ehlers, L.P., Herriges, J.D., Pernick, R.E., Hebblewhite, M. and Goetz, S.J., 2022. Mapping tundra ecosystem plant functional type cover, height, and aboveground biomass in Alaska and northwest Canada using unmanned aerial vehicles. *Arctic Science*, 8(4), pp.1165-1180.

Oscro, L.P., Wu, Q., de Lemos, E.L., Gonçalves, W.N., Ramos, A.P.M., Li, J. and Junior, J.M., 2023. The segment anything model (sam) for remote sensing applications: From zero to one shot. *International Journal of Applied Earth Observation and Geoinformation*, 124, p.103540.

Over, J.S.R., Ritchie, A.C., Kranenburg, C.J., Brown, J.A., Buscombe, D.D., Noble, T., Sherwood, C.R., Warrick, J.A. and Wernette, P.A., 2021. *Processing coastal imagery with Agisoft*

Metashape Professional Edition, version 1.6—Structure from motion workflow documentation (No. 2021-1039). US Geological Survey.

Pan, Y., Birdsey, R.A., Fang, J., Houghton, R., Kauppi, P.E., Kurz, W.A., Phillips, O.L., Shvidenko, A., Lewis, S.L., Canadell, J.G. and Ciais, P., 2011. A large and persistent carbon sink in the world's forests. *science*, 333(6045), pp.988-993.

Parmenter, R.R. and MacMahon, J.A., 1983. Factors determining the abundance and distribution of rodents in a shrub-steppe ecosystem: the role of shrubs. *Oecologia*, 59, pp.145-156.

Pasalodos-Tato, M., Ruiz-Peinado, R., Del Río, M. and Montero, G., 2015. Shrub biomass accumulation and growth rate models to quantify carbon stocks and fluxes for the Mediterranean region. *European Journal of Forest Research*, 134, pp.537-553.

Pastick, N.J., Wylie, B.K., Rigge, M.B., Dahal, D., Boyte, S.P., Jones, M.O., Allred, B.W., Parajuli, S. and Wu, Z., 2021. Rapid monitoring of the abundance and spread of exotic annual grasses in the western United States using remote sensing and machine learning. *AGU Advances*, 2(2), p.e2020AV000298.

Peláez, M., López-Sánchez, A., Wilson Fernandes, G., Dirzo, R., Rodríguez-Calcerrada, J. and Perea, R., 2024. Responses of oak seedlings to increased herbivory and drought: a possible trade-off?. *Annals of Botany*, p.mcae178.

Perino, A., Pereira, H.M., Navarro, L.M., Fernández, N. and Bullock, J.M., 2019. Ceaus, u. S., Cortés-Avizanda, A., van Klink, R., Kuemmerle, T., Lomba, A., and Pe'er, G., Plieninger, T., Benayas, JMR, Sandom, CJ, Svenning, J., and Wheeler, HC: Rewilding complex ecosystems, *Science*, 364.

Perkovich, C. and Ward, D., 2021. Aboveground herbivory causes belowground changes in twelve oak *Quercus* species: a phylogenetic analysis of root biomass and non-structural carbohydrate storage. *Oikos*, 130(10), pp.1797-1812.

Perkovich, C. and Ward, D., 2022. Differentiated plant defense strategies: Herbivore community dynamics affect plant-herbivore interactions. *Ecosphere*, 13(2), p.e3935.

Pettorelli, N., Barlow, J., Stephens, P.A., Durant, S.M., Connor, B., Schulte to Bühne, H., Sandom, C.J., Wentworth, J. and Du Toit, J.T., 2018. Making rewilding fit for policy. *Journal of Applied Ecology*, 55, pp.1114-1125.

Poorter, H., Niklas, K.J., Reich, P.B., Oleksyn, J., Poot, P. and Mommer, L., 2012. Biomass allocation to leaves, stems and roots: meta-analyses of interspecific variation and environmental control. *New Phytologist*, 193(1), pp.30-50.

Poorter, L., Bongers, F., Aide, T.M., Almeyda Zambrano, A.M., Balvanera, P., Becknell, J.M., Boukili, V., Brancalion, P.H., Broadbent, E.N., Chazdon, R.L. and Craven, D., 2016. Biomass resilience of Neotropical secondary forests. *Nature*, 530(7589), pp.211-214.

- Pringle, R.M., Young, T.P., Rubenstein, D.I. and McCauley, D.J., 2007. Herbivore-initiated interaction cascades and their modulation by productivity in an African savanna. *Proceedings of the National Academy of Sciences*, 104(1), pp.193-197.
- Puliti, S., Dash, J.P., Watt, M.S., Breidenbach, J. and Pearse, G.D., 2020. A comparison of UAV laser scanning, photogrammetry and airborne laser scanning for precision inventory of small-forest properties. *Forestry: An International Journal of Forest Research*, 93(1), pp.150-162.
- QGIS.org, 2024. *QGIS Geographic Information System*. Version 3.32. [Software] Open Source Geospatial Foundation Project. Available at: <https://qgis.org> [Accessed 25 October 2024].
- R Core Team (2024). *R: A language and environment for statistical computing*. Version 4.4.1. R Foundation for Statistical Computing, Vienna, Austria. Available at: <https://www.R-project.org/> (Accessed: 23 October 2024).
- Rincon-Madroño, M., Sánchez-Zapata, J.A., Barber, X. and Barbosa, J.M., 2024. Long-term vegetation responses to climate depend on the distinctive roles of rewilding and traditional grazing systems. *Landscape Ecology*, 39(1), p.1.
- Rooke, T. and Bergström, R., 2007. Growth, chemical responses and herbivory after simulated leaf browsing in *Combretum apiculatum*. *Plant Ecology*, 189, pp.201-212.
- Rooke, T., 2003a. *Defences and responses: woody species and large herbivores in African savannas* (Vol. 276). Swedish University of Agricultural Sciences.
- Rooke, T., 2003b. Growth responses of a woody species to clipping and goat saliva. *African Journal of Ecology*, 41(4), pp.324-328.
- Rooke, T., Bergström, R., Skarpe, C. and Danell, K., 2004b. Morphological responses of woody species to simulated twig-browsing in Botswana. *Journal of Tropical Ecology*, 20(3), pp.281-289.
- Rooke, T., Danell, K., Bergström, R., Skarpe, C. and Hjältén, J., 2004a. Defensive traits of savanna trees—the role of shoot exposure to browsers. *Oikos*, 107(1), pp.161-171.
- Roy, P.S. and Ravan, S.A., 1996. Biomass estimation using satellite remote sensing data—an investigation on possible approaches for natural forest. *Journal of biosciences*, 21, pp.535-561.
- RStudio Team, 2024. *RStudio: Integrated Development for R*. Version 2024.09. [Software] RStudio, PBC. Available at: <https://posit.co/download/rstudio-desktop/> [Accessed 25 October 2024].
- Ruiz-Peinado, R., Moreno, G., Juarez, E., Montero, G. and Roig, S., 2013. The contribution of two common shrub species to aboveground and belowground carbon stock in Iberian dehesas. *Journal of Arid Environments*, 91, pp.22-30.
- Saatchi, S., Mascaró, J., Xu, L., Keller, M., Yang, Y., Duffy, P., Espírito-Santo, F., Baccini, A., Chambers, J. and Schimel, D., 2015. Seeing the forest beyond the trees. *Global Ecology and Biogeography*, 24(5), pp.606-610.

- Salek, L., Harmacek, J., Jerabkova, L., Topacoglu, O. and Machar, I., 2019. Thorny shrubs limit the browsing pressure of large herbivores on tree regeneration in temperate lowland forested landscapes. *Sustainability*, 11(13), p.3578.
- Sankaran, M., Ratnam, J. and Hanan, N., 2008. Woody cover in African savannas: the role of resources, fire and herbivory. *Global ecology and biogeography*, 17(2), pp.236-245.
- Schmitz, O.J., Sylvén, M., Atwood, T.B., Bakker, E.S., Berzaghi, F., Brodie, J.F., Croomsigt, J.P., Davies, A.B., Leroux, S.J., Schepers, F.J. and Smith, F.A., 2023. Trophic rewilding can expand natural climate solutions. *Nature Climate Change*, 13(4), pp.324-333.
- Shataee, S., Darvishsefat, A.A. and Kellenberger, T., 2007. Forest type mapping using incorporation of spatial models and ETM+ data. *Pakistan Journal of Biological Sciences*, 10(14), pp.2292-2299.
- Siddiq, Z., Hayyat, M.U., Khan, A.U., Mahmood, R., Shahzad, L., Ghaffar, R. and Cao, K.F., 2021. Models to estimate the above and below ground carbon stocks from a subtropical scrub forest of Pakistan. *Global Ecology and Conservation*, 27, p.e01539.
- Siddiq, Z., Hayyat, M.U., Khan, A.U., Mahmood, R., Shahzad, L., Ghaffar, R. and Cao, K.F., 2021. Models to estimate the above and below ground carbon stocks from a subtropical scrub forest of Pakistan. *Global Ecology and Conservation*, 27, p.e01539.
- Siewert, M.B. and Olofsson, J., 2020. Scale-dependency of Arctic ecosystem properties revealed by UAV. *Environmental Research Letters*, 15(9), p.094030.
- Slade, G., Anderson, K., Graham, H.A. and Cunliffe, A.M., 2024. Repeated drone photogrammetry surveys demonstrate that reconstructed canopy heights are sensitive to wind speed but relatively insensitive to illumination conditions. *International Journal of Remote Sensing*, pp.1-18.
- Spiegel, M.P., Volkovitskiy, A., Terekhina, A., Forbes, B.C., Park, T. and Macias-Fauria, M., 2023. Top-Down Regulation by a Reindeer Herding System Limits Climate-Driven Arctic Vegetation Change at a Regional Scale. *Earth's Future*, 11(7), p.e2022EF003407.
- Sullivan, M.J., Talbot, J., Lewis, S.L., Phillips, O.L., Qie, L., Begne, S.K., Chave, J., Cuni-Sanchez, A., Hubau, W., Lopez-Gonzalez, G. and Miles, L., 2017. Diversity and carbon storage across the tropical forest biome. *Scientific reports*, 7(1), p.39102.
- Svenning, J.C., 2020. Rewilding should be central to global restoration efforts. *One Earth*, 3(6), pp.657-660.
- Svenning, J.C., Buitenwerf, R. and Le Roux, E., 2024. Trophic rewilding as a restoration approach under emerging novel biosphere conditions. *Current Biology*, 34(9), pp.R435-R451.
- Takahashi Miyoshi, G., Imai, N.N., Garcia Tommaselli, A.M., Antunes de Moraes, M.V. and Honkavaara, E., 2020. Evaluation of hyperspectral multitemporal information to improve tree species identification in the highly diverse atlantic forest. *Remote Sensing*, 12(2), p.244.

Tanentzap, A.J., Daykin, G., Fennell, T., Hearne, E., Wilkinson, M., Carey, P.D., Woodcock, B.A. and Heard, M.S., 2023. Trade-offs between passive and trophic rewilding for biodiversity and ecosystem functioning. *Biological Conservation*, 281, p.110005.

Tedersoo, L., Sepping, J., Morgunov, A.S., Kiik, M., Esop, K., Rosenvald, R., Hardwick, K., Breman, E., Purdon, R., Groom, B. and Venmans, F., 2024. Towards a co-crediting system for carbon and biodiversity. *Plants, People, Planet*, 6(1), pp.18-28.

The Wallacea Trust. (2023). Methodology for awarding biodiversity credits v. 3. Retrieved 2 December, 2024, from <https://wallaceatrust.org/wpcontent/uploads/2022/08/Biodiversity-credit-methodology-1.5.pdf>

Thomson, E.R., Spiegel, M.P., Althuisen, I.H., Bass, P., Chen, S., Chmurzynski, A., Halbritter, A.H., Henn, J.J., Jónsdóttir, I.S., Klanderud, K. and Li, Y., 2021. Multiscale mapping of plant functional groups and plant traits in the High Arctic using field spectroscopy, UAV imagery and Sentinel-2A data. *Environmental Research Letters*, 16(5), p.055006.

to Bühne, H.S., Ross, B., Sandom, C.J. and Pettoirelli, N., 2022. Monitoring rewilding from space: The Knepp estate as a case study. *Journal of Environmental Management*, 312, p.114867.

Tommila, T., Tahvonen, O. and Kuittinen, M., 2024. How much carbon can shrubs store? Measurements and analyses from Finland. *Urban Forestry & Urban Greening*, p.128560.

Torres, A., Fernández, N., Zu Ermgassen, S., Helmer, W., Revilla, E., Saavedra, D., Perino, A., Mimet, A., Rey-Benayas, J.M., Selva, N. and Schepers, F., 2018. Measuring rewilding progress. *Philosophical Transactions of the Royal Society B: Biological Sciences*, 373(1761), p.20170433.

Toth, C. and Józków, G., 2016. Remote sensing platforms and sensors: A survey. *ISPRS Journal of Photogrammetry and Remote Sensing*, 115, pp.22-36.

Tree, I., 2018. Wilding: The return of nature to a British farm. Pan Macmillan.

Trier, Ø.D., Salberg, A.B., Kermit, M., Rudjord, Ø., Gobakken, T., Næsset, E. and Aarsten, D., 2018. Tree species classification in Norway from airborne hyperspectral and airborne laser scanning data. *European Journal of Remote Sensing*, 51(1), pp.336-351.

Tudge, S.J., Harris, Z.M., Murphy, R.J., Purvis, A. and De Palma, A., 2023. Global trends in biodiversity with tree plantation age. *Global Ecology and Conservation*, 48, p.e02751.

Ustin, S.L., Gitelson, A.A., Jacquemoud, S., Schaepman, M., Asner, G.P., Gamon, J.A. and Zarco-Tejada, P., 2009. Retrieval of foliar information about plant pigment systems from high resolution spectroscopy. *Remote Sensing of Environment*, 113, pp.S67-S77.

Vafidis, J., Lucksted, I., Gall, M., Maxfield, P., Meakin, K. and Steer, M., 2021. Mapping scrub vegetation cover from photogrammetric point clouds: A useful tool in reserve management. *Ecology and evolution*, 11(11), pp.6789-6797.

Vesk, P.A. and Westoby, M., 2001. Predicting plant species' responses to grazing. *Journal of Applied Ecology*, 38(5), pp.897-909.

- Vorster, A.G., Evangelista, P.H., Stovall, A.E. and Ex, S., 2020. Variability and uncertainty in forest biomass estimates from the tree to landscape scale: the role of allometric equations. *Carbon Balance and Management*, 15, pp.1-20.
- Wallace, L., Hillman, S., Reinke, K. and Hally, B., 2017. Non-destructive estimation of above-ground surface and near-surface biomass using 3D terrestrial remote sensing techniques. *Methods in Ecology and Evolution*, 8(11), pp.1607-1616.
- Wang, C., 2021. At-sensor radiometric correction of a multispectral camera (RedEdge) for sUAS vegetation mapping. *Sensors*, 21(24), p.8224.
- Wang, C., Zhang, W., Li, X. and Wu, J., 2022. A global meta-analysis of the impacts of tree plantations on biodiversity. *Global Ecology and Biogeography*, 31(3), pp.576-587.
- Wickham, H., François, R., Henry, L. and Müller, K., 2020. *dplyr: A Grammar of Data Manipulation*. R package version 1.0. 2 (2020) [online]
- Wickham, H., François, R., Henry, L., Müller, K. and Vaughan, D., 2020. dplyr: A grammar of data manipulation.
- Wimberly, M.C., 2023. *Geographic Data Science with R: Visualizing and Analyzing Environmental Change*. Chapman and Hall/CRC.
- Wulder, M.A., White, J.C., Fournier, R.A., Luther, J.E. and Magnussen, S., 2008. Spatially explicit large area biomass estimation: three approaches using forest inventory and remotely sensed imagery in a GIS. *Sensors*, 8(1), pp.529-560.
- Yu, G., Li, X., Wang, Q. and Li, S., 2010. Carbon storage and its spatial pattern of terrestrial ecosystem in China. *Journal of Resources and Ecology*, 1(2), pp.97-109.
- Zandler, H., Brenning, A. and Samimi, C., 2015. Potential of space-borne hyperspectral data for biomass quantification in an arid environment: advantages and limitations. *Remote Sensing*, 7(4), pp.4565-4580.
- Zhang, C., Zhou, J., Wang, H., Tan, T., Cui, M., Huang, Z., Wang, P. and Zhang, L., 2022. Multi-species individual tree segmentation and identification based on improved mask R-CNN and UAV imagery in mixed forests. *Remote Sensing*, 14(4), p.874.
- Zhao, Zhuoyi, Fan, Chengyan, & Liu, Lin. (2023). Geo SAM: A QGIS plugin using Segment Anything Model (SAM) to accelerate geospatial image segmentation (1.1.0). Zenodo. <https://doi.org/10.5281/zenodo.8191039>
- Zianis, D. and Mencuccini, M., 2004. On simplifying allometric analyses of forest biomass. *Forest ecology and management*, 187(2-3), pp.311-332.
- Zolkos, S.G., Goetz, S.J. and Dubayah, R., 2013. A meta-analysis of terrestrial aboveground biomass estimation using lidar remote sensing. *Remote sensing of environment*, 128, pp.289-298.

5.7 Supplementary materials

Table S5.1: results of multiple linear regression models fitted to predict above-ground biomass (AGB) and below-ground biomass (BGB) for each taxon. Model performance is evaluated using R², Residual Sum of Squares (RSS), and Akaike Information Criterion (AIC). The tested models include combinations and interactions of predictor variables: log-transformed height, canopy area, and condition. Results are presented unfiltered to display the full range of tested models. P-values are excluded from this table as uninformative to these model comparisons. Each of the terms included in the various models (column 2) was significant ($p < 0.05$)

Taxon	Biomass	Model	R ²	RSS	AIC
blackthorn	AGB	log_above ~ condition * log_height * log_canopy_area	0.82	62.75	181.34
blackthorn	BGB	log_below ~ condition * log_height * log_canopy_area	0.83	31.57	143.56
blackthorn	AGB	log_above ~ log_height	0.73	92.29	190.55
blackthorn	AGB	log_above ~ log_height + log_canopy_area	0.77	80.92	185.32
blackthorn	AGB	log_above ~ log_height * log_canopy_area	0.79	73.92	182.35
blackthorn	AGB	log_above ~ condition + log_height + log_canopy_area	0.79	71.49	180.51
blackthorn	AGB	log_above ~ condition * log_height	0.78	76.77	184.42
blackthorn	BGB	log_below ~ log_height	0.63	66.61	172.62
blackthorn	BGB	log_below ~ log_height + log_canopy_area	0.71	53.05	162.09
blackthorn	BGB	log_below ~ log_height * log_canopy_area	0.71	51.94	162.93
blackthorn	BGB	log_below ~ condition + log_height + log_canopy_area	0.78	40.75	149.59
blackthorn	BGB	log_below ~ condition * log_height	0.73	48.71	159.40
dogrose	AGB	log_above ~ condition + log_height + log_canopy_area	0.83	32.10	136.46
dogrose	BGB	log_below ~ condition + log_height + log_canopy_area	0.63	30.61	133.85
dogrose	AGB	log_above ~ log_height	0.78	41.73	146.90
dogrose	AGB	log_above ~ log_height + log_canopy_area	0.80	38.95	145.10
dogrose	AGB	log_above ~ log_height * log_canopy_area	0.81	35.54	142.07
dogrose	AGB	log_above ~ condition * log_height	0.82	34.73	140.80
dogrose	AGB	log_above ~ condition * log_height * log_canopy_area	0.85	28.43	137.79
dogrose	BGB	log_below ~ log_height	0.51	40.70	145.53

Taxon	Biomass	Model	R ²	RSS	AIC
dogrose	BGB	log_below ~ log_height + log_canopy_area	0.56	36.55	141.61
dogrose	BGB	log_below ~ log_height * log_canopy_area	0.56	36.39	143.37
dogrose	BGB	log_below ~ condition * log_height	0.59	34.04	139.69
dogrose	BGB	log_below ~ condition * log_height * log_canopy_area	0.64	29.78	140.34
hawthorn	AGB	log_above ~ condition + log_height + log_canopy_area	0.88	28.33	130.77
hawthorn	BGB	log_below ~ condition * log_height * log_canopy_area	0.85	19.35	117.41
hawthorn	AGB	log_above ~ log_height	0.75	60.12	168.90
hawthorn	AGB	log_above ~ log_height + log_canopy_area	0.85	35.35	141.16
hawthorn	AGB	log_above ~ log_height * log_canopy_area	0.85	35.01	142.61
hawthorn	AGB	log_above ~ condition * log_height	0.77	55.03	167.95
hawthorn	AGB	log_above ~ condition * log_height * log_canopy_area	0.90	24.56	130.77
hawthorn	BGB	log_below ~ log_height	0.67	43.61	150.92
hawthorn	BGB	log_below ~ log_height + log_canopy_area	0.74	33.63	138.37
hawthorn	BGB	log_below ~ log_height * log_canopy_area	0.76	31.40	136.52
hawthorn	BGB	log_below ~ condition + log_height + log_canopy_area	0.82	23.75	120.89
hawthorn	BGB	log_below ~ condition * log_height	0.73	35.23	142.96
oak	AGB	log_above ~ log_height * log_canopy_area	0.79	19.71	104.44
oak	BGB	log_below ~ condition + log_height + log_canopy_area	0.74	18.94	102.48
oak	AGB	log_above ~ log_height	0.64	33.56	126.51
oak	AGB	log_above ~ log_height + log_canopy_area	0.73	25.41	114.89
oak	AGB	log_above ~ condition + log_height + log_canopy_area	0.78	20.77	106.99
oak	AGB	log_above ~ condition * log_height	0.68	30.38	125.64
oak	AGB	log_above ~ condition * log_height * log_canopy_area	0.85	14.25	96.54
oak	BGB	log_below ~ log_height	0.52	35.01	128.58
oak	BGB	log_below ~ log_height + log_canopy_area	0.67	24.21	112.50
oak	BGB	log_below ~ log_height * log_canopy_area	0.68	22.97	111.93
oak	BGB	log_below ~ condition * log_height	0.54	33.02	129.72
oak	BGB	log_below ~ condition * log_height * log_canopy_area	0.77	16.76	104.49

Taxon	Biomass	Model	R ²	RSS	AIC
sallow	AGB	log_above ~ condition * log_height * log_canopy_area	0.87	27.98	136.92
sallow	BGB	log_below ~ condition + log_height + log_canopy_area	0.70	42.14	151.43
sallow	AGB	log_above ~ log_height	0.65	76.18	180.00
sallow	AGB	log_above ~ log_height + log_canopy_area	0.80	42.10	149.38
sallow	AGB	log_above ~ log_height * log_canopy_area	0.81	40.26	148.92
sallow	AGB	log_above ~ condition + log_height + log_canopy_area	0.84	34.26	140.05
sallow	AGB	log_above ~ condition * log_height	0.73	59.03	169.97
sallow	BGB	log_below ~ log_height	0.50	70.61	175.82
sallow	BGB	log_below ~ log_height + log_canopy_area	0.66	47.32	155.81
sallow	BGB	log_below ~ log_height * log_canopy_area	0.67	46.70	157.09
sallow	BGB	log_below ~ condition * log_height	0.59	57.48	168.50
sallow	BGB	log_below ~ condition * log_height * log_canopy_area	0.74	36.81	152.00

Table S5.2: linear models predicting aboveground biomass (AGB) and belowground biomass (BGB) for different taxa using the maximal model: $\text{Biomass} \sim \text{condition} \times \log(\text{height}) \times \log(\text{canopy area})$. Each row represents a model term, with corresponding estimates, standard errors and T-values. P-values are excluded from this table as uninformative to these model comparisons. Each of the terms included in the various models were significant ($p < 0.05$).

Log (W)	Taxon	Term	Estimate	s.e.	t
BGB	blackthorn	conditionprotected:log_canopy_area	-2.43	0.97	-2.51
BGB	blackthorn	conditionprotected	15.93	8.38	1.90
BGB	blackthorn	conditionprotected:log_height:log_canopy_area	0.39	0.22	1.80
BGB	blackthorn	log_canopy_area	0.64	0.47	1.35
BGB	blackthorn	conditionprotected:log_height	-2.68	2.03	-1.32
AGB	blackthorn	conditionprotected:log_canopy_area	-1.76	1.37	-1.29
AGB	blackthorn	log_height:log_canopy_area	0.18	0.17	1.09
AGB	blackthorn	conditionprotected:log_height:log_canopy_area	0.28	0.31	0.90
AGB	blackthorn	conditionprotected	8.80	11.81	0.75
AGB	blackthorn	conditionprotected:log_height	-1.32	2.86	-0.46
BGB	blackthorn	log_height:log_canopy_area	0.05	0.12	0.41
BGB	blackthorn	(Intercept)	-1.48	4.07	-0.36
AGB	blackthorn	(Intercept)	1.28	5.73	0.22
AGB	blackthorn	log_height	-0.28	1.64	-0.17
AGB	blackthorn	log_canopy_area	-0.08	0.67	-0.11
BGB	blackthorn	log_height	0.02	1.17	0.01
AGB	dogrose	conditionprotected:log_height	-3.55	2.24	-1.58
AGB	dogrose	conditionprotected:log_height:log_canopy_area	0.36	0.24	1.50
AGB	dogrose	conditionprotected	13.82	9.98	1.38
AGB	dogrose	log_height	1.96	1.50	1.31
AGB	dogrose	conditionprotected:log_canopy_area	-1.49	1.19	-1.25
BGB	dogrose	log_canopy_area	0.54	0.63	0.86
BGB	dogrose	log_height	1.25	1.53	0.82
BGB	dogrose	conditionprotected	7.79	10.22	0.76
BGB	dogrose	conditionprotected:log_canopy_area	-0.92	1.22	-0.75
AGB	dogrose	(Intercept)	-4.49	6.00	-0.75

Log (W)	Taxon	Term	Estimate	s.e.	t
BGB	dogrose	conditionprotected:log_height	-1.69	2.29	-0.74
BGB	dogrose	conditionprotected:log_height:log_canopy_area	0.18	0.25	0.72
BGB	dogrose	log_height:log_canopy_area	-0.06	0.15	-0.38
BGB	dogrose	(Intercept)	-2.29	6.14	-0.37
AGB	dogrose	log_canopy_area	0.17	0.61	0.27
AGB	dogrose	log_height:log_canopy_area	0.00	0.14	-0.01
AGB	hawthorn	log_canopy_area	1.73	0.74	2.35
AGB	hawthorn	(Intercept)	-15.38	6.77	-2.27
AGB	hawthorn	log_height	3.38	1.59	2.13
AGB	hawthorn	conditionprotected:log_height	-4.88	2.92	-1.67
AGB	hawthorn	log_height:log_canopy_area	-0.22	0.16	-1.36
AGB	hawthorn	conditionprotected:log_height:log_canopy_area	0.42	0.32	1.31
AGB	hawthorn	conditionprotected	17.01	15.33	1.11
BGB	hawthorn	conditionprotected:log_height	-2.85	2.59	-1.10
BGB	hawthorn	log_height	1.38	1.41	0.98
AGB	hawthorn	conditionprotected:log_canopy_area	-1.40	1.75	-0.80
BGB	hawthorn	conditionprotected:log_height:log_canopy_area	0.17	0.28	0.62
BGB	hawthorn	(Intercept)	-3.10	6.01	-0.52
BGB	hawthorn	log_canopy_area	0.30	0.65	0.46
BGB	hawthorn	conditionprotected	6.07	13.61	0.45
BGB	hawthorn	conditionprotected:log_canopy_area	-0.11	1.55	-0.07
BGB	hawthorn	log_height:log_canopy_area	0.00	0.14	-0.02
AGB	oak	log_height:log_canopy_area	0.75	0.30	2.50
AGB	oak	(Intercept)	18.76	7.91	2.37
AGB	oak	log_canopy_area	-2.81	1.28	-2.21
AGB	oak	log_height	-3.85	1.89	-2.04
BGB	oak	log_height:log_canopy_area	0.56	0.33	1.71
BGB	oak	(Intercept)	13.02	8.58	1.52
AGB	oak	conditionprotected:log_canopy_area	2.18	1.47	1.49
AGB	oak	conditionprotected:log_height:log_canopy_area	-0.46	0.33	-1.41
BGB	oak	log_height	-2.87	2.05	-1.40

Log (W)	Taxon	Term	Estimate	s.e.	t
BGB	oak	log_canopy_area	-1.74	1.38	-1.25
AGB	oak	conditionprotected	-10.11	9.66	-1.05
BGB	oak	conditionprotected:log_height:log_canopy_area	-0.37	0.36	-1.04
BGB	oak	conditionprotected:log_canopy_area	1.52	1.59	0.96
AGB	oak	conditionprotected:log_height	1.87	2.18	0.86
BGB	oak	conditionprotected	-7.03	10.48	-0.67
BGB	oak	conditionprotected:log_height	1.57	2.36	0.66
AGB	sallow	log_canopy_area	0.85	0.52	1.64
BGB	sallow	log_canopy_area	0.92	0.60	1.54
AGB	sallow	conditionprotected:log_canopy_area	-0.95	0.97	-0.98
AGB	sallow	conditionprotected:log_height:log_canopy_area	0.15	0.20	0.78
AGB	sallow	(Intercept)	-2.86	5.04	-0.57
BGB	sallow	conditionprotected:log_canopy_area	-0.59	1.11	-0.53
BGB	sallow	(Intercept)	-2.70	5.78	-0.47
BGB	sallow	log_height	0.66	1.44	0.46
BGB	sallow	conditionprotected:log_height:log_canopy_area	0.10	0.23	0.45
AGB	sallow	conditionprotected	3.52	9.00	0.39
BGB	sallow	log_height:log_canopy_area	-0.05	0.14	-0.38
AGB	sallow	log_height	0.44	1.26	0.35
AGB	sallow	conditionprotected:log_height	-0.55	1.93	-0.28
BGB	sallow	conditionprotected	0.84	10.32	0.08
BGB	sallow	conditionprotected:log_height	-0.16	2.22	-0.07
AGB	sallow	log_height:log_canopy_area	0.00	0.12	0.00

Chapter 6: Conclusion

6.1 Main Findings

This thesis aimed to evaluate the carbon storage potential of scrubland ecosystems in a rewilding context, a critical step toward recognising the ecological and economic value of rewilding within natural capital frameworks. The overarching goal was to assess whether current carbon estimation methodologies adequately account for the unique characteristics of scrublands (Chapter 2), while also developing taxa-specific allometric models (Chapter 3), exploring the impact of browsing on biomass allocation (Chapter 3), quantifying the carbon content of scrub roots and shoots (Chapter 4), and investigating remote sensing methodologies for landscape-scale applications (Chapter 5).

To address the central research question, *“What is the carbon storage potential of scrubland created by rewilding?”*, the thesis pursued six interlinked research objectives:

- i. Evaluate the applicability of current methodologies for estimating carbon storage in scrubland ecosystems within a rewilding context.
- ii. Determine the carbon storage potential of scrubland through destructive sampling and the development of above- and belowground taxa-specific allometric equations for a 25-year-old rewilded landscape.
- iii. Investigate the impact of browsing on carbon storage and biomass allocation, both above- and below-ground, and develop a model to describe this impact.

- iv. Quantify carbon content in above- and below-ground biomass across five target scrub taxa, assessing the 50% carbon-to-dry-weight assumption and examining the influence of herbivory on carbon content.
- v. Evaluate the potential for remote sensing of carbon storage in scrubland ecosystems using a Structure from Motion (SfM) approach.
- vi. Develop a predictive tool for estimating total carbon storage in rewilded scrubland by integrating SfM data with multispectral imaging and above- and below-ground carbon models at a landscape scale.

The remainder of this chapter synthesises these findings within the broader context of rewilding and climate change science and discusses future research directions based on the results to emerge from the research outputs discussed in my thesis (Figure 6.1).

- i. **Evaluate the applicability of current methodologies for estimating carbon storage in scrubland ecosystems within a rewilding context. (Chapter 2)**

Findings: I found the i-Tree Eco model (i-Tree, 2021), one of the most commonly used methodologies for quantifying the carbon storage in trees and forests, is unsuitable for accurately estimating carbon storage in scrub ecosystems, and particularly those that are shaped by browsing. The model's fixed root:shoot (R:S) ratio of 0.26, derived from closed-canopy systems (Nowak, 2020), was tested against destructive sampling. The results revealed

significant discrepancies, with scrub trees at Knepp displaying an average R:S ratio of 1.07—over four times higher than the model's assumption. This ratio also exceeded those found in temperate hedgerows (R:S = 0.94; Axe et al., 2017) and global shrubland estimates (R:S = 0.32; Mokany et al., 2006). My findings underscore the unique biomass allocation patterns in rewilded scrub ecosystems and demonstrate the underestimation of belowground biomass in existing carbon storage models.

Additionally, the results showed that standard allometric relationships, commonly applied in models such as the Woodland Carbon Code (Randle & Jenkins., 2011) and i-Tree Eco, were absent in the scrub trees at Knepp. Specifically, there was no significant relationship between basal diameter and tree height below the browsing line (<2.5 m). This challenges the validity of applying traditional allometric assumptions to multi-stemmed scrub species shaped by browsing pressure.

Impact/significance: These findings highlight critical shortcomings in current carbon accounting methodologies, which are largely designed for closed-canopy forests and fail to reflect the structural and ecological characteristics of rewilded scrublands. My results show that existing models consistently underestimate belowground biomass in scrub species, particularly in landscapes influenced by herbivory and open conditions. This research demonstrates the inadequacy of these methodologies and emphasises the urgent need for tailored models that integrate scrub-specific data and account for the effects of herbivory.

Additionally, this study advances our ecological understanding of rewilded systems, illustrating how in these ecosystems, herbivory fundamentally alters biomass allocation

patterns compared to closed-canopy forests. The observed discrepancies in root:shoot ratios and the lack of standard allometric relationships underscore the unique carbon dynamics of scrublands, particularly the significant role of root systems in carbon storage.

Novelty: The study's use of scrub-specific measurements and its challenge to the widely used 0.26 root:shoot ratio represents a significant departure from traditional forest-centric models, paving the way for developing tailored allometric models.

ii. **Determine the carbon storage potential of scrubland through destructive sampling and the development of above- and belowground taxa-specific allometric equations of a 25-year-old rewilded landscape – Chapter 3**

Findings: Using a destructive sampling methodology (e.g., Huynh et al., 2021), 270 scrub trees comprising five different scrubland taxa were harvested to measure aboveground biomass (AGB) and belowground biomass (BGB). These data served as the foundation for developing predictive models tailored to rewilded scrub ecosystems.

The resulting scrub-specific allometric equations demonstrated high predictive accuracy, with R^2 values ranging from 0.63 (BGB for dog rose) to 0.95 (AGB for hawthorn). These results align with established allometric models for closed-canopy forests and shrublands (e.g., Chave et al., 2005; Mokany et al., 2006). The most effective models incorporated height, canopy area, and basal diameter as key predictors, while accounting for browsing conditions ("exposed" vs. "protected") further improved accuracy for most taxa.

These findings underscore the effectiveness of tailored allometric equations for accurately estimating biomass in scrub ecosystems. Incorporating browsing pressure into these models captures the distinct structural traits and biomass allocation patterns characteristic of rewilded landscapes.

Impact/significance: The equations developed in this chapter offer a novel framework for assessing biomass and carbon storage in rewilded scrublands. By focusing on taxa-specific measurements, this study addressed a critical gap in current methodologies, which often rely on generalised equations developed for closed-canopy forests (Chapter 2, Burrell et al., 2024). These findings underscore the necessity of ecosystem-specific approaches to allometry, particularly in landscapes undergoing secondary succession, where the structural traits of vegetation diverge significantly from those of traditional forest systems (Chave et al., 2014; Mokany et al., 2006).

The strong predictive performance of these equations highlights their utility in accurately estimating both aboveground and belowground biomass in scrub ecosystems. This has important implications for carbon accounting frameworks, which currently lack tailored tools for valuing the carbon storage potential of scrublands influenced by large herbivores. Unlike conventional models such as IPCC guidelines, i-Tree Eco, and the Woodland Carbon Code, which estimate belowground biomass (BGB) using a standardised root:shoot (R:S) ratio of 0.26 (Matthews & Mackie, 2006; Nowak et al., 2020), the equations developed here provide specific, tailored formulas for estimating BGB based on aboveground traits. This approach adds a level of accuracy not currently achieved by existing carbon accounting tools.

By incorporating detailed equations based on key structural traits, this research establishes a robust foundation for integrating scrub ecosystems into natural capital frameworks and carbon offset schemes. These findings not only improve the precision of biomass estimation in rewilded landscapes but also emphasise the need for incorporating ecosystem-specific methodologies to accurately reflect the unique contributions of scrublands to carbon sequestration.

Novelty: This chapter represents a significant advancement in allometric modelling by addressing the longstanding gap in estimating biomass for temperate scrub ecosystems within rewilding contexts (Chapter 2, Burrell et al., 2024). The innovative use of a browsing metric, combined with the development of taxa-specific equations, is among the first attempts to create models explicitly tailored to scrub trees in rewilded landscapes. Unlike traditional models that often underestimate belowground biomass, these equations provide a more accurate and comprehensive account of biomass distribution by incorporating both aboveground and belowground components.

Leveraging a large dataset of destructively sampled scrub trees ($n = 270$)—notably larger than is typical for studies of this nature—this research significantly refines the precision and applicability of allometric equations for non-forested ecosystems. This robust dataset underpins the development of replicable scrub-specific models, offering a scalable, non-destructive framework for understanding carbon dynamics. By addressing the unique complexities of scrub biomass in heterogeneous landscapes, this work establishes a new benchmark for carbon accounting in rewilding projects and beyond.

- iii. Investigate the impact of browsing on carbon storage and biomass allocation, both above and below ground, and develop a model to describe this impact –
Chapter 3

Findings: Chapter 3 revealed significant variability in root:shoot (R:S) ratios across scrub taxa and browsing conditions, highlighting unique biomass allocation dynamics in rewilded landscapes. For example, dog rose exhibited R:S ratios averaging 1.22 in exposed conditions and 1.15 in protected conditions, substantially exceeding the 0.26 standard used in models like the Woodland Carbon Code (Nowak et al., 2020). These results affirm Chapter 2's assertion that scrub ecosystems harbour a substantial belowground carbon pool, generally overlooked in traditional carbon accounting methodologies. Similarly, oak and blackthorn demonstrated substantial belowground biomass investments, indicative of adaptive responses to herbivory and competition (Perkovich & Ward, 2021).

The impact of browsing was evident in differential biomass allocation. Hawthorn and oak exhibited higher R:S ratios in exposed conditions, reflecting adaptive responses to browsing stress. Conversely, blackthorn showed greater belowground biomass in protected conditions, likely driven by its clonal propagation strategy, which promotes root expansion when browsing pressure is reduced (Gómez et al. 2008; Facciolati et al., 2024). These findings align with research emphasising scrub species' resilience in browsed landscapes, (Boege and Marquis 2005; Call and St. Clair, 2018).

Significance/Importance: These findings are significant because they address the limitations of conventional biomass models, such as i-Tree Eco and the Woodland Carbon Code, which rely on generalised assumptions developed for closed-canopy forests. The high R:S ratios

observed across scrub taxa underscore the critical role of belowground biomass as a carbon pool in scrub ecosystems. Conventional models underestimate this contribution, potentially leading to significant miscalculations in carbon storage estimates.

The study demonstrates that in rewilded landscapes browsing fundamentally alters biomass allocation patterns, emphasising the ecological complexity of rewilded landscapes. Incorporating herbivory effects into carbon accounting frameworks is essential for accurate assessment. Furthermore, the equations developed here enable non-destructive biomass estimation, overcoming the challenges posed by irregular, multi-stemmed scrub species.

Novelty: This research introduces the first set of rewilding-specific allometric equations that integrate browsing effects into biomass allocation models. Unlike conventional tools, which assume static relationships between aboveground and belowground biomass, these equations account for the dynamic influences of herbivory as well as aboveground plant traits. This represents a significant advancement in the field, enabling more accurate predictions of biomass and carbon storage in scrub ecosystems.

The inclusion of browsing conditions in the power-law scaling equations is a novel approach that enhances the predictive power of the models. This innovation challenges the prevailing notion that scrubby, smaller trees are “unmeasurable” in terms of carbon accounting (Randle & Jenkins, 2011).

By addressing the complexities of biomass allocation in browsed landscapes, this work lays the foundation for integrating scrub ecosystems into natural capital frameworks and carbon offset strategies.

iv. **Quantify Carbon Content in Rewilded Scrublands: Challenging the '50% Rule' through Elemental Analysis – Chapter 4**

Findings: This chapter builds upon the findings of the previous chapters by addressing a critical gap in our understanding of the carbon content of scrub species in rewilded landscapes. The results found significant variability in carbon content between aboveground and belowground biomass across all taxa. On average, aboveground components exhibited higher carbon percentages than belowground components. For instance, blackthorn showed a mean aboveground carbon content of 51.1%, compared to 48.8% belowground, while dog rose displayed 52.2% aboveground versus 47.5% belowground. These differences may reflect structural adaptations to herbivory, such as increased lignification (Agrawal & Fishbein 2006; Barrere et al. 2019), chemical defence, i.e. by investment in carbon-based compounds such as phenolics (Royer et al. 2013; Barrere et al. 2019) or wood density (Facciolati et al., 2024), enhancing resilience to browsing pressure (Salek et al., 2019) thus increasing the carbon content.

The study also identified significant variability within and between taxa. Sallow, for example, exhibited aboveground carbon percentages ranging from 48.9% to 53.8%, underscoring the complexity of carbon content across scrub taxa. Such findings challenge the utility of the widely assumed 50% carbon:biomass ratio, which is commonly applied in forest carbon accounting models (Randle & Jenkins et al., 2011).

Significance/Importance: These findings underscore key differences in biomass allocation and carbon content between nascent scrub ecosystems and other woody landscapes. The higher carbon percentages in aboveground components reflect unique structural adaptations

to herbivory, highlighting the importance of distinguishing between aboveground and belowground biomass in carbon storage assessments for rewilded landscapes.

The observed variability within and between taxa reinforces the need for scrub-specific carbon content values. Reliance on generalised assumptions, such as the 50% rule, risks substantial inaccuracies in estimating carbon storage potential.

Novelty: This chapter makes a novel contribution by demonstrating that the 50% carbon-to-biomass ratio, widely used in forest models, is not applicable to rewilded scrub ecosystems.

Furthermore, the study provides carbon content values for above- and belowground scrub which can be used alongside the allometric equations developed in Chapter 3, providing a comprehensive framework for estimating carbon storage in rewilded scrublands. This combination enhances the accuracy of carbon storage assessments and sets a new standard for valuing scrub ecosystems within natural capital and carbon offset strategies.

The implications of these findings extend beyond carbon accounting. It establishes a critical foundation for future studies, advocating for larger sample sizes and more detailed investigations into the factors driving carbon variability in scrub ecosystems.

v. **Integrating Structure from Motion and 5-Band Imaging to Estimate Above- and Belowground Biomass in a Rewilded Scrubland Ecosystem – Chapter 5**

Findings: In order to meet the objective, this chapter focused on integrating UAV RGB photogrammetry using a Structure-from-Motion (SfM) workflow and multispectral imagery to develop a scalable, non-destructive methodology for estimating biomass in rewilded scrublands. The findings revealed several key outcomes. SfM-derived canopy height and area metrics demonstrated strong alignment with field measurements (taken from Chapter 3), validating the accuracy of these predictor variables. Using an XGBoost classification model, the study achieved moderate success in differentiating scrub taxa based on spectral and structural data, with taxa like hawthorn and oak showing balanced accuracy scores of 0.78 and 0.79, respectively. However, structurally complex taxa such as blackthorn and dog rose proved more challenging to classify, with balanced accuracy scores of 0.65 and 0.64, respectively.

Importance/significance: The significance of this research lies in its demonstration of the potential for UAV-based SfM photogrammetry and multispectral imaging to remotely estimate biomass in rewilded scrub ecosystems. By enabling robust above- and below-ground biomass assessments without the need for labour-intensive field methods, it significantly expands the feasibility of biomass modelling through remote sensing in heterogeneous and structurally complex ecosystems. This finding challenges the exclusion of scrub from traditional carbon accounting frameworks and advocates for its inclusion in natural capital valuation and carbon offset schemes. The ability to apply these methods across broader spatial

scales is particularly significant for monitoring rewilding projects and evaluating their contributions to ecological restoration and carbon sequestration goals.

Furthermore, the use of SfM over LiDAR is particularly noteworthy due to its cost-effectiveness and accessibility, making it a viable option for large-scale biomass assessments despite its reduced capability to penetrate dense vegetation compared to LiDAR (Liao et al., 2021; James & Robson, 2012; Westoby et al., 2012). The ability to apply these methods across broader spatial scales is particularly significant for monitoring rewilding projects and evaluating their contributions to ecological restoration and carbon sequestration goals cost effectively.

Novelty: The novelty of this research is evident in several aspects. First, by incorporating spectral and structural data, the study developed a unique, non-destructive methodology for scrub-specific biomass modelling. It represents one of the first successful integrations of UAV-based SfM with multispectral imaging for the purpose of carbon estimation. Additionally, the research bridged destructive sampling-derived allometric models with remote sensing technologies, creating a replicable framework for biomass and carbon estimation at the landscape level, encompassing both above and belowground biomass. By incorporating scrub-specific carbon content data derived in Chapter 4, this study offered a refined understanding of the carbon sequestration potential of scrub ecosystems. Finally, the scalable workflow developed here provides a transferable framework for applying SfM and multispectral imaging to other rewilding or scrubland systems, facilitating comprehensive, large-scale biomass and carbon assessments and setting a new standard for remote sensing applications in heterogeneous landscapes.

- vi. **Develop a predictive tool for estimating total carbon storage in rewilded scrubland by integrating SfM data with multispectral imaging and above- and belowground carbon models at a landscape scale – Chapter 5**

Findings: This chapter demonstrated the successful development of a remote sensing predictive tool that integrates taxa-specific and condition-specific allometric equations (developed in Chapter 3) with scrub-specific carbon content data (derived in Chapter 4) and a Structure-from-Motion (SfM) photogrammetry and multispectral imaging framework (Chapter 5). The approach enabled accurate and non-destructive estimation of both aboveground biomass (AGB) and belowground biomass (BGB) across a rewilded scrubland landscape.

Using the combined allometric equations and carbon content values, total carbon storage across the 13-hectare study area at Knepp Wildland was calculated at a minimum of 1,950 kg C ha⁻¹, partitioned into AGB (1,710 kg C ha⁻¹) and BGB (240 kg C ha⁻¹). Blackthorn emerged as the dominant contributor to AGB, with a total biomass of 25,804.22 kg across the site, while sallow showed the highest BGB allocation, contributing 1,641.45 kg/13 ha. These findings reflect unique structural traits and biomass allocation patterns that distinguish them from forest ecosystems.

Importance/significance: The development of this predictive tool marks a significant advancement in carbon accounting for rewilded scrublands by addressing key methodological gaps identified in Chapter 2. This scalable and efficient framework provides a practical solution for estimating carbon storage in complex, heterogeneous landscapes

where traditional field-based methods are often impractical. By incorporating both aboveground biomass (AGB) and belowground biomass (BGB), the tool offers a more comprehensive assessment of scrubland carbon dynamics, particularly for ecosystems that have been historically undervalued or excluded from natural capital and carbon market frameworks. Additionally, the integration of the novel "browsing" metric developed in this thesis allows the model to account for the substantial effects of herbivory, ensuring its relevance and applicability to remote sensing methodologies.

This approach enhances ecological valuation by accurately capturing the carbon storage potential of scrublands, reinforcing their role as essential components of rewilding projects and climate mitigation strategies. It challenges the historical exclusion of scrublands from mainstream carbon accounting models and provides robust evidence for their integration into policies aimed at achieving global climate targets.

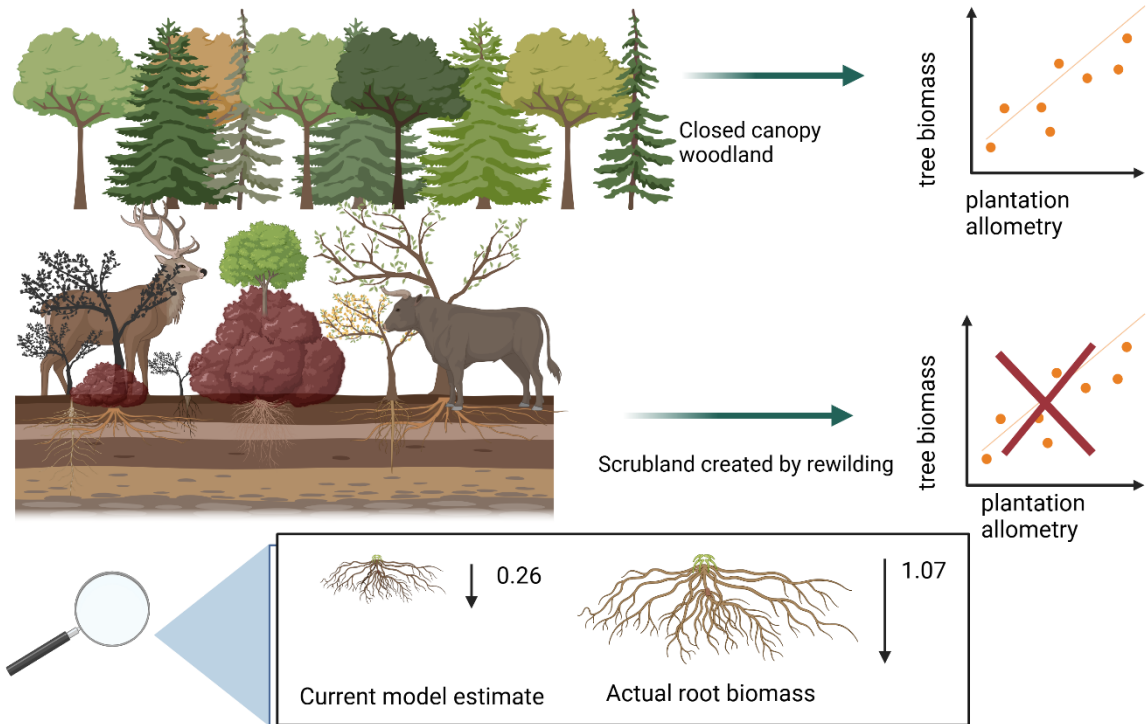
Novelty: This research represents a pioneering step in biomass and carbon storage estimation, offering several innovative contributions to the field. The integration of SfM photogrammetry, multispectral imaging, and scrub-specific carbon models is the first scalable methodology tailored explicitly to rewilded scrub ecosystems. Unlike recent forest models that focus on aboveground biomass estimation (e.g. Luo et al., 2024; Wu et al., 2024; Tian et al., 2023), this tool incorporates both above-and belowground biomass, addressing critical gaps in conventional carbon accounting frameworks.

The workflows developed throughout this thesis are transferable and adaptable, enabling application to other temperate lowland rewilding projects and scrubland systems. By providing a replicable framework for landscape-scale biomass and carbon assessments, this research bridges the gap between field-based allometry (Chapter 3) and remote sensing

technologies (Chapter 5). Furthermore, the inclusion of multispectral data, which accounted for seasonal and spectral variability, demonstrated a novel application for improving taxa classification and vegetation analysis in rewilded landscapes.

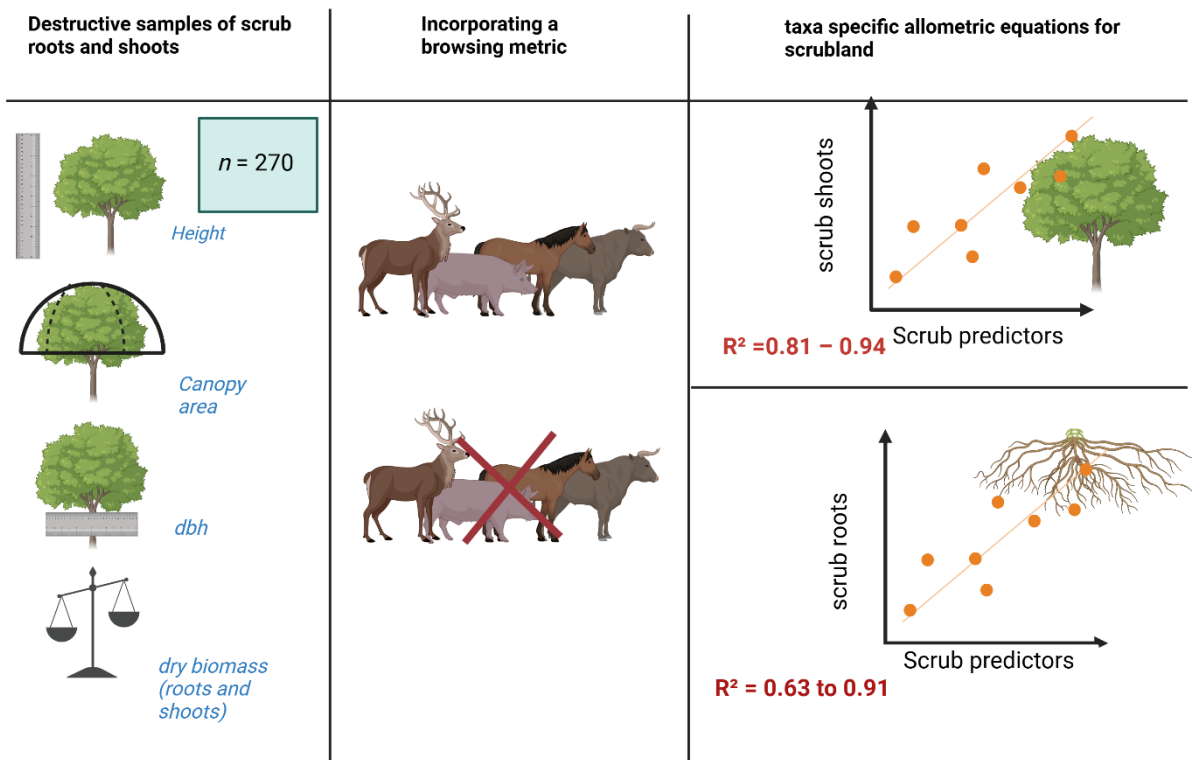
Chapter 2 - Current biomass models are ineffective for rewilding systems

[A]



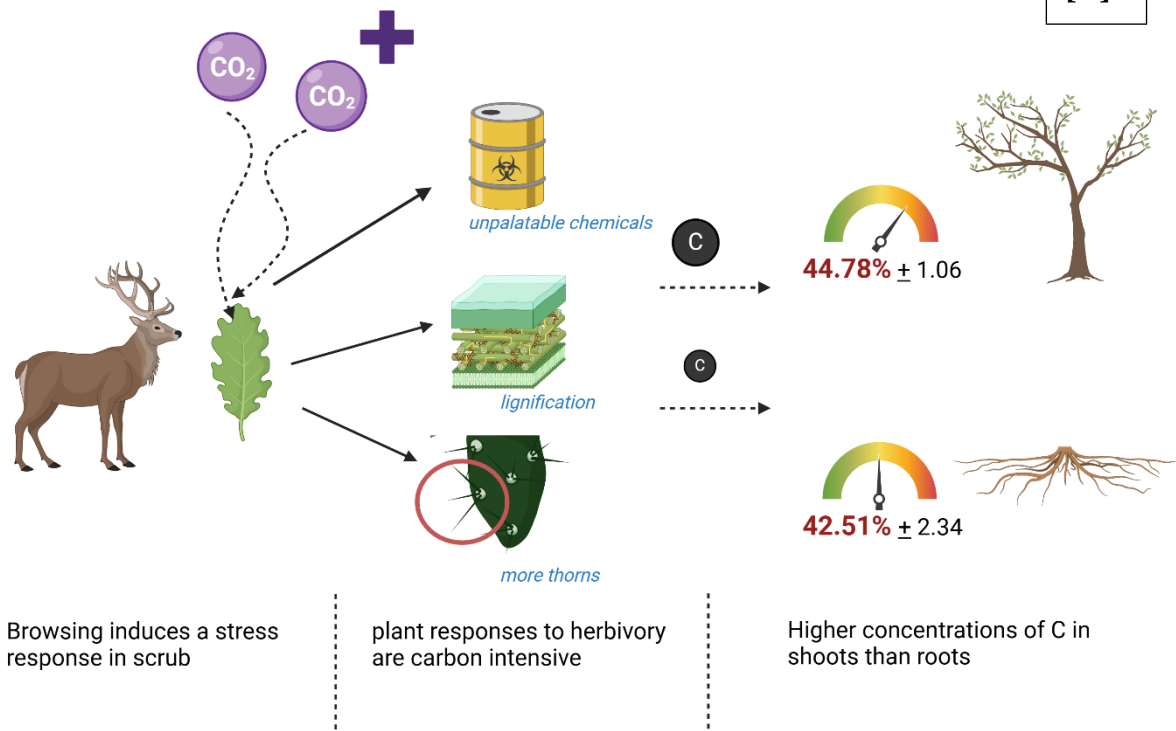
Chapter 3 - Building of the first scrub biomass estimating model for rewilding

[B]



Chapter 4 - Carbon content of rewilded scrubland

[C]



Chapter 5 - development of a scrub-specific carbon model using drone technology

[D]

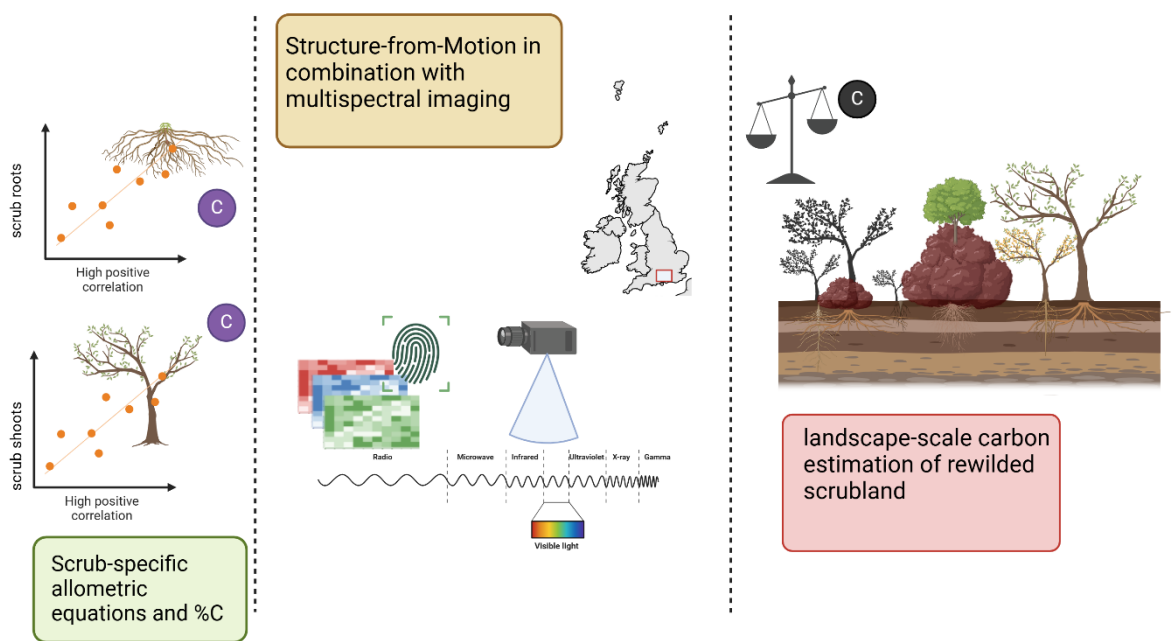


Figure 6.1: Diagrams (A – D) summarising the findings of this thesis. Created in <https://BioRender.com>, by Nancy C. Burrell.

6.2. Future directions

The findings of this thesis highlight several key areas for future research to advance our understanding of carbon storage and ecosystem dynamics in rewilded landscapes. The following avenues of investigation emerge as particularly promising:

1. **Long term research:** The scrubland at Knepp is in its early stages of development, representing a nascent phase of ecosystem succession. Repeating this research in 10 years and at subsequent intervals would provide invaluable insights into how biomass allocation, root:shoot ratios, and carbon storage potential evolve as the ecosystem matures. Long term studies are crucial for understanding how carbon sequestration rates may change over time (Marin-Spiotta et al., 2007; Powers & Marin-Spiotta, 2017).
2. **Bramble Carbon Accounting:** The carbon storage potential of bramble (*Rubus fruticosus*) has been previously noted by Axe et al. (2017), yet it remains underexplored in current carbon accounting frameworks. This thesis demonstrated that bramble dominates a large portion of temperate lowland rewilded landscape classes (Balandier et al., 2013), as seen in the canopy identification results from Chapter 5. Future research should incorporate destructive sampling methodologies to evaluate bramble's contribution to carbon storage models, particularly in the context of rewilding and its integration into natural capital assessments. Its prevalence and rapid growth suggest it could play a significant role in overall carbon sequestration within rewilded ecosystems not just because it sequesters carbon (Axe et al., 2017) but also by facilitating nutrients for sapling growth through leaf litter and providing protection from browsing ensuring a higher survival rate (Harmer et al., 2010).

- 3. Integration of Soil Carbon:** Soil carbon has been increasingly recognised as a critical component of carbon storage (Tudge et al., 2023; Lal et al., 2021), especially in rewilding contexts where soil structure and organic matter improve over time (Kastovska et al., 2024; Schmitz et al., 2023). Although this thesis focused on aboveground and belowground woody biomass, future studies should incorporate soil profiles to develop a more comprehensive understanding of the carbon storage potential of scrub ecosystems. Combining soil carbon measurements, such as the work done by Agri Carbon and Arup (Knepp Wildland Carbon Project, 2024) with the scrub-specific allometric models developed here could provide insights into the total carbon balance of rewilded landscapes.
- 4. Whole Root Excavation Studies:** The conservative destructive sampling methodology of the roots presented in Chapters 2 and 3 indicate that belowground biomass is underestimated in this thesis. Future research should focus on whole root excavation to profile the complete root systems of scrub taxa across browsing conditions. Such studies would provide a more accurate assessment of belowground carbon pools and improve our understanding of how browsing impacts root development. This is particularly relevant given the significant role of belowground biomass in carbon storage identified in this thesis.
- 5. Integration of Ecosystem Services into a Rewilding Carbon+ Unit:** While this thesis primarily focused on carbon storage, rewilded scrublands provide a wide range of additional ecosystem services, including biodiversity support (Svenning et al., 2024; Schmitz et al., 2023), flood mitigation (Harvey et al., 2024), pollination (Wallace, 2019), and soil stabilisation (Schmitz et al., 2023). Future research should aim to integrate

carbon models with assessments of these services to create a comprehensive valuation framework. For instance, combining BTO Breeding Bird Survey (BBS) data with scrubland maps to evaluate habitat use by nesting birds and territories could serve as a biodiversity metric, highlighting the role of rewilded scrub in supporting diverse ecosystems (e.g., Broughton et al., 2022). The development of a "Rewilding Carbon+ Unit" offers an exciting opportunity to encapsulate metrics for carbon storage alongside biodiversity enhancement, soil health improvement, and water regulation. This multidisciplinary approach, exemplified by tools such as the Wallacea Trust Biodiversity Calculator (Wallacea Trust, 2022), aligns with global climate and biodiversity goals, providing a robust framework for recognising and valuing rewilded landscapes within natural capital frameworks and carbon markets.

6. **Advancing Remote Sensing Methodologies:** The successful application of UAV-based Structure-from-Motion (SfM) and multispectral imaging (Chapter 5) points to further potential for advancing remote sensing technologies. Future research could refine these methods for even broader spatial scales (e.g. 10 band multispectral imaging (Carnegie et al., 2023)) and integrate them with technologies such as LiDAR and satellite imagery (Zhang et al., 2024). This would enable the monitoring of larger rewilded landscapes with greater precision (Pettorelli et al., 2023; to Buhne et al., 2022), particularly for dynamic ecosystems undergoing rapid succession.
7. **Refining Browsing Metrics:** This research used bramble as a proxy for browsing pressure, but this approach has limitations as it does not directly quantify herbivore density or browsing intensity. Future research should refine this method by incorporating direct measures such as faecal pellet counts (Forsyth et al., 2007), remote

sensing of vegetation damage (Spiegel et al., 2023), or herbivore exclusion experiments (Tanentzap et al., 2023). These methods would improve the accuracy of biomass and carbon storage models in rewilded ecosystems, providing a more precise understanding of herbivory's role in shaping biomass allocation.

6.3. Concluding Remarks

Rewilding offers a powerful and innovative approach to addressing the climate crisis, delivering a suite of ecosystem services that benefit both nature and society (Cerqueira et al., 2015; Torres et al., 2018). From bolstering biodiversity to enhancing soil health and water regulation, rewilded landscapes offer immense ecological potential (Svenning et al., 2024). Yet these diverse benefits often go underappreciated and undervalued in natural capital frameworks. The inherent heterogeneity of rewilding ecosystems makes them challenging to quantify and assign a clear market value, limiting their recognition and integration into broader environmental and economic strategies.

This thesis provides a foundation for addressing this gap by developing a robust framework to assess the carbon storage potential of rewilded ecosystems. Carbon, as a widely recognised and traded commodity (Griscom et al., 2017), offers a practical entry point for valuing rewilding's contributions. By extending this valuation to include the broader suite of ecosystem benefits—such as biodiversity gains, flood mitigation, and climate resilience—through a "Carbon+ Credit," we can redefine the ecological and economic significance of rewilding. This approach not only highlights the critical role of carbon storage but also

provides a way of attaching the full spectrum of rewilding benefits to be valued within a natural capital framework.

Integrating rewilding into climate mitigation and natural capital strategies bridges the gap between ecological restoration and actionable market solutions. By showcasing that the carbon storage potential of rewilding can indeed be measured, it strengthens the case for rewilding as a vital tool to combat the twin crises of climate change and biodiversity loss, incentivising its broader adoption.

6.4 References

- Agrawal A.A. and Fishbein M. 2006. Plant defense syndromes. *Ecology* 87: 132–149.
- Axe, M. S., Grange, I. D., & Conway, J. S. (2017). Carbon storage in hedge biomass—A case study of actively managed hedges in England. *Agriculture, Ecosystems & Environment*, 250, 81–88.
- Balandier, P., Marquier, A., Casella, E., Kiewitt, A., Coll, L., Wehrlen, L. and Harmer, R., 2013. Architecture, cover and light interception by bramble (*Rubus fruticosus*): a common understorey weed in temperate forests. *Forestry*, 86(1), pp.39-46.
- Barrere, J., Saïd, S., Morin, X., Boulanger, V., Rowe, N., Amiaud, B., Bernard, M. 2019. The cost of deer to trees: changes in resource allocation from growth-related traits and phenolic content to structural defence. *Plant Ecology and Evolution* 152: 417–425.
- Boege, Karina, and Robert J. Marquis. 2005. Facing Herbivory as You Grow up: The Ontogeny of Resistance in Plants. *Trends in Ecology & Evolution* 20: 441–448. <https://doi.org/10.1016/j.tree.2005.05.001>
- Broughton, R.K., Bullock, J.M., George, C., Gerard, F., Maziarz, M., Payne, W.E., Scholefield, P.A., Wade, D. and Pywell, R.F., 2022. Slow development of woodland vegetation and bird communities during 33 years of passive rewilding in open farmland. *PLoS One*, 17(11), p.e0277545.
- Burrell, N.C., Jeffers, E.S., Macias-Fauria, M. and Willis, K.J., 2024. The inadequacy of current carbon storage assessment methods for rewilding: A Knepp Estate case study. *Ecological Solutions and Evidence*, 5(1), p.e12301.
- Call, A. and St Clair, S.B., 2018. Timing and mode of simulated ungulate herbivory alter aspen defense strategies. *Tree Physiology*, 38(10), pp.1476-1485.

- Carnegie, A.J., Eslick, H., Barber, P., Nagel, M. and Stone, C., 2023. Airborne multispectral imagery and deep learning for biosecurity surveillance of invasive forest pests in urban landscapes. *Urban Forestry & Urban Greening*, 81, p.127859.
- Cerqueira, Y., Navarro, L.M., Maes, J., Marta-Pedroso, C., Pradinho Honrado, J. and Pereira, H.M., 2015. Ecosystem services: the opportunities of rewilding in Europe. *Rewilding European Landscapes*, pp.47-64.
- Chave, J., Andalo, C., Brown, S., Cairns, M.A., Chambers, J.Q., Eamus, D., Fölster, H., Fromard, F., Higuchi, N., Kira, T. and Lescure, J.P., 2005. Tree allometry and improved estimation of carbon stocks and balance in tropical forests. *Oecologia*, 145, pp.87-99.
- Chave, J., Réjou-Méchain, M., Búrquez, A., Chidumayo, E., Colgan, M.S., Delitti, W.B., Duque, A., Eid, T., Fearnside, P.M., Goodman, R.C. and Henry, M., 2014. Improved allometric models to estimate the aboveground biomass of tropical trees. *Global change biology*, 20(10), pp.3177-3190.
- Facciolati, V., Zarek, M., Blonska, E., Lasota, J., Orman, O. and Ciach, M., 2024. To be browsed or not to be browsed: differences in nutritional characteristics of blackthorn *Prunus spinosa* subject to the long-term pressure of herbivores. *bioRxiv*, pp.2024-04.
- Forsyth, D.M., Barker, R.J., Morriss, G. and Scroggie, M.P., 2007. Modeling the relationship between fecal pellet indices and deer density. *The Journal of Wildlife Management*, 71(3), pp.964-970.
- Gómez, Sara, Yusuke Onoda, Vladimir Ossipov, and Josef F. Stuefer. 2008. Systemic Induced Resistance: A Risk-Spreading Strategy in Clonal Plant Networks? *New Phytologist* 179: 1142–1153. <https://doi.org/10.1111/j.1469-8137.2008.02542.x>
- Griscom, B.W., Adams, J., Ellis, P.W., Houghton, R.A., Lomax, G., Miteva, D.A., Schlesinger, W.H., Shoch, D., Siikamäki, J.V., Smith, P. and Woodbury, P., 2017. Natural climate solutions. *Proceedings of the National Academy of Sciences*, 114(44), pp.11645-11650.
- Harmer, R., Kiewitt, A., Morgan, G. and Gill, R., 2010. Does the development of bramble (*Rubus fruticosus* L. agg.) facilitate the growth and establishment of tree seedlings in woodlands by reducing deer browsing damage?. *Forestry*, 83(1), pp.93-102.
- Harvey, G.L., Hartley, A.T., Henshaw, A.J., Khan, Z., Clarke, S.J., Sandom, C.J., England, J., King, S. and Venn, O., 2024. The role of rewilding in mitigating hydrological extremes: State of the evidence. *Wiley Interdisciplinary Reviews: Water*, 11(3), p.e1710.
- Huynh, T., Lee, D.J., Applegate, G. and Lewis, T., 2021. Field methods for above and belowground biomass estimation in plantation forests. *MethodsX*, 8, p.101192.
- i-Tree. (2021). *i-Tree Eco user's manual*, 2021. <https://www.itreetools.org/documents/275/EcoV6 UsersManual.2021.09.22.pdf>
- James, M.R. and Robson, S., 2012. Straightforward reconstruction of 3D surfaces and topography with a camera: Accuracy and geoscience application. *Journal of Geophysical Research: Earth Surface*, 117(F3).

- Kaštovská, E., Mastný, J. and Konvička, M., 2024. Rewilding by large ungulates contributes to organic carbon storage in soils. *Journal of Environmental Management*, 355, p.120430.
- Knepp Estate, Arup & Nattergal Ltd., 2023. *Knepp Wildland Carbon Project*. Available at: <https://www.arup.com/globalassets/downloads/insights/knepp-wildland-carbon-project.pdf> [Accessed 8 Dec. 2024].
- Lal, R., Monger, C., Nave, L. and Smith, P., 2021. The role of soil in regulation of climate. *Philosophical Transactions of the Royal Society B*, 376(1834), p.20210084.
- Liao, J., Zhou, J. and Yang, W., 2021. Comparing LiDAR and SfM digital surface models for three land cover types. *Open Geosciences*, 13(1), pp.497-504.
- Luo, M., Anees, S.A., Huang, Q., Qin, X., Qin, Z., Fan, J., Han, G., Zhang, L. and Shafri, H.Z.M., 2024. Improving Forest Above-Ground Biomass Estimation by Integrating Individual Machine Learning Models. *Forests*, 15(6), p.975.
- Maczik, D.M., Jansen, V.A. and Rossberg, A.G., 2024. Evaluating Biodiversity Credits Using Metacommunity Modelling. *bioRxiv*, pp.2024-06.
- Marín-Spiotta, E., Silver, W.L. and Ostertag, R., 2007. Long-term patterns in tropical reforestation: Plant community composition and aboveground biomass accumulation. *Ecological Applications*, 17(3), pp.828-839.
- Matthews, R. W., & Mackie, E. D. (2006). *Forest mensuration: A handbook for practitioners*. Forestry Commission.
- Mokany, K., Raison, R.J. and Prokushkin, A.S., 2006. Critical analysis of root: shoot ratios in terrestrial biomes. *Global change biology*, 12(1), pp.84-96.
- Nowak, D. J. (2020). *Understanding i-Tree: Summary of programs and methods*. US Department of Agriculture, Forest Service, Northern Research Station.
- Perkovich, C. and Ward, D., 2021. Herbivore-induced defenses are not under phylogenetic constraints in the genus *Quercus* (oak): Phylogenetic patterns of growth, defense, and storage. *Ecology and Evolution*, 11(10), pp.5187-5203.
- Pettorelli, N. and Schulte to Bühne, H., 2023. Current and future opportunities for satellite remote sensing to inform rewilding. *Remote Sensing in Ecology and Conservation*, 9(3), pp.301-310.
- Powers, J.S. and Marín-Spiotta, E., 2017. Ecosystem processes and biogeochemical cycles in secondary tropical forest succession. *Annual Review of Ecology, Evolution, and Systematics*, 48(1), pp.497-519.
- Randle, T., & Jenkins, T. (2011). The construction of lookup tables for estimating changes in carbon stocks in forestry projects. *A background document for users of the Forestry Commissions' Woodland Carbon Code*.
- Royer M., Lariat R., Le Bot J., Adamowicz S., Robin C. 2013. Is the C:N ratio a reliable indicator of C allocation to primary and defence-related metabolisms in tomato? *Phytochemistry* 88: 25–33.

- Salek, Lubomir, Jaromir Harmacek, Lucie Jerabkova, Osman Topacoglu, and Ivo Machar. 2019. Thorny Shrubs Limit the Browsing Pressure of Large Herbivores on Tree Regeneration in Temperate Lowland Forested Landscapes. *Sustainability* 11(13): 3578. <https://doi.org/10.3390/su11133578>
- Schmitz, O.J., Sylvén, M., Atwood, T.B., Bakker, E.S., Berzaghi, F., Brodie, J.F., Crowsigt, J.P., Davies, A.B., Leroux, S.J., Schepers, F.J. and Smith, F.A., 2023. Trophic rewilding can expand natural climate solutions. *Nature Climate Change*, 13(4), pp.324-333.
- Spiegel, M.P., Volkovitskiy, A., Terekhina, A., Forbes, B.C., Park, T. and Macias-Fauria, M., 2023. Top-Down Regulation by a Reindeer Herding System Limits Climate-Driven Arctic Vegetation Change at a Regional Scale. *Earth's Future*, 11(7), p.e2022EF003407.
- Svenning, J.C., Buitenwerf, R. and Le Roux, E., 2024. Trophic rewilding as a restoration approach under emerging novel biosphere conditions. *Current Biology*, 34(9), pp.R435-R451.
- Tanentzap, A.J., Daykin, G., Fennell, T., Hearne, E., Wilkinson, M., Carey, P.D., Woodcock, B.A. and Heard, M.S., 2023. Trade-offs between passive and trophic rewilding for biodiversity and ecosystem functioning. *Biological Conservation*, 281, p.110005.
- Tedersoo, L., Sepping, J., Morgunov, A.S., Kiik, M., Esop, K., Rosenvald, R., Hardwick, K., Breman, E., Purdon, R., Groom, B. and Venmans, F., 2024. Towards a co-crediting system for carbon and biodiversity. *Plants, People, Planet*, 6(1), pp.18-28.
- Tian, L., Wu, X., Tao, Y., Li, M., Qian, C., Liao, L. and Fu, W., 2023. Review of remote sensing-based methods for forest aboveground biomass estimation: Progress, challenges, and prospects. *Forests*, 14(6), p.1086.
- to Bühne, H.S., Ross, B., Sandom, C.J. and Pettoirelli, N., 2022. Monitoring rewilding from space: The Knepp estate as a case study. *Journal of Environmental Management*, 312, p.114867.
- Torres, A., Fernández, N., Zu Ermgassen, S., Helmer, W., Revilla, E., Saavedra, D., Perino, A., Mimet, A., Rey-Benayas, J.M., Selva, N. and Schepers, F., 2018. Measuring rewilding progress. *Philosophical Transactions of the Royal Society B: Biological Sciences*, 373(1761), p.20170433.
- Tudge, S.J., Harris, Z.M., Murphy, R.J., Purvis, A. and De Palma, A., 2023. Global trends in biodiversity with tree plantation age. *Global Ecology and Conservation*, 48, p.e02751.
- Wallace, C., 2019. The Impacts of a Rewilding Project on Pollinator Abundance and Diversity at a Local Scale.
- Wallacea Trust, 2022. *Biodiversity Credit Methodology: Version 2.1*. Available at: <https://wallaceatrust.org/wp-content/uploads/2022/12/Biodiversity-creditmethodology-V2.1.pdf> [Accessed 6 December 2024].
- Westoby, M.J., Brasington, J., Glasser, N.F., Hambrey, M.J. and Reynolds, J.M., 2012. 'Structure-from-Motion' photogrammetry: A low-cost, effective tool for geoscience applications. *Geomorphology*, 179, pp.300-314.

Wu, Z., Yao, F., Zhang, J. and Liu, H., 2024. Estimating Forest Aboveground Biomass Using a Combination of Geographical Random Forest and Empirical Bayesian Kriging Models. *Remote Sensing*, 16(11), p.1859.

Zhang, L., Zhao, Y., Chen, C., Li, X., Mao, F., Lv, L., Yu, J., Song, M., Huang, L., Chen, J. and Zheng, Z., 2024. UAV-LiDAR Integration with Sentinel-2 Enhances Precision in AGB Estimation for Bamboo Forests. *Remote Sensing*, 16(4), p.705.